A New Energy Absorber for Earthquake Resistant Buildings

By:

Habib Saeed Monir

Thesis submitted to the City University for the degree of Doctor of Philosophy

Department of Civil Engineering, School of Engineering
City University
London

January of 2001

ABSTRACT

The research work which has been reported in this thesis is associated with the design of an energy absorbing device. The device as well as being capable to absorb high amount of energy, possess all the necessary properties of a structural member.

Most energy absorbing devices have not the necessary conditions to be used as a structural members. Their problems have been demonstrated in chapter 1 and chapter 3 of the this thesis. In order to overcome these problems an alternative kind of energy absorbing device, has been proposed.

The inversion of tubes has been proposed as the basic of the work. This is a well-known energy-absorbing principle and has been widely used in industry and many mechanical engineering cases as the basic of design. However, the device has some disadvantages and these required improvement. The following steps have been taken to improve the energy absorbing characteristics:

1- Normally the energy absorbing capacity of the device is limited due to buckling. This problem has been improved by including an adhesive within the device.

2- The second problem in this energy-absorbing device is that its elastic stiffness is very low and this is unacceptable for a structural member. The elastic stiffness has been improved by forming a stiff shell at the top of the tube.

3- The device undergoes a significant change in length during the energy absorbing process and if it is not compensated in some way, the device will be useless in the subsequent cycles of vibration. A special mechanism has been installed in the device to solve this problem. This enables the deformation to be compensated after the absorption process.

Two major applications for the device have been considered to be studied in the thesis:

First because of its special response at high speed loading, it has been installed in a simply supported framework. The middle member of this framework has been replaced by the energy absorbing device and the behaviour of the framework has been analysed under an explosive load. In order to determine the advantages of the installation of this device in a framework, this framework has also been analysed without the inclusion of the device. The comparison of these results showed that when the framework is equipped with the absorber, a great reduction in the forces and strains of the members

of the framework have been achieved. The framework has become 2.5 times stronger, when just one device was used in the frame.

In the second application of the device, its behaviour has been studied as an absorber of a first soft story method. The first soft story is one of the ideas which has been presented for the isolation of buildings from earthquake effects, however, no proper absorber has been suggested to be used in this method. This device has an excellent performance in this regard, because of its shortening ability and its compact form along with its high energy absorbing capacity.

Two energy absorbing devices were inserted in the braces of a single degree freedom structure and subjected to a high rate base acceleration. For a comparison, the behaviour of the frame, when it was not equipped with the devices, was also analysed. The results indicated that by the inclusion of the absorber, the acceleration has been decreased more than three times. The forces in the members were also three times less than the frame without the device.

Finally, the behaviour of a multi story building has been examined when it was equipped with two energy absorbing device in the braces of the first floor. The results showed that a great reduction in the accelerations, velocities and also the forces and moments has been achieved, as was the case in the previous example. By using this absorber in the braces, the accelerations and velocities were four times less than the case which the frame did not include any absorber.

In simple words, this energy absorber is similar to the dampers, which are used in the vehicles to reduce vibrations, but with this difference that the dampers in the car are active all the time while this damper is activated only when a high rate loading is applied.

ACKNOWLEDGEMENTS

I would like to thank my supervisor, Professor L F Boswell, for his guidance in the preparation of this thesis.

I am indebted to Iranian Government who supported the financial expenses of my education at City University.

I would like to give my thanks for Urmia university in Iran for all of their collaborations during my study at London.

And finally I wishes to express my thanks to my wife for her continuous encouragement and assistance throughout the period of this research work.

Content

Abbreviations

ADAS	Added damping and stiffness
CBF	Concentric braced frame.
DEBF	Disposable element braced frame
EBF	Eccentrically braced frame
FD	Friction damped
FDBF	Friction damped braced frame
KBF	Knee bracing frame
MDFS	Multi degree freedom structure
MRF	Moment resistant building.
SDFS	Single degree freedom structure
VE	Viscoelastic

Notation

A	cross section area of the bar
A_s	effective shear area
b	width of wedges
D	the diameter of tube
e	depth of teeth
E	elastic modulus
E_k	reduced elastic modulus
f_{yc}	compressive yield limit
f_{yt}	tensile yield limit
F_y	concentrated uniform loading
G_c	fracture toughness
h	height of teeth
I_{ZZ}	second modulus in z direction
L	length
m	density
m_t	peak to peak value
M_a	mass
M_p	full plastic moment of peeling tube
M	moment
p	point load
R	radius
R_b	radius of bar
S	triangular elements side lengths
t	response time
t_t	the thickness of tube
t_g	the thickness of glue
U	displacement at X direction
V	displacement at Y direction
W	displacement at W direction
W_e	external work

absorbed energy by friction

W_F absorbed energy by fracture

W_p absorbed energy during bending

x length of tube in the curl

y the separated length of peeling tube

Y equivalent yield stress

α thermal coefficient

α_c Curvature hardening modulus

α_t angle of teeth

β ratio of tube thickness to die radius

δ deflection

δ_r failure elongation of adhesive

γ ratio of initial to final curvature

μ coefficient of friction

ν Poisson coefficient

θ angle of the stiffeners

θ_r angle of rotation during failure

σ_0 yield stress

τ peeling strength of the adhesive

Δ_a elastic deflection of the device

Δ^b the deflection of the device at the start of peeling process

Chapter one: Introduction

Impact and its destructive effect has been the subject of research programmes for many years. A great deal of numerical and experimental work has been undertaken to determine the behaviour of structures under impact and dynamics loads. This research work has been carried out in two different areas of impact effects: the behaviour of materials and components under high strain rates and the behaviour of structures which are assemblies of these components. The results of this research work indicates that by raising the energy absorbing capacity of a structure, instead of its overall strength, a more safe and economical structure could be achieved. Two choices are available for increasing energy absorption . These are the raising of the damping coefficient and energy absorbing qualities of the structural components or by using individual substructures named energy absorbing devices.

Materials and components possess some degree of internal damping in the elastic range. However, the structure cannot be called an absorbing system only by relying on this limited amount of energy absorbing capacity.

In properly designed structures, a high energy absorbing capacity may be achieved in the plastic deformation of the components. In this design, some unrecoverable damage is left in these members after tolerating the impact forces. In fact, these components are sacrificed for the overall safety of the structure. These members should be properly repaired or changed after the damage has occurred.

The replacement of a main structural member is not an easy task, but apart from this matter, in view of safety and confidence, subjecting such members to the danger of high strains is not always advisable. Therefore, the idea of creating individual substructures as absorbing points in the structure, is worth consideration.

Energy absorbing devices are the most suitable places for dissipating the energy of applied dynamic loads. Many attempts have been made by different researchers to design increasingly more efficient devices. For this purpose, a variety of energy absorbing and damping systems have been created and tested by using different kinds of energy dissipating phenomena. In each case, a particular type of impact was considered and the application of the absorbing device was restricted to a specific type of loading and condition. These devices have been designed to have high energy absorbing capacity combined with the lowest volume and weight.

As a general assessment, all of the available devices suffer from some disadvantages. In each case, some properties of an ideal absorber have been disregarded to satisfying other essential properties, which were crucial for the considered condition. In other words, an absorber is basically suitable for a special type of impact situation.

Devices used in constructions for absorbing seismic or explosion shocks, are expected to possess many qualities for their application. A suitable absorber for a structure, i.e. a framework, is one that would be able to function as a structural component and a high capacity absorber simultaneously, but due to the disadvantages which exist in the available absorbers, it is not possible to satisfy all the necessary conditions. For this reason, usually these energy absorbers are left unloaded in structures during the service loading.

The possession of a low yield point is one of the problems that prevents the absorber being used as a structural component because under service loads, it is expected to behave elastically in a reasonable range of loading and this is not achievable with a low yield limit.

In some of the absorbers, the yield limit (or load deflection curve) is poorly defined or unstable with respect to time history. Obviously, such devices do not satisfy the important quality of a structural member and, therefore, cannot be use as load carrying component.

The low capacity of energy dissipation is another disadvantage which exists in some other energy absorbing devices. They may carry some parts of service loads but they have not enough capacity to absorb substantial amounts of energy. They are, therefore unsuitable for use in structures.

Large volume, absence of post impact strength are typical of the problems which are to be found in energy absorbing devices. In addition to these problems, some of the energy absorbing devices affect the natural frequencies of the structure and shift them to an undesired range.

Existence of these problems has meant that the use of energy absorbing devices in structures would face some restrictions and for this reason, there is a necessity for the development of a new energy absorbing device.

In an attempt to create an energy absorbing device, with the properties which satisfy simultaneously the essential necessities of a structural member and a high energy

absorbing capacity, a new energy absorbing device has been developed in the theme of the present thesis.

Peeling and the inverting of a tube is the absorbing phenomenon which has been used in this new energy absorbing device. By developing this idea, a device has been created which can be used as a tensile bar in structures and has high energy absorbing capacity for impact shocks. In fact, by accompanying peeling process with the inversion of the tube in this device, the properties of a pure tube inversion device have been improved substantially. A low yield limit, which is a major disadvantage of a tube inverting system, has been completely improved in this new energy absorbing device. The yield limit is a very important parameter for a structural member and as well as being high enough, it should be well defined and stable with respect to time. Having a precise yield limit is one of the advantages of this new energy absorbing device. Besides, its energy absorbing capacity is functional at much higher level of load than pure tube inversion devices, because there is no buckling restriction in this new device.

One of the most important properties of this new energy absorbing device is its ability to shorten under compressive force. This is a unique property for this device. By implementing a special mechanism, the device can compensate its lengthening during the absorption process and therefore the brace becomes taut again in the structure. This means that the device will be able to continue its absorbing process without degradation of strength and its response will remain rectangular until the end of its absorbing capacity. By using this device, energy dissipation is concentrated at special points within a structure that have been already considered for this purpose and energy dissipation demands on other structural members is minimised.

This property gives the best opportunity for the device to be used as a seismic shock absorber. Until now, much research has been performed for the creation of proper absorbers for protecting buildings from earthquake damages. A review of this work will be reported in chapter two and it will be seen that despite a huge effort in this research work, there is still no widely accepted use of these devices in structures.

Devices which have been made for earthquake resistant buildings, can be classified into two major groups, which are called active and passive respectively.

For each type, many devices have been designed and made, but generally there is more attraction for the use of passive devices compared to active devices, because passive devices have usually simpler designs and therefore less complicated.

The new energy absorbing device, which will be introduced in this thesis, is a passive device and can be used as a tensile bar in frameworks, grids and in the braces of moment resisting frames and so on.

The thesis is divided into the following six chapters:

The first chapter is the introduction.

In the second chapter, a review of the available energy absorbing devices will be presented. The description of some of these energy absorbing devices will be explained first, and then the discussion will be continued by reviewing the energy absorbing devices of seismic protection.

Chapter 3 is exclusively for introducing the new energy absorbing device. The details of the device will be presented in this chapter and its unique properties will be explained and discussed.

In chapter 4, the response of device under impact shocks will be analysed. Numerical and analytical methods will be used in this chapter.

In Chapter 5, application of this new energy absorbing device will be assessed. Different kinds of structure with and without the inclusion of the energy absorbing device will be analysed. The results will be compared to demonstrate the effectiveness of the energy absorbing device in increasing the impact strength of structures.

Finally, chapter 6 is conclusion and considers suggestions for future work for the development and application of this energy absorbing device.

Chapter Two: Literature review

Introduction

There are many methods for attenuating shock energy. Basically for absorption of the energy, only damping properties of structural members, either in their elastic or plastic deformation range need be considered. This is the method which is used frequently in design[42]. Alternatively the design of a special kind of device, called an energy absorbing device, can be considered. Such a device dissipates the energy of impact loads and prevents damage to the main structure [77].

The application of energy absorbers has been commonly used to reduce the effects of machinery vibrations for example. Implementation of these devices in structural engineering however is only a recent development.

For machinery, the energy absorbing devices are located at suitable points to eliminate the propagation of dynamic waves to the other parts of the system. Depending on the type of vibration and its amplitude, these devices may work either in the elastic or plastic range of deformation of solid parts. A liquid containing device also might be used in these systems.

Car accidents have been a subject of considerable investigation in impact and crash-worthiness problems and the research results have affected the design of recently manufactured vehicles[29, 74].

For direct impact, the usual method of protection is to place the energy absorbing device in front of this load. By elastic or plastic deflection or fracture of this energy absorbing part, the energy is dissipated and the system is kept safe.

The necessity of energy absorbing systems to be included within structures was related to the possibility of explosion, vehicle collision or falling of heavy objects causing potential damages. But it is only in recent decades that these devices have been used for the attenuation of earthquake shocks[31]. In this regard many systems have been suggested and tested experimentally. These can be classified in three groups:

(i) devices in the base isolation system,

(ii) devices in the first soft storey system,

(iii) and devices which are distributed over suitable locations of the structure for absorption of energy.

In this chapter a review of the most usual energy absorbing devices, which are currently being used in practice, will be given. This will be followed by a discussion of the application of energy absorbing devices in structures subjected to seismic effects.

2-1 Energy absorbing devices

2-1-1 Bar in tension

The permanent deformation of a strip makes the simplest form of energy absorbing device which can be used in the case of a tensile load[35]. A ductile material strip is stretched until fracture occurs and appreciable amounts of energy can be absorbed during this plastic deformation and failure Fig(2-1). It is insensitive to the direction of loading if it is arranged so that it aligns itself with the direction of the loading. With metals the material can be a rod, strip or tube. With textiles it can be a webbing strap or a rope.

Despite its simplicity and substantial energy absorbing capacity, it has some major disadvantages. The main problem is its catastrophic failure which may be aggravated with localised failure of the material because of imperfections or stress wave effects. By increasing the absorbing capacity of bar, its rigidity will be decreased. This contradiction of its high energy absorbing capacity and the sufficient rigidity is another drawback for this device.

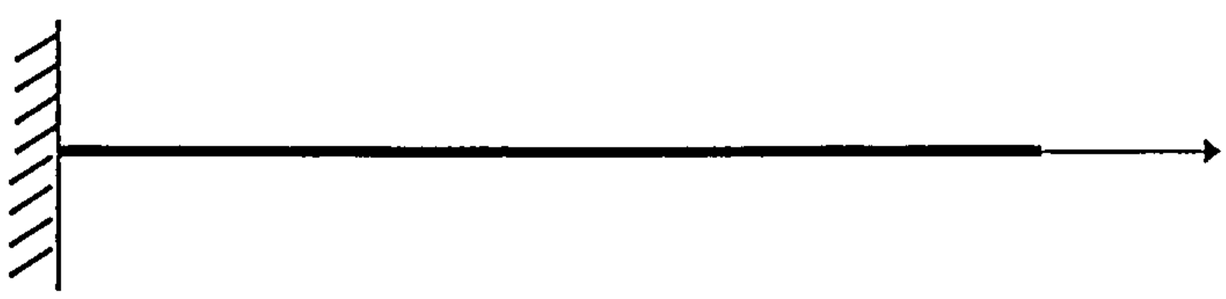

Fig 2-1: Tensile bar as energy absorbing device.

2-1-2 Axially compressive thin walled tubes

Thin walled tubes, which have circular cross sections, are used as energy absorbing devices. The simplest form is the compression of a ductile tube between two parallel platens. The tube is crushed into its natural deformed pattern, which consists of a number of small local buckles. At first there will be an initial peak load, and then

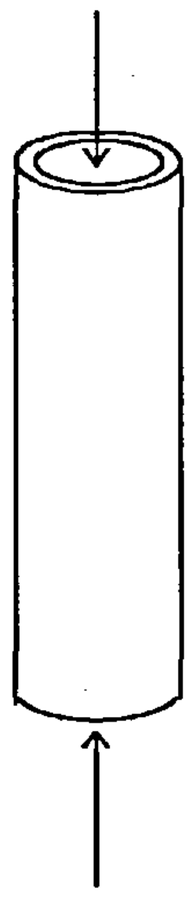

Fig 2-2: Axially compressive thin walled tube as energy absorbing device

there is successive buckling causing a load which fluctuates about a mean value.
This mean static crumpling load for a tube of thickness t, diameter D and yield stress Y is given approximately[35] by

$$P = 6Yt\sqrt{Dt} \qquad (2.1)$$

If the length of a tube is more than a few diameters, it fails by overall bending rather than by crumpling and consequently absorbs much less energy.
If the dimensions of tubes made from brittle fibre reinforced composite material are chosen properly then they crush progressively to powder from one end, if this end is tapered suitably to help initiate of the crushing process. The load deflection curve is much flatter than for metal tubes and the specific energy can be much higher because of the low weight of the material[21].

2-1-3 Laterally compressed metal tubes as impact energy absorbers-single tube system

Single or a system of laterally compressed rings can be used as energy absorbing devices. The behaviour of a single tube is more easily analysed theoretically than a tube system. De Runtz and Hodge[65] considered the large geometric changes of a rigid perfectly plastic deforming tube (fig 2-3).

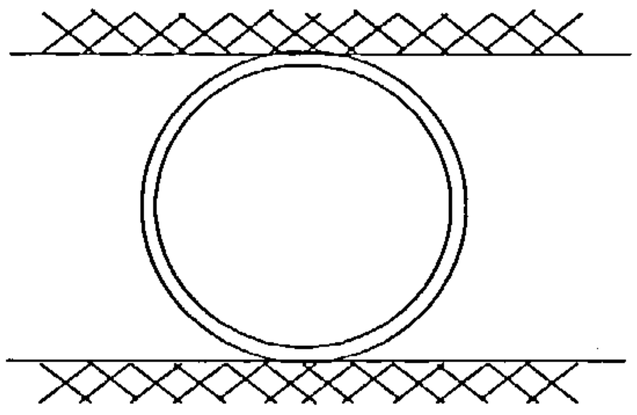

Fig 2-3: Laterally compressed metal tubes for absorption of energy

The mode of failure will be one of the following forms[58] which are shown in Figures 2-4(a) and (b).

a b

Fig 2-4: Collapse modes of laterally compressed tube

The failure mode (a) is common in tubes made from mild steel, due to the upper and lower yield point phenomena, hinges form and remain at cross sections where bending is initiated. Most other materials deform in mode form (b).

Whichever mechanism happens, the following equation[58] relates load p to the deflection δ :

$$p = \frac{p_0 L}{[1-(\delta / D)^2]^{1/2}} \qquad (2.2)$$

in which L and D are length and mean diameter of the tube respectively, P_0 is the initial collapse load per unit length of tube and is given by:

$$p_0 = 8M_0/D = 4M_0/R \qquad (2.3)$$

where M_0 is the plastic moment of hinges and given by:

$$M_0 = Yt^2/4 \qquad (2.4)$$

If σ_o is considered as a tensile yield stress then, $Y=2\sigma_o/3^{1/2}$ for a tube length not less than the diameter of the tube and $Y=\sigma_o$ for a tube length not greater than a few times the thickness. Formula (2.1) can be written as

$$p = \frac{2YtL}{D[1-(\delta/D)^2]^{1/2}} \qquad (2.5)$$

This equation gives an underestimated value for p, due to the strain hardening effect. Redwood[57] has given a modified equation:

$$p = \frac{p_0 L}{[1-(\delta/D)^2]^{1/2}}[1+\frac{E_p}{3Y\xi}\sinh^{-1}(\xi/D)] \qquad (2.6)$$

If a tube is compressed diametrically by two opposed concentrated loads, the load deflection curve could become more flat[59]. This is explained by the fact that in flat plate compression, the contact lines with the plate split and move outwards, as the deformation progresses, so reducing the moment arm of the applied force. This requires an increase in the applied load to maintain the deformation. This effect, in addition to strain hardening, causes a steep response. But in compressing by a two point load (in a ring), or two line load (in a tube), the moment arm increases and if a rigid perfectly plastic model is used, a falling load deflection curve will be achieved. The corresponding equation for p will be:

$$p = \frac{p_0 L}{[1+2(\delta/D)-(\delta/D)^2]^{1/2}} \qquad (2.7)$$

For a tube constrained in a grooved block, the tube collapse will occur in higher modes than the fundamental mode. In this case the collapse load per unit length will rise by a factor of approximately 2.4. For a tube in a V-block, the response will differ and can be calculated in terms of various ring parameters[56].

2-1-4 Laterally compressed metal tubes as impact energy absorbers- A layered system of tubes

In tube systems, although there is a similarity to single tube response, the effect of mutual constraints between adjacent tubes may produce modes of deformation and load-deflection characteristics significantly different from the fundamental flat plate mode. The prediction of yield load or energy absorbing capacity in a tube system takes on a statistical nature and usually the formulas have an experimentally defined form which cover the lower or higher bound of results[22].

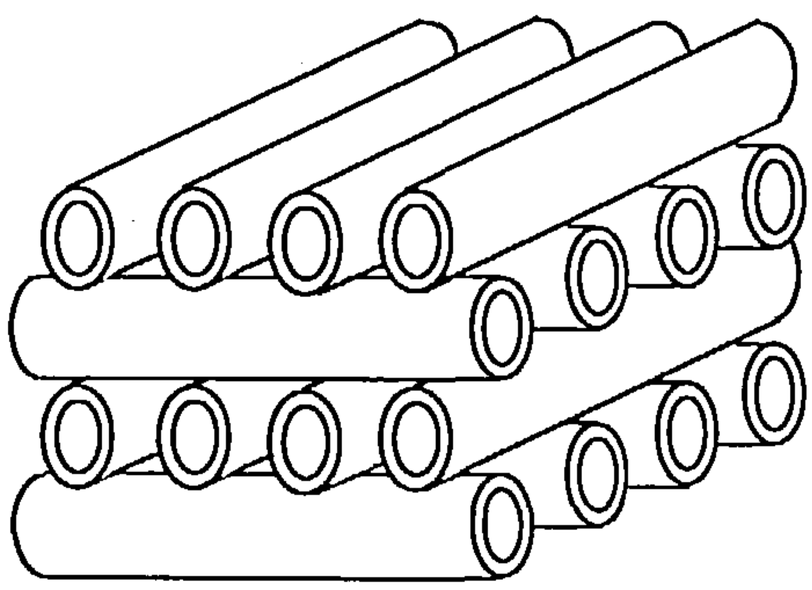

Fig 2-5: System of laterally compressed metal tubes for absorption of energy

The tube systems (fig 2-5) could be made in open crossed layer system or in a closed system. An open system is one that has sufficient initial lateral separation between adjacent tubes that there is no contact between them after deformation.

If the separation is of the order of the diameter of the tubes, each tube will have a deformation which is essentially the same as that of a single tube crushing between flat plates. This is despite the fact that each tube in the system is loaded only at discrete areas of contact with the adjacent layers tubes and not along all of the length.

If the separation is so large, then the mode of deformation is rather more complex and the tubes will have a variation in shape of the cross section along the length.

If a closed system is considered, in which adjacent tubes are in contact before deformation and the system is confined in a box, then the system's behaviour will be similar to that of the single laterally constrained tube. Such a system will absorb three times energy as absorbed by an open system.

The dynamic response of tubes and rings both as individual elements or as a system of tubes is more difficult to assess. The effects of strain rate and system inertia has been

considered by Reid[58] and it is shown that in some situations the inertia effect plays a secondary role in the deformation, so in these cases the global mode of deformation is very similar to the quasi static mode and, therefore, approximate methods can be used to include strain rate effects[59, 60].

2-1-5 Energy Absorbing Device with Cylindrical Systems

N.G. Shrive , K.R.F. Andrews and G. L. England[73] tested another kind of tube system for energy absorbing purposes. They compressed a system of tubes diametrically. In this system, intermediate layers of tubes between the inner and outer tubes was considered (Fig 2-6). Sherive *at al* tested the system in different conditions of intermediate tube fixidity and length. It was found that in an intermediate layer with a tack weld to both inner and outer rings, the energy absorption capacity will be increased with little effort and with virtually no increase in weight.

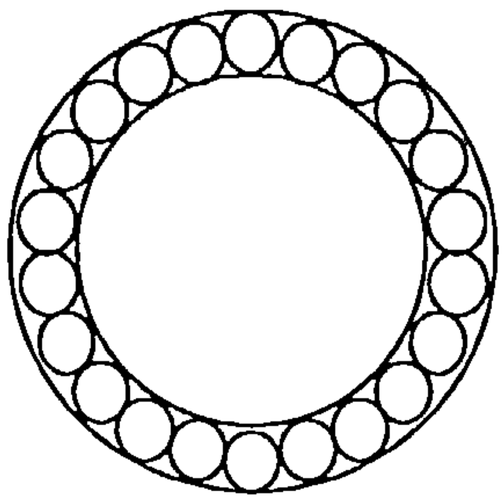

Fig 2-6: Cylindrical System for absorption of energy

It was also shown that the impact loading produces quasi static behaviour.

2-1-6 Tubular Ring as an Energy absorber

Reid, Austin and Smith[60] introduced tubular rings as energy absorbing devices. These were built by welding together four lengths of metal tubing with mitred joints (Fig 2-7).

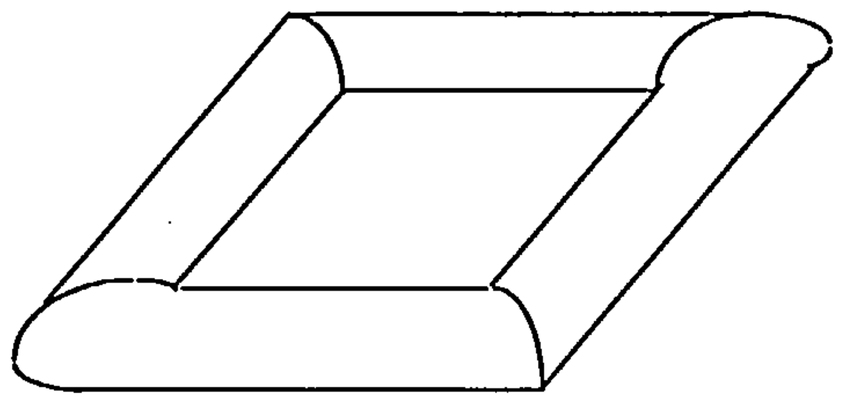

Fig 2-7: Tubular ring as energy absorbing device

Laterally compressed tubes have less capacity than axially compressed tubes and are not sensitive to impact parameters (like direction of impact). Therefore, the energy absorbing capacity of a laterally compressed tube is enhanced by welding the tubes together. The load deflection curve of a series of single tubular rings under static loads were obtained and compared with a free tube with the same length by Reid *et al.* These results show that the tubular ring configuration provides a significantly more efficient means of energy absorbing than a free tube of equal length. The collapse load per unit length is increased by a factor of approximately 3 to 6 and the energy absorption per unit length by a factor of approximately 4.5 to 9, both with respect to a free tube.

In a dynamic test, the collapse load is almost twice the corresponding quasi static load. The collapse load is related to the influence of strain rate sensitivity of its material properties. With regard to a six layer system it should be noted that the load pulse is virtually rectangular. This is a consequence of both strain rate effects and possibly inertia effects.

2-1-7 Stiffened Metallic Tubes as Energy absorbing Device

An attempt has been made by J.F. Carney and Veillette[9] for developing a new type of energy absorbing device by stiffening metal tubes. They stiffened cylindrical tubes with tensile members, the component that has minimal compressive strength, and put them under lateral quasi static and impact loading.

A high tensile strength steel wire was used to provide tension bracing (fig 2-8). These stiffeners can affect dramatically a tube load deflection behaviour and result in stiffness properties which are directionally sensitive.

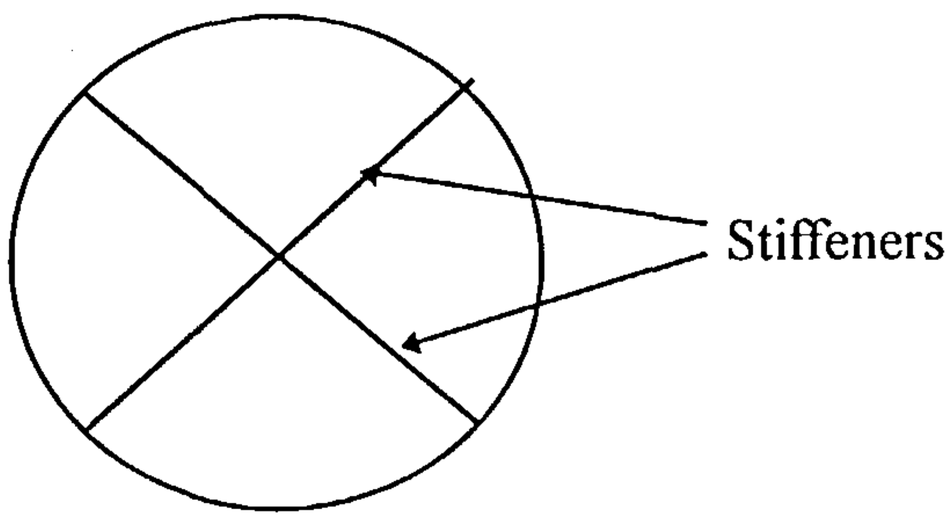

Fig 2-8 : Stiffened metallic tubes

Tests were undertaken in two different support conditions. In the first case, the tube was tested without any external constraint and in the second, the centre of tube was forced to move in vertical direction in a special rig. For the first case, the collapse is asymmetric with respect to the loading axis of tube. In the second case, the collapse tubular configuration was symmetrical with respect to the vertical diametrical axis of the tube.

From quasi static tests it was concluded that in order to maximise the energy dissipation over large deformations (δ /D=0.7) , θ the angle of bracing should be in the region of $0° \leq \theta \leq 10°$. If $\theta \geq 45°$, the bracing has no effect upon the load deflection shapes. For $\theta \leq 25°$, the load deflection curve has three regions. These involve a pre-collapse stiff linear portion, followed by a less stiff but stable region in which the load continues to increase with deflection, which is followed by an unstable region in which the applied load decreases with additional deformation. With increasing θ, the second region is reduced and for $\theta > 30^o$, it completely disappears. The result obtained by Carney for the constrained mode were within a few percent of an unconstrained mode with only a change of different collapse mode.

For impact, Carney *et al* only investigated the behaviour of unconstrained tubes. As would be expected, the initial impact velocity is arrested most rapidly in the lower bracing angle cases. Conversely for a given impact velocity, the maximum tube deflection increase significantly as θ increases beyond 30°. The family of tests corresponds to an impact velocity range from 12.42 m/sec, to 18.32 m/sec and an increase in energy dissipation of from 1.5 to over 2.5 times the quasi static levels was achieved under impact loading condition.

2-1-8 Energy Dissipation by splitting and curling tubes.

W.J. Stronge, Tx Yu and W Johnson[76] tested a system that eliminates transmitted impact forces by the fracture and plastic deformation of tubes. In this system (fig 2-9), metal tubes are split axially and deformed plastically by the passage of a mandrel through the tube. It has been found that tube splitting and curling is more efficient than axial buckling or tube inversion and it has a better stroke - to - length ratio than any alternative deformation mechanism.

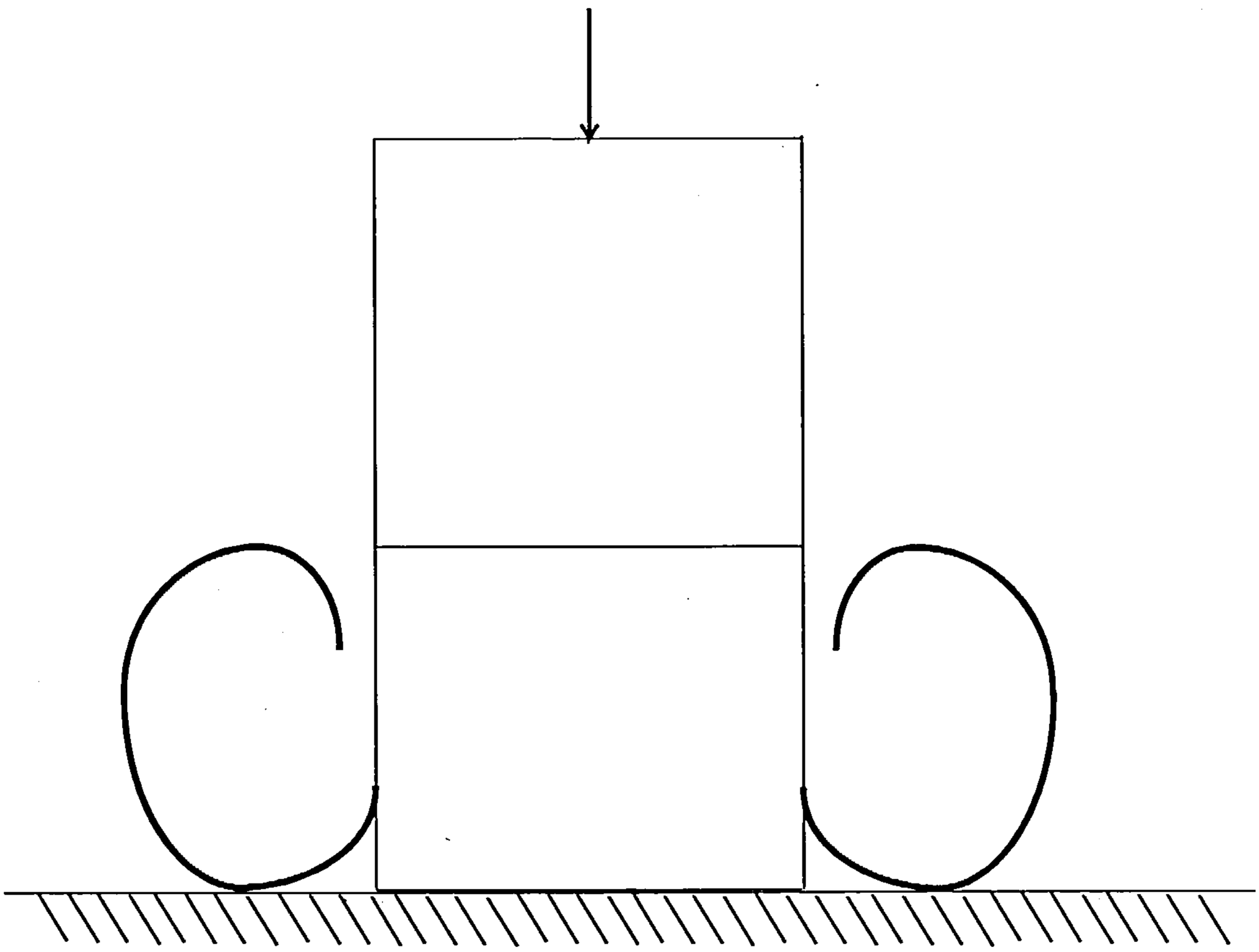

Fig 2-9 : Energy Dissipation by splitting and curling tubes.

In the quasi-static experiments of Stronge *et al* , thin walled square cross section tubes were split and curled by being passed axially against a die as shown in Fig. 2-9. Two sets of tubes have been tested, a set of aluminium alloy HE30 tubes and a set of mild steel tubes. In these tests, the axis of the die was parallel to the axis of the tube and it contained four identical cylindrical surfaces of 8, 12 or 16 mm radius that controlled the initial radius of the curl.

During pressing, the tube is split at the four corners by spreading die surface and the sides curl outward to form four rolls. The fracture occurs continuously in steel and the fracture surface appears smooth. In the aluminium alloy, the fracture surface is jagged. Due to strain hardening, the force gradually increases as pressing proceeds in the aluminium alloy. Two sets of mild steel tubes were tested to study fracture energy. One set had corners shaved on the outside to half thickness whilst the other set without any change in the thickness of corners. The tubes with full corners require a steady press force that is 50% larger than the shaved corner tubes. The fracture energy (the energy which is absorbed during the fracture of a material) is clearly a significant component of the total energy dissipated in splitting and curling mild steel tubes. There are three primary sources of energy dissipation during splitting and curling and these are: work done in plastic deformation, fracture propagation and friction. The rate of work done by external press force P is $W_e^o = PV$ and this is equal to the rate of energy dissipation.

$$W_e^o = W_p^o + W_f^o + W_F^o \qquad (2.8)$$

From this equation the following equation can be obtained[76]:

$$P = 4\{(M_o / R_o)[\gamma + \alpha_c t(\gamma^2 - 1)/2R_o] + G_c t\}/(1-\mu) \qquad (2.9)$$

Where γ is the rate of initial to final radius of curvature for the curl and is equal to

$$\gamma = R_o / R_f = (1 - 2\beta x / R_o)^{-1/2} \qquad (2.10)$$

in which x is the length of tube in the curl, μ is coefficient of friction and R_0 is the radius of the curl.

In these tubes, the fracture energy required to split the tube and the plastic work performed in curling are comparable for aluminium. The plastic work is between one and three times the fracture energy. For steel, the converse is true, fracture energy is two or three times the plastic work in tubes for the dimensions tested. These results are consistent with the reduction in pressing force that occurred when the corner thickness of mild steel tubes was decreased.

In the Stronge et al experiments, tubes were split and curled by impact with a 38 kg mass falling freely at 6.3 m/s. The average force during the impact pulse was calculated by dividing the kinetic energy of the impacting mass by the deformation of tube, ΔL. The average dynamic force is always larger than the quasi static deformation force for the same tubes. For aluminium this increase is 15% to 40% of the quasi static force.

For mild steel tube, the dynamic force for deformation is a factor of 2.5-3.0 larger than the quasi static force.

2-1-9 Tube Inversion

Ductile material tubes may be inverted by suitably formed dies for absorbing energy of impact. They may be inverted inside or outside. Fig(2-10) shows some different kinds device. The load deflection characteristic of these devices are rectangular but in comparison to the other devices, they have a low yield limit.

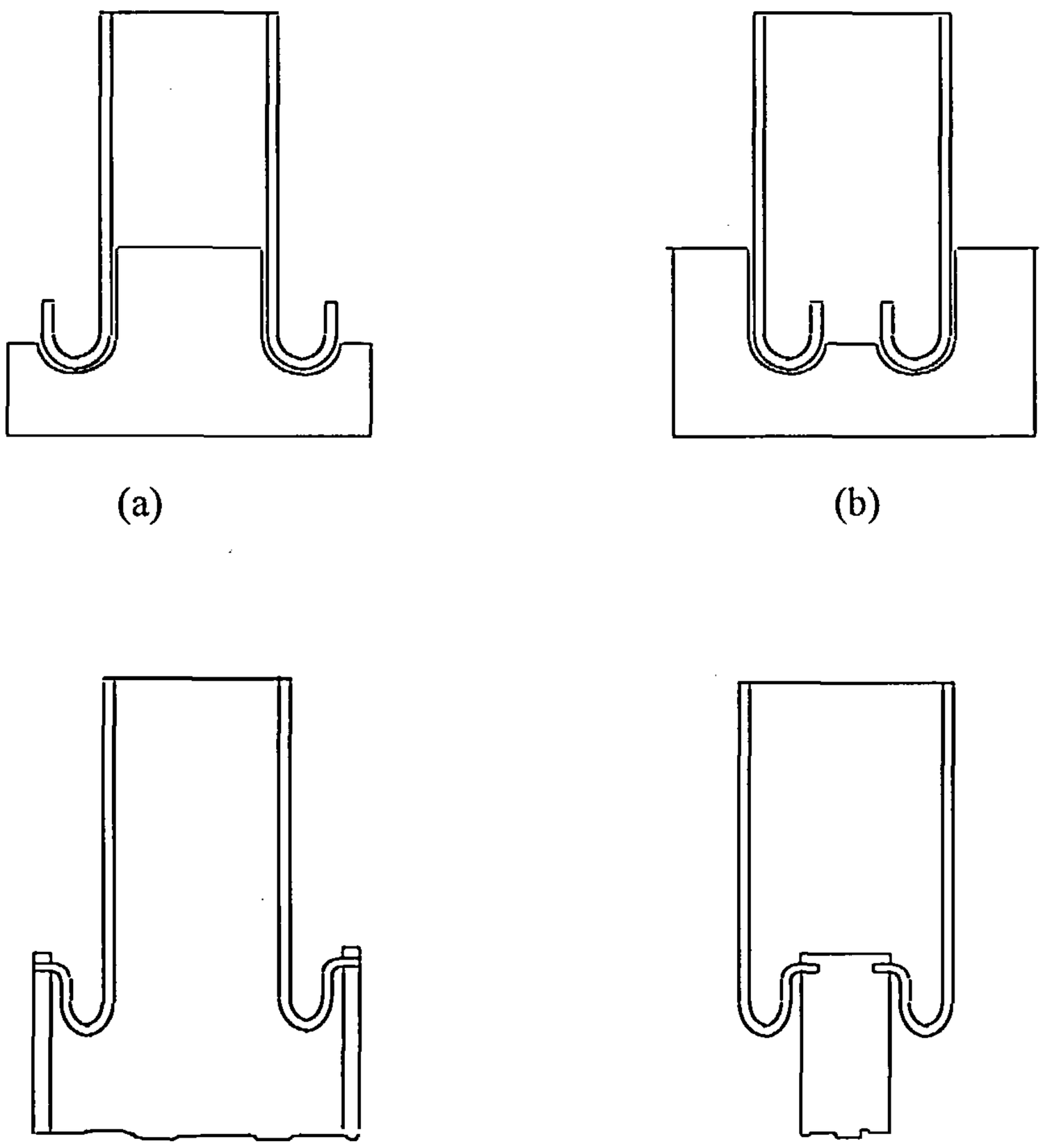

Fig 2-10 : Energy Dissipation by inversion of tubes.

Inversion tubes have been considered in relation to the design of force attenuating collapsible steering wheels, for facilitating lunar and planetary soft landing of spacecraft, for cushioning air drop cargo, as over load protectors for railway rolling stock, as a safety factors for elevators, as buffer elements for nuclear reactor control

rods and as yieldable air craft seat anchors. The rectangular force displacement characteristic ensures substantially uniform retardation.

An approximate analytical expression for the steady compressive load necessary to maintain an inside-out inversion is easily arrived at by assuming that the tube material is perfectly plastic, that no tube length or thickness changes occur during bending, that energy dissipation consists solely in (i) bending and unbending the tube and (ii) in increasing its radius, any interaction between bending and other imposed stress is neglected and buckling or instability is not envisaged. With these assumption the yield load of the device will be[23]:

$$P = \pi_o . t_o Y(8D.t_o)^{1/2} \qquad (2.11)$$

In which Y, D and t_0 are the yield limit, diameter and thickness of the tube respectively. If the system shown in Fig. 2-10c or 2-10d is considered, then the compressive force is just P/2. Experiments shows that this equation gives an underestimated result by 25% of the experimental result. Tubes with low strain hardening rates buckle rather than invert. It may be shown from ref. 45 that the axisymmetric buckling load P_z for a tube whose reduced modulus is E_k is approximately $P_B = 4\pi t_o^2 E_k / 3$. Thus, inversion would occur only if $P<P_B$ or $E_k/Y>3(D/2t_0)^{1/2}$.

2-1-10 Zigzag Structures

In energy absorbers which utilise plastic bending there is usually a mechanism which converts other types of loading into bending. A simple device is the W frame, shown in figure (2-11).

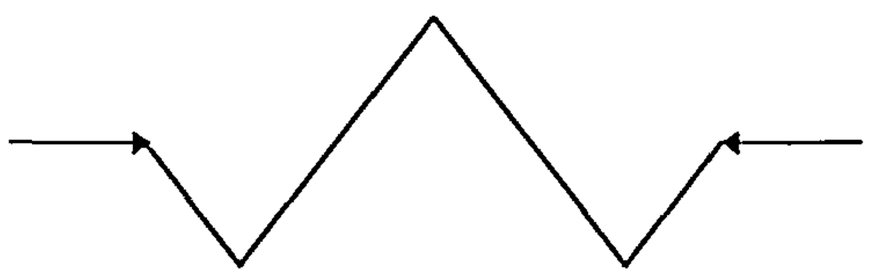

Fig 2-11 : Zigzag structures for absorbing the energy

When compressed from the ends this device has the load-deflection characteristic shown in fig. 2-12[35] .

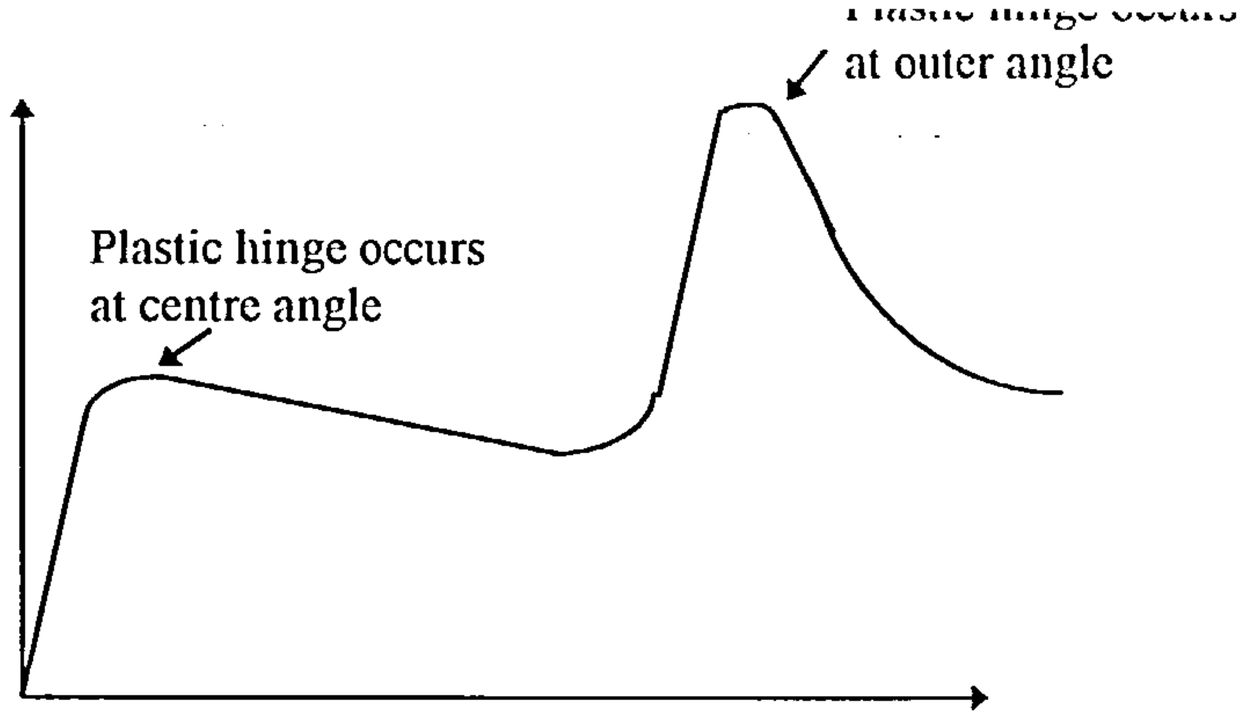

Fig 2-12 : Load deflection curve of zigzag structures

There appear to be major problems with obtaining adequate joints at the angles of the W. These can be overcome to some extent by having an S frame, where sharp changes in angle at joints do not occur.

2-1-11 U shape devices

The mechanism of energy absorption in the U shaped strips is very simple. The strip is initially in a semicircular form with two equal straight sections on either. When one side is moved relative to the other, the semicircular portion rolls along the strip and work is done at the two points when the radius of curvature is changed from straight to the radius of the semicircle and then from this radius to straight again which is a reverse movement. Thus at any instant, the energy dissipation is concentrated at two transverse surfaces but these two surfaces move along the strip[1].

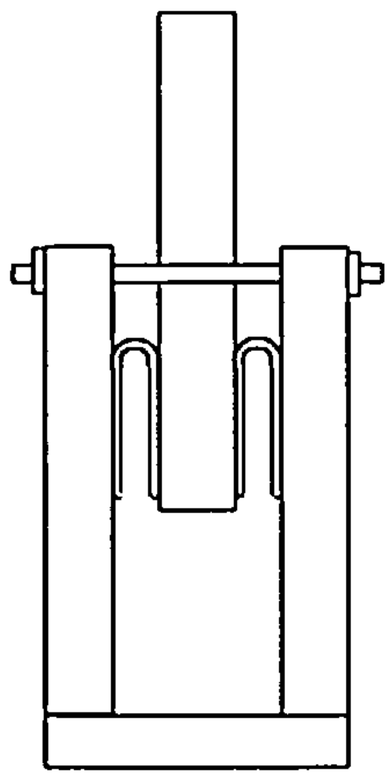

Fig 2-13 : U element for absorption of the energy

The maintenance of the semicircular shape can be enhanced by including a roller held in position in such a way that it can move with the semicircular portion but this is not essential for the energy absorbing dissipation process.

Load deflection relationship of this device is calculated by equation 2-12:

$$P=Ybt^2/4R \qquad (2.12)$$

in which Y is the yield stress of the strip, b is its width and t is its thickness[1]. R is the mean radius of the semicircular.

2-1-12 Torsional Energy dissipaters

Members which work in torsion could absorb more energy than members working in flexure. Most of time bending and torsion work together for the absorption of energy[25]. A simple form of this device is shown in Figure 2-14.

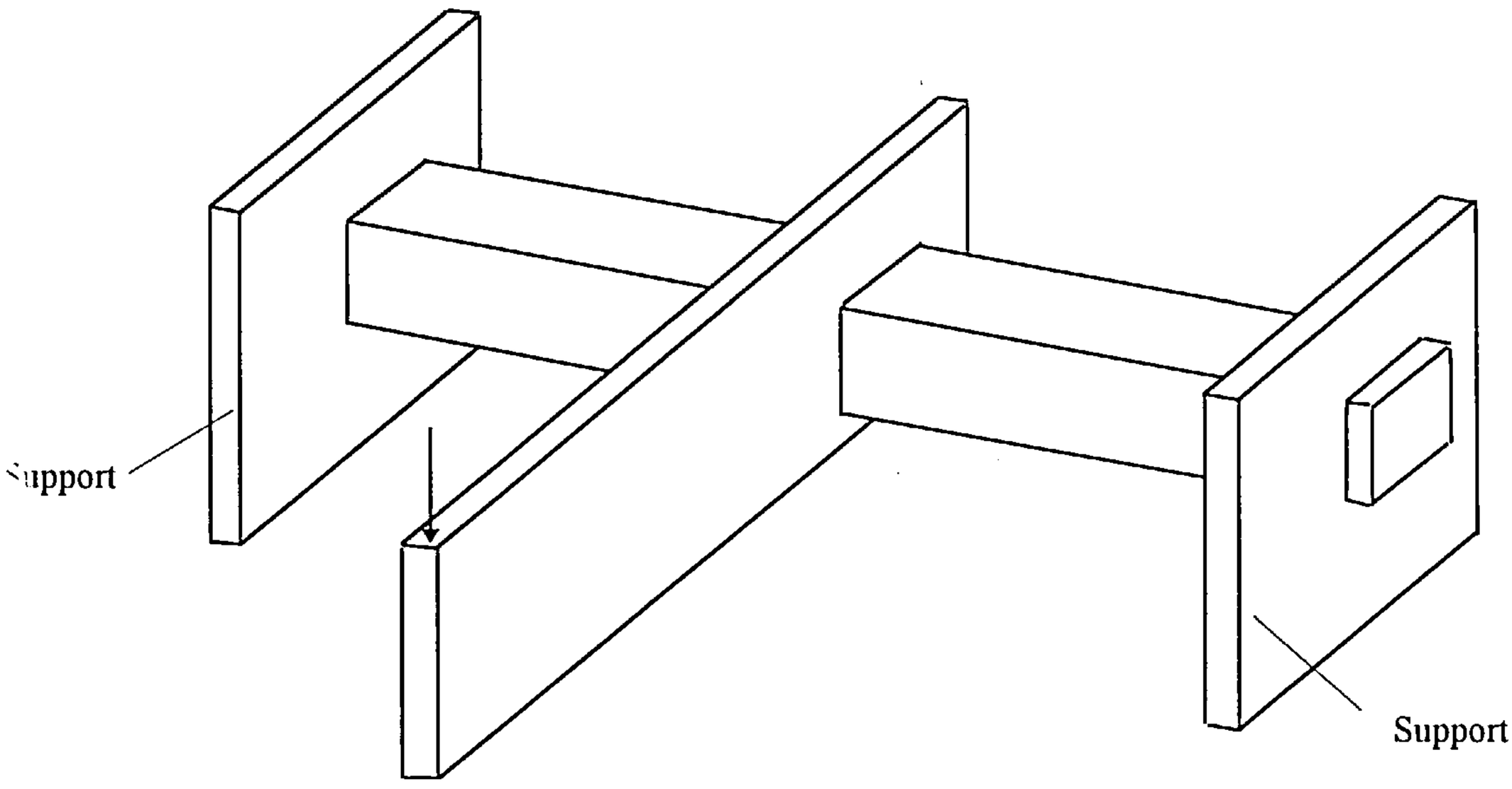

Fig 2-14 : Torsional bending device for absorption of energy

2-1-11 Efficiency of Energy Absorbing Devices:

The efficiency of an energy absorber can be specified in a number of ways. Two widely used definitions are specific energy, which is the energy absorbed per unit weight and the volumetric efficiency, which is percentages of the total volume of the absorber which is employed usefully for the absorption of energy[35]. The later is often simplified to stroke efficiency, which is the length of stroke divided by the total length of the absorber. It is also possible to measure efficiency in terms of an ideal energy absorber. The characteristic of this vary with the dynamics of the system, but as a general comparator, an ideal absorber is usually taken to be one which instantaneously reaches the maximum allowable retarding force and retains this force throughout the stroke, giving a rectangular force time pulse.

Often, it is possible to incorporate energy absorbing properties into a component which has another function and in this case efficiency becomes less important. A common example is a structural member which is designed to collapse in a controlled manner, absorbing a significant amount of energy. This can be less than optimum as a structural member and relatively inefficient as an energy absorber, but it may be the best overall compromise.

So far the most popular forms of passive energy absorbing devices, which are frequently used in the practice, have been reviewed in the last section. In the next section, the implementation of energy absorbing devices in structures for reducing shock effects is investigated.

2-2 Structures and Energy Absorbing Devices

Energy absorbing devices may be used in structures for different reasons. Depending on the condition of the impact, which is applied to a structure, the type of energy absorbing device is chosen. In marine structures impact shocks may be induced by explosion, collision, slamming of sea waves or falling objects.

When an impact force is frequently applied to a structure, the economic solution is to design an energy absorbing devices which work in the elastic range. Devices which apply energy absorbing phenomenon like the use of viscous liquid or generating friction between solid parts are suitable for these cases[26]. The damping coefficient does not degrade in these energy absorbing devices, but usually they cost more than

other passive devices. Besides, they usually have large volume and need to be regularly inspected and checked.

The energy absorbing devices which have been reviewed in the previous section, use the plastic deformation of solid parts for absorbing the energy. Such devices have more efficiency than the elastic range working devices, but they have problems of degradation of strength with the process of energy dissipation and the reduction of damping coefficient.

Energy absorbing devices have only been introduced recently for the protection of structures against earthquake effects, however such devices have not found their place among the most popular methods for creating earthquake resistant buildings[43].

In the next section a review of some of the most common passive energy absorbing techniques, which have been used so far for the seismic effects, will be given. As well as classifying them, some technical detail for each one will be presented.

2-3 Energy absorbing methods for seismic resistant buildings

Energy absorbing devices can be classified into two categories of seismic resistant buildings, and these are: isolated and none isolated buildings.

The isolation may be arranged to occur at the base of a building, in which case it is called base isolation, or in some other part of the building. Creating a soft story is an alternative method of isolation in which the building is kept away from the base excitation. In what follows, a review of existing methods for each case will be given.

2-3-1 Base Isolation method

Isolation is providing a discontinuity between two bodies which basically are in contact. Therefore no motion in the direction of the discontinuity, can be fully transmitted. The discontinuity consists of a layer between the bodies which has low resistance to shear compared with the bodies themselves. Such discontinuities may be used for isolation from horizontal seismic motions of whole structures, parts of structures, or items of equipment mounted on structures. Because they are generally located at or near the base of the item concerned, such systems are commonly referred to as base isolation[12].

There are various forms of layer providing the discontinuity, ranging from infinitely thin sliding surfaces (e.g. PTFE bearings), through rubber bearings a few centimetres

thick, to flexible or lifting structural members of any height. In order to provide the required rigidity under serviceability loads, such as wind or minor earthquakes, to control the seismic deformations which occur at the discontinuity, and to provide a reasonable minimum level of damping to the structure as a whole, the discontinuity must be associated with energy-dissipating devices. It is apparent that seismic isolation is only appropriate for horizontal motions.

Obviously, the location of the isolating devices should be at the lowest possible position of the structure to protect most of the structure. However, cost and practical considerations influence the choice of location. On bridges it may be convenient to isolate only the deck, because isolation from thermal movements is required there anyway. In buildings, the choice may lie between isolating at ground level, or below the basement, or at some point up a column. Each of these locations has its advantages and disadvantages relating to accessibility and to the very important design consideration of dealing with the effects of the shear displacements on building services, partitions, and cladding.

In the following, the usual base isolation methods are explained.

Base isolation using lead-rubber bearings

The lead-rubber bearing is conceptually and practically an attractive device for base isolation, as it combines the required design features of flexibility and deflection control into a single component[12].

The bearing figure 2-15, is similar to the laminated steel and rubber bearings used for compensating temperature effects on bridges, but with the addition of a lead plug energy dissipater.

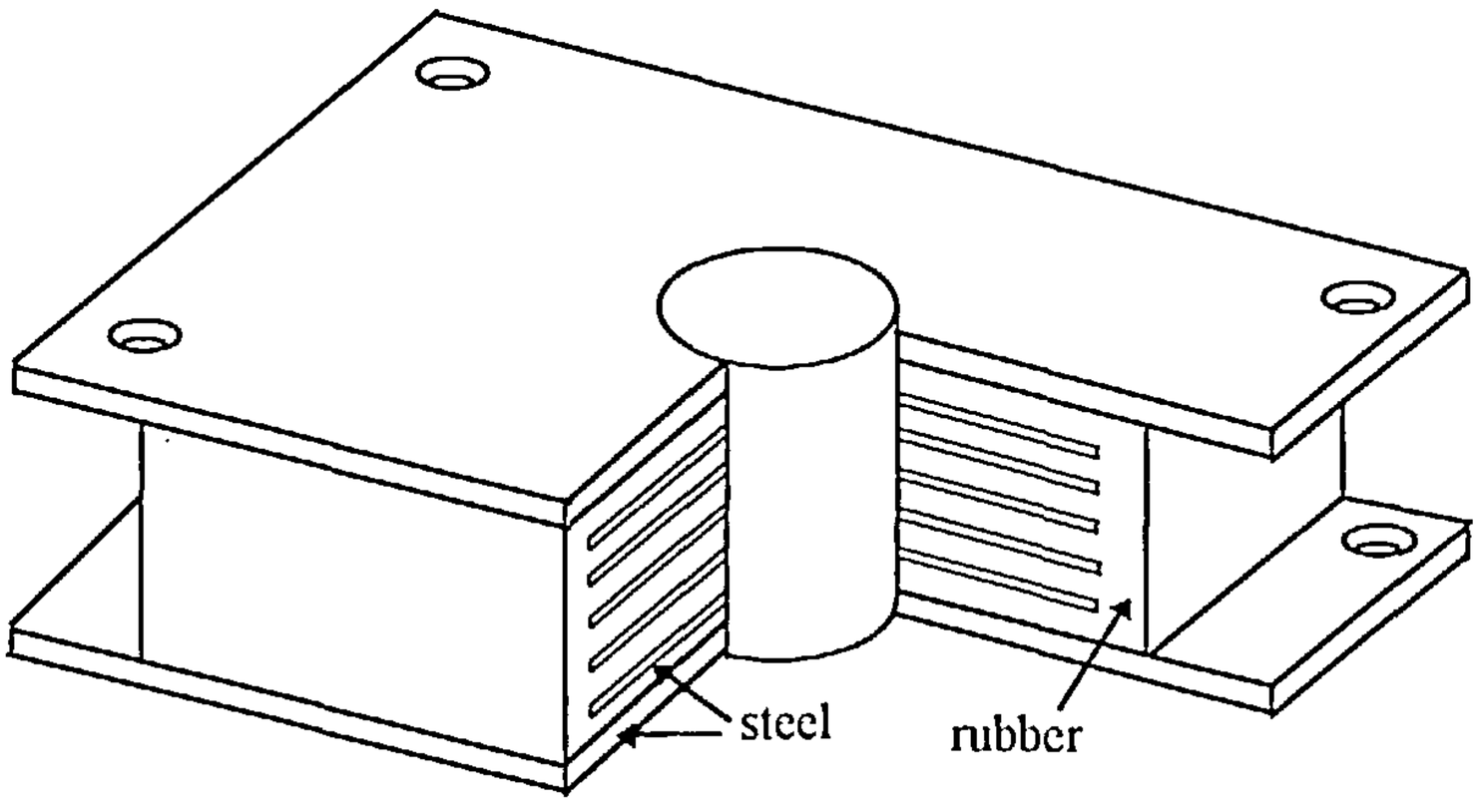

Fig 2-15 : Lead - Rubber bearing

Under cyclic shear loading the lead plug causes the bearing to have high hysteretic damping behaviour, of almost pure bilinear form. The high initial stiffness is likely to satisfy the deflection criteria for serviceability limit state loading, while the low post-elastic stiffness gives the potential for a large increase in period of vibration desired for the ultimate limit state design earthquake.

The first building to be built using lead-rubber bearings for seismic isolation was the William Clayton Building in Wellington, New Zealand[39], designed 1978 and it had a four-storey ductile moment-resisting frame. The inter-storey drifts calculated for the isolated building were about 10 mm and were uniform over the building's height. For comparison, the maximum drift for the non-isolated model was 52 mm per storey for the top two storeys.

Lead-rubber bearings have also been used in a rapidly growing number of 2 bridges in New Zealand (over 30 in 1985) and the USA. These bearings have a wide range of applications where they are likely to lead not only to less damaged structures in earthquakes but also to cheaper construction.

Curved plate as absorber of base isolated structures

A curved plate energy absorber was suggested by S. F. Stiemer and F.L.Chow[75] for earthquake resistance structures. The proposed devices would be used in parallel with isolating systems in building or other structures. The plates are designed to deform elastically under minor loads such as wind and to deform plastically when subjected to major earthquake loading.

For one directional application, X shape was chosen fig (2-16). To avoid stress concentrations at the clamped boundaries or in the middle of plate, rounded transitions were chosen. When this flat plate of mild steel was loaded in the weak direction, the fixed bending stresses at the apex of the tapers became uniform along the length, thus allowing yielding to develop over the full length of both tapered sections.

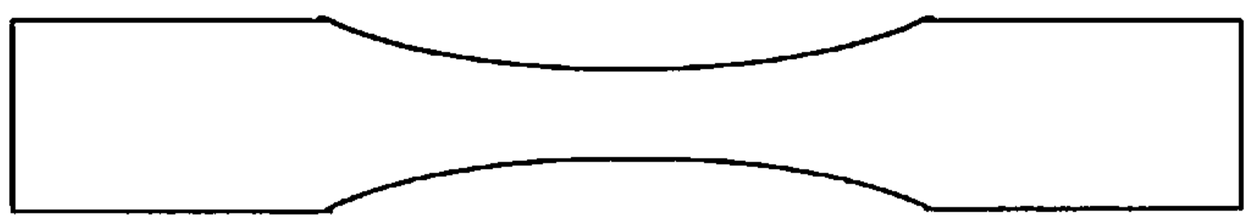

Fig 2-16: X form plate as absorber of isolated base

The second type of energy absorbing device, consists of two curved plates in pairs like rings with planes perpendicular to each other (fig 2-17). This arrangement enables energy absorption in any horizontal direction and even in the vertical direction.
The main goal of Stiemer *et al* was to design an element, which shows a stable behaviour, that is, after having experimental elastic and plastic deformation and then being brought back to the initial position, the geometric shape of the device should not change. This type of energy absorber was aimed at an application in base isolated structures where bearing pads like roller bearings undergo lateral parallel displacement or rubber pads in which even three dimensional displacements have to be accommodated. These energy absorbers (fig 2-17) could be put from the opposite directions as well.

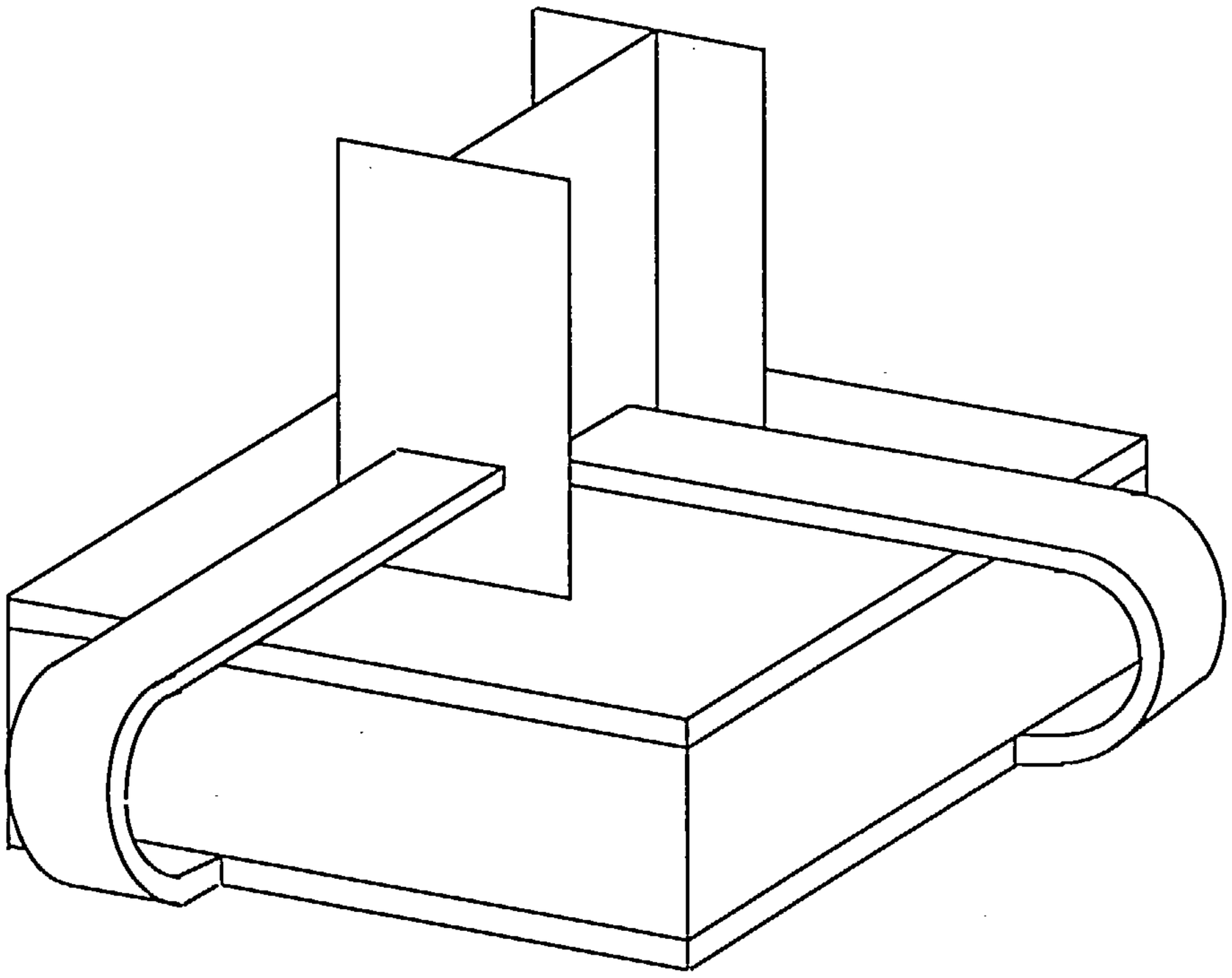

Fig 2-17: Curved plate as absorber of isolated base

Isolation using flexible piles and energy dissipaters

An alternative to the use of lead-rubber bearings is the isolation system used for Union House[7], a 12-storey office block in Auckland, New Zealand, completed in 1983. As the building required end-bearing piles about 10 m long, the designers took the opportunity of making the piles flexible and separating them from lateral contact with the soft soil layer overlying bedrock by surrounding them with a hollow sleeve, thus creating the flexibility required for base isolation. Deflection control was imposed by X shaped steel energy dissipaters located at the ground level. The structure was built of reinforced concrete except that the superstructure was diagonally braced with steel tubes. Lateral flexibility of the piles was attained by creating hinges of low moment resistance at the top and bottom of each pile.

The earthquake analysis was carried out using non-linear dynamic analysis.

Under the design earthquake loading the horizontal deflection of the first floor relative to the ground (i.e. at the dissipaters) was calculated to be $\pm$60 mm.

The response of the building was also checked under a 'maximum credible earthquake' to ensure that adequate clearance was provided at the energy dissipaters, and that no significant yielding would occur in the superstructure.

In this survivability state the horizontal deflection at the dissipaters was $\pm$130 mm and a provision for $\pm$150 mm was made.

Cost and time comparisons of the isolated and none-isolated equivalent structure estimated a capital cost saving of $300 000 and a construction time saving of 3 months, representing $150 000. Together these equal a substantial saving of nearly 7 percent in the total construction cost of $NZ 6.6 million.

Isolation using uplift

As well as the methods described in the preceding sections, the flexibility required to reduce seismic response in isolation systems may be obtained by allowing a part of the structure to lift during large horizontal motions. This mechanism is referred to variously as uplift, rocking, or stepping, and involves a discontinuity of contact between part of the foundations and the soil beneath, or between a vertical member and its base[12].

The response of structures experiencing uplift has been a subject of increasing

interest in recent years and a variety of systems have been studied, generally showing a considerable reduction in structural responses compared with non-uplift alternatives. Some of the systems studied have not incorporated energy dissipaters relying solely on uplifting columns or rocking of the raft or local pad foundations to produce the desired effects. However, despite apparently favourable results such structures have not yet been enthusiastically adopted in practice. This is probably due to continuing design uncertainties regarding factors such as soil behaviour under rocking foundations in the design earthquake, the possible overturning of slender structures in survivability events, or possible impact effects when the separated interfaces slam together. However, with the addition of energy absorbers the above hazards are lessened, and utilisation of the advantageous flexibility of uplift has been put to practical effect in completed constructions.

The first such structure to be built was the South Rangitikei Railway Bridge in New Zealand[6], the design of which was carried out 1971. The bridge deck is 320 m long, comprising six prestressed concrete spans, about half of which is at a height of 70 m above the riverbed. The piers consist of hollow reinforced concrete twin shafts 10.7 m apart coupled together with cross beams at three levels, so that they act as a kind of portal frame lateral to the line of the bridge. At their base, these shafts are seated on an elastomeric bearing and lateral rocking of the portals is possible under the control of a steel torsion-beam energy dissipater of the type shown in Figure 2-13. As with the other forms of base isolation, substantial reductions in earthquake stresses are possible, as described for an early investigation of this bridge by Beck and Skinner[6] the final configuration differing in detail, but not in principle.

Despite recent advances in base isolation research, the wide spread application of this technology is still impeded by over conservative attitudes. For example, in the United states of America, the number of bureaucratic mandates (i.e. feasibility studies, peer reviews, plant and site inspectors) that an engineer must satisfy in order to isolate a structure, make it remarkable that anyone undertakes a base isolated project. Unless bearings become a catalogue commodity with certified characteristic and allied to reasonably simple design and analysis procedures that promote the benefit of base isolation, this technology will remain difficult to implement and restricted to a few

projects a year. More importantly, while base isolation provisions are now in the UBC (Uniform Building Code), the requirements are so conservative that the potential advantages of using base isolation (reduced design requirements in the superstructure) are lost[43].

2-3-2 First soft storey method

The essential characteristic of a soft first story method consists of a discontinuity of strength and stiffness which occurs at the second floor column connection. This discontinuity is caused because lesser strength or increased flexibility, in the first floor vertical structure results in a concentration of forces at the second floor connections. This is a great disadvantage for this type of building, but if it is done in a controlled way, it can produce savings in the cost of superstructure and a great reduction in non-structural damage[3]. In this case most of the displacements will appear in this soft floor and upper stories will not be highly effected. Apparently, the induced vibrations in this soft story should be damped by using proper energy absorbing devices and only the damping quality of the structure is insufficient for achieving this purpose. In the following, the absorbing system of a building which has been made with first soft story will be reported. In the next chapter, a new energy absorbing device with a high capability to be used as an absorber for a first soft story will be introduced.

First soft floor with Teflon Sliders:

Figure 2-18a Shows the structure of Tianjing City hospital in China[40]. Mo L. Y. and Chang Y. F. proposed an alternative frame with first soft floor, as is shown in Figure 2-18b. In the framing, Teflon sliders are placed on the top of the first story of reinforced concrete framed shear walls, as its energy absorbing system Figure 2-19. These shear walls are framed by columns and beams, and are designed to carry a portion of weight of the superstructure. The lateral load is determined by the frictional characteristics of the Teflon sliders. The remaining first storey columns are designed for ductile behaviour in order to accommodate large drifts. Although the proposed system appears to be promising, the absence of systematic tests of this proposed system precludes an experimental check of the calculated dynamic response.

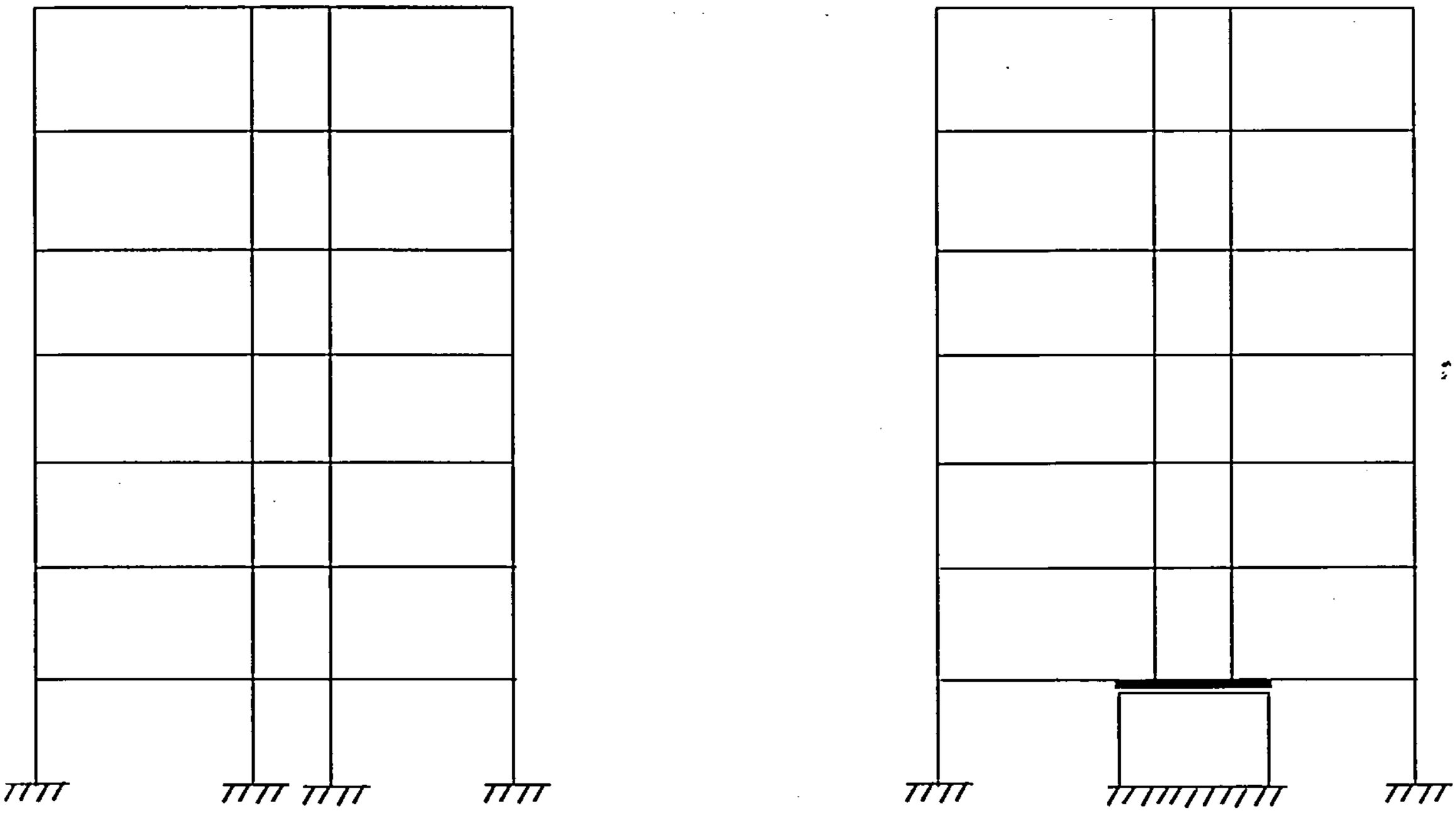

(a) (b)

Fig 2-18 : Elevation of Tianjing City Hospital, China: (a) the conventional design
(b) proposed first soft story system

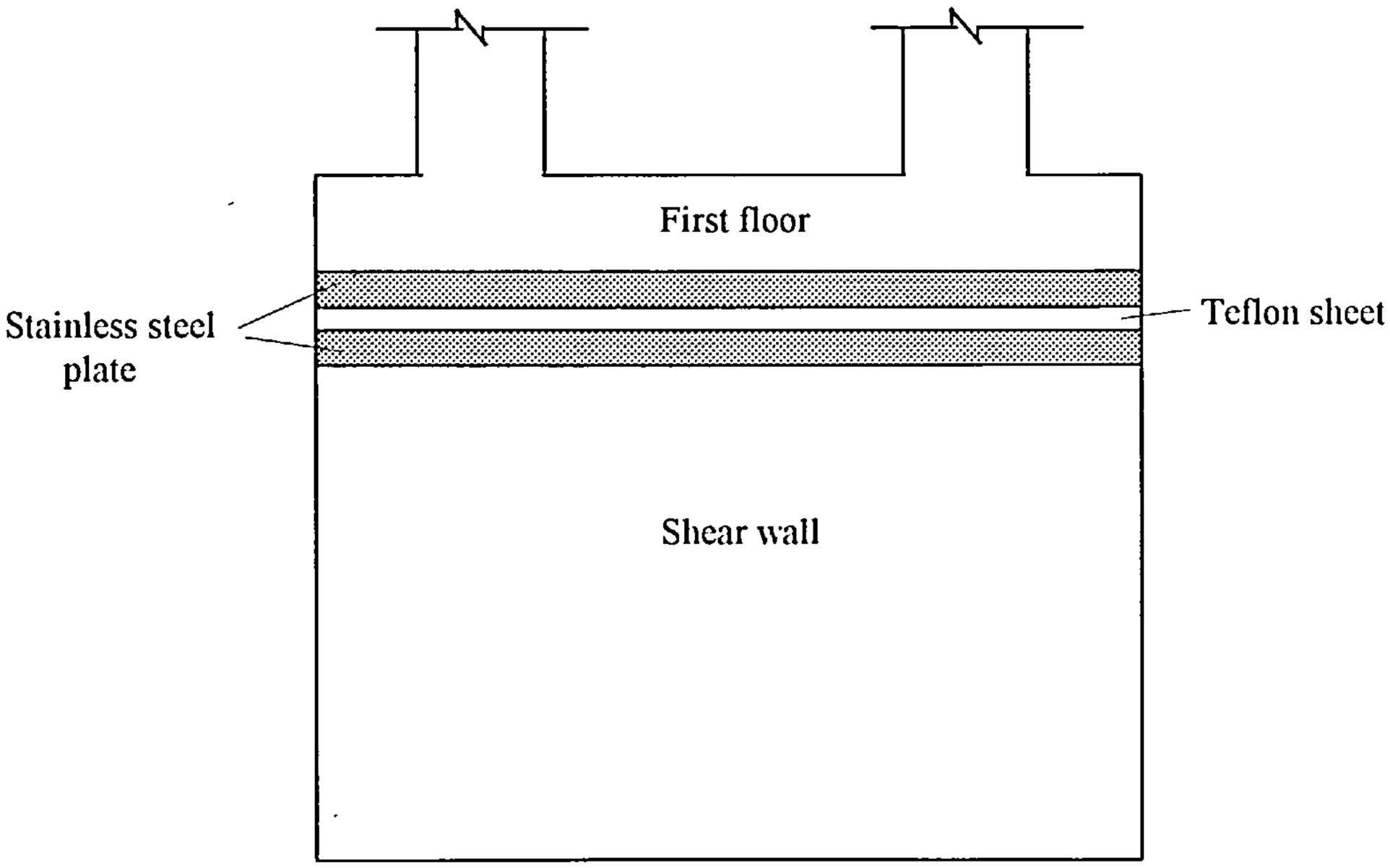

Fig 2-19 : First storey shear wall with Teflon Slider

2-4 Non-isolated structures

The structures which are not isolated from seismic shocks, either by base isolation or first soft storey, may be equipped with energy absorbing devices which are located in the most suitable positions for absorption of energy. Various forms of energy dissipaters have been developed for such structures and in the following a discussion is given.

2-4-1 Slitted Reinforced Concrete Wall

The first kind of these energy absorbing parts was developed by Muto[42] in 1960 and has been used effectively in a number of tall buildings in Japan. The wall is a precast panel which fits between adjacent pairs of columns and beams in a moment resisting steel frame. The panel is divided by slits into some vertical beam elements which are supported by two horizontal beams at the top and bottom of panel, Figure 2-20. The wall is connected to the beam of the steel frame and effectively stiffens the building against wind loads while providing high energy absorption in larger earthquakes.

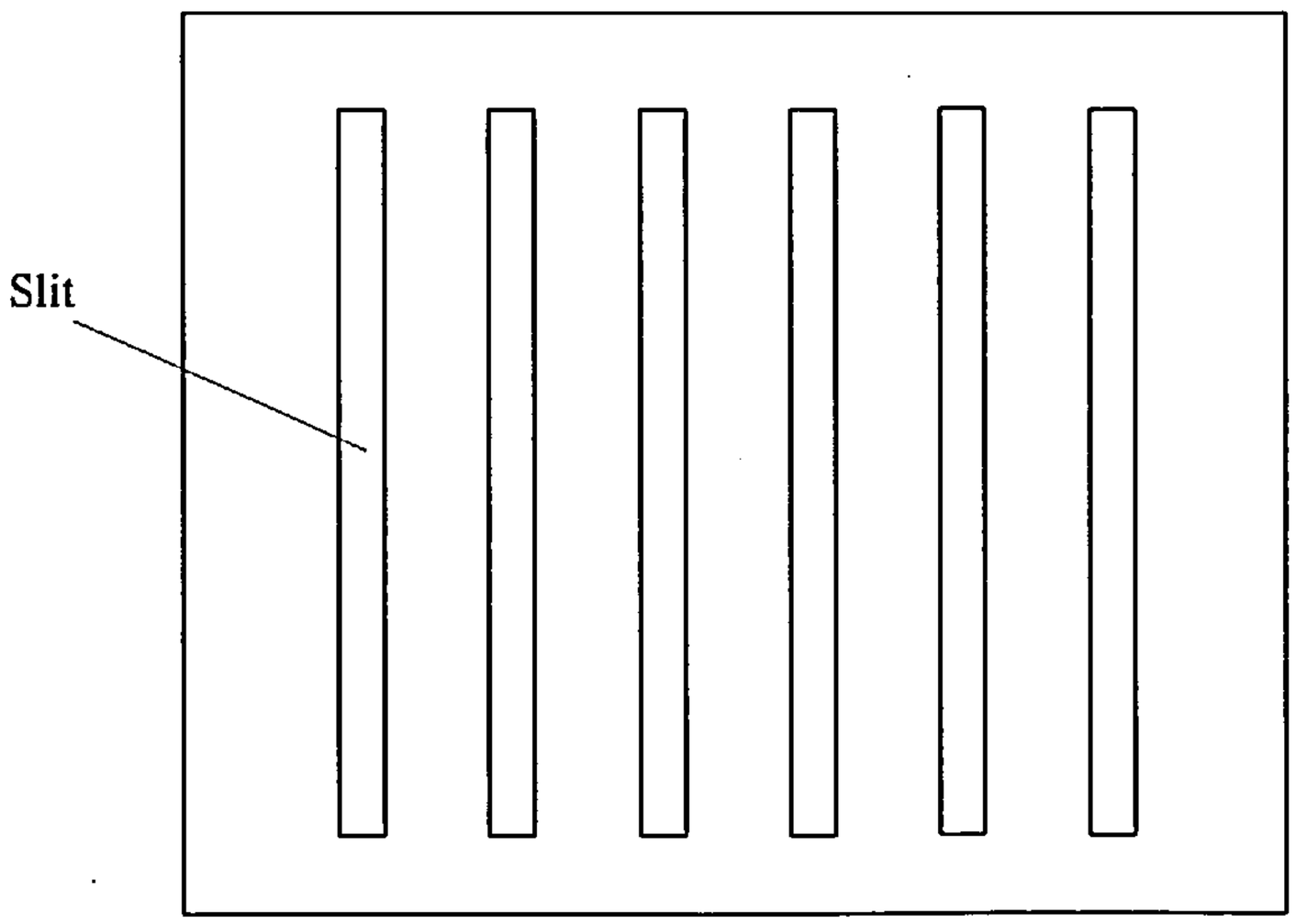

Fig 2-20 : Slitted shear wall for absorption of energy

2-4-2 Energy dissipaters in diagonal bracing

Concentric braced frames (CBF) are known to be economical and effective in controlling lateral deflections due to wind and moderate earthquakes, but during major earthquakes, these structures do not perform well, firstly being stiffer, they tend to invite higher seismic forces and secondly their energy dissipation capacity is very much limited due to the pinched hysteretic behaviour of the braces. The performance is still poorer when the brace is designed to be effective only in tension. A tension brace stretches during a severe shock and buckles in compression during reversal of load. On the next application of load in the same direction, this elongated brace is not effective even in tension until it is taut again and is being stretched further. As a result, energy dissipation degrades very quickly.

Moment resisting frames (MRF) are favoured for their earthquake resistance capacity because they have stable ductile behaviour under repeated reversing loads. This preference is reflected in various seismic codes by assigning lower lateral forces. However, these structures are very flexible and it is often economically difficult to develop enough stiffness to control story drifts and deflections to prevent non-structural damage.

The disadvantages of both of MRF and the CBF can be partially avoided by combining these systems. The concentrically braced MRF would be stiff enough during a severe earthquake. But the contribution of the braces is limited to the lower excitation levels and the only line of resistance during a major earthquake is the MRF, which means that this system does not protect against severe damage to the main structure.

An eccentric braced frame is another step in this direction. In this method, the brace joints are eccentric to force the beam into inelastic action to dissipate more energy. After a major earthquake, large inelastic deformations must be expected at all floors of a structure. Although the structure is saved from total collapse, the main beams are sacrificed and actual structure would need major repair or replacement.

Diagonal bracing incorporating energy dissipaters provides an alternative to the eccentric braced MRF in which they control the horizontal deflections of the frame and also the locations of damage, thus protecting both the main structure and non-structural components. Several kind of dampers have been suggested to be used in the diagonal bracing and in the following the most important cases will be review.

Friction damped braced frames

Pall and Marsh[49] suggested an improvement for the behaviour of steel frame structures. The system described as a friction damped braced frame employs a friction damping device at the intersection of the braces (Fig 2-21). For a high level of energy dissipation, it is necessary to provide either a large slip force or large displacements. The displacement is limited by the storey drift, therefore a large slip force equal to the tensile yielding limit of the brace is preferred. To avoid buckling of the compressed brace, the friction device is designed so that it deforms under the force applied by the tension brace and pulls back the compression brace Figure 2-22. A number of contact surfaces have been tested under cyclic loads. The brake leaning pad have demonstrated the best energy dissipation capacity, which is almost ideally rectangular hysteretic loops. Figure 2-23 and 2-24 demonstrate other kinds of friction damped braces.

On the basis of the analysis carried out by the means of a simplified inelastic model D. Jurukovski *et al* [27] concluded that: (1) the structure behaves as a dual system (braced MRF) at service loads, (2) its stiffness is reduced in extremely high excitation levels (softening due to activation of the slip joints), reducing the seismic forces, and (3) large amounts of energy are dissipated in the friction mechanism. Finally, the main structure remains elastic and there is no damage in the FD devices.

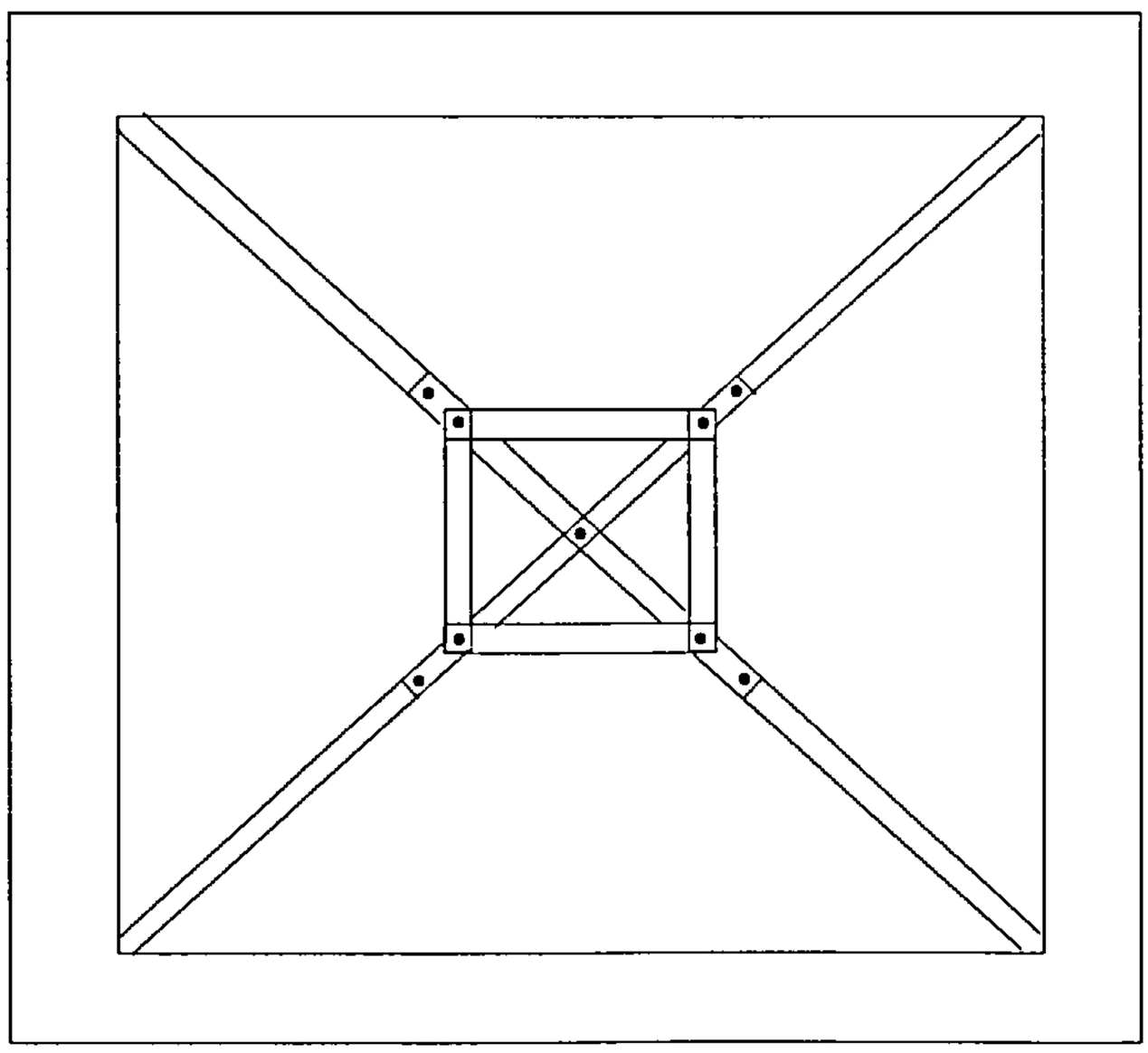

Fig 2-21 : Friction damped bracing

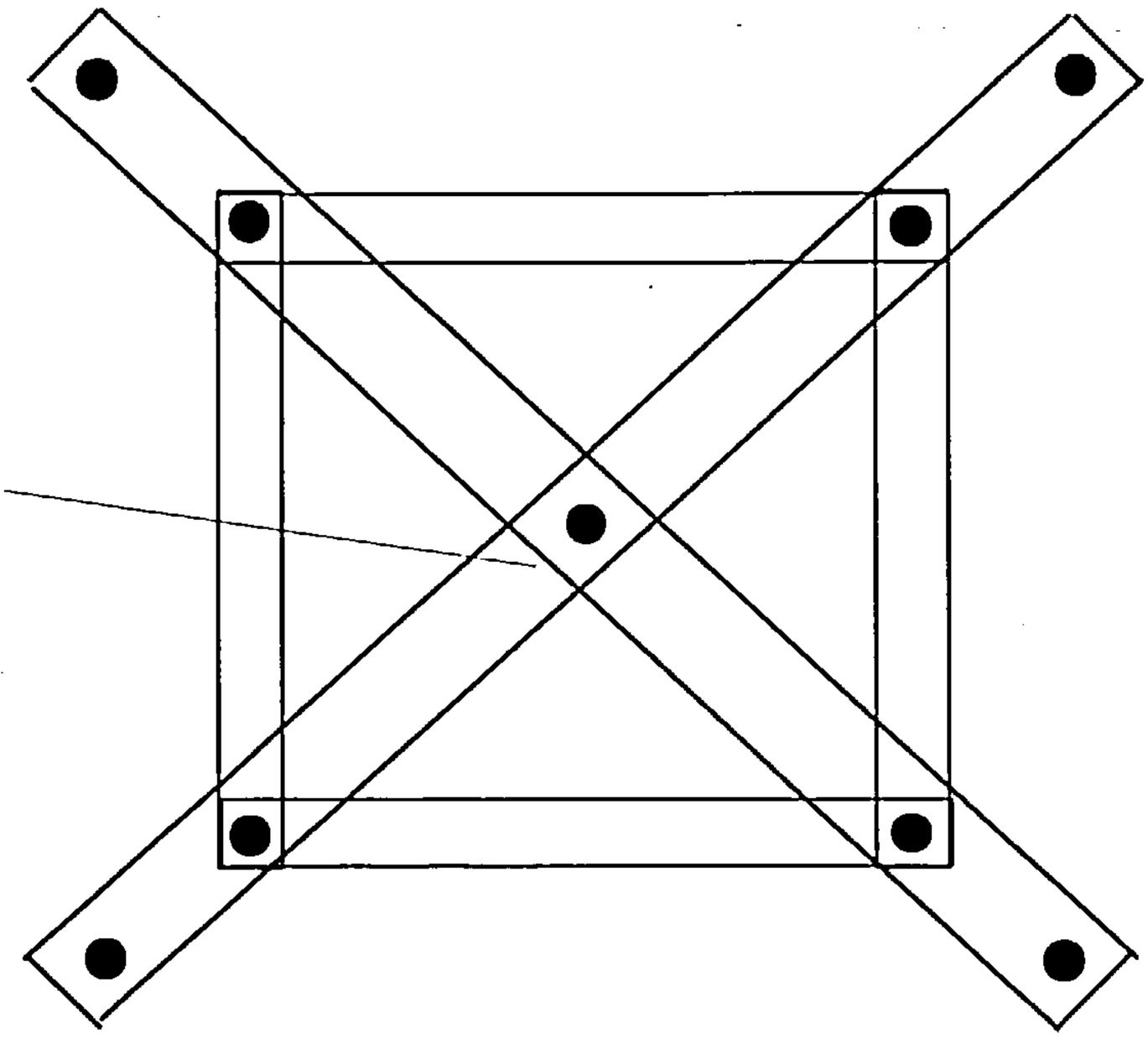

Fig 2-22 : Friction damped device

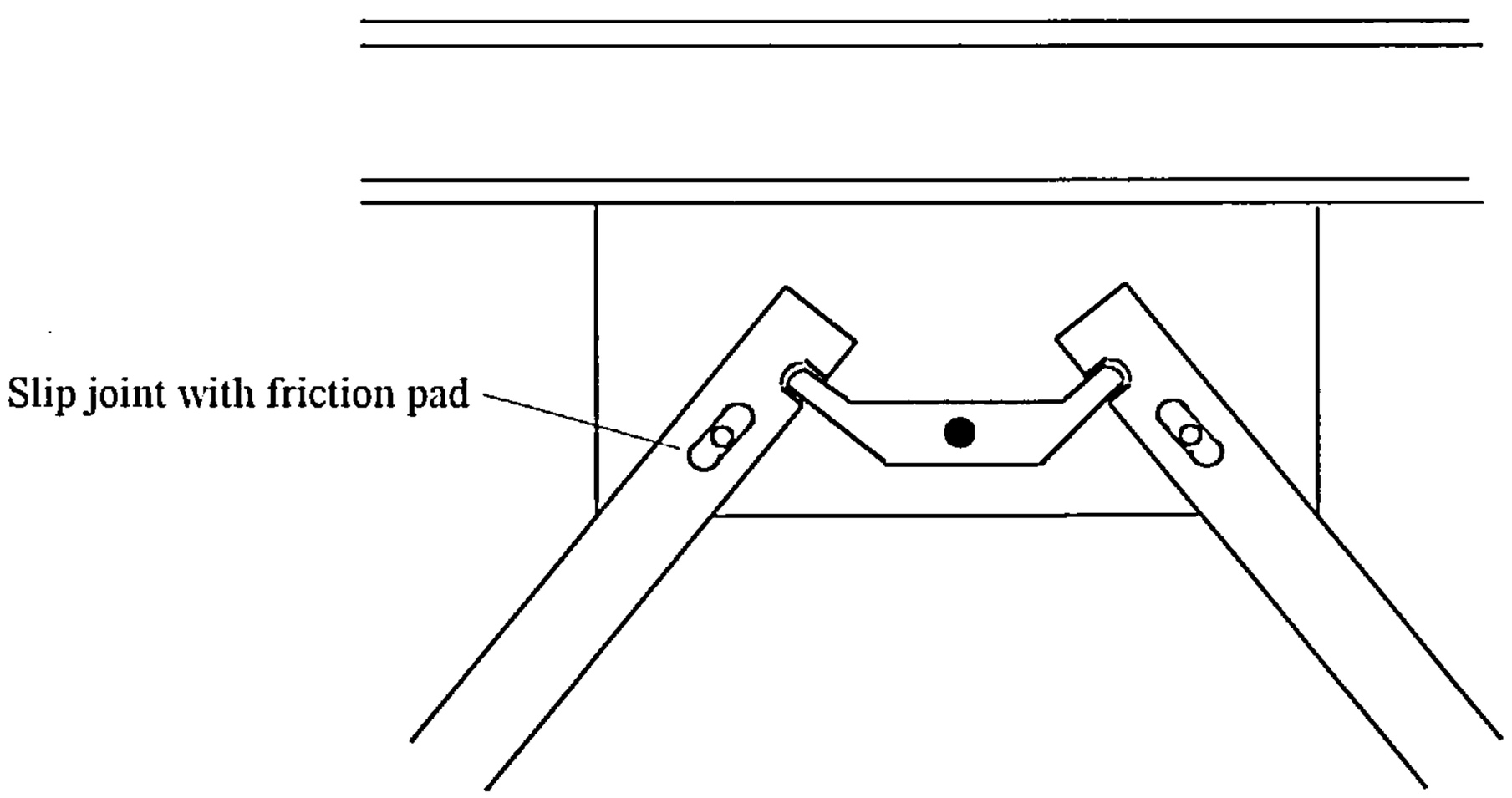

Fig 2-23 : Alternative model for friction damped brace

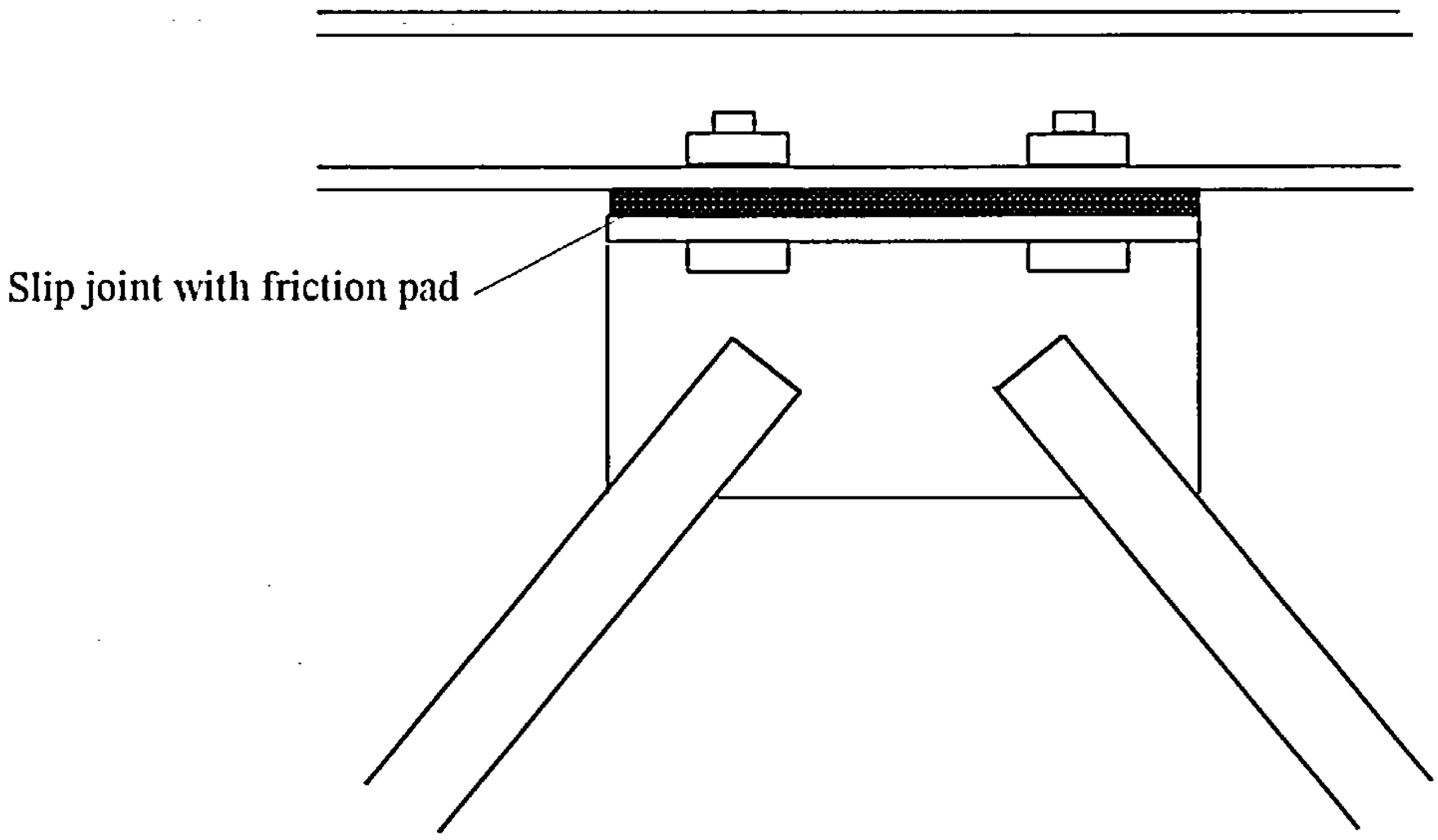

Fig 2-24 : An other model of friction damped brace

Further, research on this system was carried out by Filiatrault and Cherry[15]. They noticed that the compressed brace is safe against buckling failure only if the tension brace slips at every load cycle. But the load reversal is not usually symmetric and the compression brace would not always been pulled back by the friction device. This means that the model suggested by Pall and March has overestimated the energy dissipation capacity of the system. However, the results of the shaking table tests proved that the performance of the FDBF was superior to that of the MRF and the Dual systems (braced MRF). There is no doubt that the FDBF is an advanced idea that introduces a higher level of control than other systems based on the development of yielding mechanisms. Pall and Marsh stated that the motion of a vibrating building is slowed down by braking rather than breaking.

There are still two important features that require further consideration and experimental research: (1) the failure of the braces due to buckling and (2) the softening of the frame at higher response levels. The latter does not necessarily mean an improvement on performance, particularly when applied to high rise buildings. Also, the possibility of lock ups of the relatively complicated and heavily pre-stressed friction device should not be neglected.

Rotating plates braces:

Oiles Industry Co. of Tokyo, Japan[63] developed a brace damper. The Mechanical damper in this system consists of four links and two rotating plates. The brace damper is typically installed at the cross point of diagonal braces in an X -braced system. Four links attach the damper to the bracing. When inter story drift imposed by lateral forces occurs, the two plates are forced to counter- rotate. The principal engineering feature of the brace damper is that the counter rotary motion of the plates produces two type of forces: a spring force proportional to displacement (drift) and a damping force proportional to the velocity.

In this system, damping is achieved by using a heavy viscous fluid which is inserted between plates and is held there by a rubber elastic material ring.

ADAS Elements

The steel plate Added Damping and Stiffness device (ADAS), Fig.2-25 is an assemblage of steel plates that is designed for installation in a building frame such that the relative story drift causes the top of the device to move horizontally relative to the bottom Fig. 2-26. The ADAS device can dissipate substantial energy during an earthquake by yielding a large volume of steel[86].

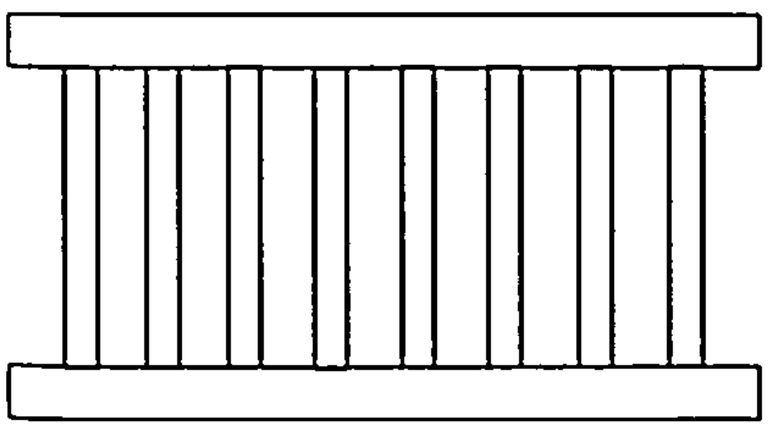

Fig 2-25 : ADAS energy absorbing device

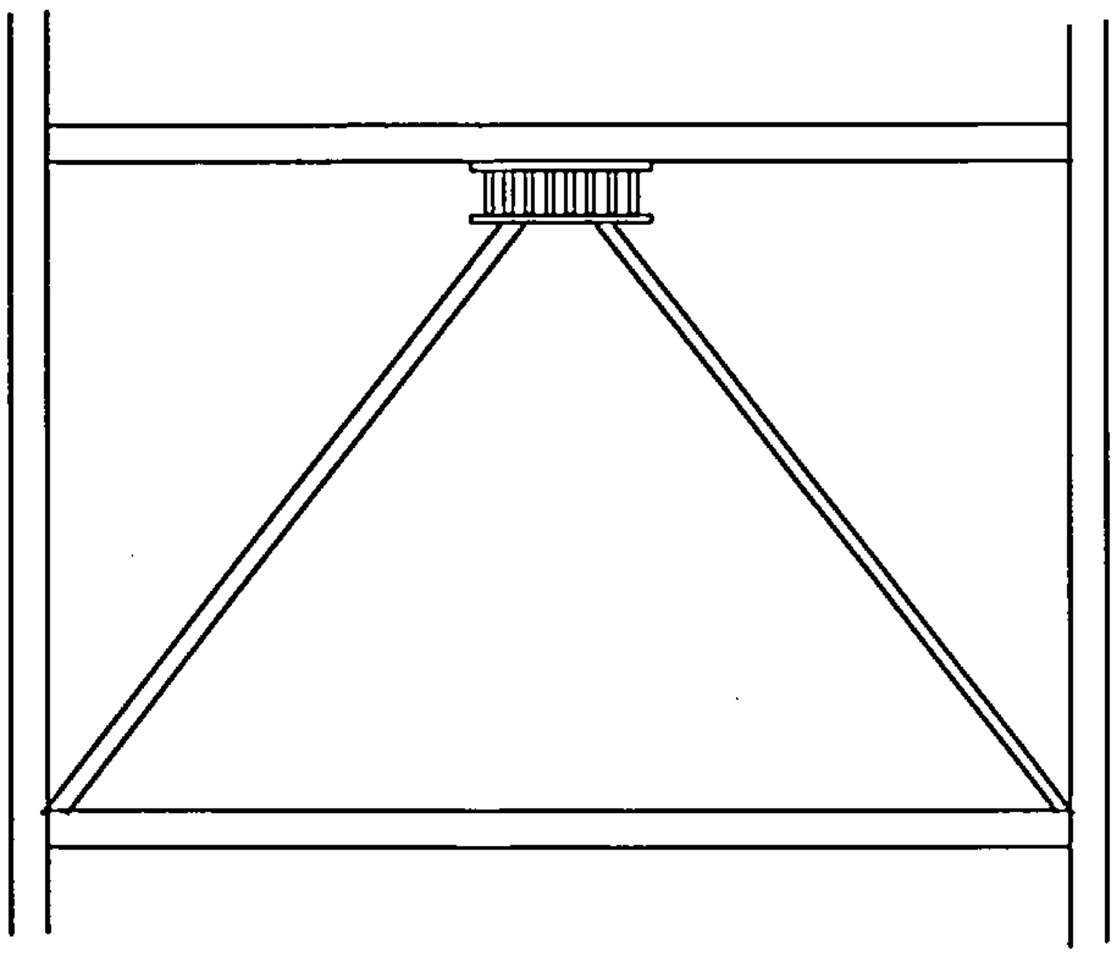

Fig 2-26 : ADAS bracing

The mechanical characteristic of yielding steel devices was investigated by Steimer and Chow 1984, Scholl 1990, Hansen 1986, Bergman and Hansen 1986,1990. The test of ADAS devices and frames with ADAS elements showed that these devices are reliable energy dissipaters and that they exhibit stable hysteretic behaviour for displacement amplitudes as large as 14 times Δ_y , yield displacement of the device, and are well situated for use in building structures situated in high seismic risk zones. The tests at the University of California at Berkley found that in the displacement range of 6 Δ_y or less, the ADAS devices hysteretic behaviour is dependent only on the yield force, P_y , and yield displacement, Δ_y , and can sustain an extremely large number of yielding reversals (more that 100 cycles in the tests).

Knee elements in the braces of the frames

An Eccentrically Braced Frame (EBF) was a solution to the low energy absorbing capacity of concentric braced frames. In this regard many attempts were made to improve the disadvantages of this sort of framing by de-coupling the control mechanism from the main structural elements, whilst maintaining the advantages of the EBF. This has led to the employment of auxiliary disposable elements within the bracing system. The introduction of additional non-structural elements may seem uneconomical compared to the EBF system but since these elements are not part of the MRF, they can be lighter and are able to develop a yielding mechanism even when slender braces are used. Heavy braces are essential for the EBF, this approach does not necessarily lead to an increase in the total weight of the system.

The disposable knee bracing frames (KBF), shown in Figure 2-27, was proposed by Aristizabal-Ocho[2]. Using simple elasto-plastic analyses for comparison of the KBF and EBF, Jurukovski *et al*[27] has demonstrated the advantages of the proposed system These are greater lateral stiffness and strength, as well as higher energy dissipation capacity, without damage to the main frame.

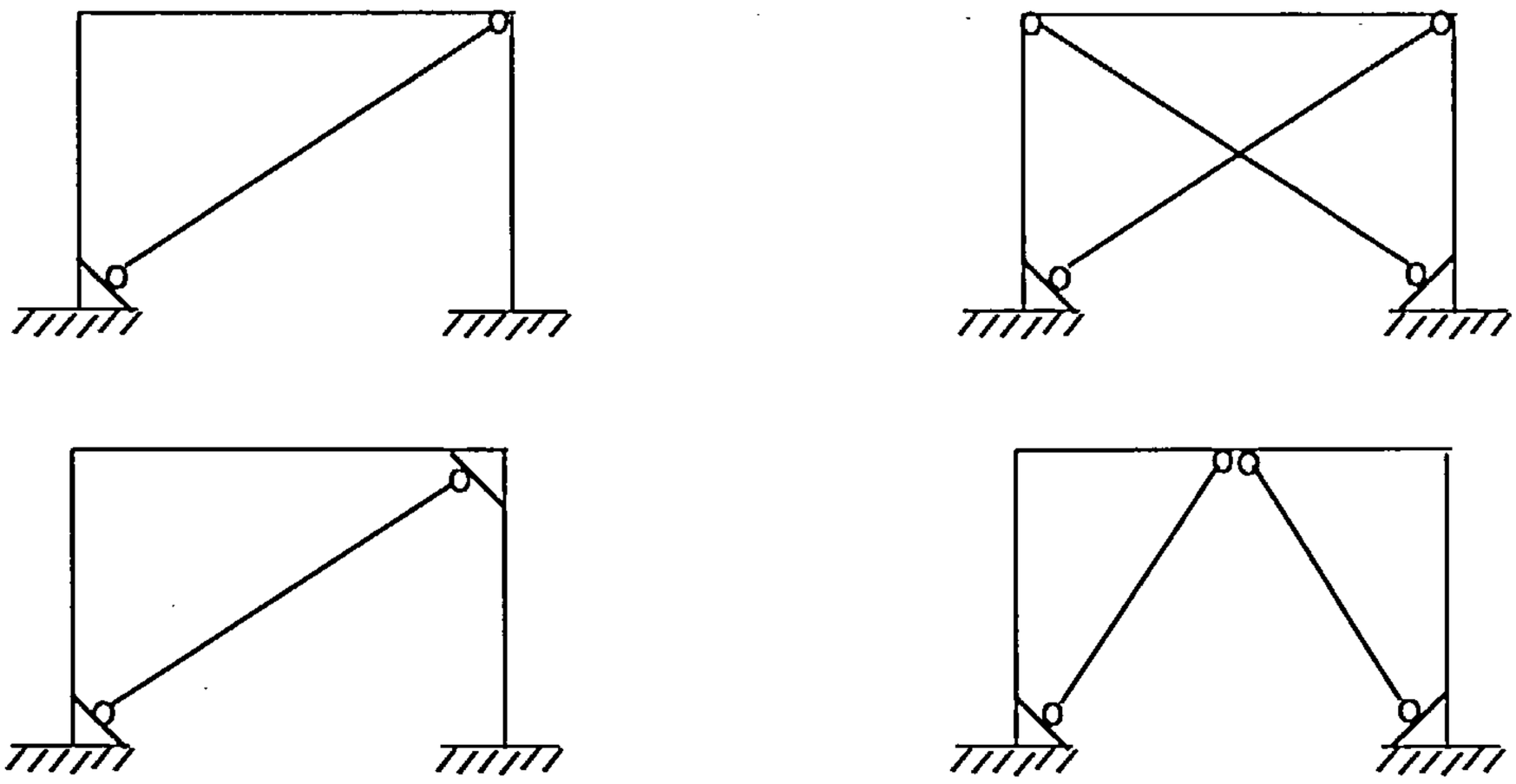

Fig 2-27: Knee braced steel frames

An extensive analytical and experimental research programme has been undertaken by Bourahla and Blakeborough[8], to verify the efficiency of KBF. In a series of shaking table tests of 1/12 scale models of one storey three bay steel frames, considering various frame configurations (MRF, X and K-shaped KBFS) the excellent performance of the KBF was confirmed. The development of the yielding initiated by the occurrence of a flexural-yielding mechanism in the knee and followed by tension-yielding of the braces, prevented serious damage to the main frame. This damage development pattern proved that the knee acts as a 'fuse-like element, imposing an extra line of defence. The comparative analyses of KBF and both the corresponding MRF and dual-CBF have demonstrated the superior behaviour of KBF, under any load conditions.

A similar approach to improve the energy dissipation capacity of braced steel frames was investigated by Jurukovski *et al*[28]. In that study a rectangular ring, fixed in the intersection of the braces, was used as a disposable element (DEBF) Figure 2-28. The cyclic tests at full-scale single-bay single storey, for both MRF and DEBF, have proved that the energy dissipation capacity of the latter is considerably higher.

Furthermore, the non-linear response analyses based on experimentally obtained results confirmed that no damage to the main structure occurred until the yielding mechanisms had been developed in all the disposable elements, and in most of the braces . However, this behaviour has not been verified by the result of the investigation of real earthquake damage.

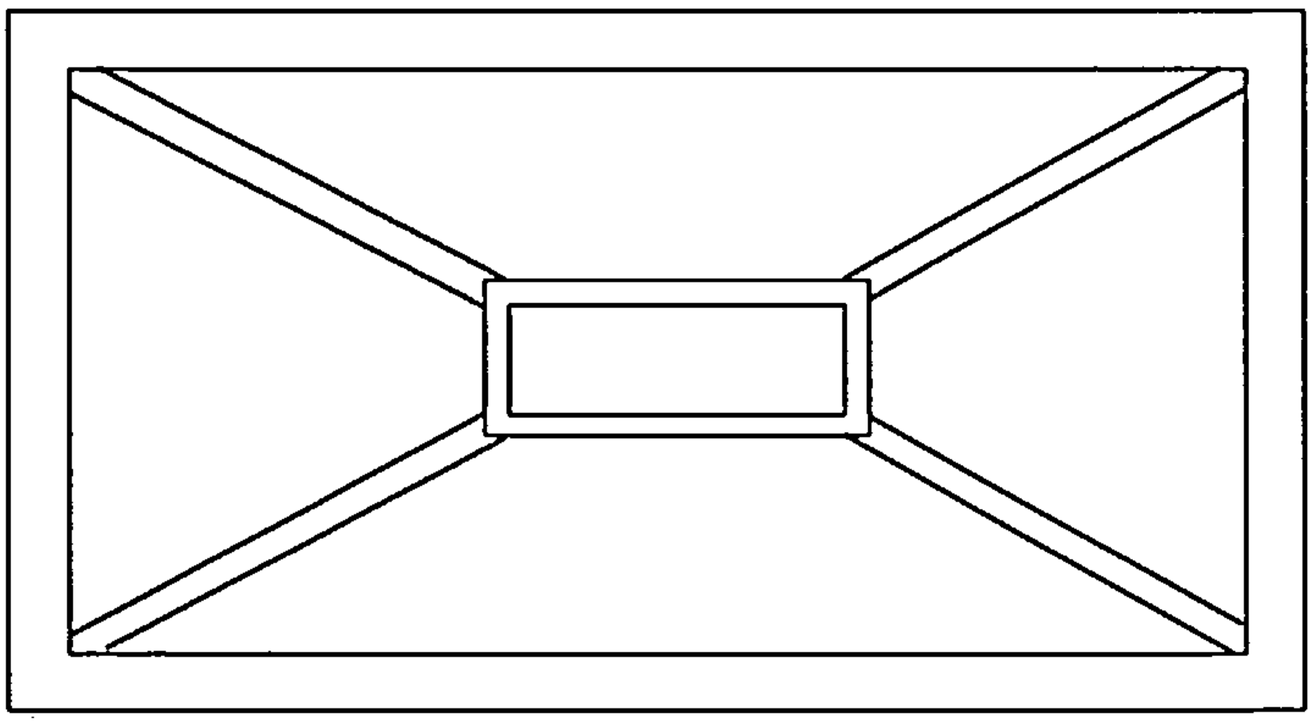

Fig 2-28 : Braced steel frame with disposable rectangular element

Although both systems with disposable control elements have demonstrated an apparently favourable behaviour under both moderate and severe earthquakes, they have inherited several drawbacks. In the case of lower intensity excitations (minor to moderate earthquakes), when the MRF remains elastic, certain damage to the disposable elements can be observed, whilst during a moderate earthquake most of the auxiliary system is destroyed.

Another practical example for the use of disposable element in the braces of frames is the six-storey government office building constructed in Wanganui[39], New Zealand, in 1980 (Fig 2-29). This building obtains its lateral load resistance from diagonally braced precast concrete cladding panels, thus minimising the amount of internal structure to suit architectural planning. A steel insert consisting a sleeve housing a specially fabricated steel tube 90 mm diameter and 1.4 m long was considered for absorbing the energy. It was designed to yield axially at a given load level. A movement gap was provided through the surrounding structure, and buckling was prevented by the surrounding sleeve and concrete.

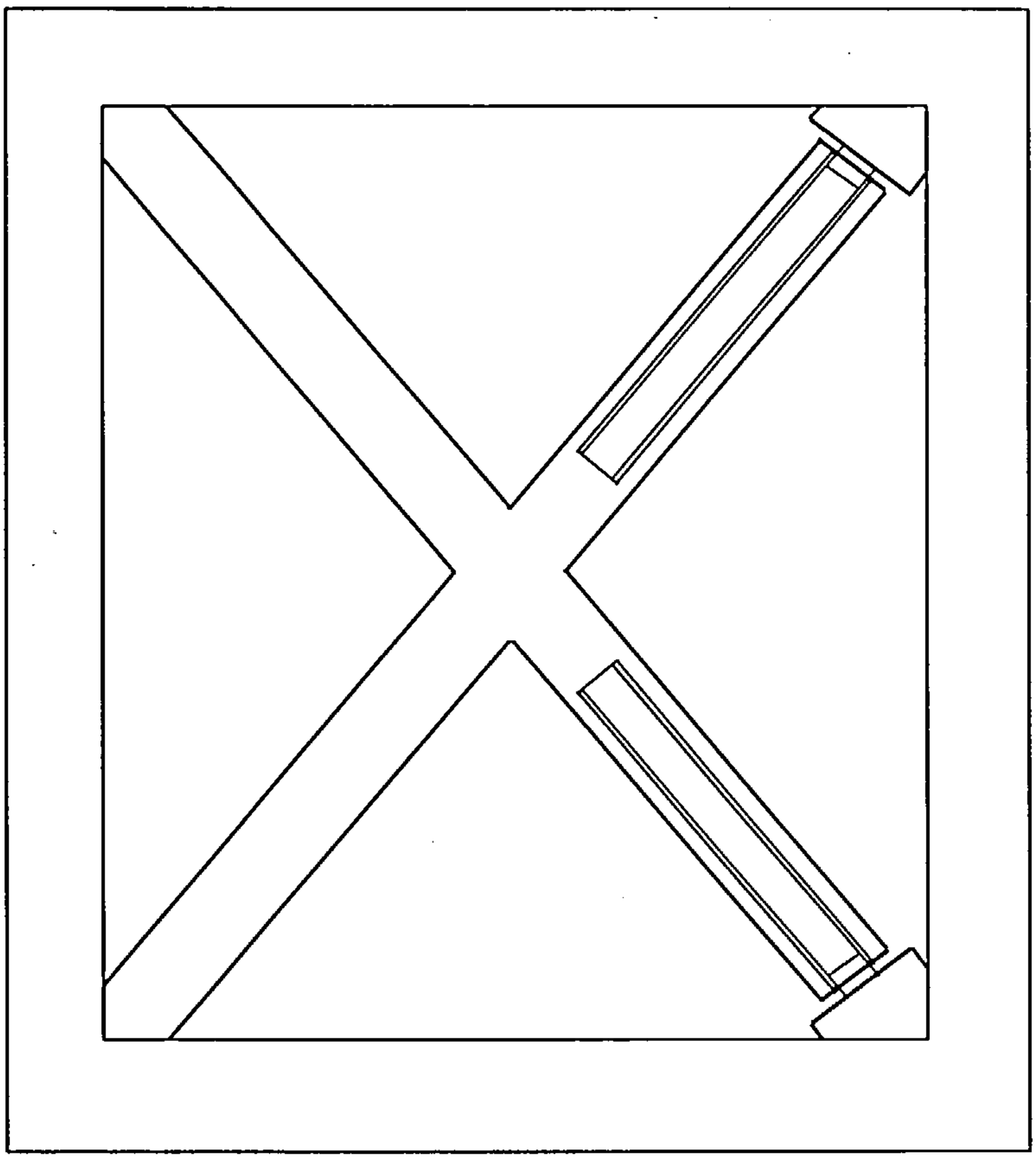

Fig 2-29 : Precast concrete bracing with steel insert absorbers

U device in the bracing of the frames

The devices which utilises the deformation of 'U' shape or oval strips could be applied in the braces of frames for absorbing the energy (Fig 2-30). The fundamentals of this device were demonstrated in the previous section. Using a multiplicity of smaller U elements, instead of using one larger element, has certain advantages. The smaller elements are easier to form, and an unexpected failure of one or more of them is not likely to be as catastrophic as failure of larger elements[1]. Additionally, it should be pointed out that forming the 'U' elements out of strip stock as has been recommended because this requires no machining or heat treating. The elements may be fixed by welding, because their support points do not coincide with their points of maximum strain and all of this provide substantial cost savings. A low elastic limit and low stiffness in the serviceably state are disadvantages of this energy absorbing device.

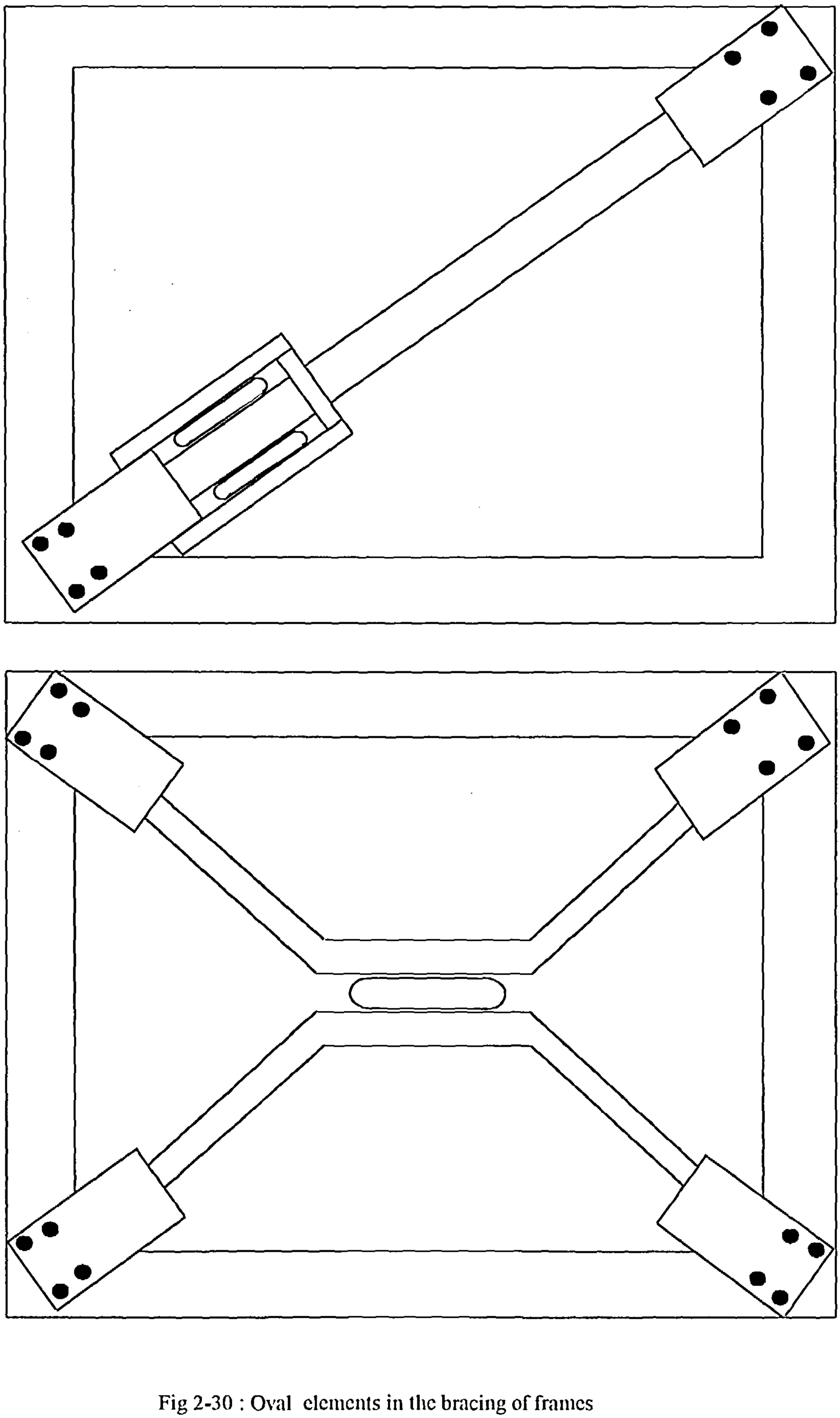

Fig 2-30 : Oval elements in the bracing of frames

Viscous damping devices in the bracing of frames

Viscoelastic (VE) dampers are among the earliest types of passive dampers which have been successfully installed in a number of tall buildings and other structures to reduce the motion amplitude and the acceleration occurring due to wind and earthquake forces. One of the earliest and more significant works on VE dampers has been the work of Mahmoodi[37], who studied and established the properties of VE materials following and extensive experimental program.

Properly employed, these dampers are capable of reducing the building motion by converting a portion of the mechanical energy of wind or earthquake to heat. In the case of wind induced motion, the additional damping provided by the viscoelastic damper is primarily for the comfort of building occupants and is a viable solution for tall and slender buildings where motion is likely to be noticeable and possibly and objectionable. In seismic situations, this technology can be incorporated either new construction or as viable candidate for the retrofit of existing buildings[67].

Earlier research into viscoelastic dampers and their applications focused on the suppression of wind induced sway of high rise buildings. Mahmoodi[38], Keel[39] showed that the wind induced sway of high rise buildings can be significantly reduced by adding viscoelastic dampers to the structure.

Viscoelastic dampers are non-load carrying elements and are designed such that part of the mechanical energy of the building motion is transferred into heat, which result in a reduction of the amplitude of the vibrating motion. The medium in which this transfer of energy takes place is a viscoelastic material.

There are basically three methods of employing a viscoelastic material as a damping medium. One is the direct application of a viscoelastic layer to the vibrating part such as plates and beams where damping is accomplished by extensional deformation of the viscoelastic layer (Fig 2-31a). The second type is an extension of the first, but by adding another layer of a rigid material on top of the viscoelastic part to form a constraint layer (Fig 2-31b). Thus the viscoelastic material will experience both extensional and shear deformation. The achieved damping is mostly due to shear deformation rather than extensional displacement. There are a number of variations of these type of damper to increase the deformation and consequently obtain higher capacity. The third type of damper is one where nearly all of the deformation is in

hear (2-31c). Each of these configurations has some merits and disadvantages, but generally, for a given amount of viscoelastic material, the third type is more efficient and is more suitable where large amounts of energy are to be damped out. Hence a typical viscoelastic damper is of the third type.

A typical structural damper is, therefore, constructed of two viscoelastic layers bonded between three parallel rigid surfaces (Fig 2-31d). The position of the damper, with respect to application of the load is such that the viscoelastic material undergoes virtually pure shear deformation. This type of damper could be suitably placed in the braces of structural frames.

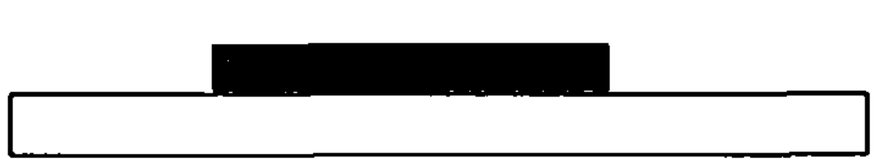

a) Extensional single layer VE damper

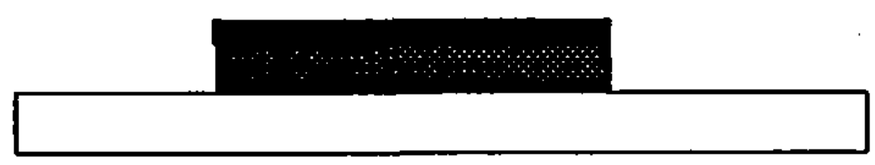

b)Extensional shear deformation constrained VE damper

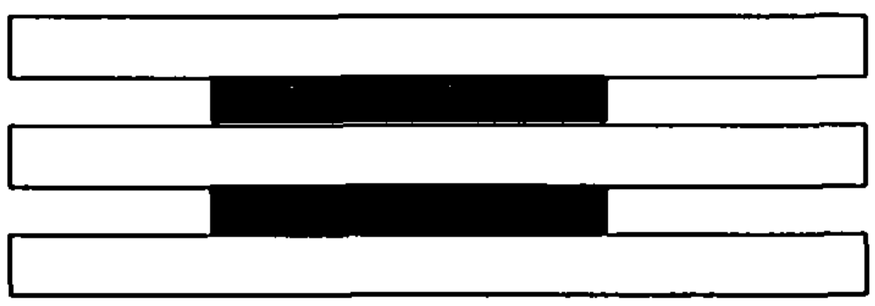

c) Extensional shear deformation VE damper

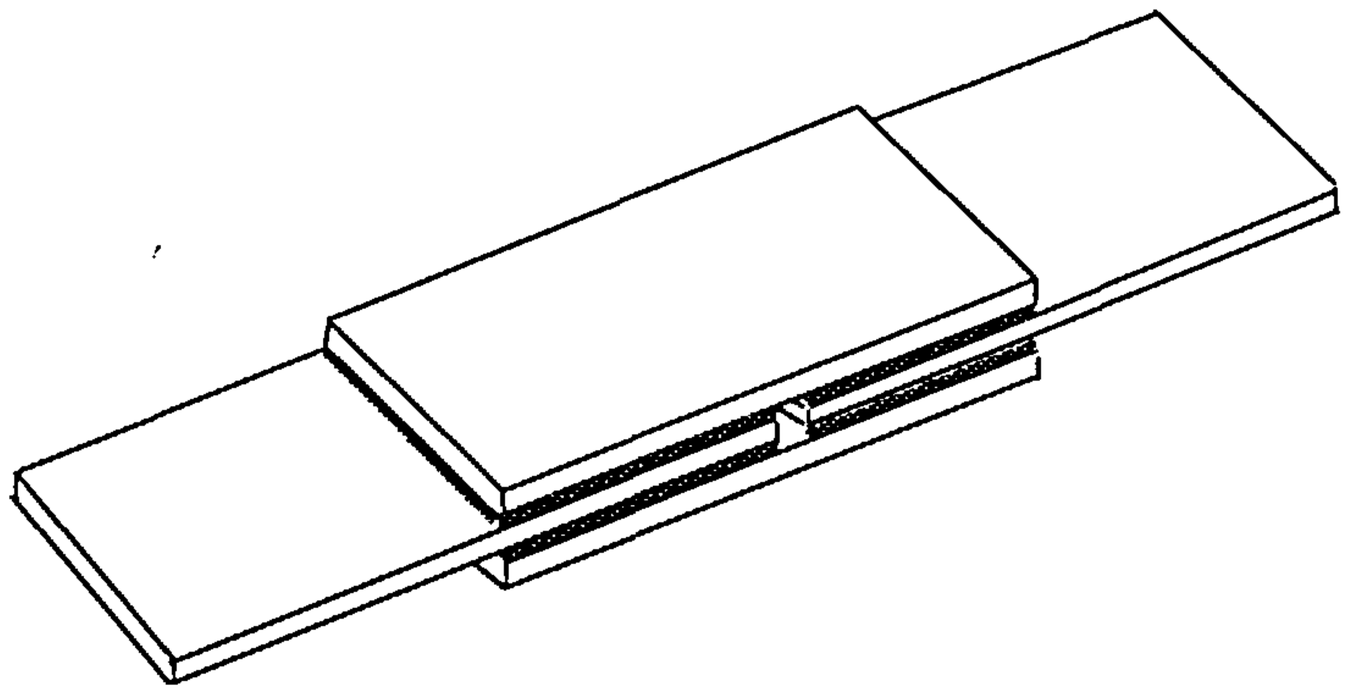

d) A typical VE damper

Fig 2-31: Different forms of VE Damper elements

Another kind of viscoelastic damper was created by Hsu and Fafitis[20]. They designed a connection which incorporates viscoelastic layers to absorb the energy. This viscoelastic connection which had been designed to carry axial forces only, is shown in Fig 2-32.

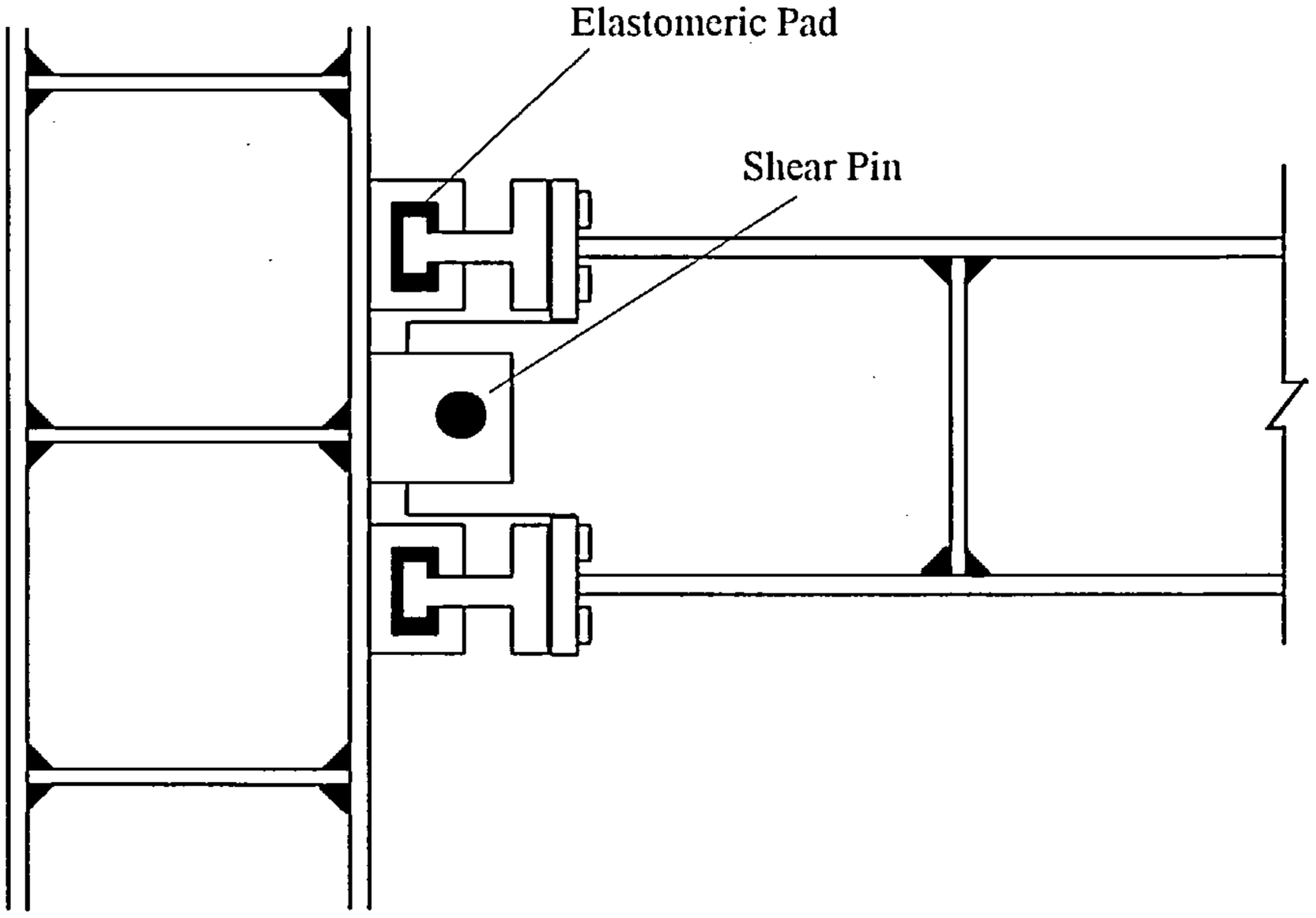

Fig 2-32 : Viscoelastic damper in the beam column connection

2-4-3 Ductile Cladding Systems

The interaction between structural and none structural elements which has been studied extensively to protect structures from their harming effects, may be used to dissipate energy from seismic shocks by applying energy absorbing devices in the links between parts[51]. Apparently this will raise the complexity of calculations of the structure but may be balanced by the overall efficiency of the building in terms of dynamic response. Apart from additional damping which this arrangement will provide, it will also raise the stiffness of structure by the bracing effects of the links. Therefore, it may shift key structural frequencies of the building to the ground motion spectral ranges which could be disastrous. Thus, any arrangement of this type should be carefully designed. A method, for reducing the negative effects of cladding systems is to carefully design of advanced suitable connections between elements. These

connections should exhibit superior properties of ductility, without failure. They should also limit the force transmission into or through the panels.

Although there are many kinds of connection systems but they are generally composed of three main compartments: (1) the anchor point, or insert, built into the precast panel, (2) connection body or connector, which forms the structural connection between the cladding panel and the main structure (Fig 2-33).

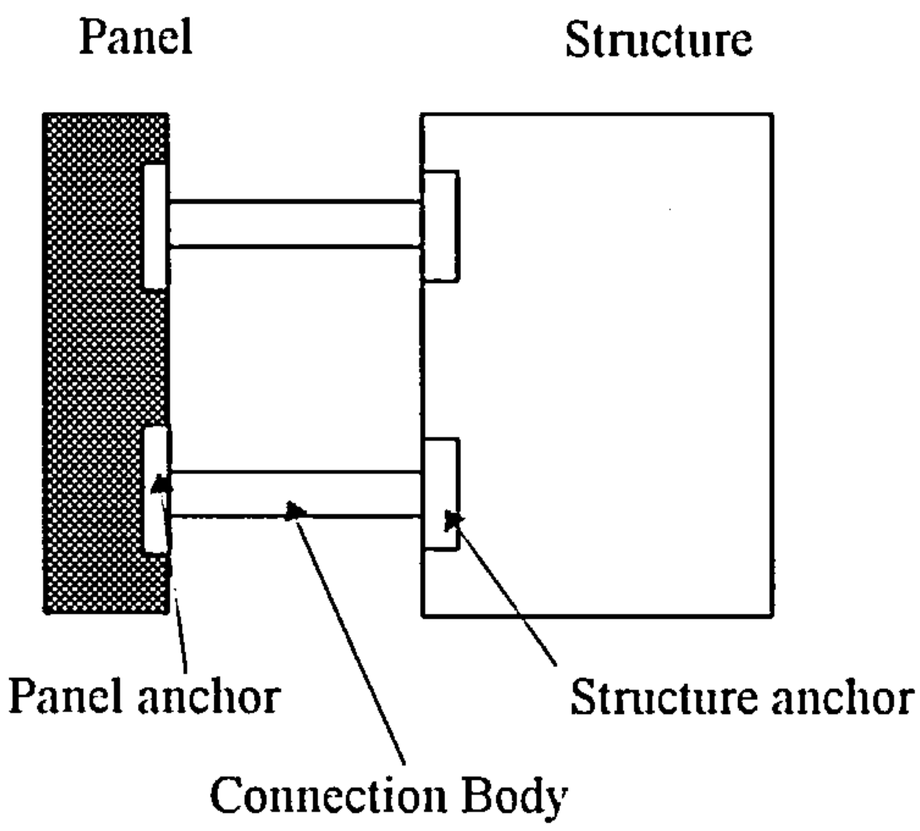

Fig 2-33 : Ductile cladding connection

The connection anchor usually consists of a steel insert embedded in the concrete of the panel of the structure. Unlike the case of a load carrying structural panel connection, the anchorage of architectural cladding connections may be subjected, in addition to possible shear of pull out, to torsional and bending moments due to eccentricity of most of the connection designs. The data available from the tests showed that inserts embedded in concrete are not by themselves capable of providing the level of ductility and damping required from an advanced connection without loss of strength and integrity. This is due to extensive cracking of the concrete surrounding the insert. The conclusion is that, in an advanced connection, the energy dissipation must occur in the connector body if the integrity of the concrete panels is to be maintained and the anchor must be kept in the linear range. The yielding of the connectors body serves two purposes: (1) it produces the necessary energy dissipation

and (2) it protects the anchor by limiting the load that can be transferred to the connectors.

The advantage of mild steel which provides high stiffness in the elastic range and absorbing energy with moderate hardening in the plastic deformations plays a key role in the most of these connection systems.

In this chapter the absorbers which are frequently used in the industry, were discussed. It was noticed that there are many restrictions for the use of each device and despite of considerable effort made in this field, still there is a necessity for more research to create devices with better responses. In the next chapter, a new energy absorbing device, which fulfils the characteristic of a high energy absorbing device and a structural member simultaneously, will be introduced.

Chapter Three : A New Energy Absorbing Device

The peeling and inverting of tubes is an idea that has been used for producing a new energy absorbing device. In this new device, as well as retaining the advantages of the pure inversion of tubes, which was illustrated in chapter 2, its properties have been improved to produce an excellent absorber for seismic and other cyclic shocks. In this chapter the details of this energy absorbing device will be introduced.

Peeling and Inverting Tubes for the Absorption of Energy

The general arrangement of the device is shown in Fig3-1 and the longitudinal cross is shown in Fig 3-2. This latter section is illustrated to a larger scale in Fig 3-3. The device is formed from three major parts: The peeling tube (Fig 3-4), which absorbs the energy of impact, the support tube (Fig 3-5) and the peeler bar (Fig 3-6). The peeling tube is located inside the support tube and they have a common longitudinal central axis. The peeling tube is glued to the support tube by an industrial adhesive. The thickness of the glue depends on its type and usually is recommended by its manufacture. The top edge of the peeling tube has been formed as an axisymmetric shell with metal forming methods (fig 3-4).The other end of this tube is bolted (or welded) to the support tube to reduce the stresses in the glue and to provide a safe transmission for the load. The peeling tube and the support tube are shown in Fig (3-7).

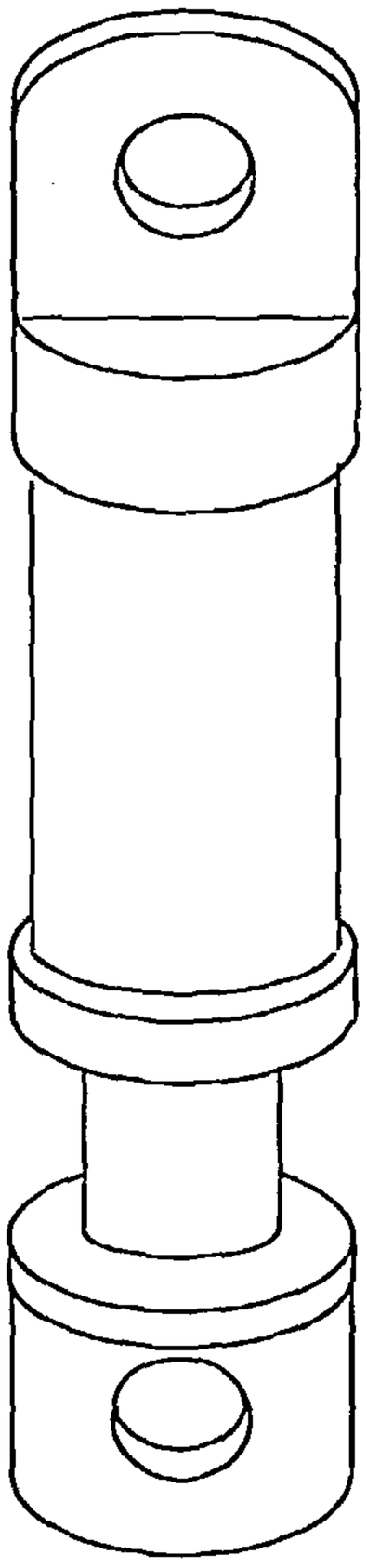

Fig3-1: The general arrangement of the device

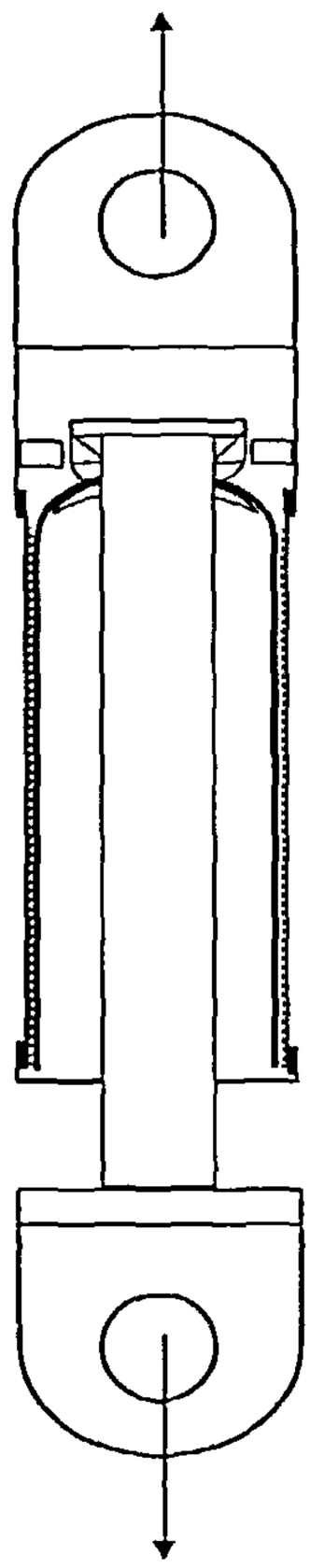

Fig 3- 2 : Longitudinal section of the Device

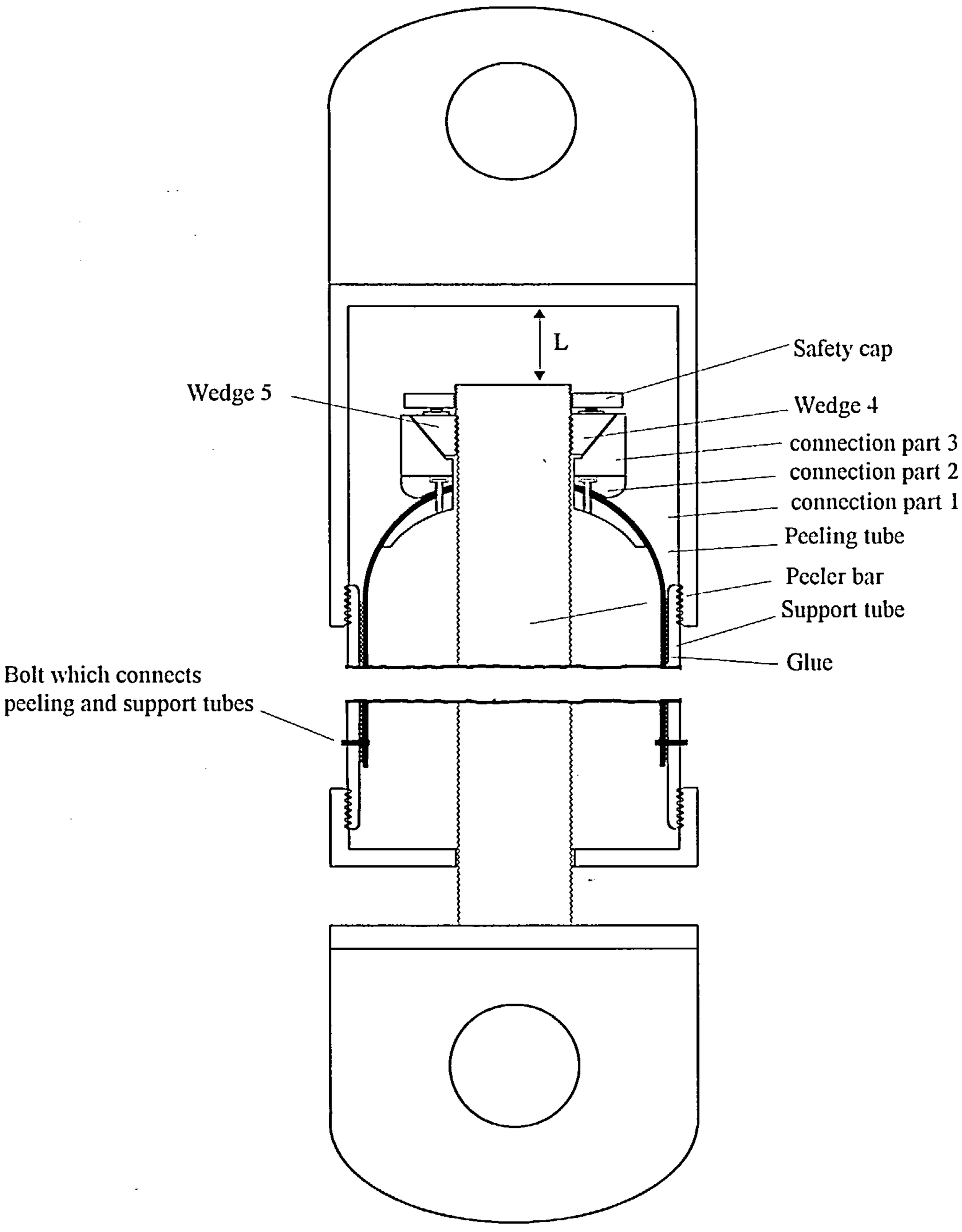

Fig 3-3: The longitudinal section of the device

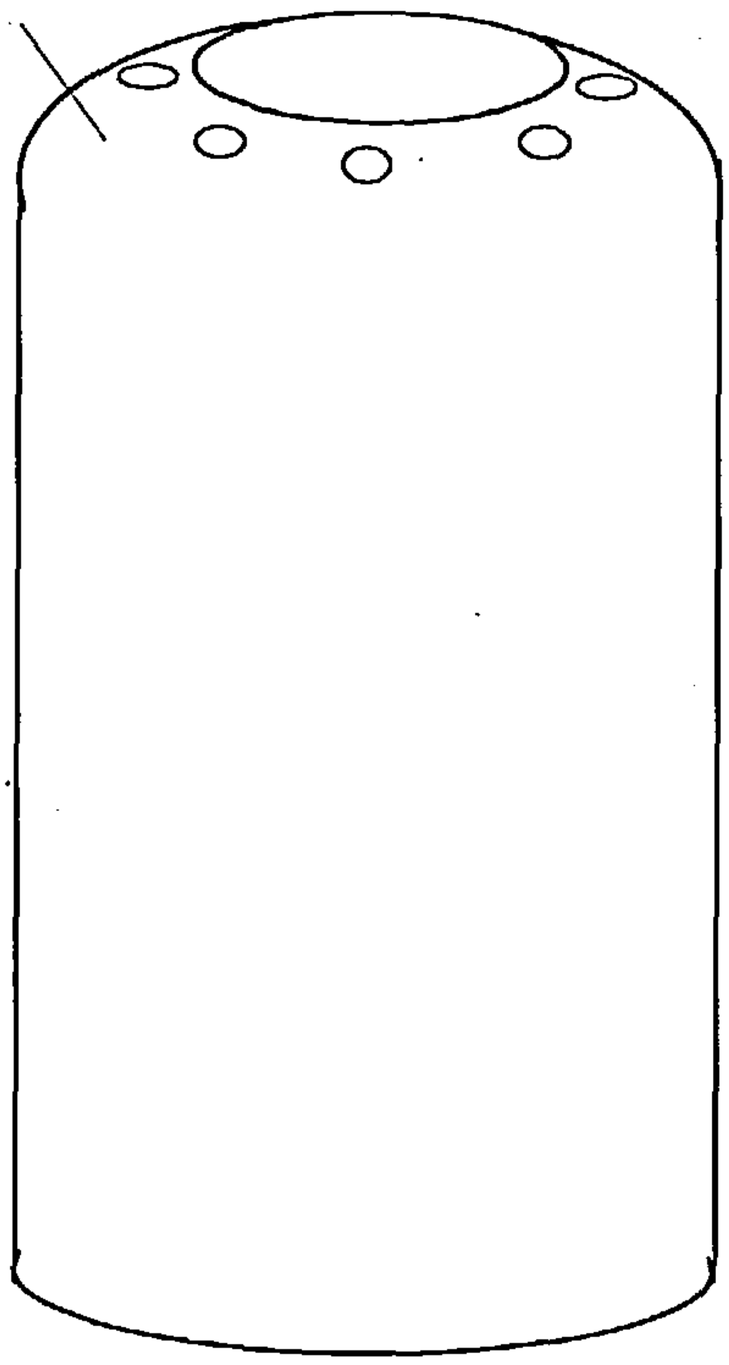

Fig 3- 4 : The peeling tube

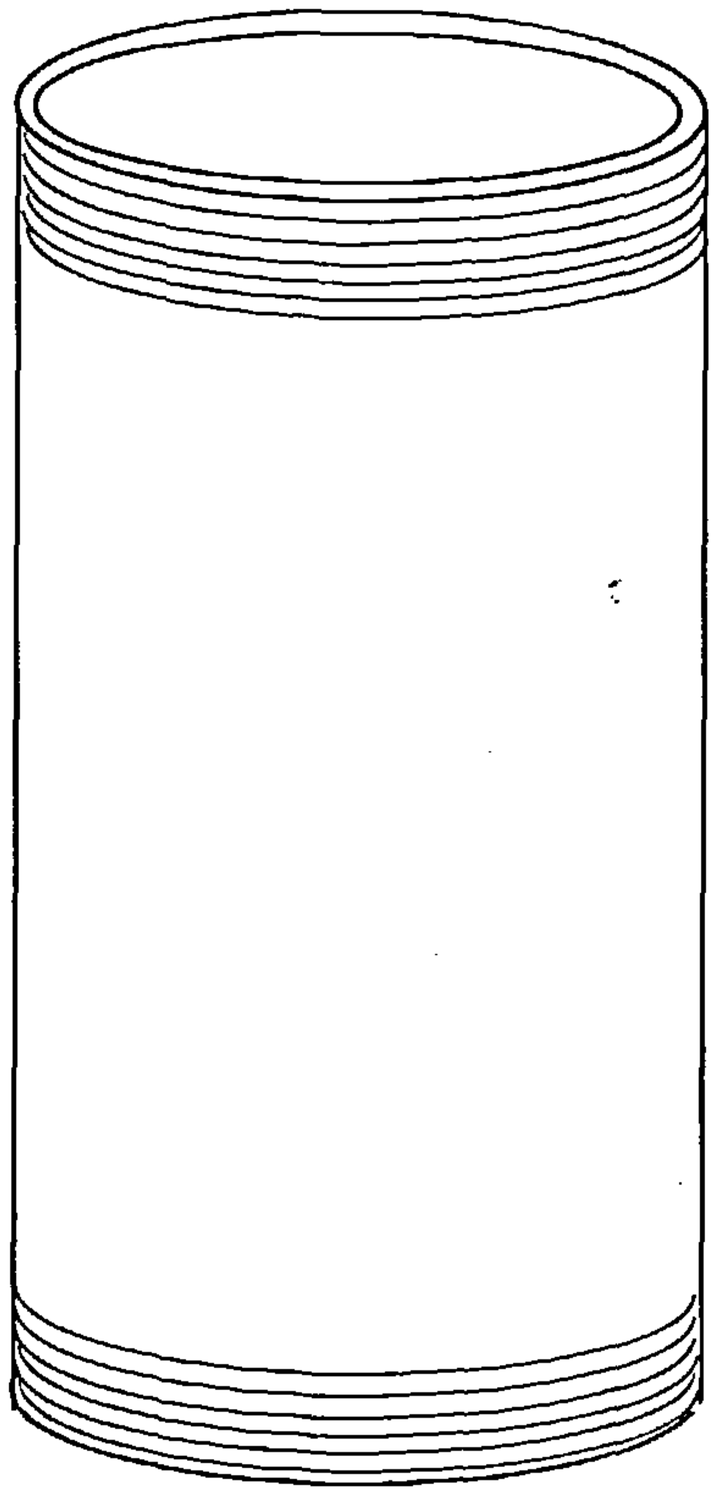

Fig3- 5: The support tube

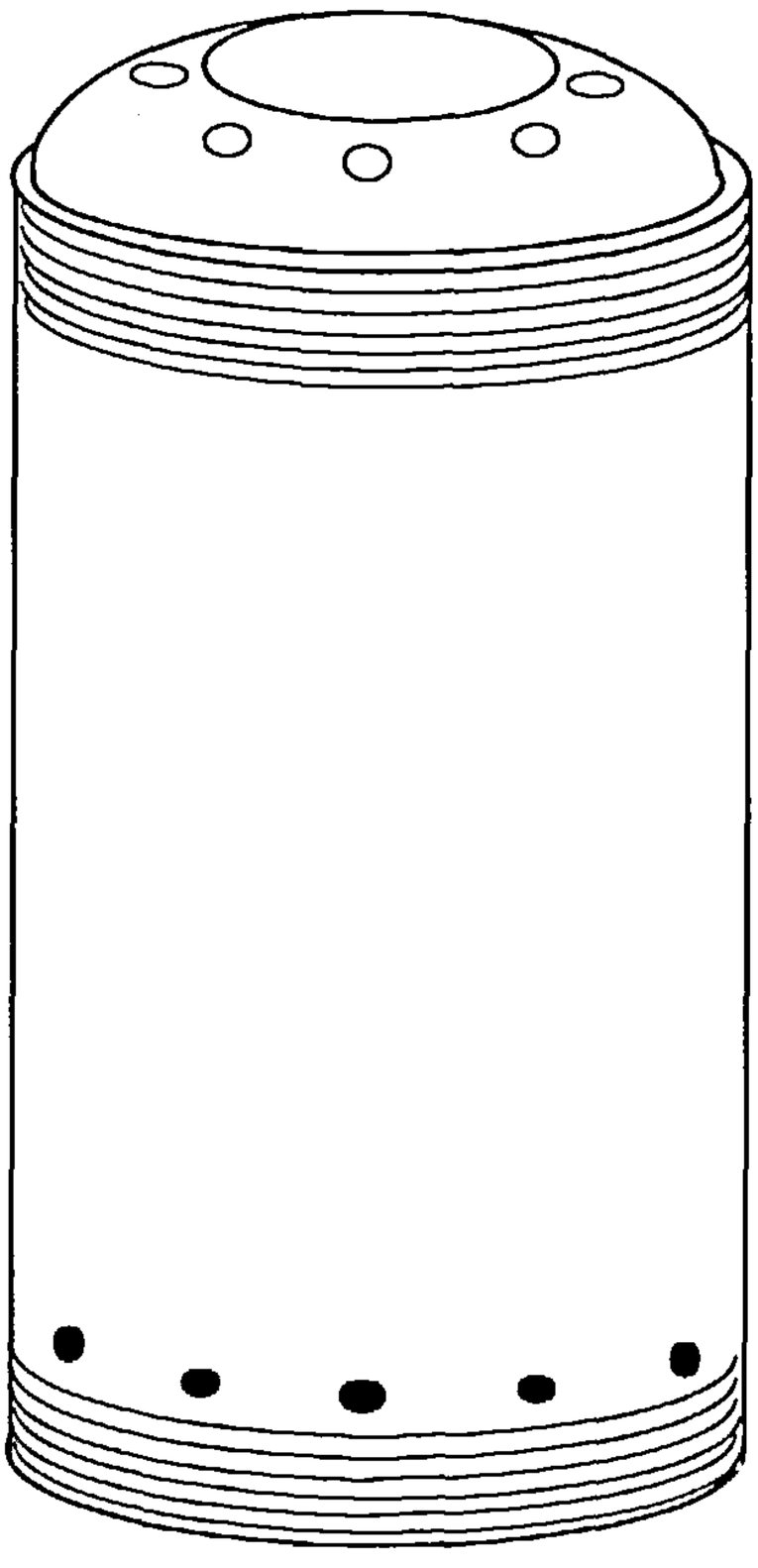

Fig 3- 6: The set of support tube and peeling tube

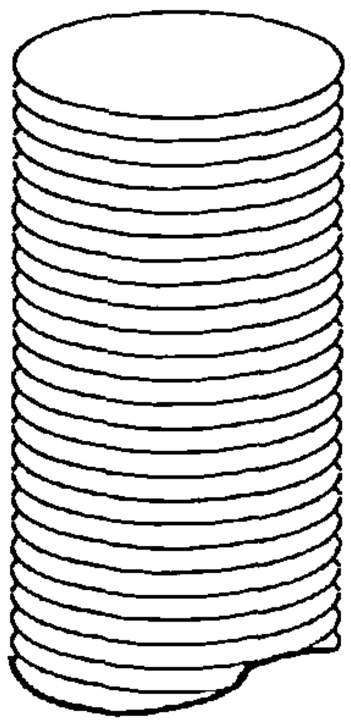

Fig 3- 7 : The peeling bar

The peeling tube and the peeler bar are connected by three connection parts. The connection part 1 (Fig 3-8) is glued to the shell of the peeling tube and is then screwed or bolted to the connection part 2 (Fig 3-9 and fig 3-10). The shell will be fixed firmly between these two parts. Connection part 2 is screwed to the connection part 3, which is in contact with the peeler bar using the two wedges 4 and 5.

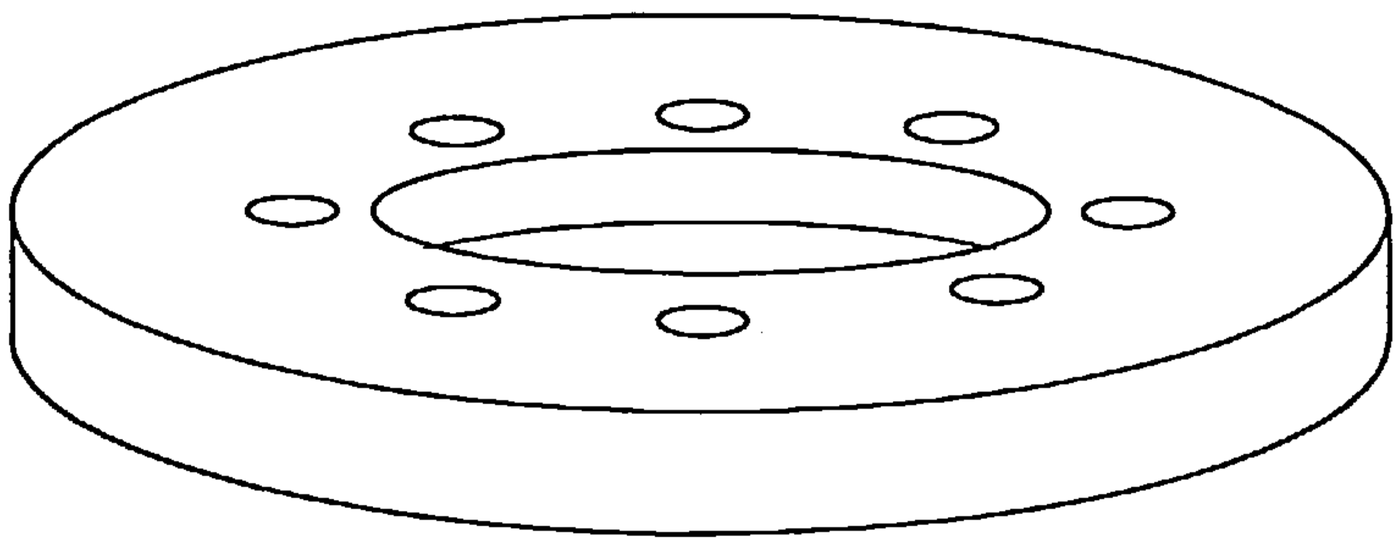

Fig 3- 8 : connection part 2

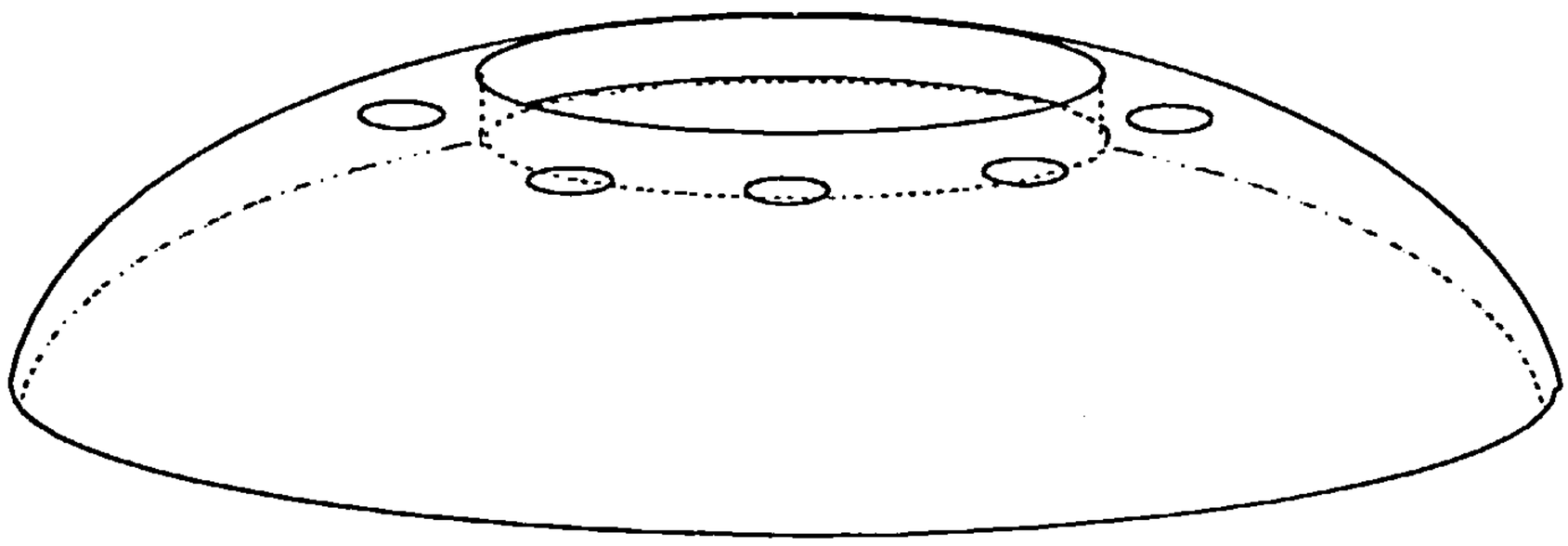

Fig 3- 9 : Connection part 1

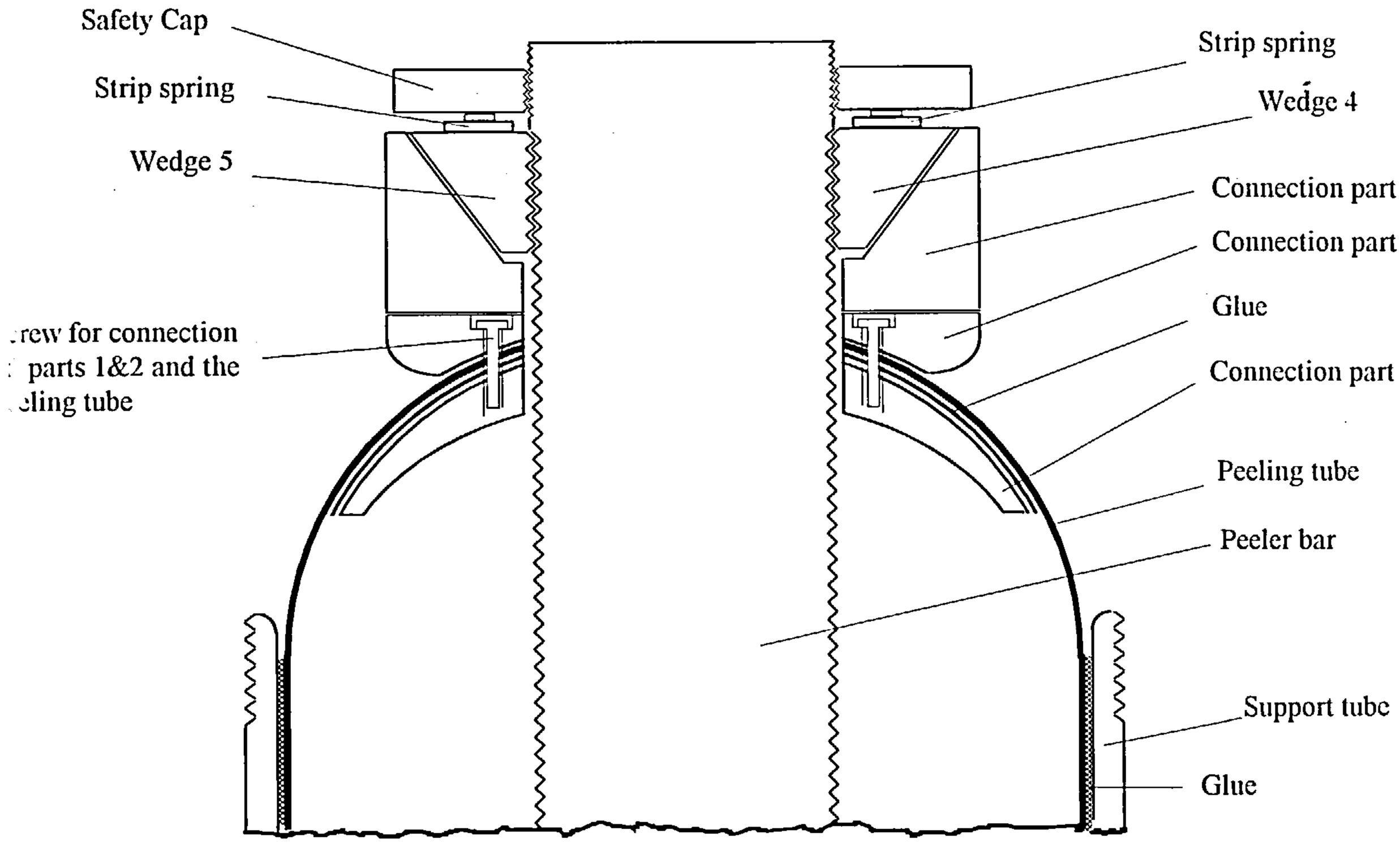

Fig 3-10: Connection of peeler tube to
the peeler bar and support tube

The top edge of the peeling tube, which is formed as an axisymmetric shell (Fig 3-4), is crucial for the device. The strength of this shell is the yield limit of the device. Its strength depends on the parameters of the shell (its shape, thickness and material properties) and the conditions of its supports, especially connection part 1. By suitably choosing the dimension of these items, which will be discussed in the next chapter, the collapse load of the shell can be adjusted to whatever value desired. In the figures this shell has been shown by a full thick uniform line, which represents its middle line. The real thickness of the shell may be variable along its longitudinal section to achieve the highest strength. In figure 3-11 a typical form of variation in the thickness of this shell has been shown.

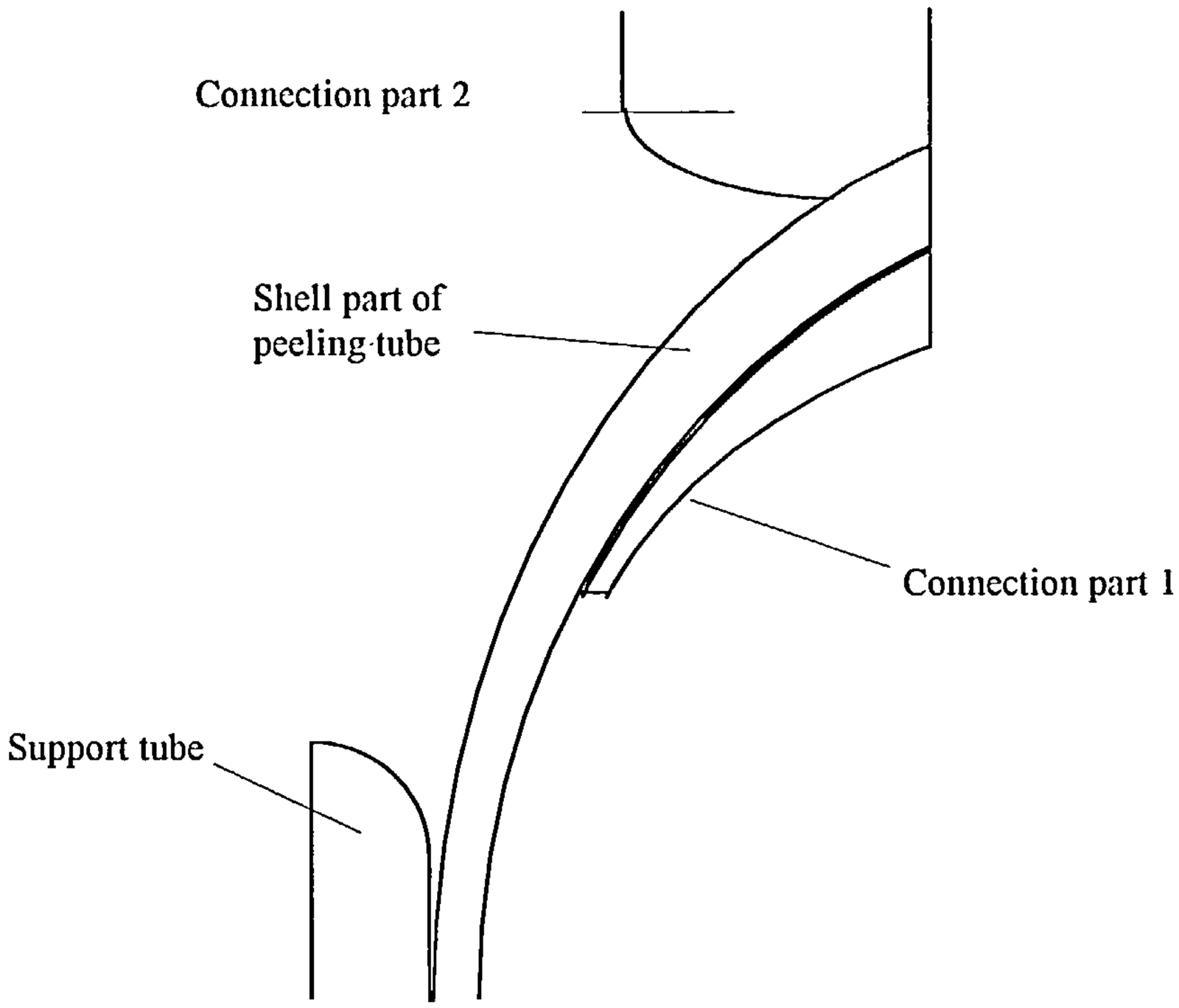

Fig 3-11: The detail of the shell

When a force is applied to the energy absorbing device, the shell part of the peeling tube will sustain the applied load so long as the load is lower than that to cause plastic yielding of the shell. If the force exceeds this limit, the shell will collapse and will undergo plastic deformations (Fig 3-12) and finally the peeling tube will start to peel away from the support tube (Fig3-13).

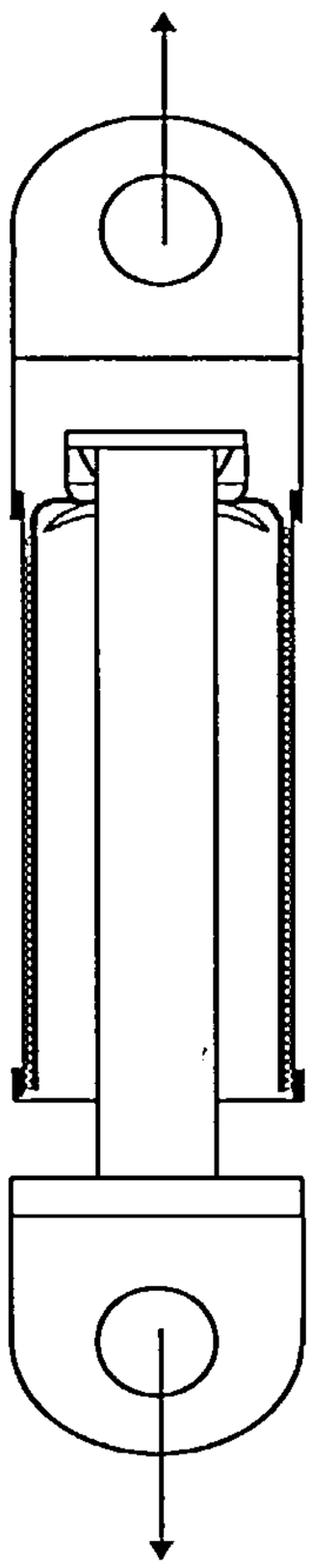

Fig 3-12: The plastic deformation of shell

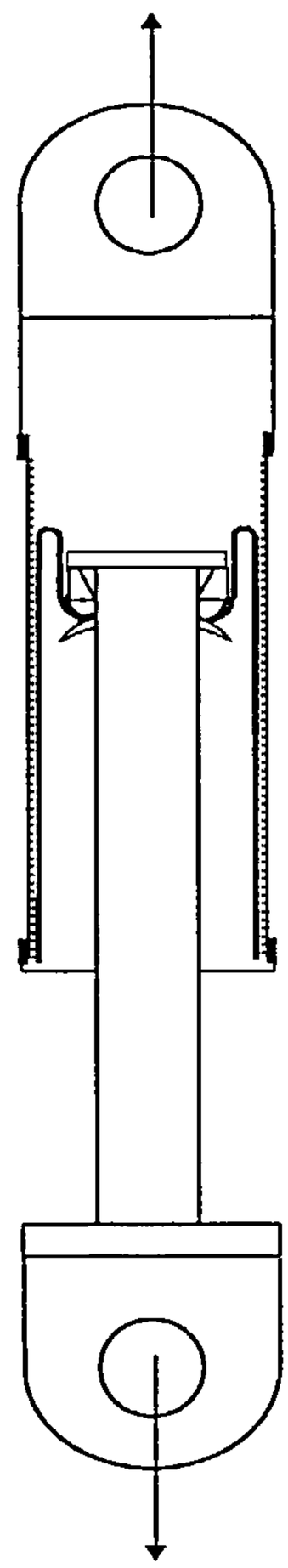

Fig 3-13: The start of peeling process

In order to ensure that the plastic deformation of the shell occurs smoothly before the peeling process begins and to avoid plastic buckling in an undesired mode, a special mechanism has been arranged by gluing connection part 1 with adhesive to the bottom face of the shell (Fig 3-10). During the loading of the device, this shell will have vertical and lateral deflections. It will be demonstrated in the next chapter that if the form of connection part 1 and also the form of the support tube in the A region (Fig 3-14) are chosen properly, then for small deflections, the stresses in the adhesive in the B region will be compressive and there will be no separation of connection part 1 and the shell. As result of large lateral deflection the glue between shell and part 1 in the B region will experience tensile stresses, which will cause the separation of the shell and part 1 (Fig 3-15). Successive separation of part 1 and the shell will ensure that the peeling tube will start peeling from the support tube smoothly.

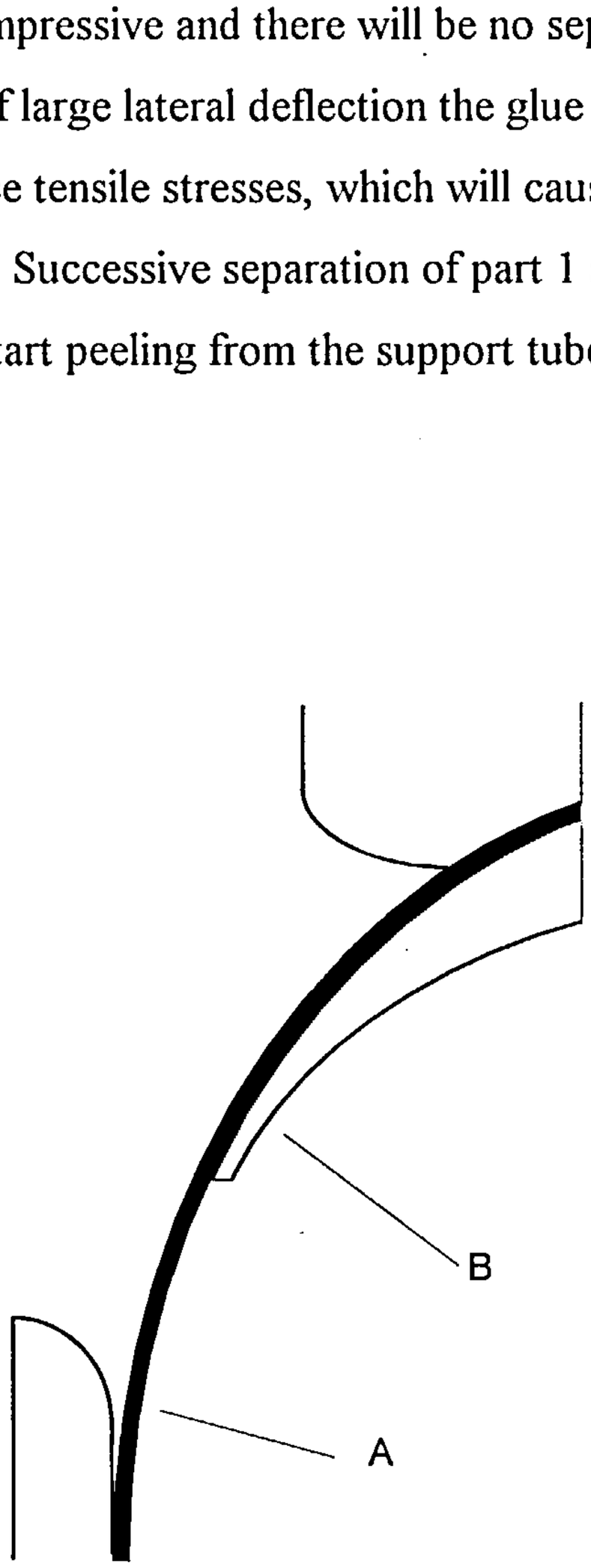

Fig 3-14: The detail of the connection of the shell to part 1. For small deflections, there is no separation between the connection part 1 and the shell.

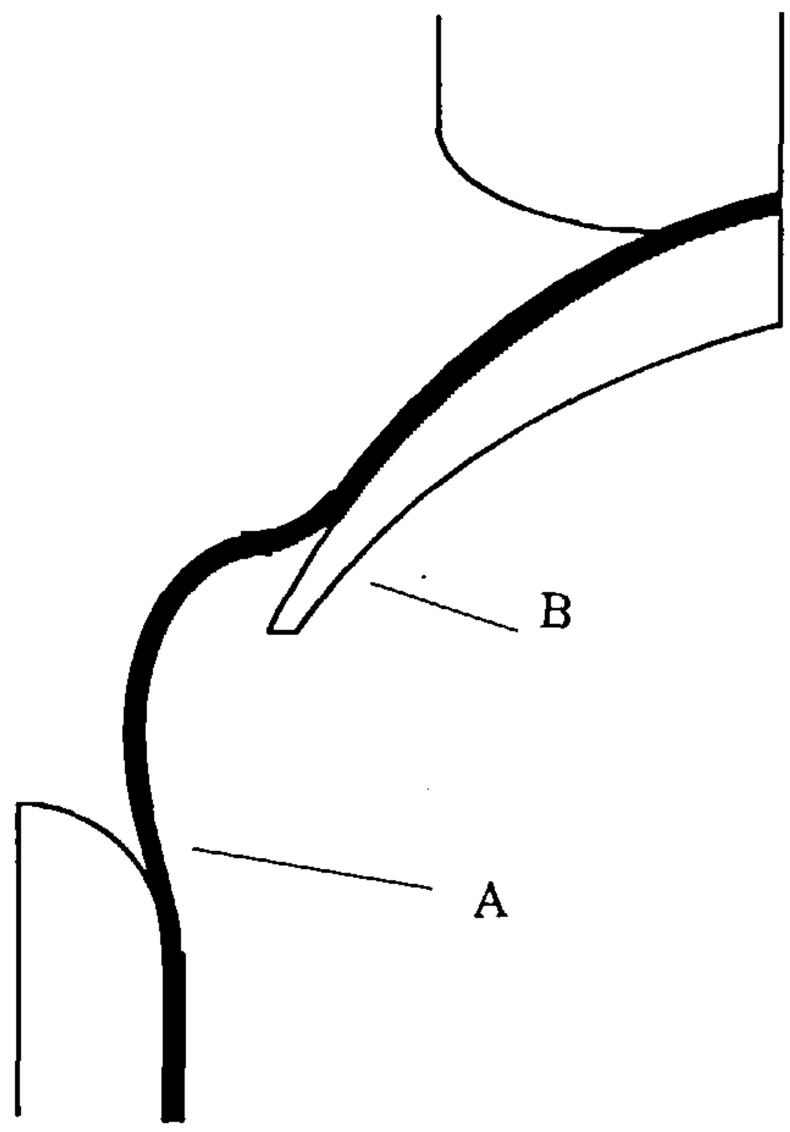

Fig 3-15: The shell starts to peel away from the connection part 1

Connection part 1 has a strengthening role for the shell and as result of the separation of this part from the shell at collapse, the load deflection curve of the device will reduce after a maximum deflection of Δ_a (Fig 3-16). The curve will gradually rise again to a constant level at the start of the peeling process at deflection Δ_b. The device will create a low potential point when it is used in a structure at the start of the energy absorbing process. This is due to the decrease of resistance and will cause all shock waves to be diverted from other directions toward the device. The subsequent rise in the load deflection curve of the device will not reduce the flow of the impact energy into this device because the stiffness of device, even in this stage, is less than the stiffness of other components. This safe and controlled dropping of load deflection is one of the advantages of this device. The thickness and the form of connection part 1 should be designed properly. It must not be too rigid (in comparison to the shell) since this will produce a tensile stress in the B region of the glue under any loading. It should not be too weak to support the upper part of the shell firmly.

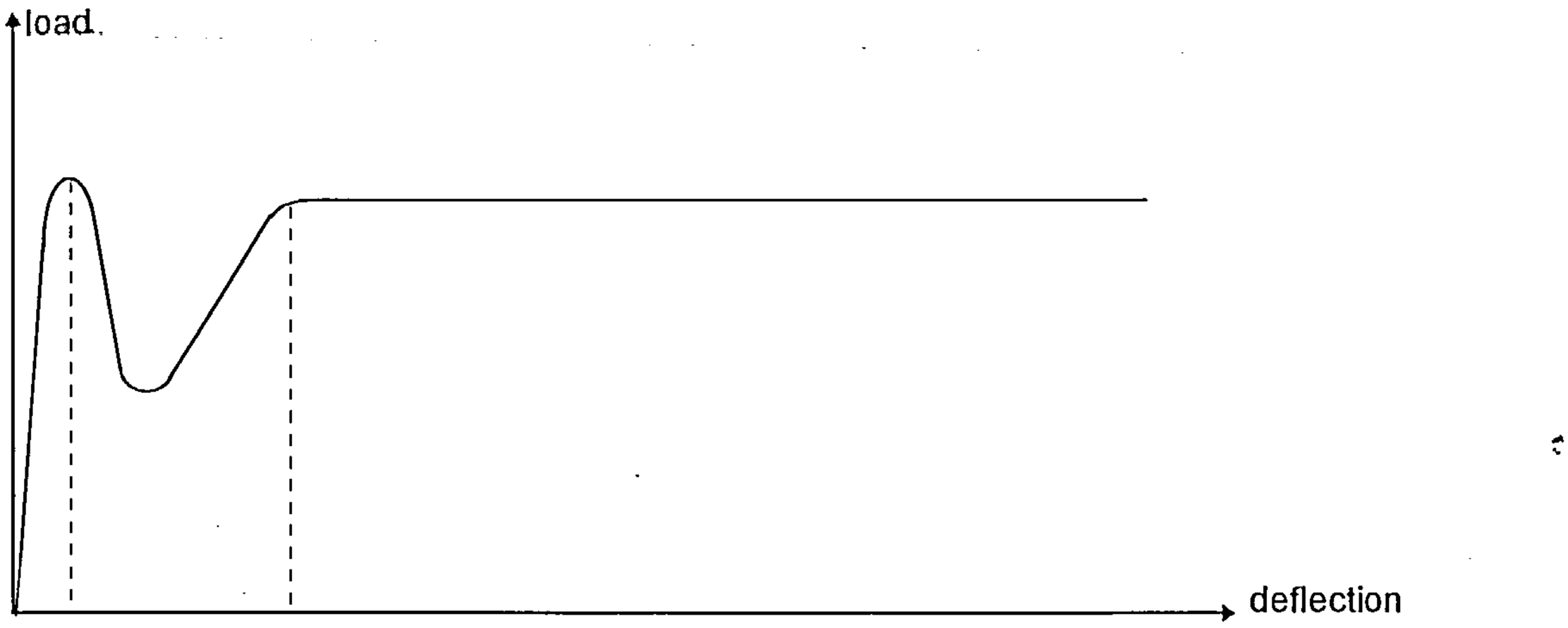

Fig 3-16: Typical load deflection curve of the device

During peeling of the tube from the support tube and the failure of the glue, the peeling tube will be inverted and, therefore, a great amount of energy will be dissipated.

The load is transferred from the peeler bar to the peeling tube via a connection set which consists of connection part 3 and wedges 4 and 5 (Fig3-17). These wedges are placed inside part 3 and are held there by strip springs (Fig3-19). On the surface of the peeler bar and the inner surface of wedges 4 and 5 teeth are formed (Fig3-18). When a tensile load is applied to the device, these wedges interact with the cogs of the peeler bar and ensure that the bar is firmly held (Fig3-20).

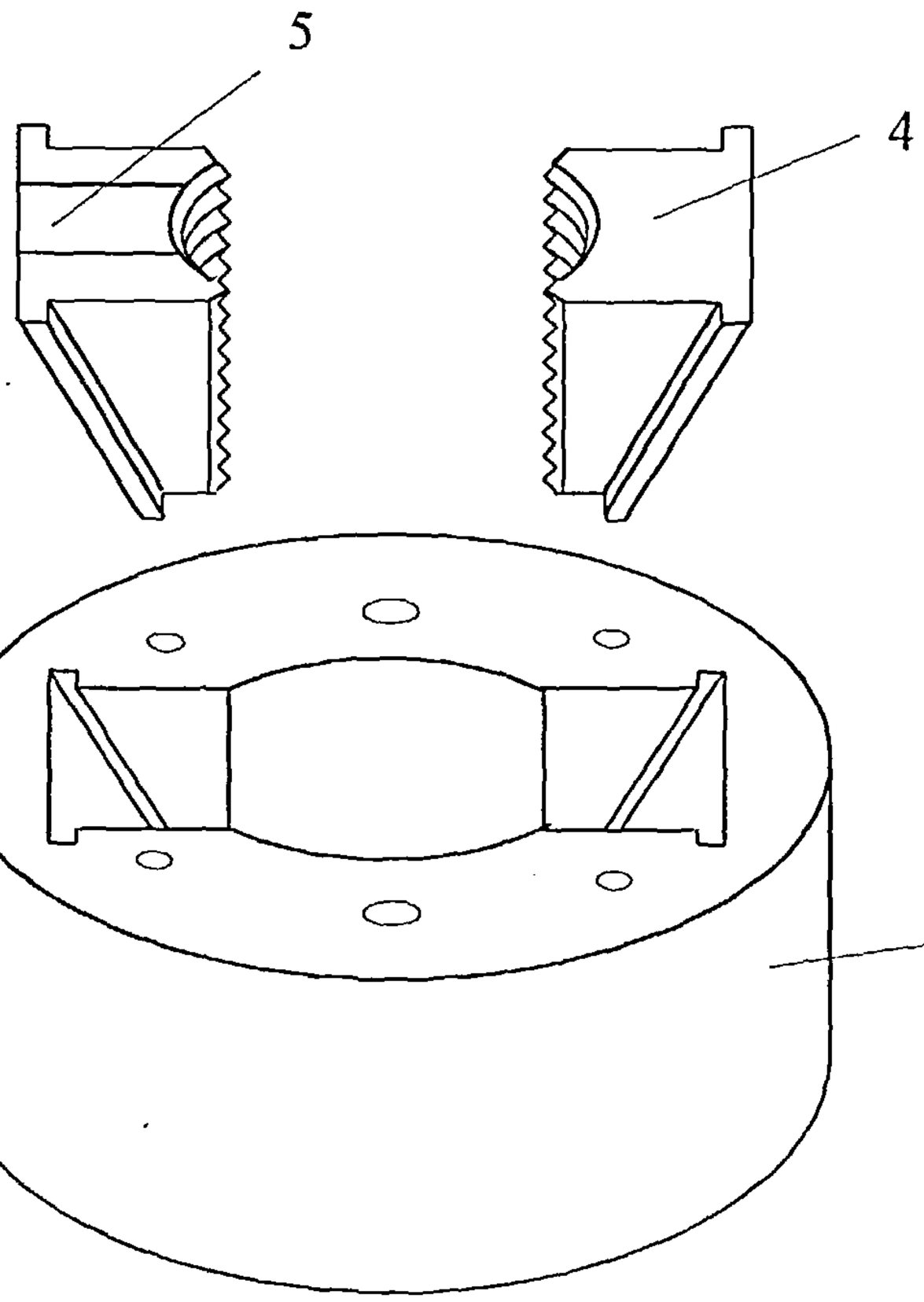

Fig 3-17 Connection set

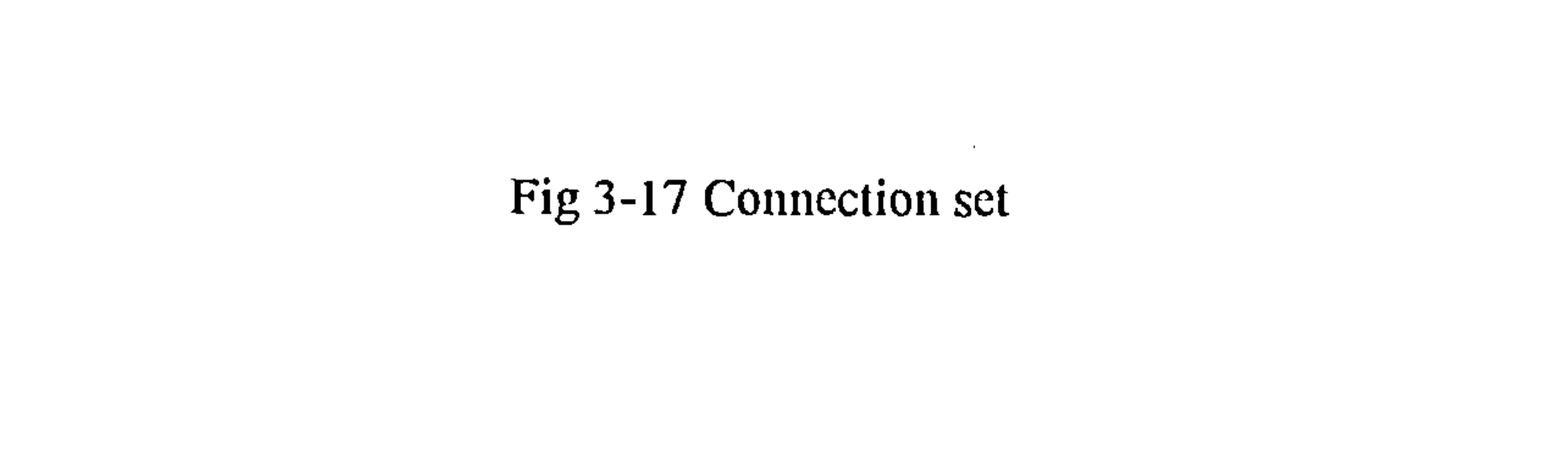

Fig 3-18 : Wedges 4 and 5

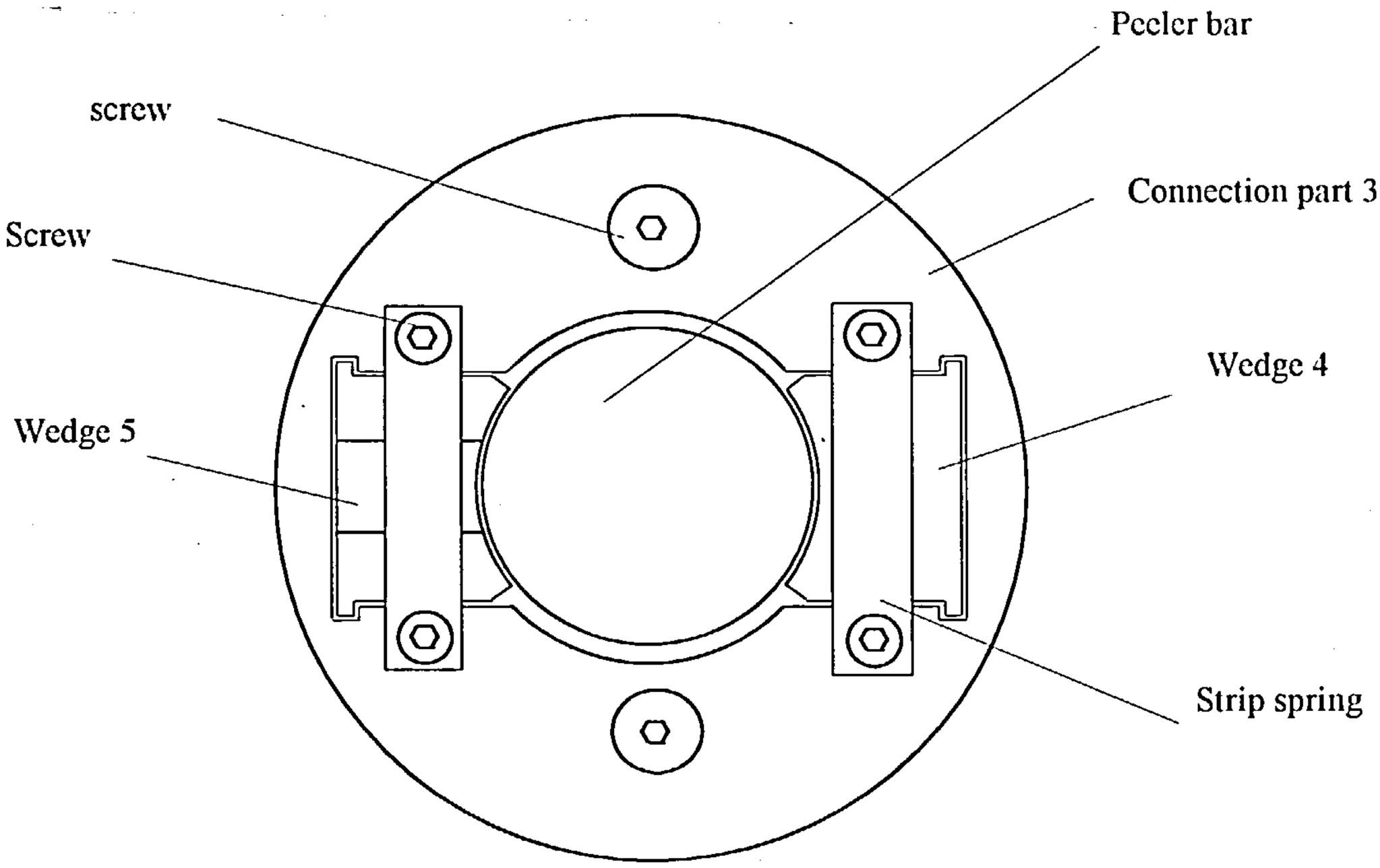

Fig3-19: Connection set from top view

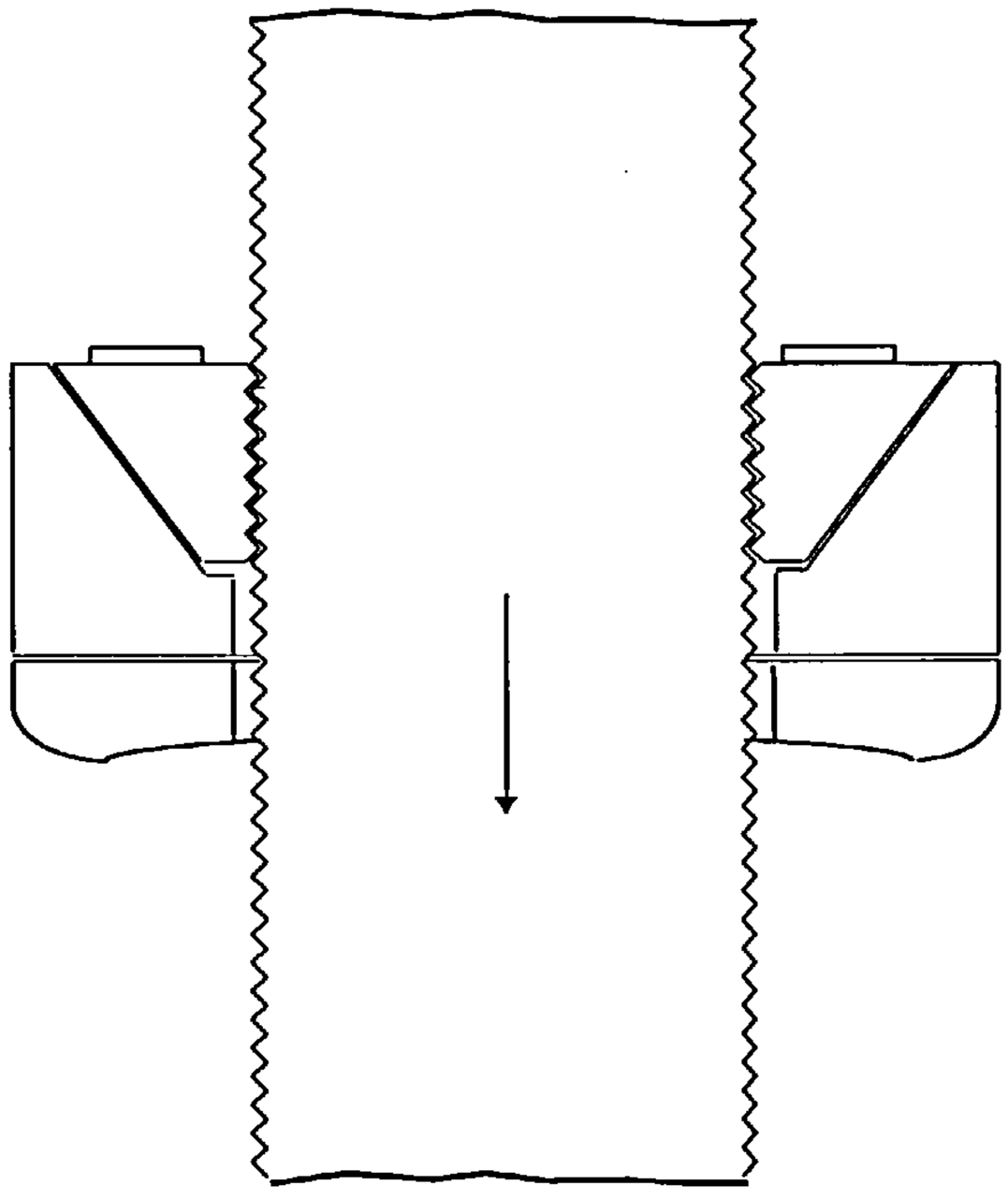

Fig 3-20: The connection set holds the bar firmly during the application of the tensile load

If the loading changes its direction during a loading cycle to become compressive, the connection set will let the bar to move through freely (Fig 3-21). In this case the wedge 5 will move outward and produce a clearance, which will result in the release of the bar from the interaction of these wedges (Fig3-22). Wedge 4 will remain almost unmoved because it has flat top surface and the spring will not let this wedge move significantly outward during a compressive force. Wedge 5 has a inclined top surface and the amount of slope will determine its maximum outward movement. By this arrangement the bar will move in a 'zigzag' path through the connection set and the device will become shorter under this compressive loading.

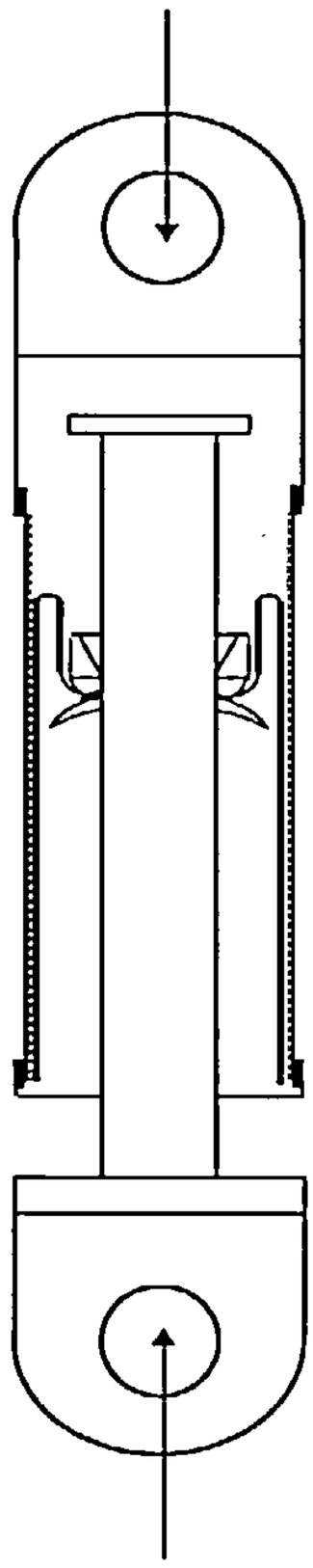

Fig 3-21: Compressive loading of the device

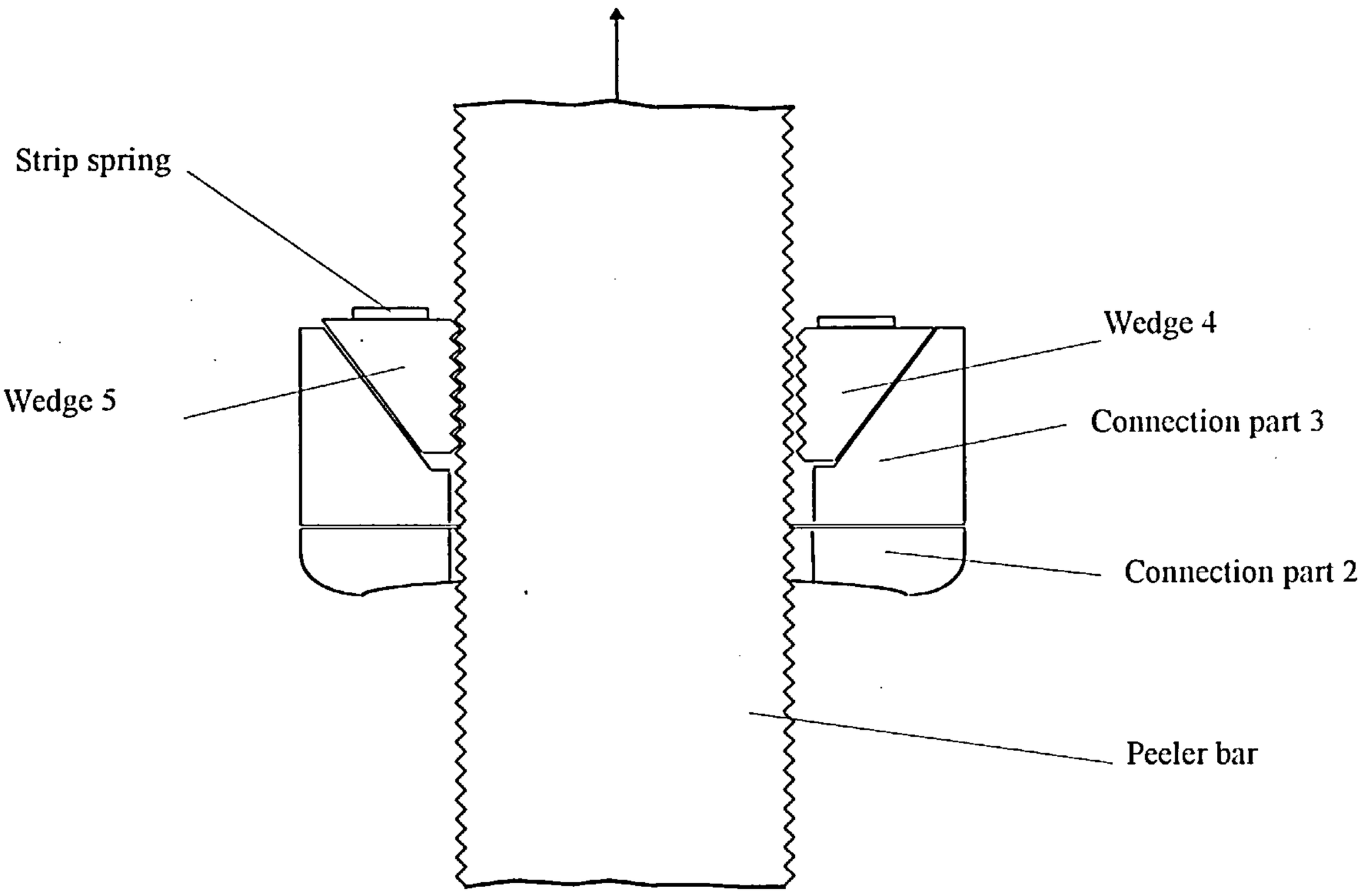

Fig 3-22: Wedge 5 moves outward and releases the bar

As soon as the compressive motion of the bar stops and the direction of force changes again to tensile, wedge 5 will return back quickly to its original position and then immediately the teeth of the wedges and bar will interact. The free movement of the bar is halted and the device acts as a tensile member (Fig 3-22). This quick interaction of the bar and the set of wedges is the reason why wedge 4 is not allowed to move outwards during a compressive loading. This ensures that the bar will not slip from the wedges if the load becomes tensile again. Wedge 4 is not firmly fixed to part 3, because some small movement, especially downward, is needed for this wedge to have proper interaction with the bar. Otherwise the bar or the wedges may be damaged.

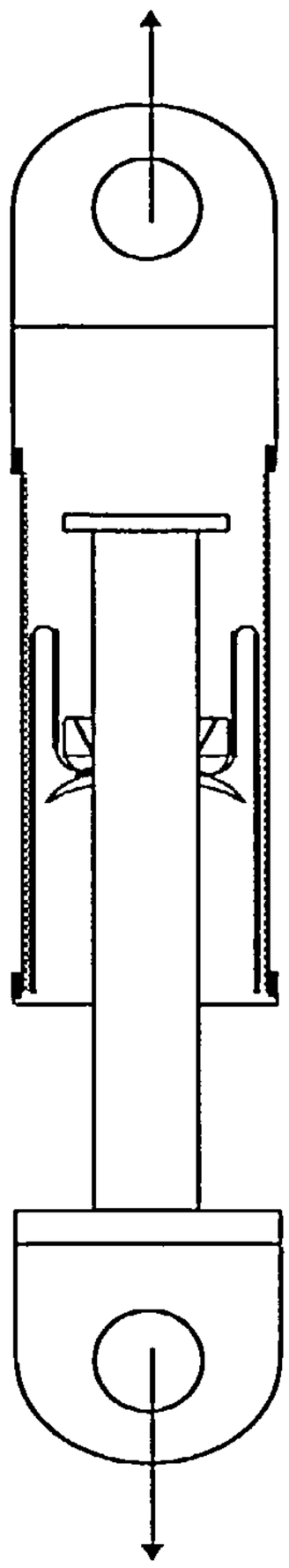

Fig 3-23: The tensile loading of the device after applying a compressive loading

In order to illustrate the importance of this mechanism and the 'zigzag' movement of the bar during a compressive loading, the release and hold process of the bar will be reviewed.

It has been mentioned that in this energy absorbing device, the load is transferred from the peeler bar to the peeling tube via a connection set which consists of connection part 3 and wedges 4 and 5. In the case of a tensile force, the teeth of the bar and wedges 4 and 5 interact and the wedges hold the bar firmly. In the case of a compressive force, this connection set will release the bar and the device will not have any resistance to this loading:

The top surfaces of wedge 5 is inclined while wedge 4 has a flat surface. This will prevent wedge 4 from moving outward any significant amount. In the case of a compressive force, the bar pushes wedge 5 outward to produce a clearance and to disengage a tooth from wedge 4 (Fig 3-24). After this, the bar moves toward wedge 4 for disengaging a tooth from wedge 5 (Fig3-25). Again the bar will move toward wedge 5 in order to disengage another tooth from wedge 4 and this procedure will continue so long as a compressive force is applied on the device. Thus the bar will move freely through the connection set in a 'zigzag' path. The device has the ability to become shorter than its original size in the structure and a limit can be defined for this by considering a restriction for free movement of the bar (for example by limiting L in Figure 3-3).

If wedge 5 has an excessive outward movement during a compressive loading, the 'zigzag' motion will be eliminated. The prohibition of wedge 5 from excessive movement can be achieved by limiting the slopes of the top surface of wedge 5. In the following the importance of this zigzag movement for the device will be demonstrated.

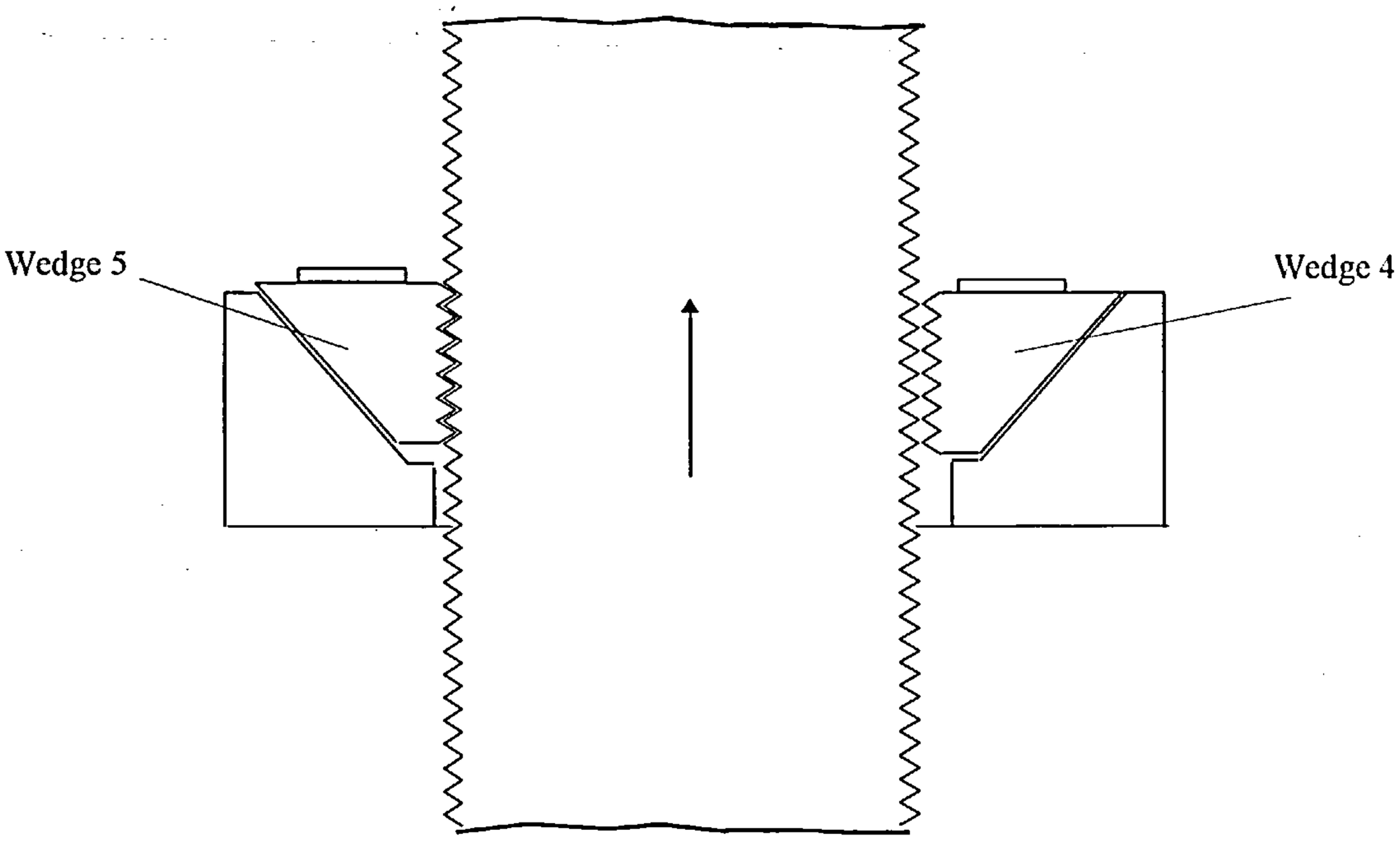

Fig 3-24: The bar has moved toward wedge 5 in order to disengage a tooth from wedge 4

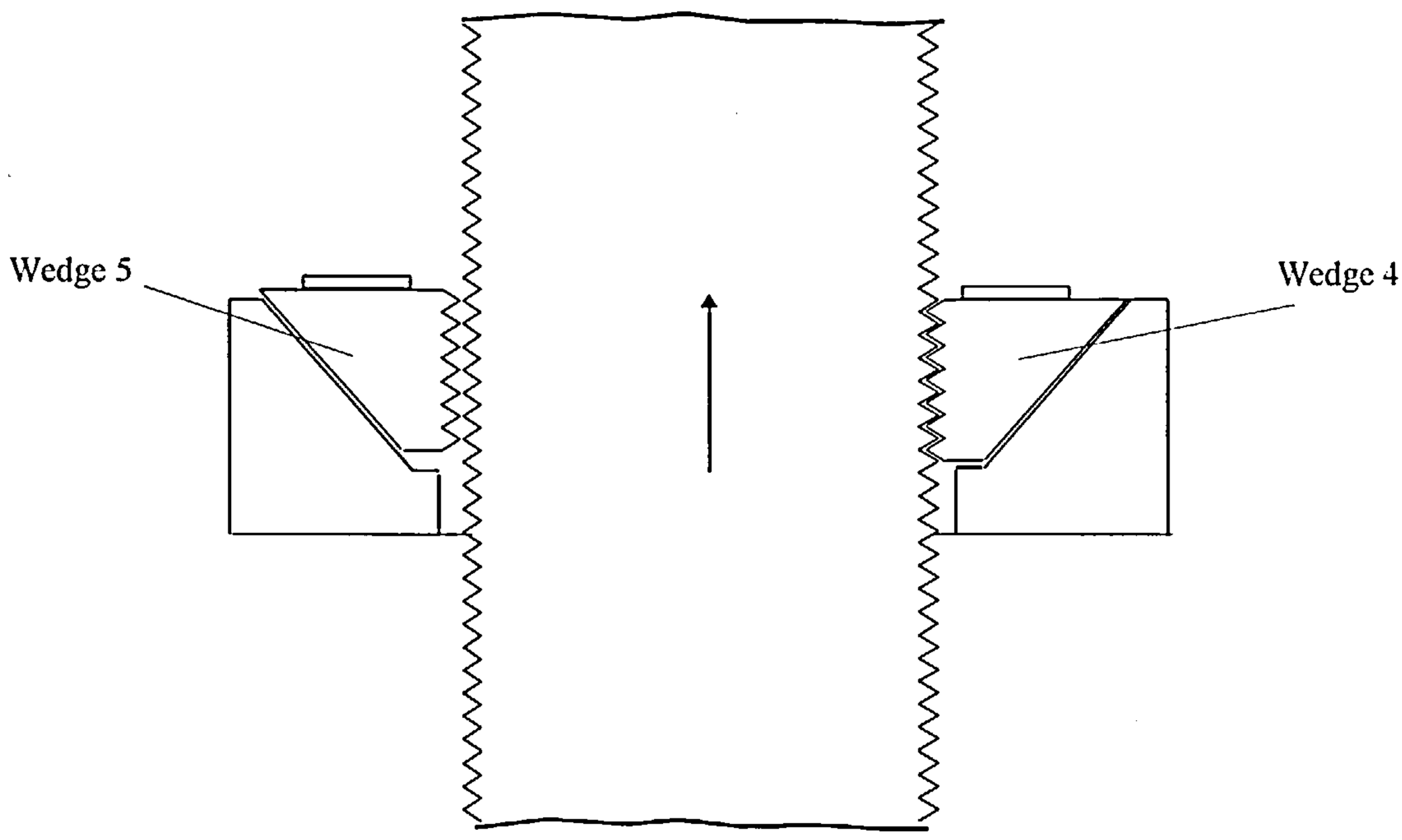

Fig 3-25: The bar has moved toward wedge 4 in order to disengage a tooth from wedge 5

If the load suddenly becomes tensile while the wedge 5 is out (Fig3-26), which is the worst situation, then the bar will move toward wedge 5 in order to disengage a tooth from wedge 4 (Fig3-27).The bar will attach to this wedge and as well as disengaging a tooth from wedge 4, will bring down wedge 5 immediately. By returning wedge 5 to its original position, both of the wedges will interact with the teeth of the bar and hold it firm. The bar will not slip from the connection set and this is the advantage of the 'zigzag' movement, which causes wedge 5 to return back quickly to its original position as soon as loading becomes tensile.

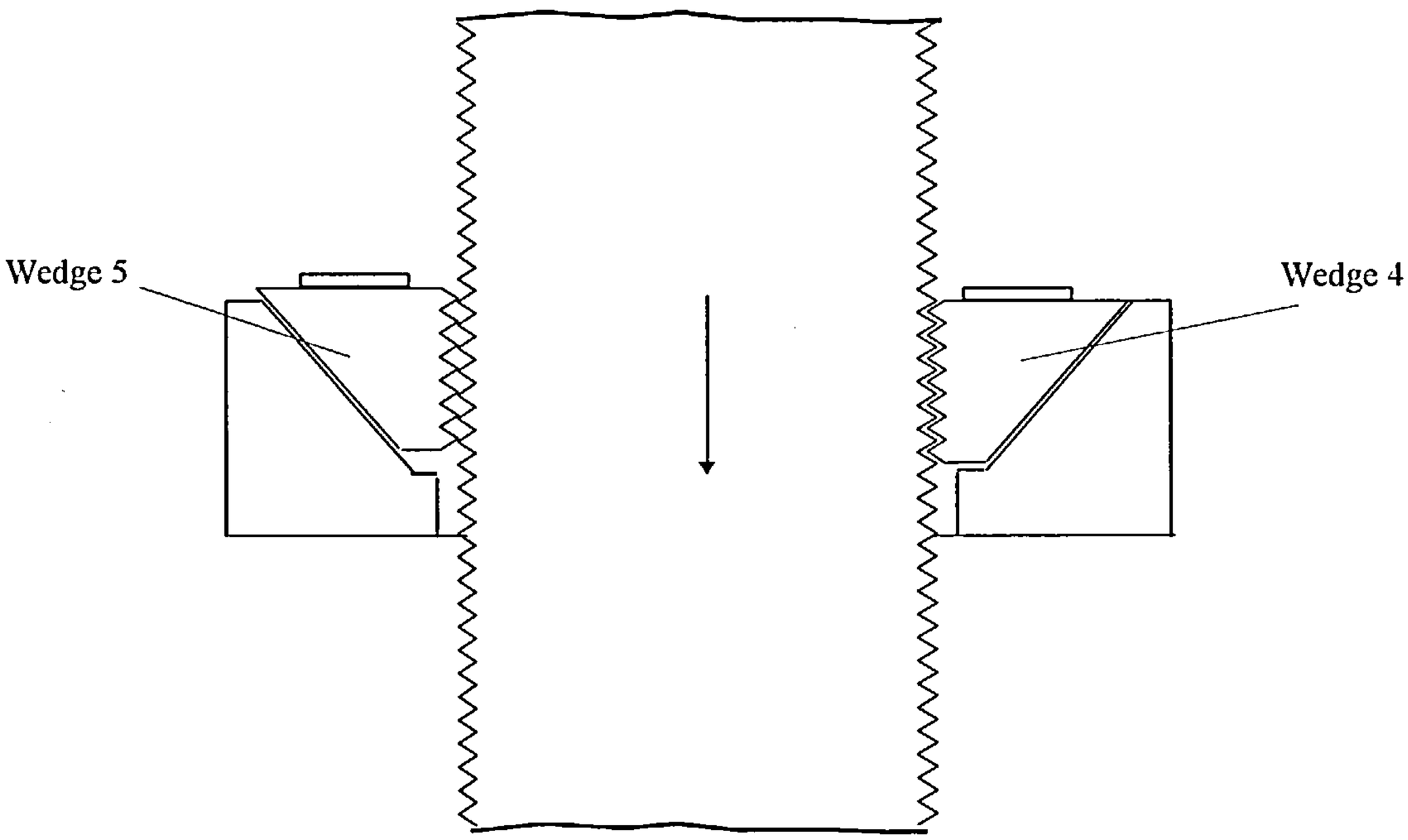

Fig 3-26: Loading becomes tensile while wedge 5 is out

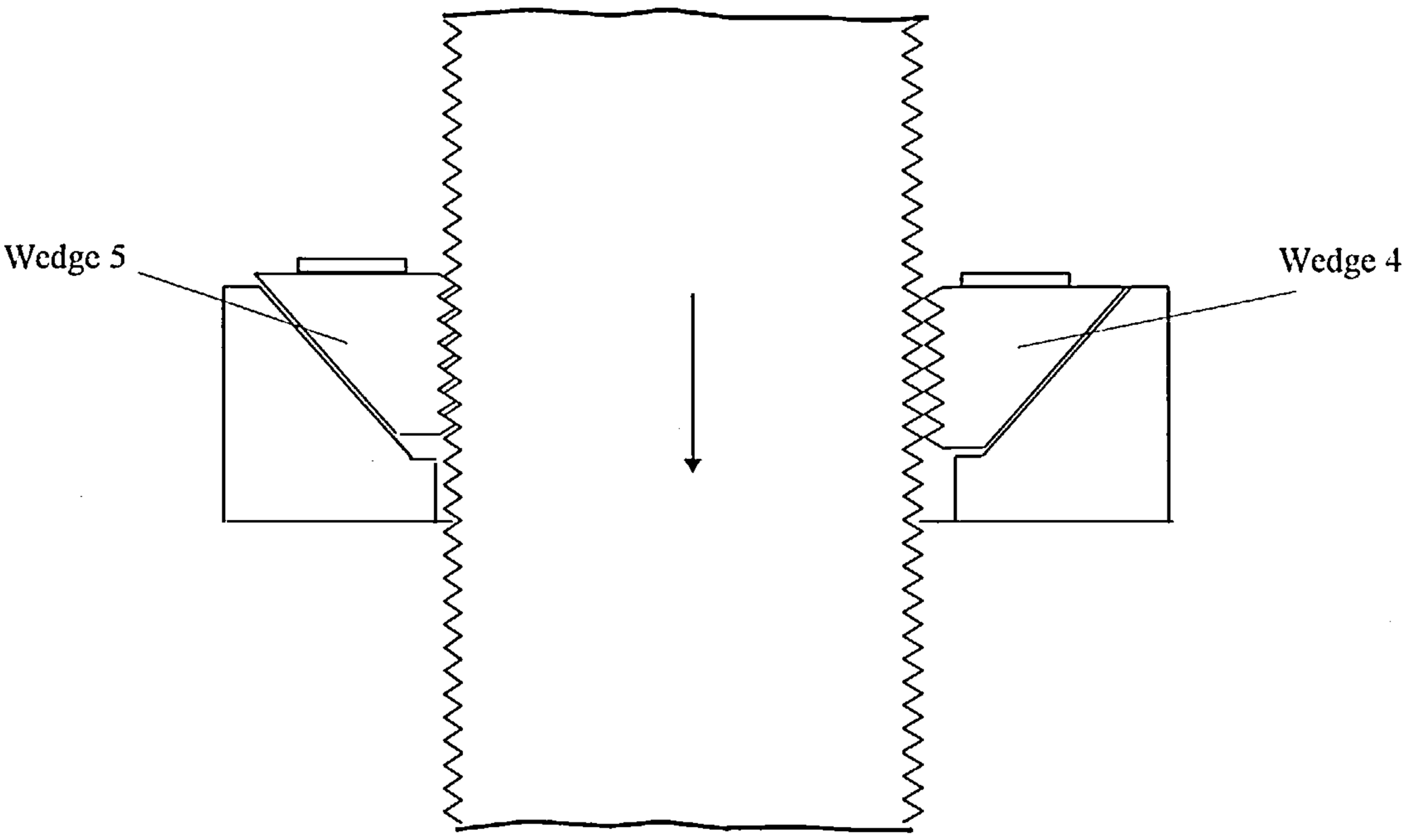

Fig 3-27: The bar has moved toward wedge 5 in order to disengage a tooth from wedge 4 and, therefore, assists the spring to return wedge 5 quickly back to its original position

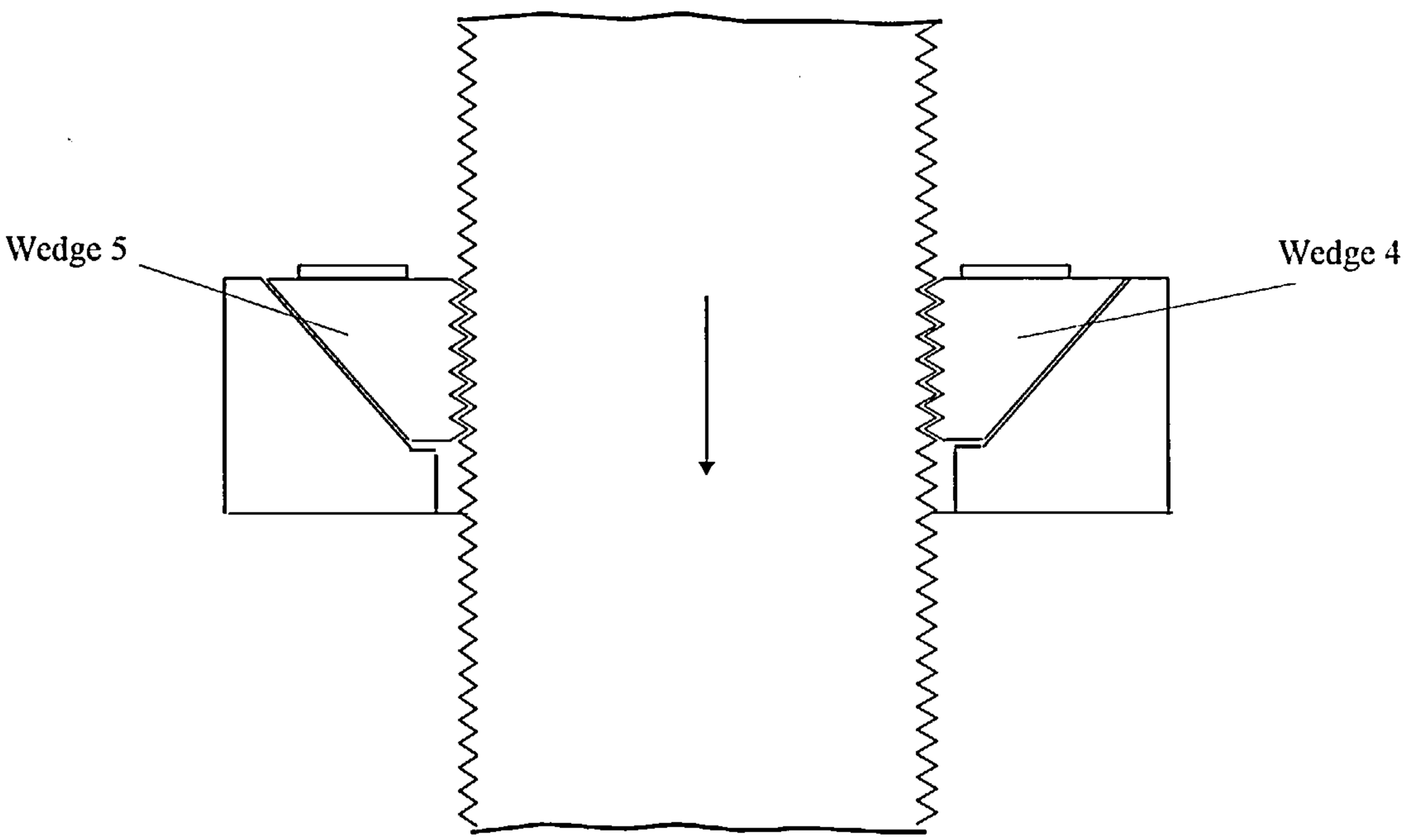

Fig 3-28: The wedges have held the bar firmly

In order to explain the importance of this arrangement, the behaviour of the device, when the both of these wedges have been allowed to move outward during a compressive loading, will be examined.

Fig3-29 shows the moment at which both of the wedges have come out during a compressive loading and the strip springs applies pressure on them to return to their original place. In this instance, if the loading changes suddenly to tensile, the bar will move downward quickly, before the wedges are able to return to their initial position under the pressure of the springs. In this case the cogs of the bar will make contact with the cogs of the wedges only by their tips (Fig3-30) and consequently after yielding them, the bar will escape. This yielding and escaping will never occur if the wedge 4 is not allowed to move outward during a compressive loading.

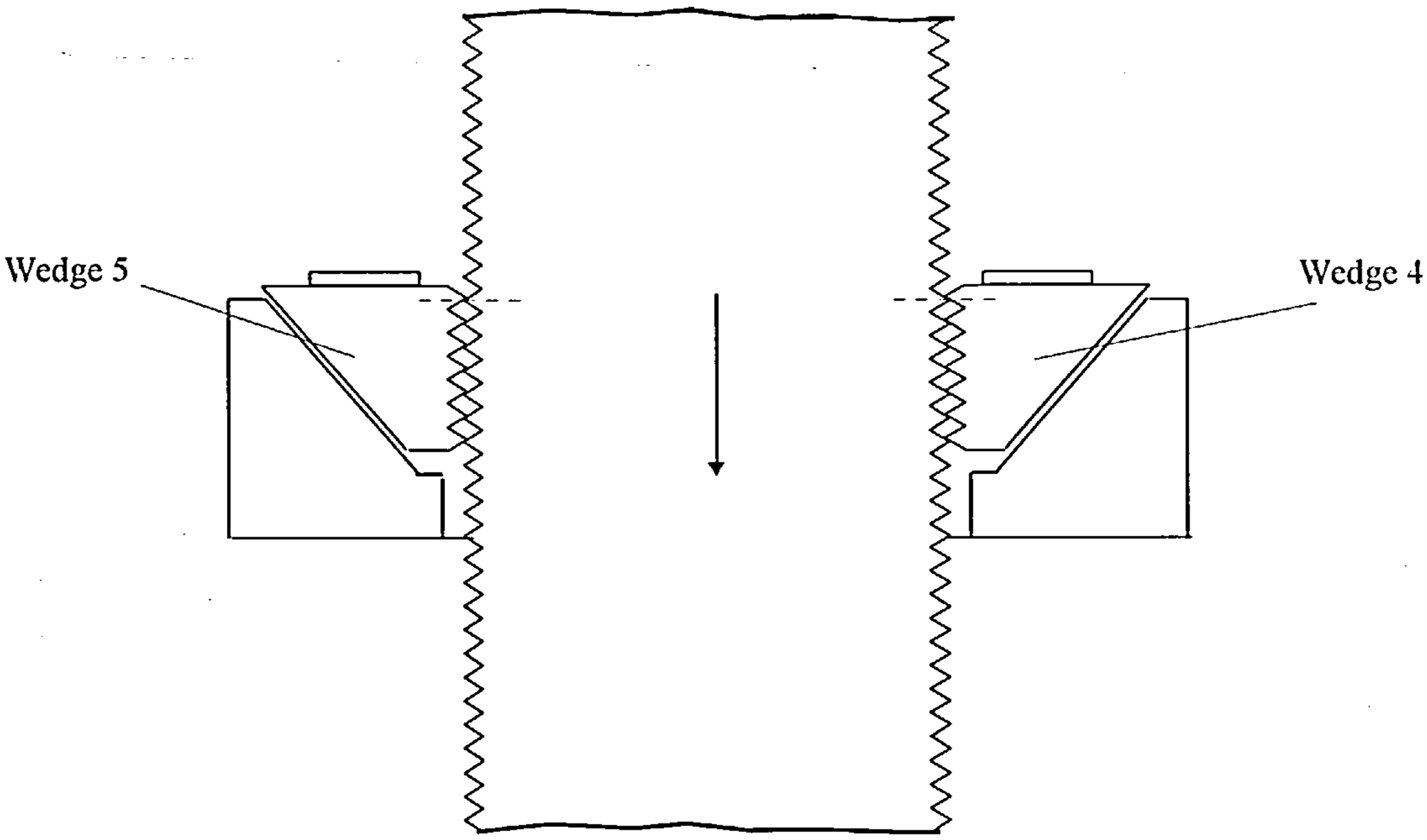

Fig 3-29: This figure shows the instance when both of the wedges have come out during a compressive loading and load becomes suddenly tensile.

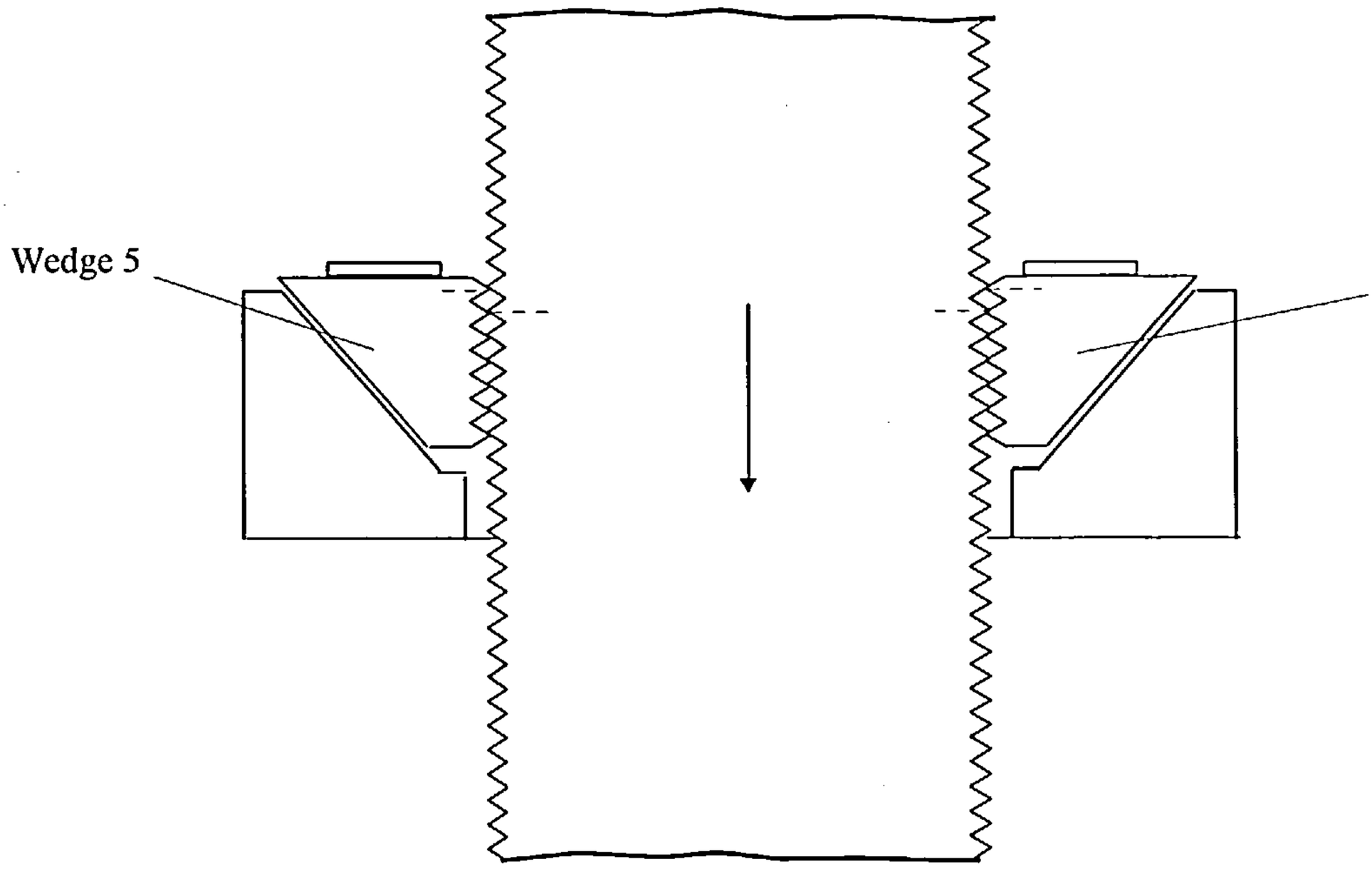

Fig 3-30: The figure shows the instance that the bar has made contact with the wedges at their tips

Figure 3-31 shows the configuration in which a guiding ring has surrounded the connection set in order to guide it during the failure of the shell and the start of the peeling process.

In order to be able to install the device in structures with long spans a fixing part should be added. Figure 3-32 shows a configuration in which the device has been lengthened by using an additional tube.

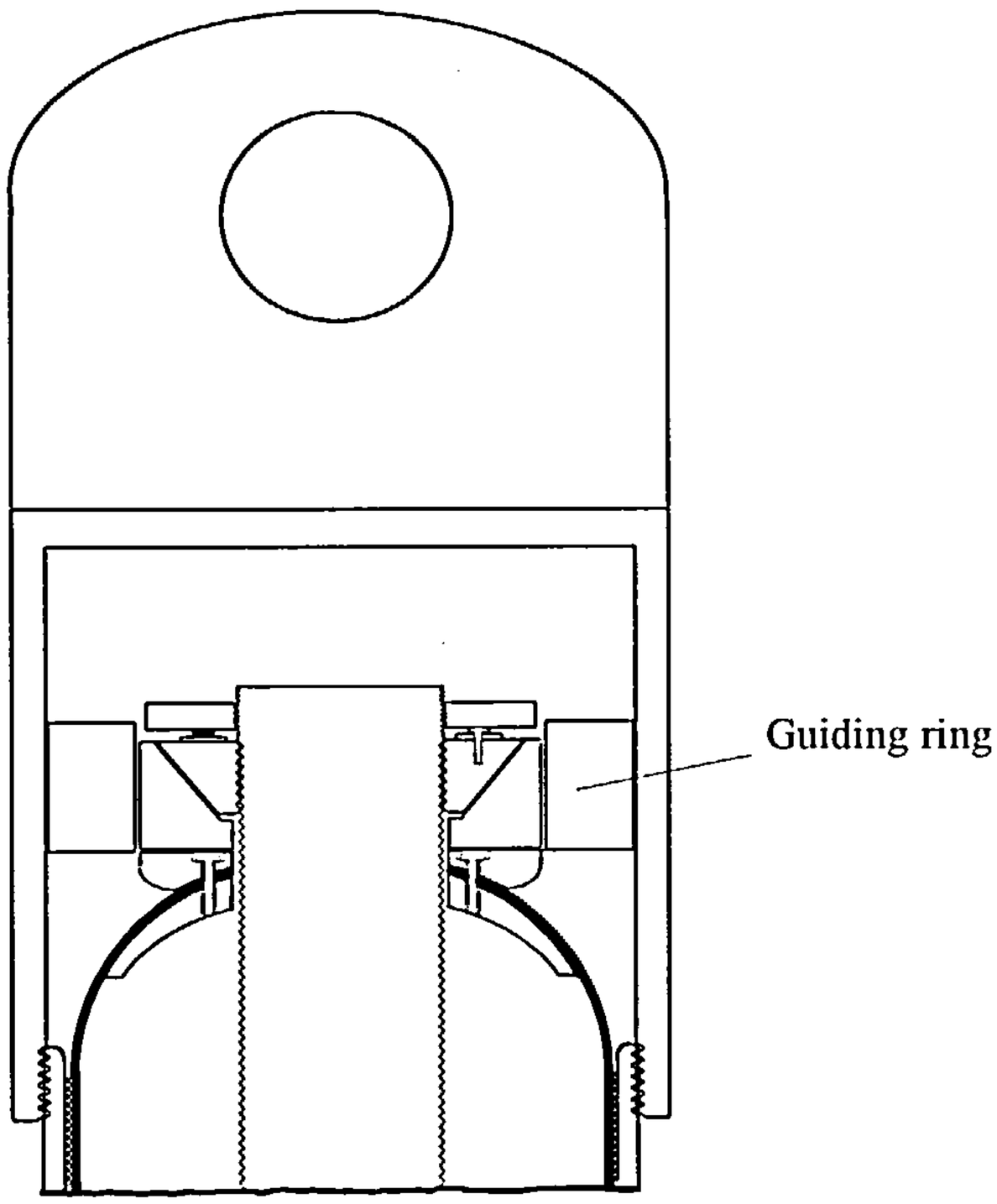

Fig 3-31: A ring has been used to guide the connection set during failure of the shell

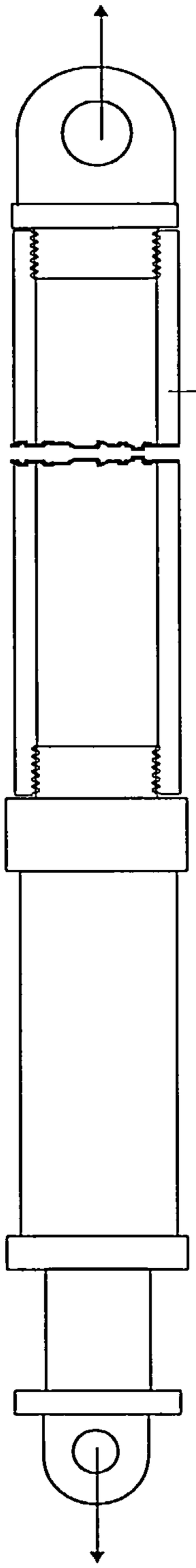

Tube for lengthening the device

Fig 3-32: Elongated configuration of the device which can be used in large spans

The device is reusable by replacing the set of peeling and support tubes and connection part 1.

Hinge connections are used to insert the device into structures. In two dimensional structures, simple pin connections and in three dimensional, sphere hinges are used.

The following properties are associated with the device:

- In a compact form, it has the capacity of dissipating high amounts of energy.
- It has a well defined and stable yield point that can be adjusted to any desired load.
- Its post impact resistance is perfectly reliable.
- under cyclic loading it will keep its energy absorbing capability.

So far, these properties have not been found together in a single device.

In view of these properties it can be seen that the device could be used as a tensile bar in a structure to resist dynamic loading, i.e. in seismic resistant design. Under service load, it will behave like ordinary member, but during large seismic loading it will limit the translation of force and will protect the structure.

For example, if two devices are used as the braces of a single degree freedom structure Fig 3-33, a high resistance against dynamic load is achieved. If a high impact on the mass M_a (either by the movement of supports or a direct impact on it) is considered, in a direction to cause a rightward movement (Fig3-34), the device L will be activated and as well as increasing in length, will absorb the energy of impact. Simultaneously the device R will not have any resistance to the applied compressive load and, therefore, will reduce in length. This reduction in length is very important for the device because, when the leftward movement of mass M_a starts (Fig3-35), the device R acts quickly as a tensile member without waiting for the structure to return back to its original situation. During the leftward movement (Fig3-36) the energy will be absorbed by device R and device L will shorten and compensate the deformation, which had occurred during the pervious cycle. By the start of the next rightward motion, again device L will act quickly to absorb the energy and device R will shorten. This procedure will be repeated until the total energy is dissipated.

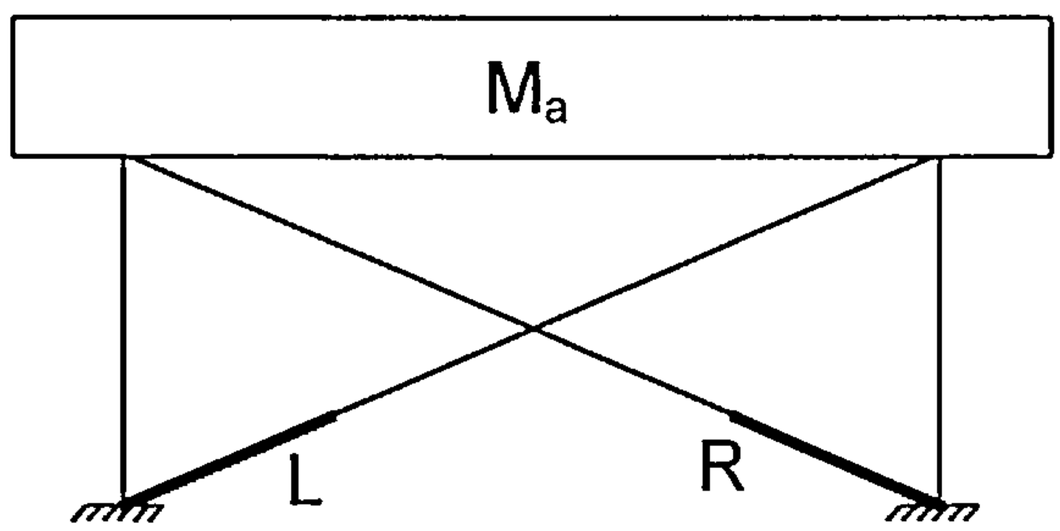

Fig 3-33: A single degree freedom structure equipped with the energy absorbing device

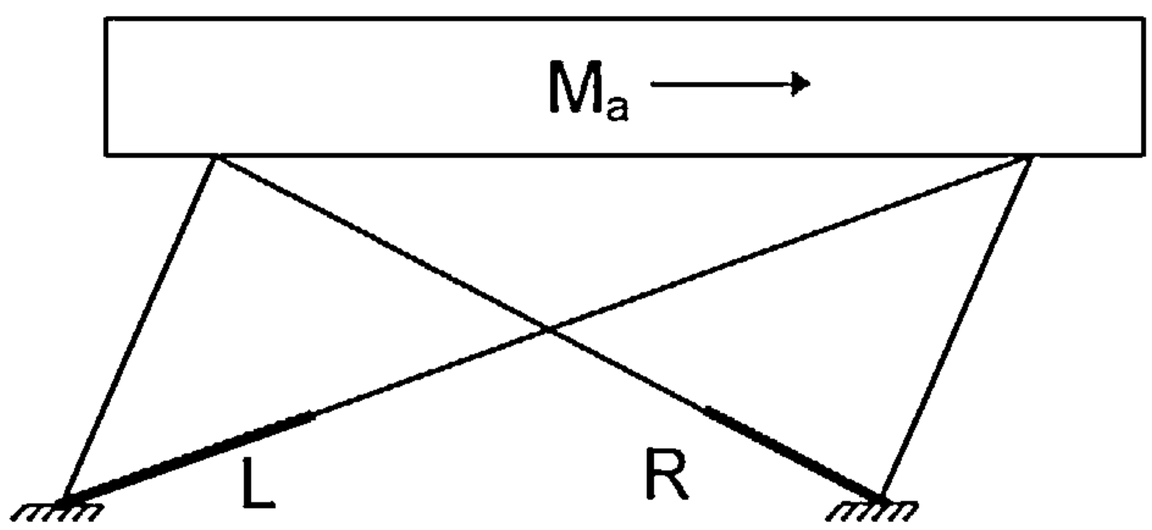

Fig 3-34: The single degree freedom structure when it is impacted from the right. Device L absorbs the energy

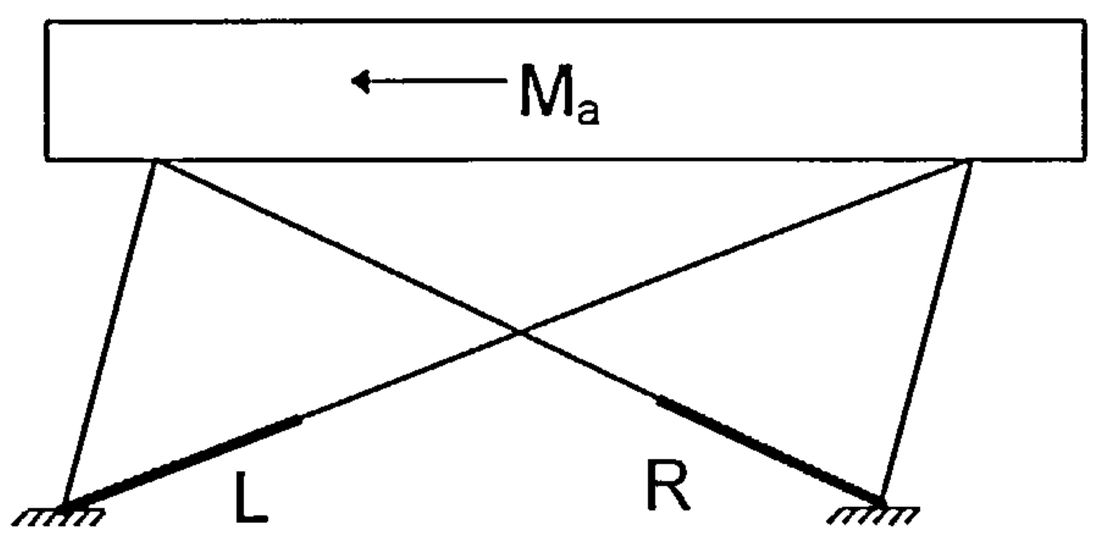

Fig 3-35: Starting of the leftward movement of the structure, device R starts to absorb the energy.

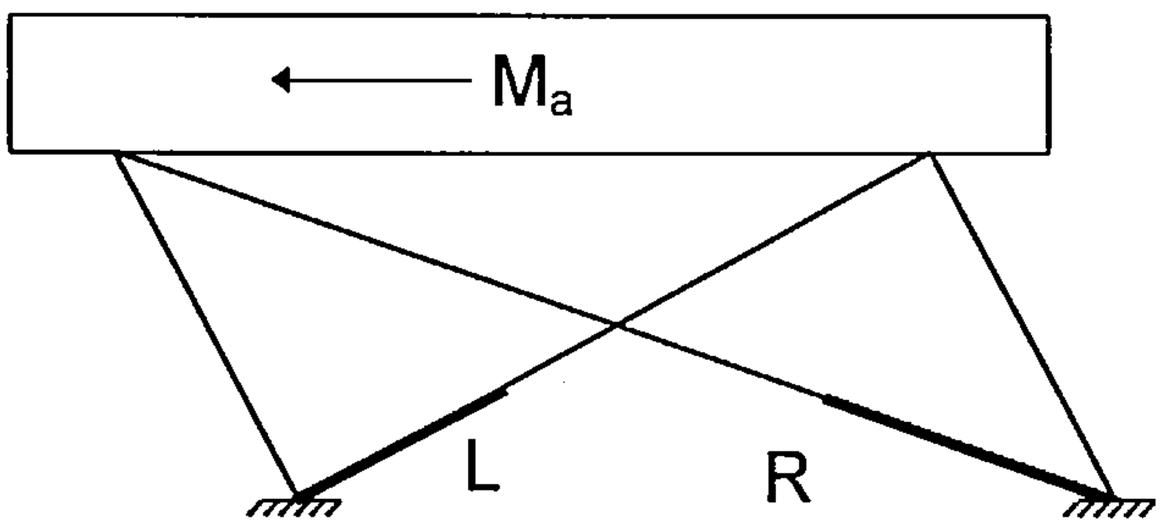

Fig 3-36: The leftward movement of the structure which causes device L gets shorter than it original length

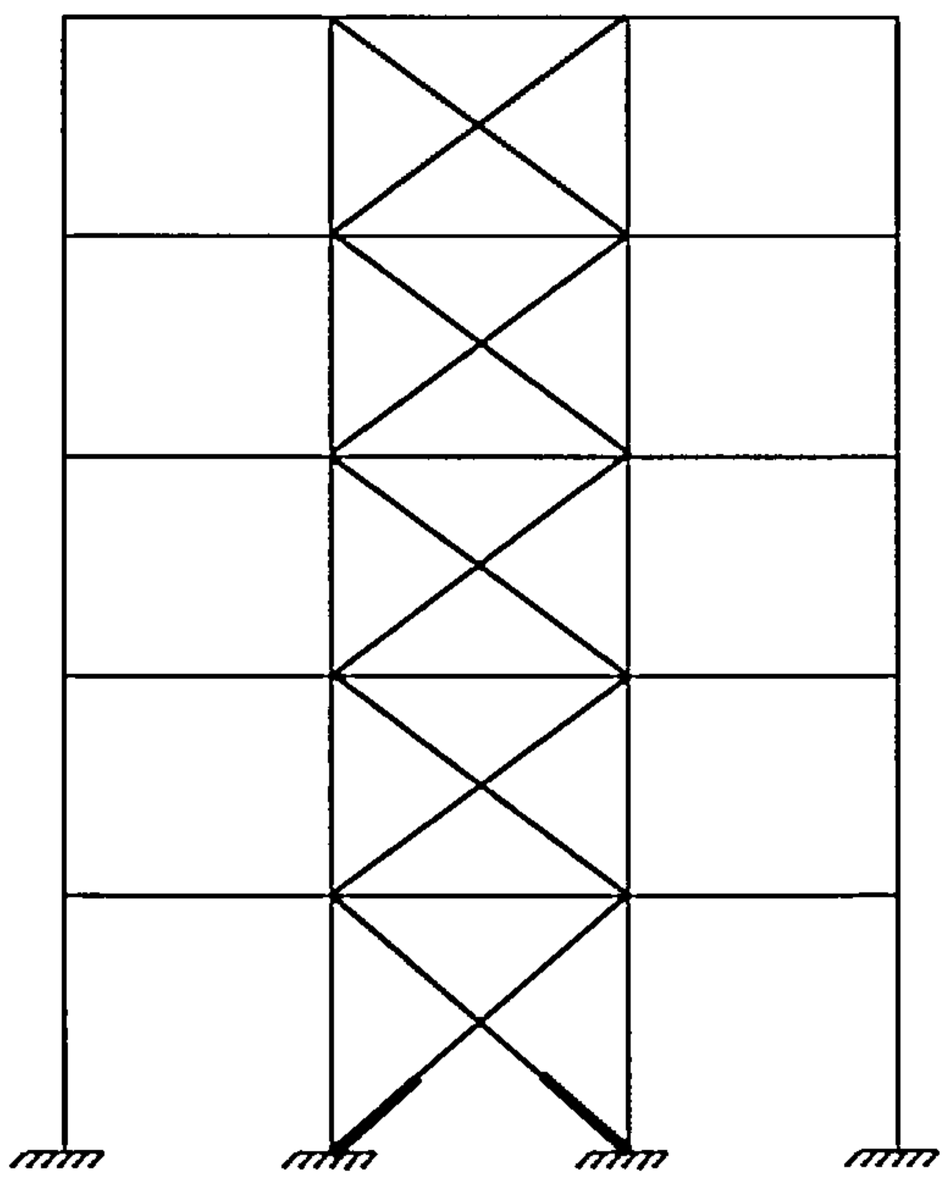

Fig 3-37: A multi-storey building equipped with the energy absorbing device

At the end of motion, only the damaged parts of the energy absorbing device need be repaired or replaced.

The behaviour of the device is the same if it is used in a multi-storey building (Fig3-37). A first soft storey will be created to isolate the structure from seismic shocks. In this configuration the frame will behave as a braced moment resistant frame which resists low rate lateral forces. In the case of a severe earthquake shock on the bases, however, the devices will act and as well as absorbing the energy, it will limit the translation of energy to higher levels in the structure. The main part of the displacement will appear in this isolator level and the other floors will not have so much movement and acceleration. The bracing of the upper floors will be provided by the ordinary structural members with sufficient rigidity to have enough stiffness in these floors.

As a final example, if one energy absorbing device is inserted as a member of a framework, a high impact resistance will be achieved. A typical framework has been shown in Figure 3-38. Figure 3-39 shows the deflected form of this framework.

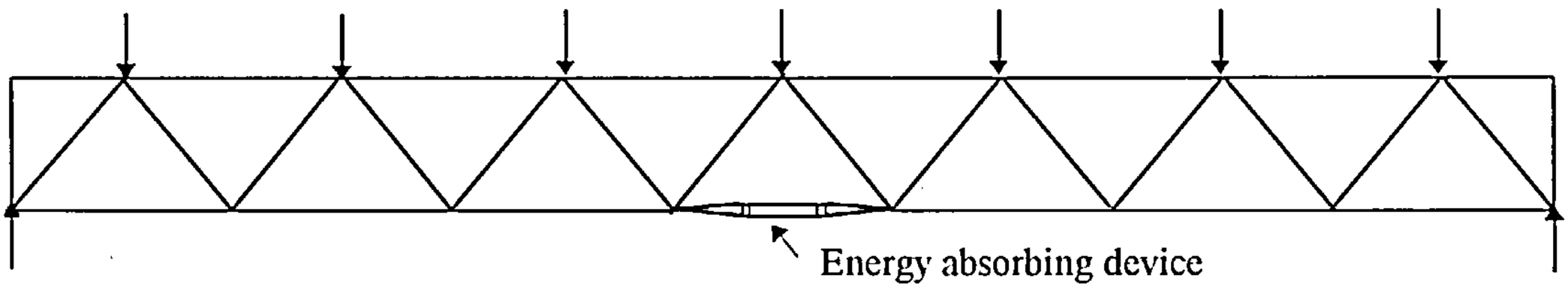

Fig 3-38: A framework which has been equipped with energy absorbing device

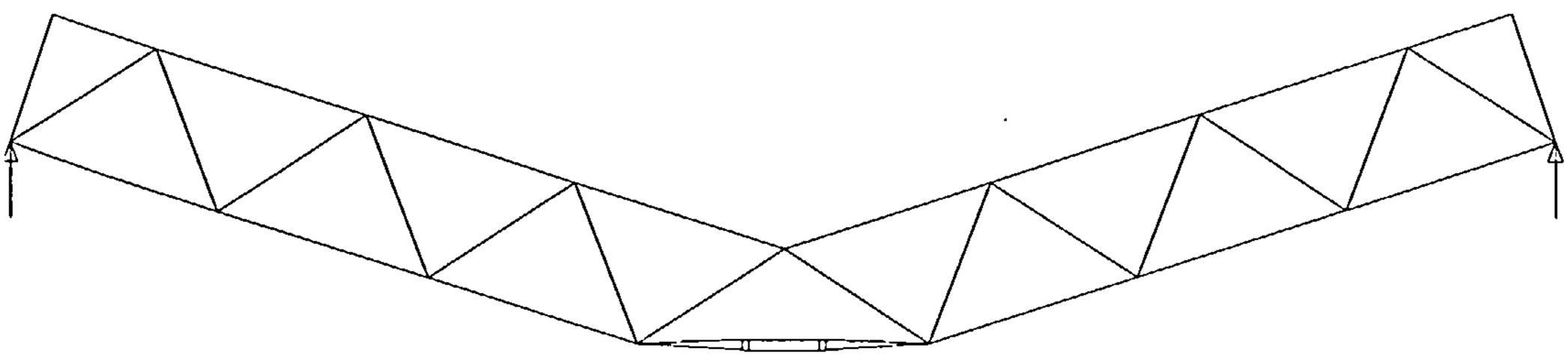

FIG 3-39: The deflected form of the framework.

The examples of the figures 3-33, 3-37, 3-38 will be discussed in detail in Chapter 5.

The following are the advantages for the use of the device in structures:

- Improved dynamic strength of structures, by absorbing the energy.
- Isolation of the structure from its supports and the controlled shock wave transfer to the other parts of structure.
- Damping of structures will remain high at all times due to the ability of the device to reduce in length under compressive forces.

The numerical and analytical computation of this device is represented in the next chapter.

Chapter 4- Computational modelling of the Energy absorbing device

The numerical modelling of the device will be explained in this chapter.

The design and associated calculation of the shell part of the peeling tube will be considered first. This is because it is the most importance part in the determination of the load deflection curve for the device subjected to axial loading.

4-1 Analysis of the shell

In this section typical forms of shell will be considered and calculations will be carried out for different dimensions of the shell.

Three stages will be considered for the numerical work for determining the behaviour of shell and these are :

(i) A nonlinear dynamic analysis for the plastic deformation of shell.

(ii) The peeling process.

(iii) Elastic Buckling analysis.

The Lusas Finite Element Program has been used for the nonlinear analysis of the shell. Initially, a decision for the general form of the shell must be made. For doing this, two aspects for the design should be considered. Firstly, the highest yield limit for the shell for all possible dimensions of tubes must be achieved. Secondly, the effect of connection part 1 should be considered in this decision.

In the following a description of some general conditions for suitable forms of shell together with design points will be given. Most of the assumptions are the same for all shells, therefore, only shell no 1 is reported in detail. Any changes for the remaining shells will be noted. The co-ordinate of the beginning and end of the chord of the shells are almost the same, therefore by performing numerical analyses, the most suitable form among them for the device can be found. Since the Lusas programme cannot represent softening behaviour for the glue, the load deflection curve is valid only until the yield limit and after that the shape of curve should be estimated from the total behaviour of the plastic deformation and peeling process.

4-1-1 Verification of Lusas:

In order to demonstrate that the non-linear finite element procedures, which have been used for the numerical work, are correct a benchmark study has been carried out. For this purpose the elasto-plastic analysis of a clamped spherical cap is considered. This shell structure is analysed by Lusas and then compared to the results of the analysis of Wood's[85] and Oliver and Onate's[46] for this shell. The analysis was carried out with two material properties, first an elastic material and second a plastic material have been assigned for the properties.

Feature definition: The cap is formed from a truncated sphere of radius 120 mm. It has a base radius of 26 mm, a central height of 2.2 mm, and a thickness of 0.4 mm inches. The shell is fully restrained at its base and is subject to an increasing concentrated transverse load at its apex.

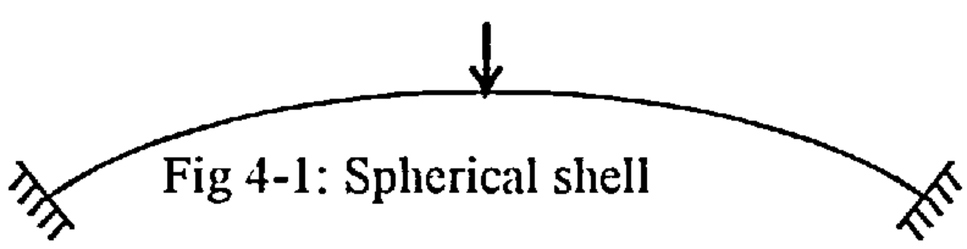

Fig 4-1: Spherical shell

Geometric definition: A thickness of 0.4 mm is considered for the shell.

Material definition: The nonlinear material behaviour is modelled by a Von-Mises elasto-plastic model with the following material properties:

Young's Modulus E	6.9 E10 N/m^2
Poisson's Ratio	o.3
Yield Stress	3.45E8 N/m^2

Mesh definition: Due its doubly symmetric nature, only a quarter of the structure is considered in the finite element model. The shell is discretised using 32 semiloof shell (QSL8 and TSL6) elements Fig 4-2.

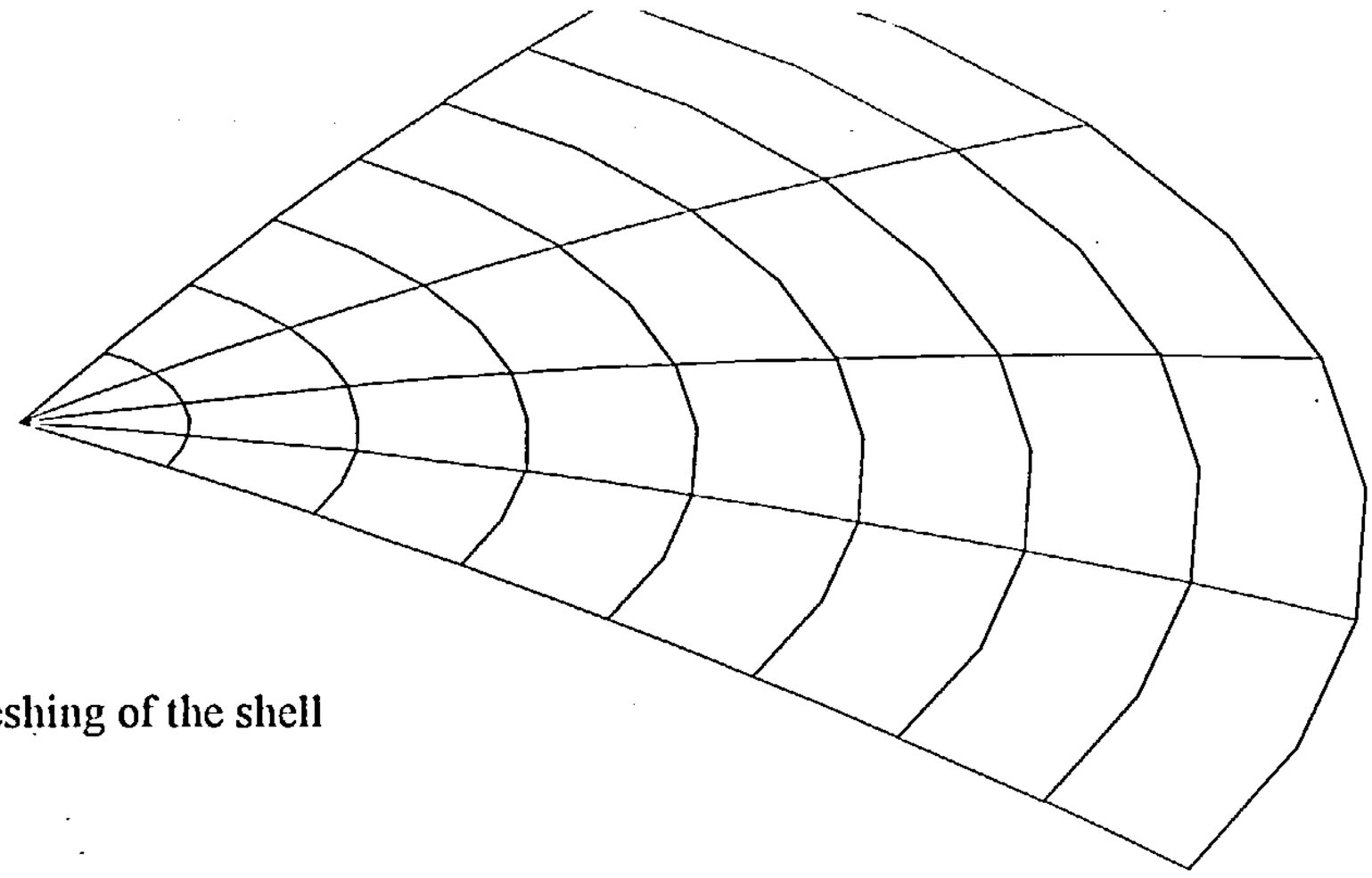

Fig 4-2: Meshing of the shell

Support definition: Symmetric boundary conditions (restraint of the loof rotations and the appropriate lateral translations) are imposed on the internal boundaries of the mesh, and the nodes at the base of the structure are restrained against translation and rotation.

Loading definition: A prescribed displacement at the apex with the increment of 0.25 mm are defined and assigned to the apex of the shell.

Results: The result of this nonlinear analysis with Lusas has been shown in Figure 4-4 The deformed mesh has been illustrated in Figure 4-3.

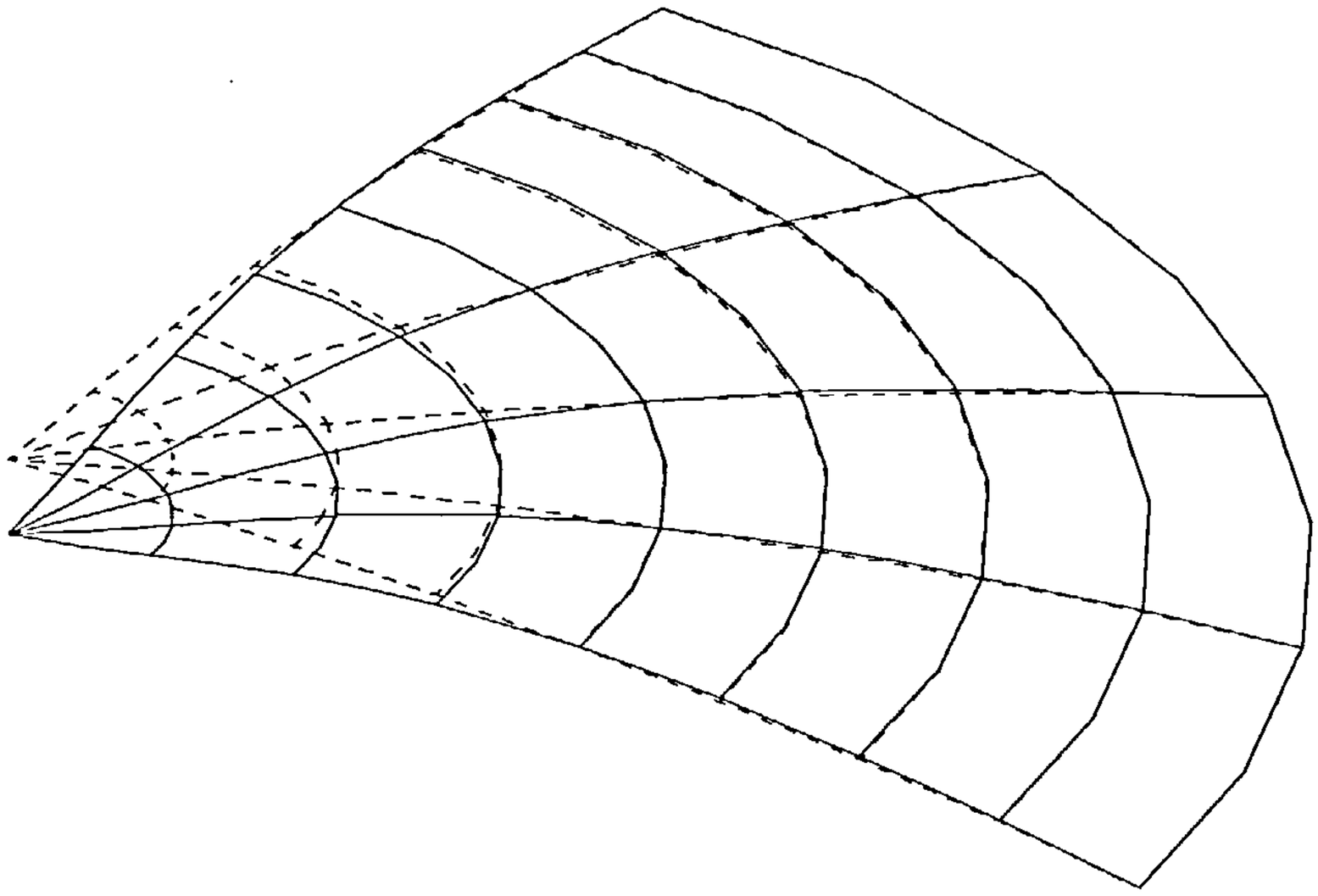

Fig 4-3: Deformed mesh

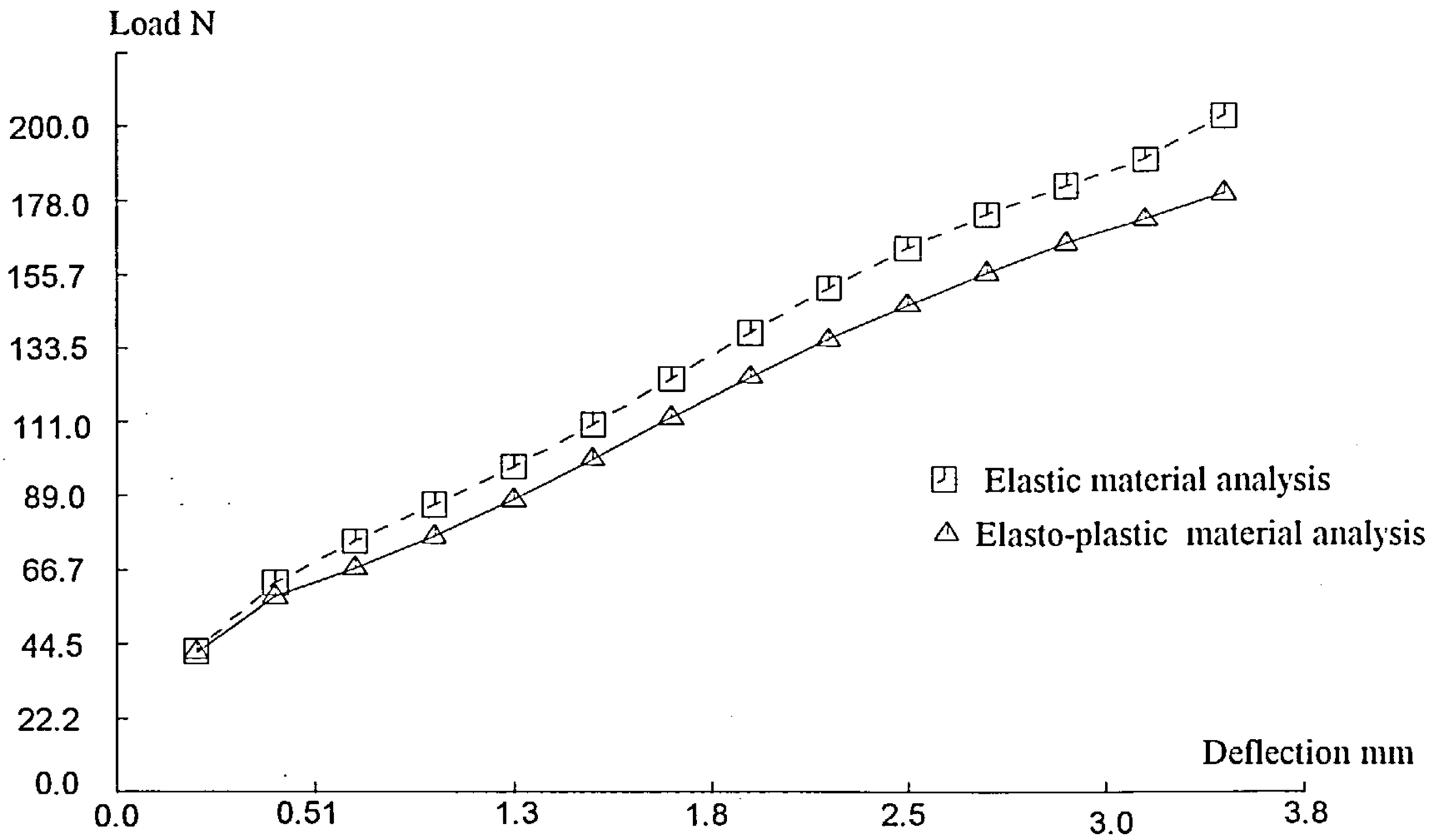

The results of the analysis from Wood and Oliver & Onate have been shown in the Figures 4-4 and 4-5 . From these Figures it is recognised that the result achieved from Lusas analysis is close to that of the Wood and Oliver& Onate's results.

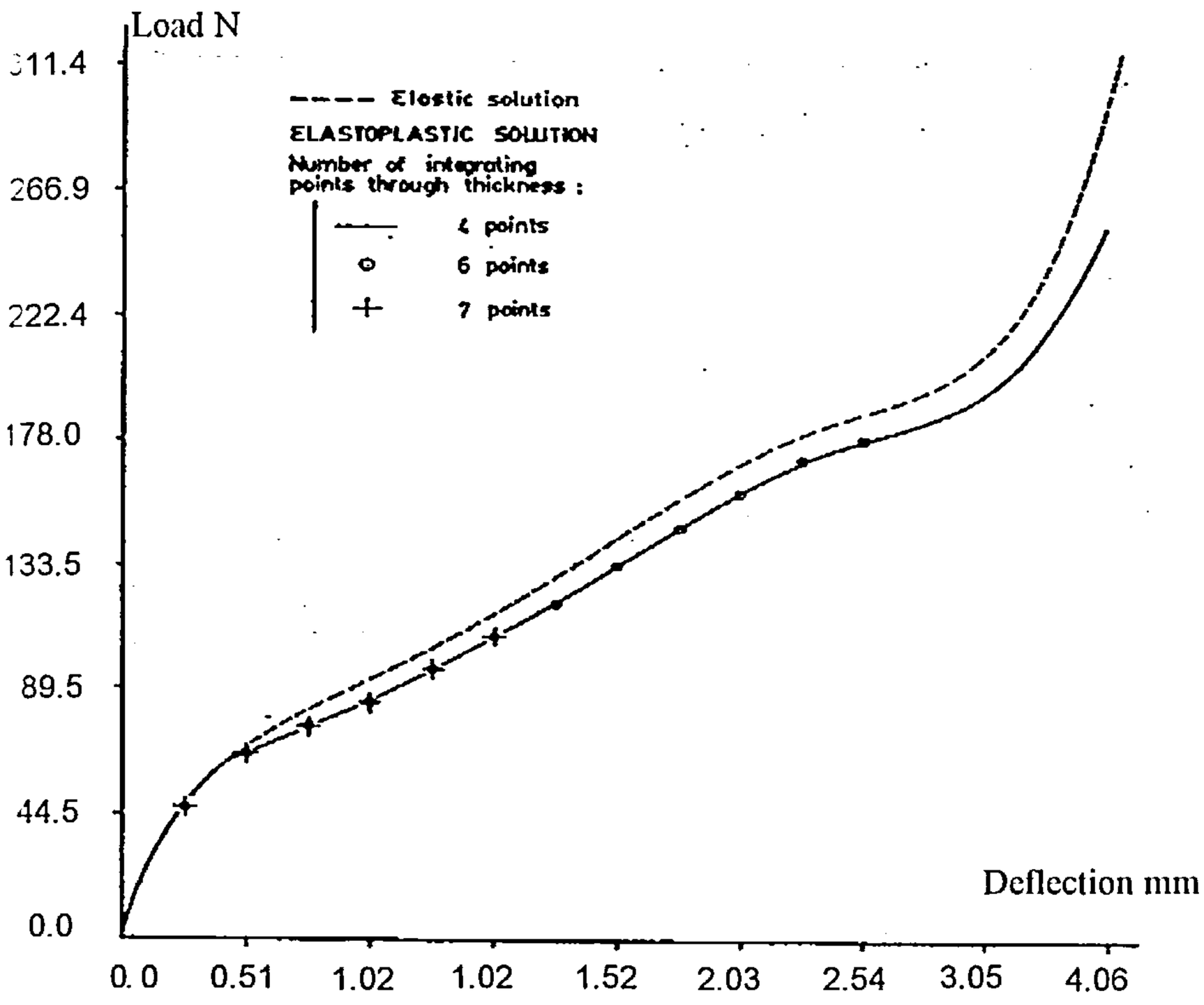

Fig 4-5: Oliver & Onate results for nonlinear plastic analysis

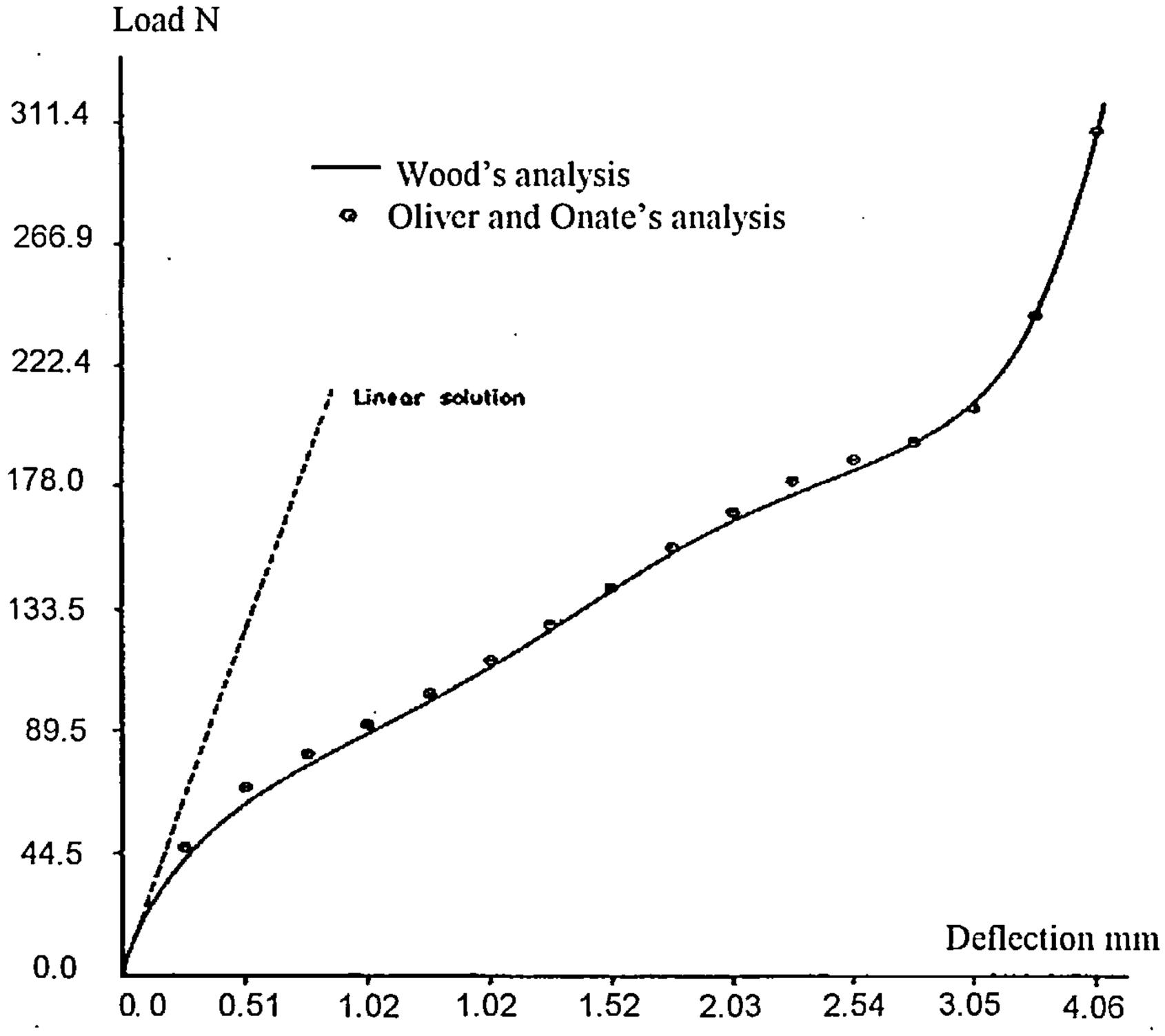

Fig 4-6: Wood's and Oliver's Results for elastic analysis

4-1-2 Shell number 1: Single arc for the shell

4-1-2-1 Nonlinear dynamic analysis

In this section, single curvature is considered for the entire shell with uniform thickness. An important behaviour for the shell with single curvature is that the slope of the shell at its contact to the connection parts should be suitable for a firm attachment. Therefore, there is a restriction to the height of the shell. In the following, a typical form of shell has been considered as an example and examined numerically.

Feature definition:

By considering a 2 mm thickness of the tube and outer diameter of 60 mm, a shell detail with uniform thickness and suitable slope at its connection edge is illustrated in Figure (4-7):

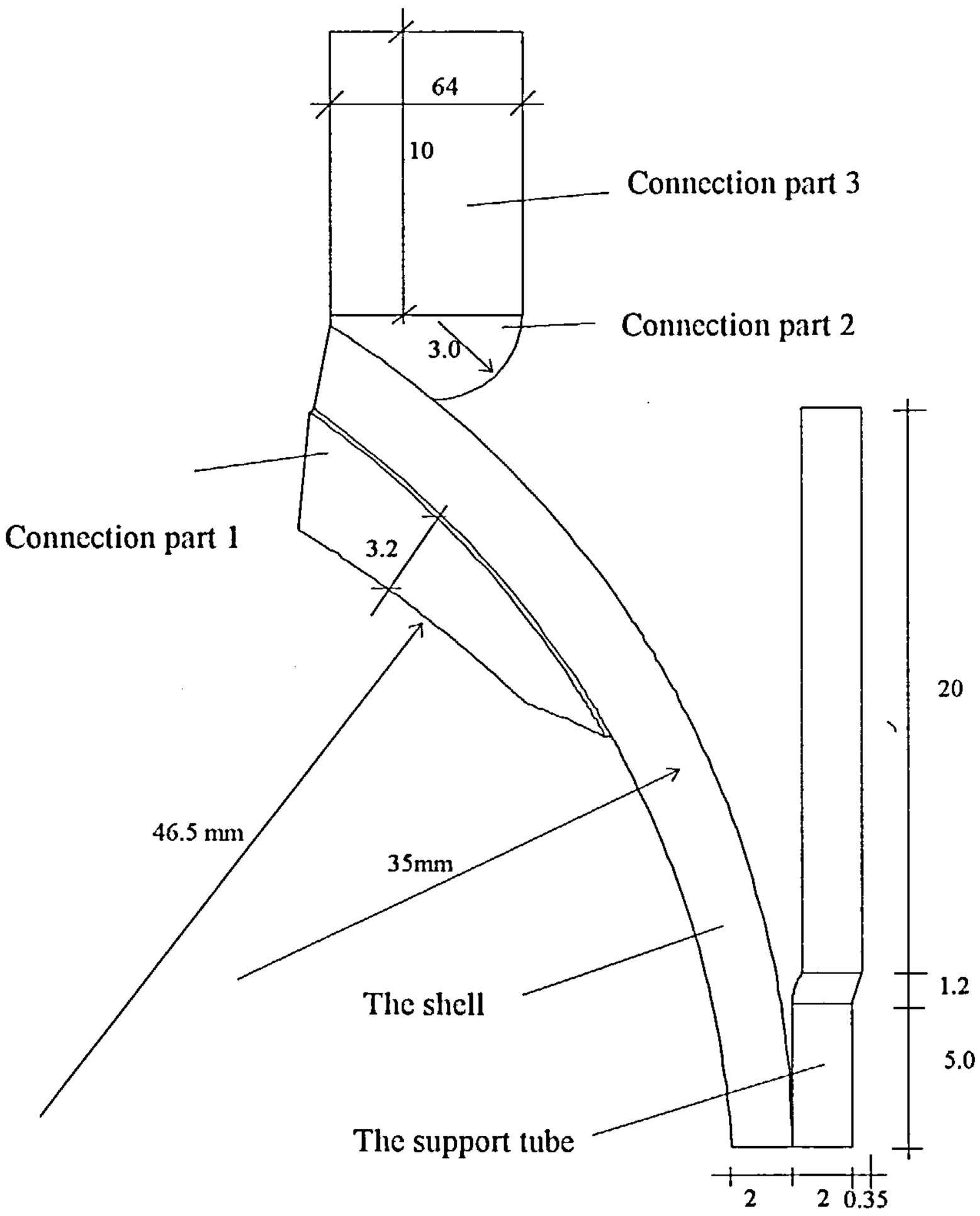

Fig 4-7: Feature definition of the shell

Meshing: The Parabolic Quadrilateral Axisymmetric Solid element QAX8 from the Lusas program has been used for the mesh of the shell. The element is part of a family of isoparametric 2-dimensional elements with higher order models capable of representing curved boundaries. Its formulation applies over a unit radian segment of the structure, and the loading and boundary conditions are axisymmetric. The Y-axis is taken as the axis of symmetry. Figure 4-8 shows the element.

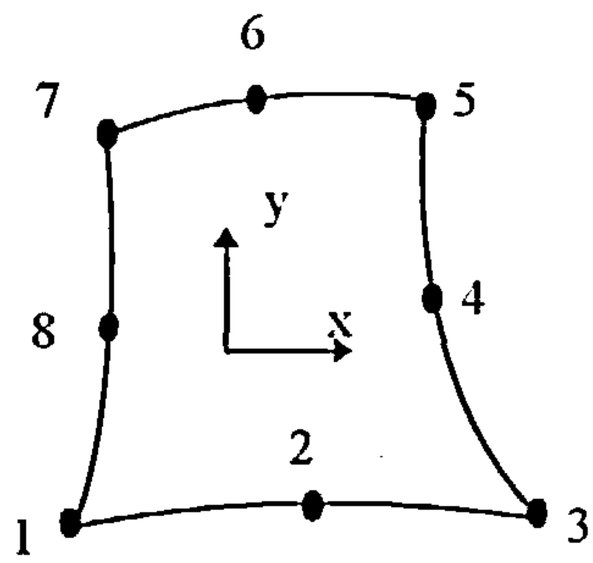

Fig 4-8: Axisymmetric Quadrilateral QAX8 element

The elements are numerically integrated. The mid-length node should be equidistant from the end nodes and the elements must not be excessively curved. The following inequalities should be applied for the element curvature:

a) Mod $(S_1-S_2)/(S_1+S_2)<1.02$

b) $(S_1+S_2)/S_3<1.02$

S_1 , S_2 and S_3 are shown in figure 4-3.

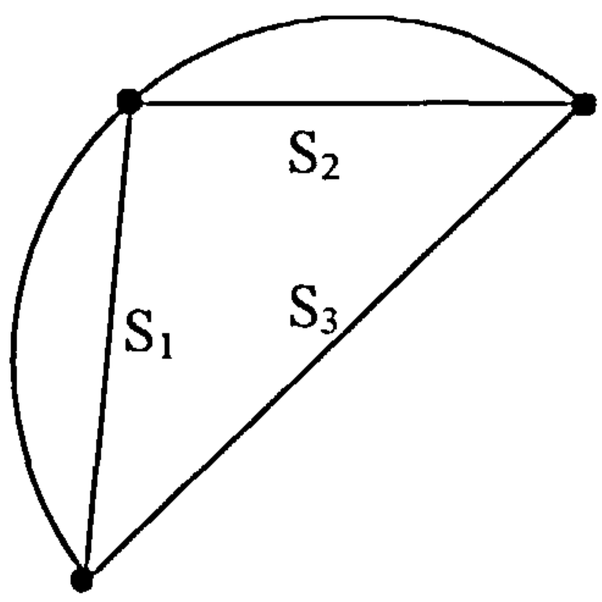

Fig 4-9

A Lusas warning will be invoked if the element curvature is not in accordance with these inequalities, but the analysis will be proceed.

Six elements in the thickness and 22 element in y direction have been considered for the shell. The meshing of the shell and its support and connection parts are shown in figure 4.10:

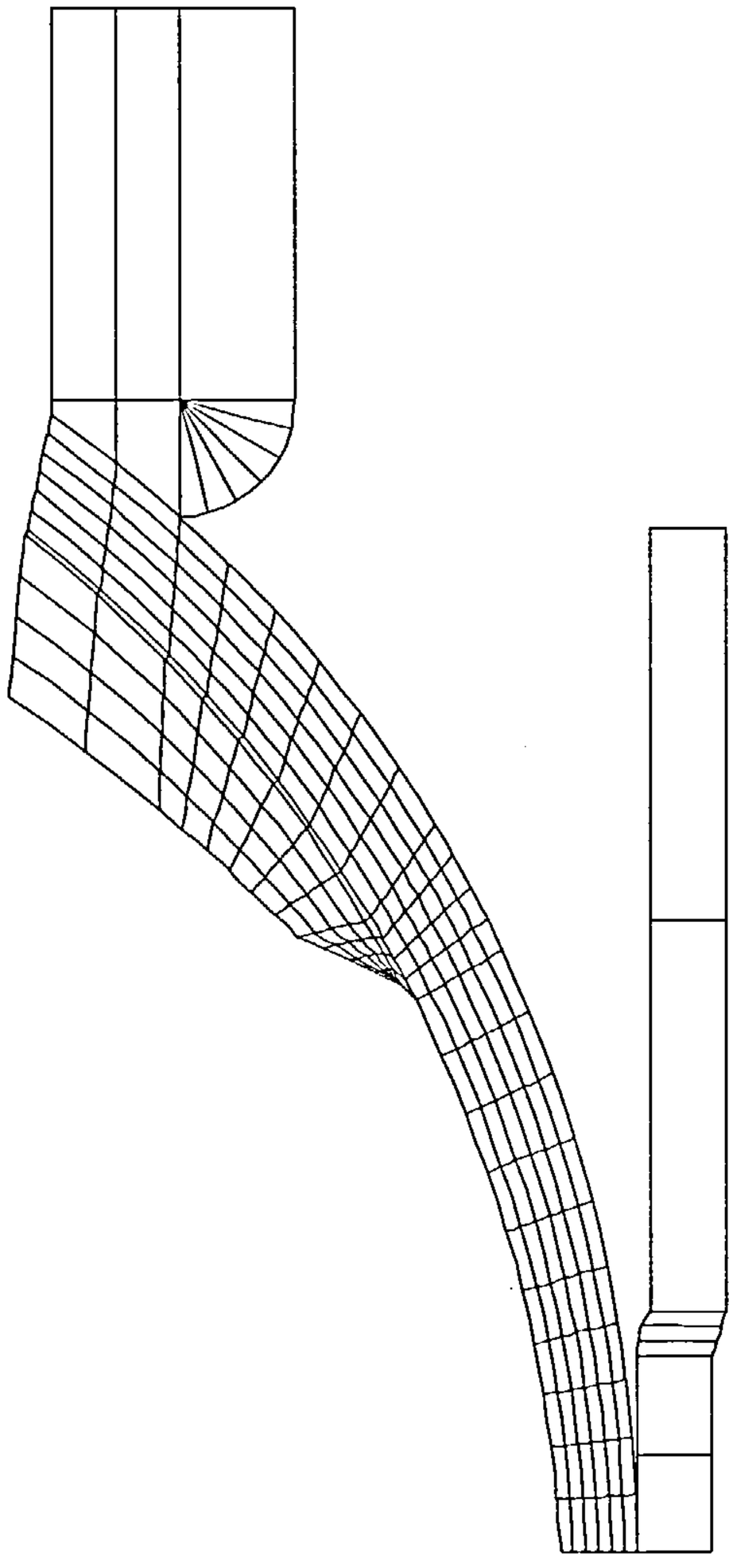

Fig 4-10: Finite element model for the shell

Geometric definition: This data section is used to define the geometric property values for the specified element type. Not all elements will require the input of geometric properties; for example, the geometric properties for a membrane element will be the element thickness at each node, whilst there is no equivalent property for the solid elements. The *LUSAS Element Library* should be consulted for geometric property details of each element type. No geometric property is required for QAX8 element.

Material Definition:

The peeling tube was considered from mild steel and the typical material properties of table 4-1 with Von Mises plastic behaviour have been assumed for it. These are the characteristics which usually considered for mild steel[18].

Table 4-1

Elastic modulus E	2.1E11 N/m^2
Poisson coefficient ν	0.3
mass m	7800 KG/m^3
yield limit	3E8 N/m^2

Figure 4-11 represents the plastic hardening properties which were assigned for the peeling tube.

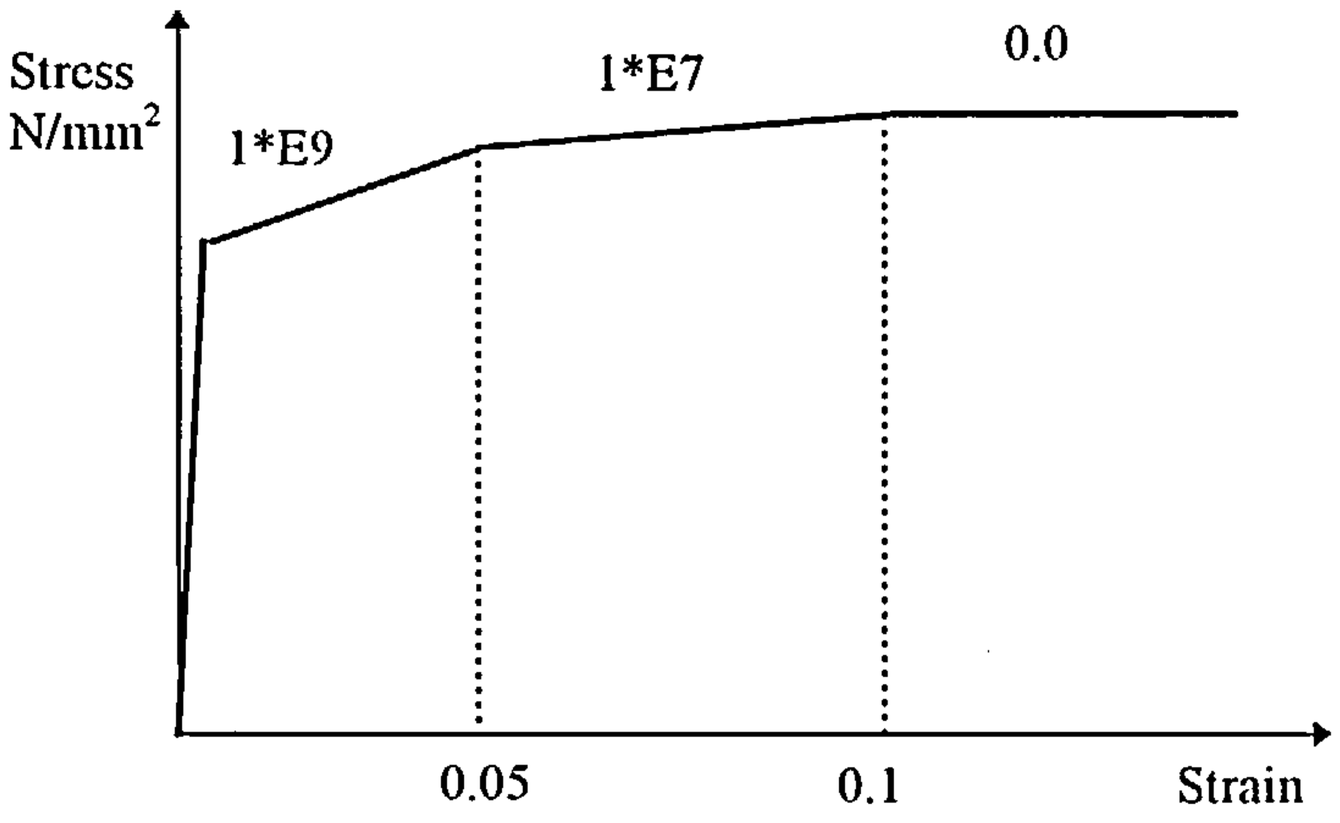

Fig 4-11: Material model for peeling tube

Except for connection part 1, no plastic material properties have been assigned to the connection parts. These other parts have been considered to be made from high strength steel and behave elastically. The connection part 1 has the same material as the peeling tube.

A modified Von-Mises material model has been used for the glue. The compressive strength of the glue is high, but its has low tensile yield limit. The following quantities have been assumed to the glue (table 4-2). These are typical characteristics which frequently used for the structural adhesives[17].

Table 4-2

E	2.0E10 N/m^2
v	0.3
m	5000 KG/m^3
f_{yt}	2E7 N/m^2
f_{yc}	1E8 N/m^2

No hardening effect has been assigned to the glue.
The applied plastic characteristics are valid for the deformation of the glue up to its yield limit and the softening behaviour starts soon after yielding of the glue. Since Lusas cannot represent strain softening behaviour, the load deflection curve of the shell will be not accurate after this softening occurs. This is not a major problem for this analysis because the peak values were mostly asked from the computations.

Slide line: Slide lines may be used to model contact and impact problems. Several slide line options are available in Lusas finite element program and they are:

(i) Tied sliding
(ii) General sliding without friction
(iii) General sliding with friction and
(iv) Sliding only (without friction or lift off)

The tied slide line option eliminates the requirement of a transition zone in mesh discretisation comprising differing degrees of refinement and is extremely useful in creating a highly localised mesh in the region of high stress gradients.
The general slide line options may be utilised for modelling finite relative deformations of colliding solids in two or three dimensions which involve sliding (with or without friction) and constant or intermittent contact conditions. The sliding only option is similar to the general sliding options, but does not permit intermittent contact conditions. Figure 4-12 shows the use of both the general and the tied slide line options.

Each slide line comprises two surfaces; designated the master surface and the slave surface. These surfaces are defined using an orderly definition of nodes in the region of the potential contact zone.

This definition ensures that each slide line surface comprises a number of contact segments in which each segment is a boundary face of an underlying element. Note that the slide line facility is inherently nonlinear and requires use of the nonlinear control data chapter, except for tied slide lines used in an implicit dynamic or static analysis, where the solution may be linear.

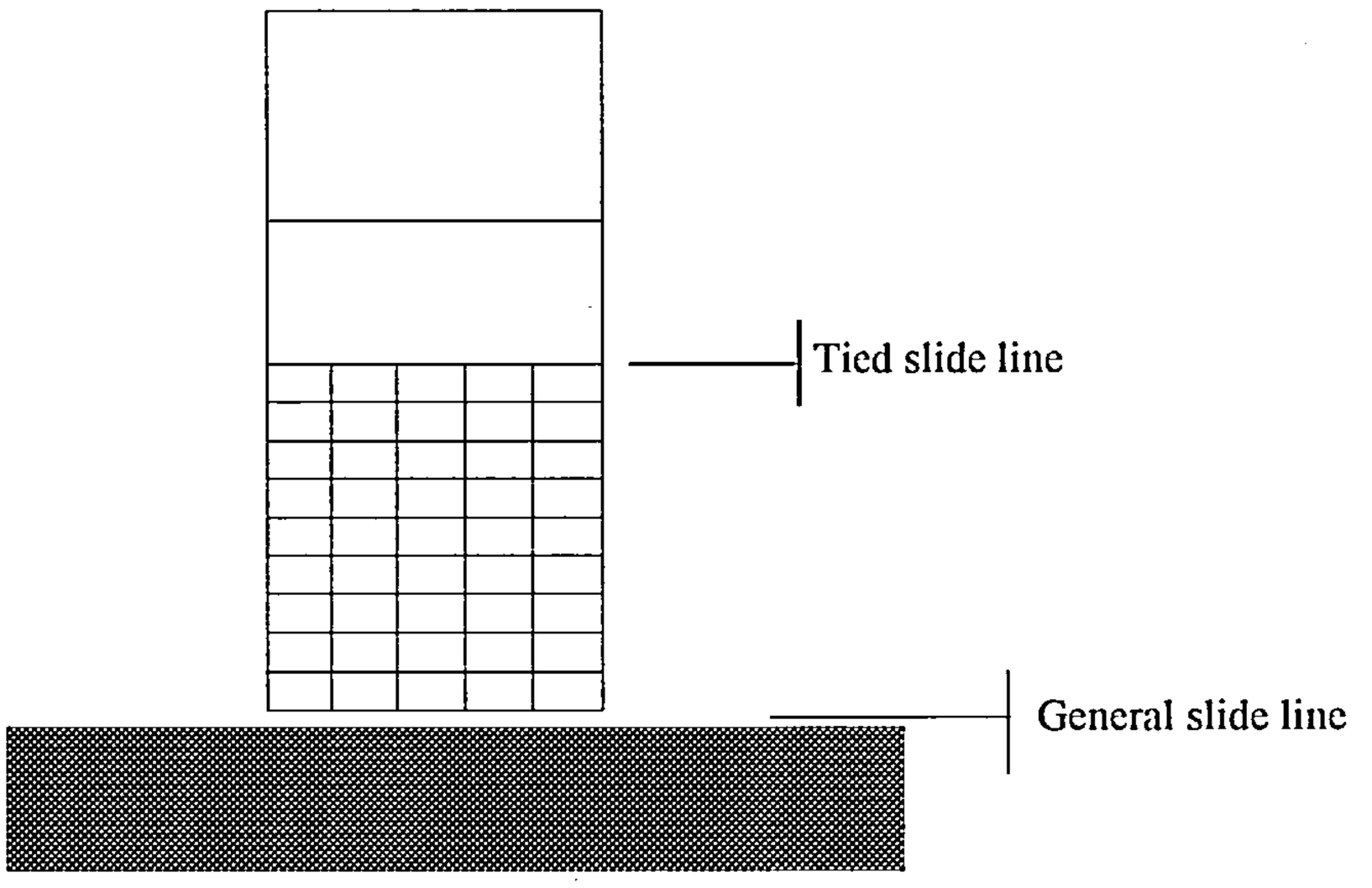

Fig 4-12: Slide lines applications

This facility was used in this analysis to represent the support tube and the connection parts. For the a convenient solution, support tube and also connection parts were considered as slave surfaces and the peeling plate as master surface. This is a common rule in Lusas to use the surface with more compact mesh as the master surface.

Geometric Nonlinearity: Geometric nonlinearities arise from significant changes in the structural configuration during loading. Common examples of geometric nonlinearity are plate structures which develop membrane behaviour, or the geometric bifurcation of truss or shell structures. The changing application of loads or boundary conditions are also geometrically nonlinear effects.

In Lusas geometric nonlinearity is accounted for using four basic formulations:

(i) Total Lagrangian

(ii) Updated Lagrangian

(iii) Eulerian and

(iv) Co-rotational

All four formulations are valid for arbitrary large deformations. In general, if rotational degrees of freedom are present, rotations must be small for a Total Lagrangian formulation. Large rotations are allowed for an Updated Lagrangian or Eulerian (provided that they are small within each load increment). The co-rotational formulation is unconditionally valid for large rotations and results are generally independent of load step size.

All formulations are valid for small strains. For some elements the Updated Lagrangian formulation is valid for moderately large strains. The Eulerian formulation is generally valid for large (finite) strains. In general, the Total Lagrangian is a stable formulation, which is usually able to cope with substantial load increments. The Updated Lagrangian, and particularly the Eulerian, formulations generally require smaller load increments in order to avoid a divergent solution. The consistent co-rotational formulation performs well for large load increments.

Standard geometrically nonlinear formulations account for the change in position of the loading, but not the change in direction relative to the deformed configuration.

Loading is always conservative for the Total Lagrangian geometrically nonlinear formulations (that is, the load is always applied in the same direction as was initially prescribed). Using an Updated Lagrangian formulation, the geometry is updated at the end of each increment and the applied loads maintain the same relative orientation to the original surface. Non-conservative loading is therefore increment size dependent. True non-conservative loading may only be achieved by using the Eulerian and co-rotational formulations.

The Eulerian geometric nonlinearity has been chosen for this numerical analysis because of the presence of large rotations.

Loading: Concentrated uniform loading of Fy=-50000 N has been applied to the connection parts as the loading of the shell (Fig 4.14). This load was sufficient to cause the failure of the shell and start the peeling process. Since the analysis involves non-

linear dynamics, a loading-time curve to represent this variation has been considered, Figure 4-13. This curve shows the increase of the load with time. At t=0 the load factor is zero which means that the applied load on the device is zero. At t=1 sec, the load factor is 1 which indicates the load F_y=-50000 N has been completely applied on the device. Between time 0 and 1 the applied load is a fraction this load.

For t>1 sec, the loading remains constant with time. Therefore, according to this assumed curve, the load is applied on the device within 1 sec, which is a moderate speed dynamic loading.

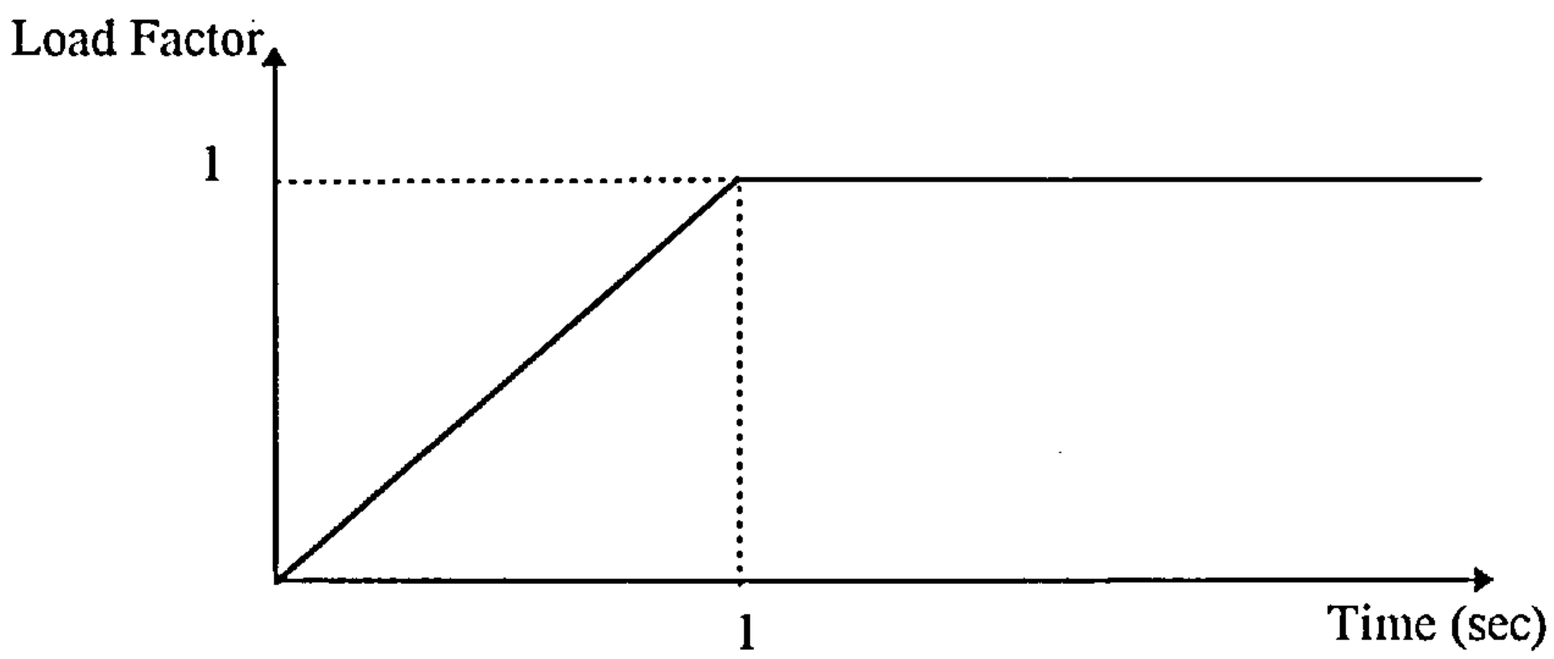

Fig 4-13: Load factor definition

Supports: A fully restricted support is used in this modelling for the base lines of the peeling and support tubes. This support definition restricts only displacement in X and Y directions because the elements of this model have only two degrees of freedom.

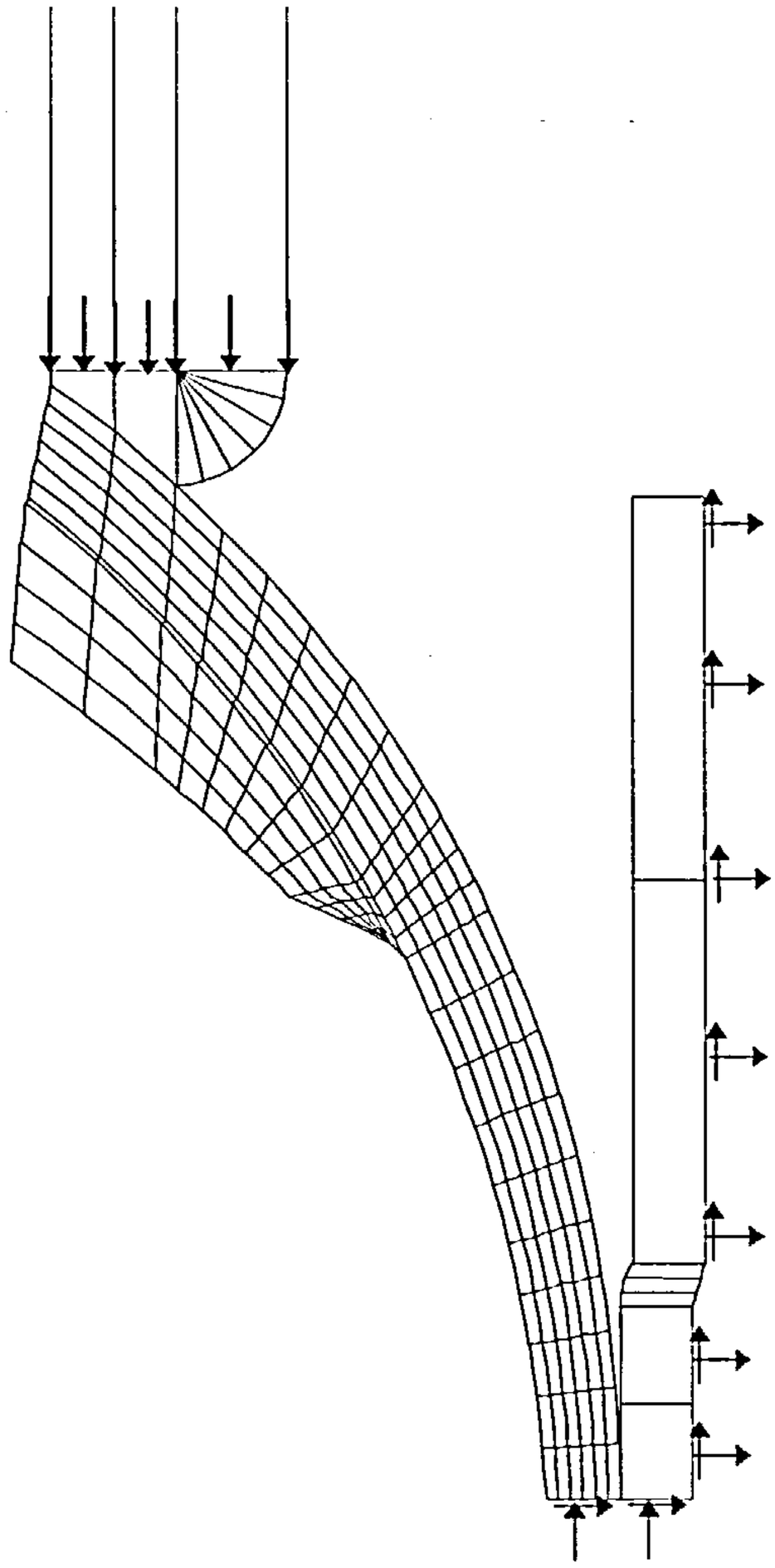

Fig 4-14: The loading and the support conditions of the device

Solution control: Nonlinear dynamic controls are assigned to this model. The computation is carried out in two stages. In the first stage large time steps (0.002 sec) are used and in the second stage small time steps (0.00001 sec).

In each increment 12 standard Newton-Raphson iterations are used. For quick convergence and to improve the slow convergence of the Newton-Raphson method, a maximum of 2 line searches is allowed. The line search procedure involves an extra optimisation iteration, in which the residual forces in subsequent iterations are minimised.

Convergence of the solution in LUSAS is controlled by several parameters. These are:

(i)-The sum of the squares of the iterative displacements as a percentage of the sum of the squares of the total displacements.

(ii)-The sum of the squares of the residual forces as a percentage of the sum of the

squares of the all external forces including reactions.

(iii)-The sum of the squares of the iterative displacements as a percentage of the sum of the squares of the incremental displacements.

All of degrees of freedom were considered in this model by invoking option 187 in Lusas finite element programme.

Results:

The load deflection curve for the device is the most important outcome of the analysis and is shown in figure 4-9. It has been already mentioned in this chapter that there is a restriction for modelling of the glue and in LUSAS it is not possible to model softening behaviour. Therefore, the resulting load deflection curve is not accurate when the shell starts to peel away from connection part 1.

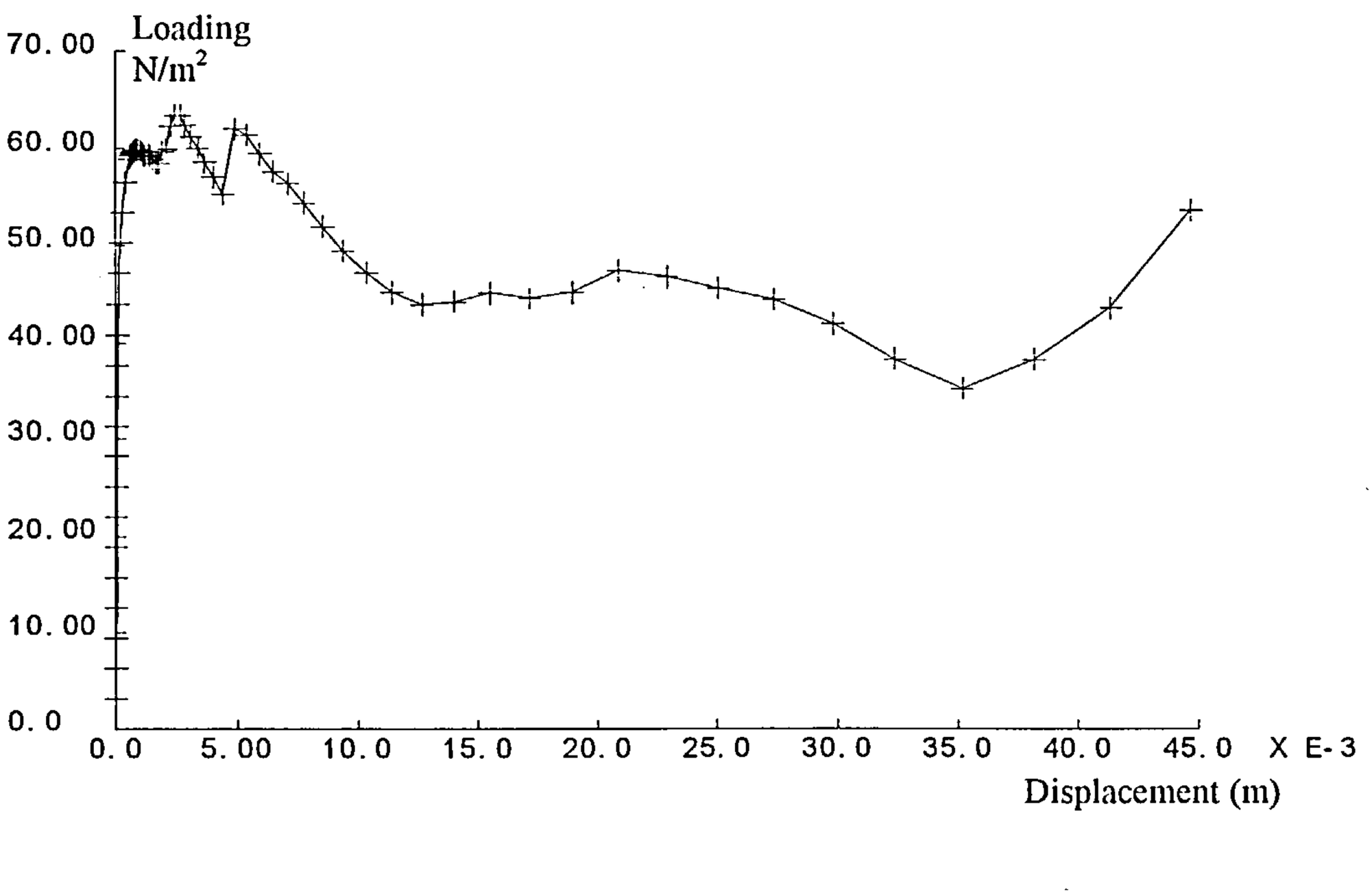

Fig 4-9: Load-deflection curve of the device

A deformed mesh of the shell is shown in figure 4-16. It shows how the interaction of the connection part 1 with the shell ends and the complete failure of the glue is initiated. By proceeding of this failure, the shell will support the load with a redistribution of the stresses. It will buckle and collapse in a proper manner and will start the peeling process without high fluctuation of its resistant. This separation is occurred at the peak load, 60000 N.

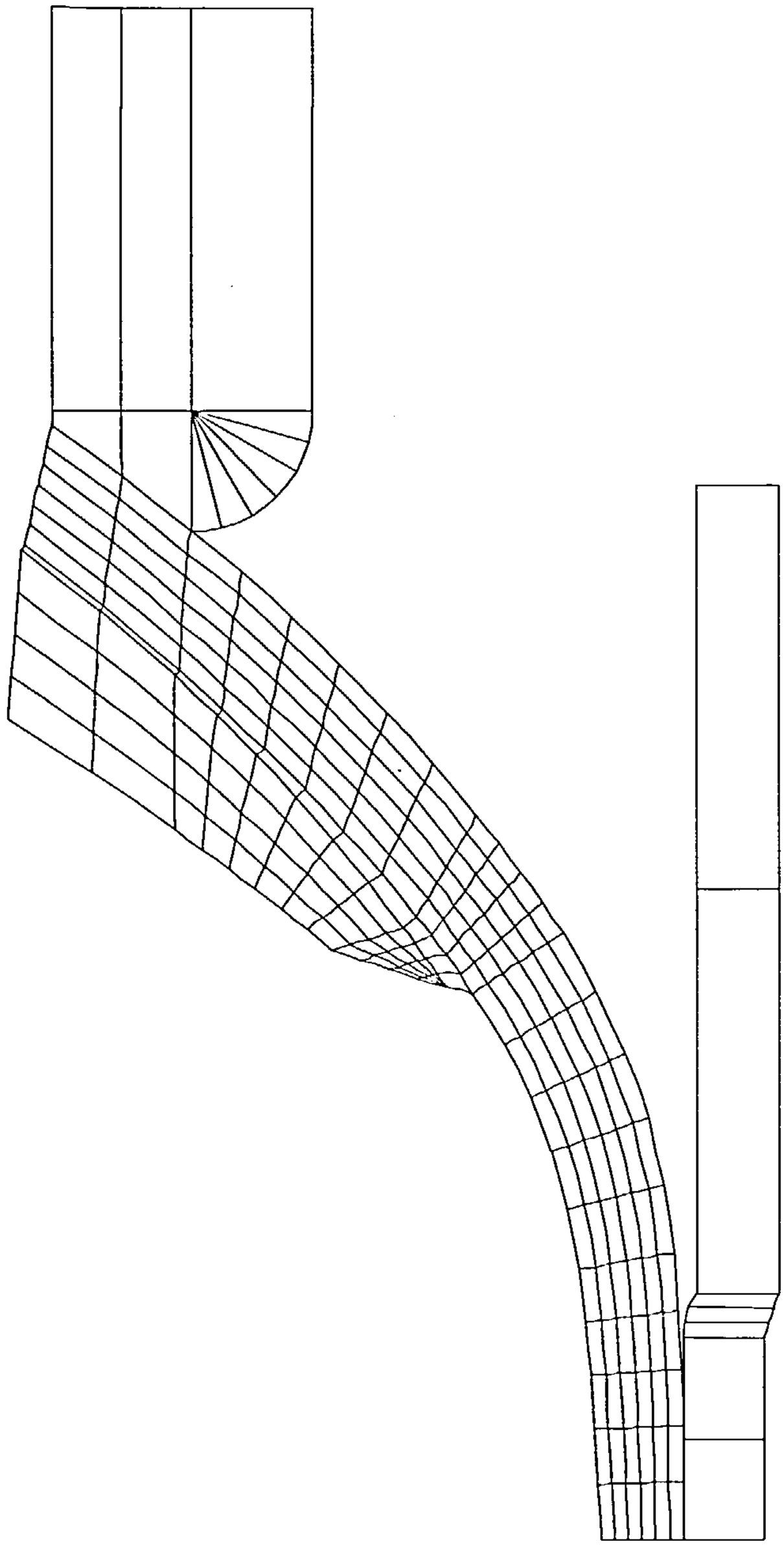

4-16: The separation of connection part 1 and the shell which is nd of interaction of these two parts.

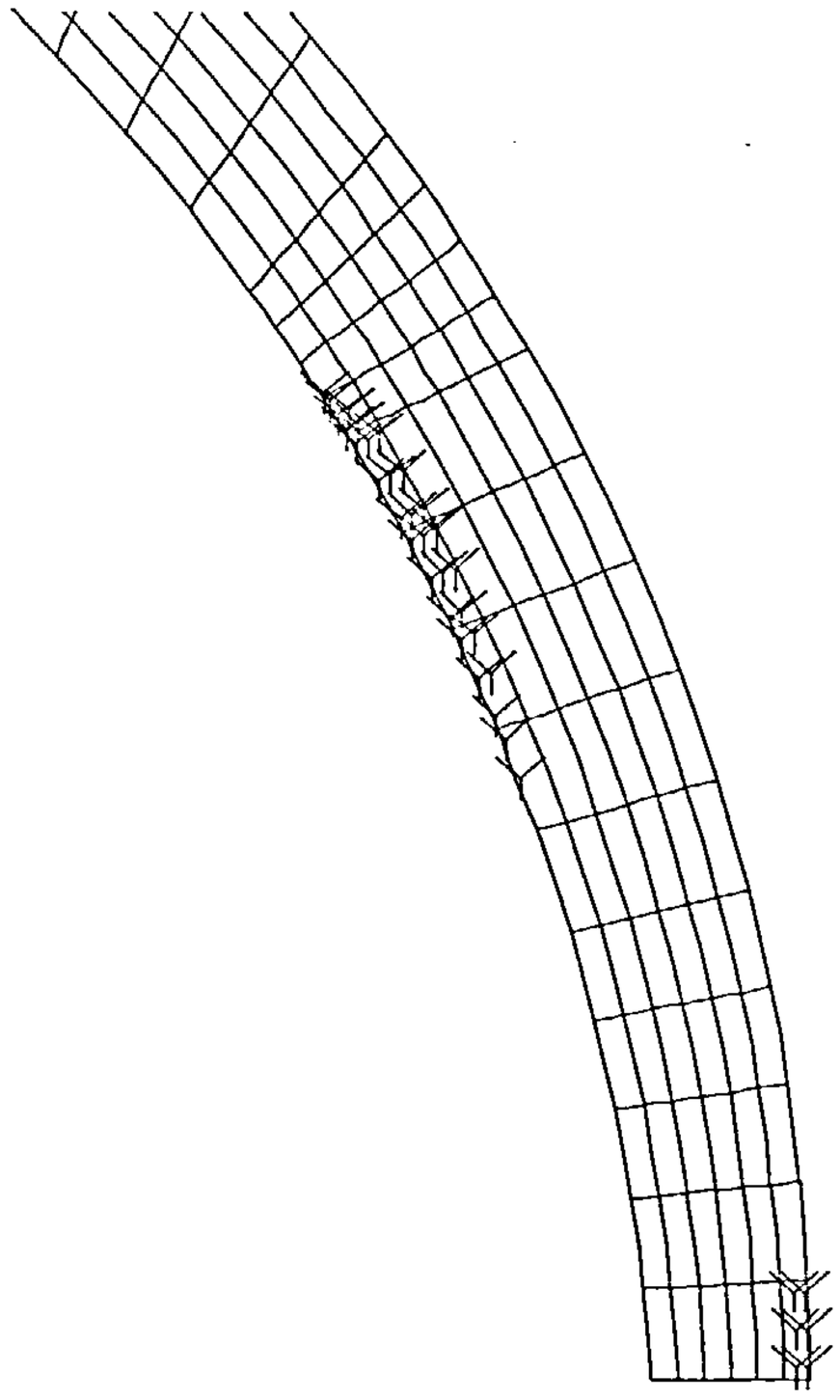

Fig 4-17: Initiation of yielding in the shell

The initiation of yielding in the shell at load 32000N has been shown in Figure 4-17. The yielded points in the shell are located below the contact area of the connection part 1 and the shell. This shows the effect of this part on the plastic behaviour of the shell. The upper part of the shell is protected by the connection part 1 and has not yielded at this stage of loading.

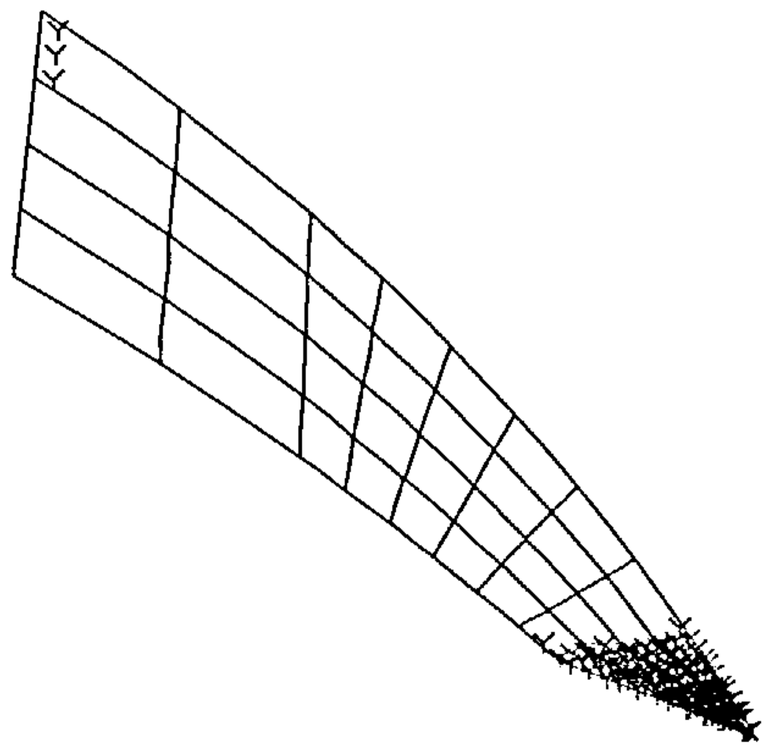

Fig 4-18: Initiation of yielding in the connection part 1

Yielded points in the connection part 1 at load 32000N have been shown in figure 4-18. It shows the stress concentration at the tip of this part, which is the end of its contact with the shell. This figure is another representation for the interaction of the shell and connection part 1.

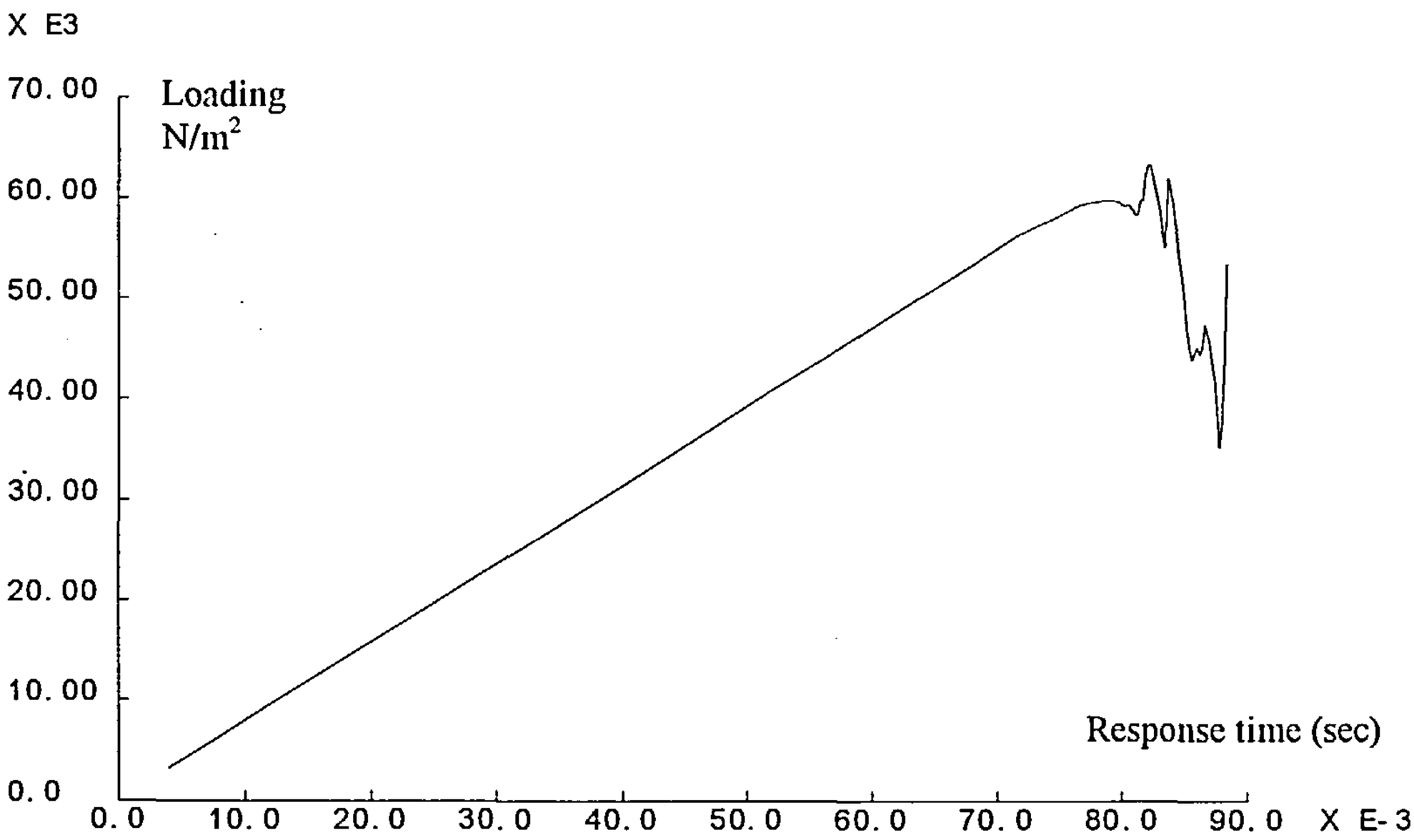

Fig 4-19: Load- response time curve of the device

Figure 4-19 shows the load- response time curve for the shell. The linear part, until its yield limit is noticeable in this figure. It also shows that after a maximum load there is a reduction in the load. This reduction is due to failure of the glue and the buckling of the shell.

The large deflection of the shell is shown in Fig 4-20. In this Figure the elements representing the glue have been removed.

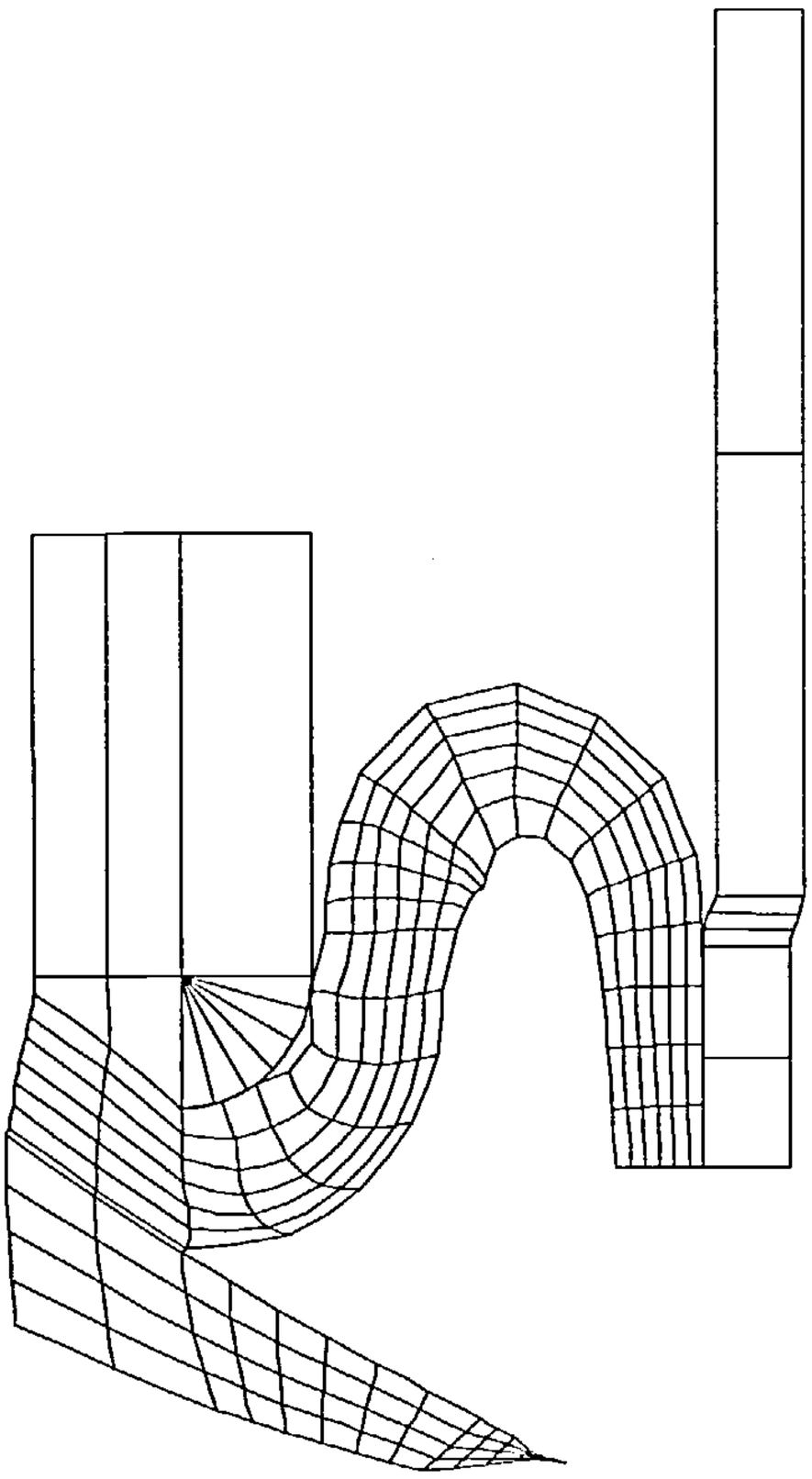

Fig 4-20: large deflection of the shell part of the peeling tube

This is the stage that the shell has collapsed and yielded between the connection part 2 and 3 and the support tube. The connection part is now detached from the shell and peeling process is to start. By the start of peeling process, the load of the device will remain at a constant level.

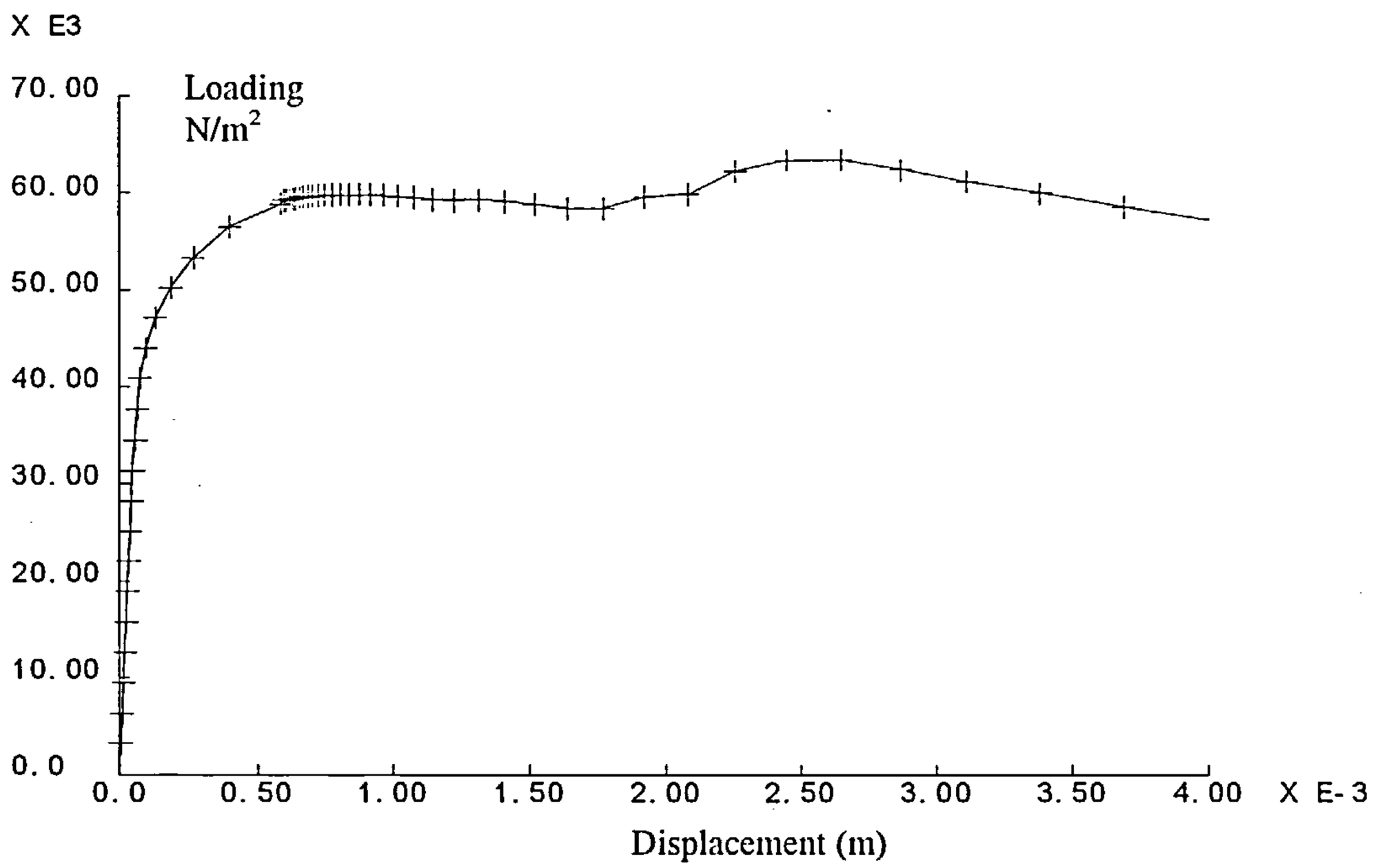

Fig 4-21: Load deflection curve of the device in short range

In Figure 4-21 the load deflection curve of the device, in its yielding state, has been shown at a large scale. It is easy to distinguish the end of linear behaviour and the ultimate load of the device.

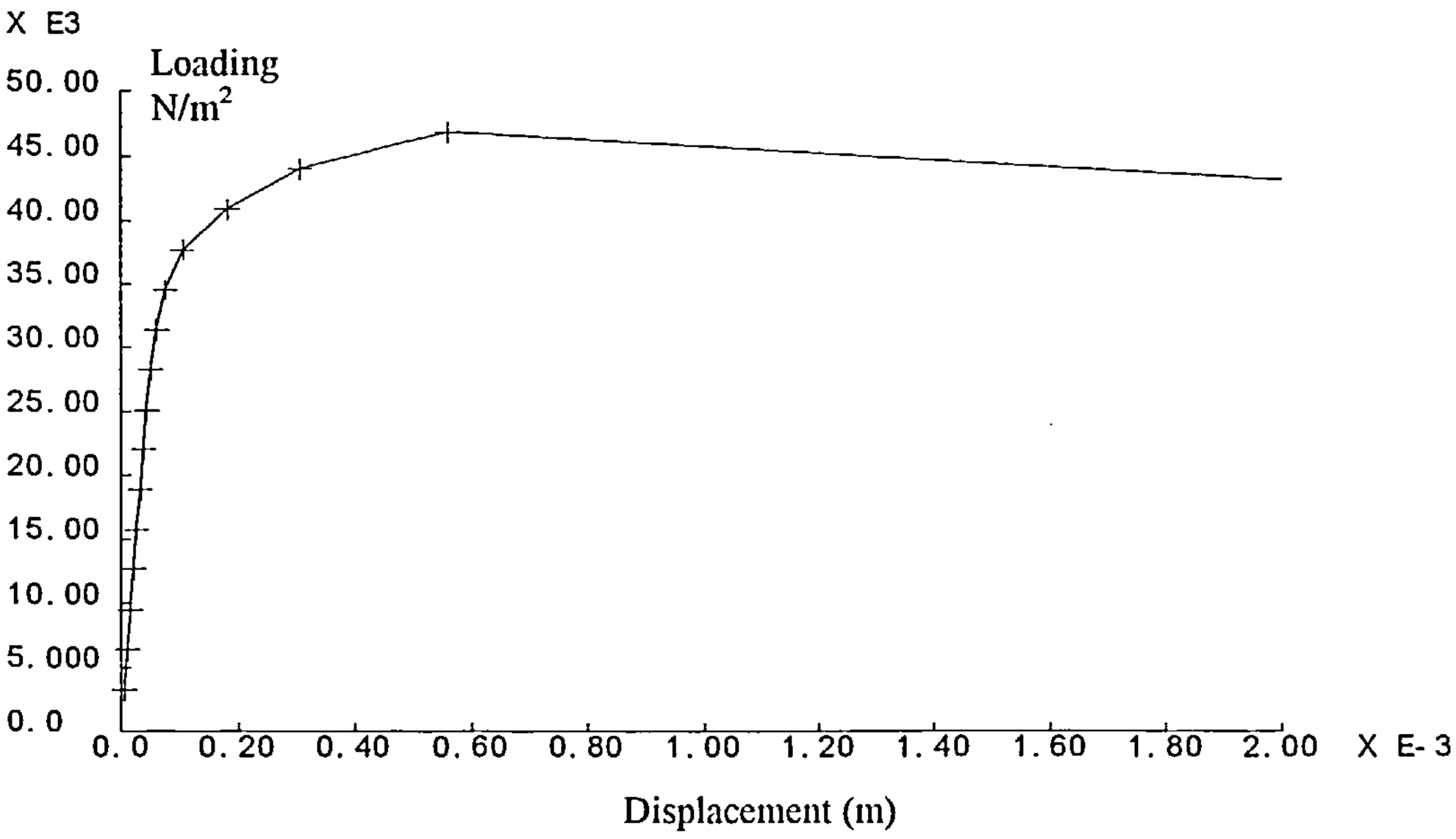

Fig 4-22: Load deflection curve of the sell without connection part 1

In order to determine the effect of connection part 1 upon the yield limit of the device, the model was analysed with the same configurations, but without this part and without the adhesive. The result has been shown in load deflection curve of the device (Fig 4-22).

From a comparison of figures 4-21 and 4-22 it may be seen that the application of connection part 1 has extended the load deflection curve such that the maximum load which may be resisted by the device has been increased by 15000 N. In fact, the shell has been strengthened by 30%. Therefore, not only the connection part 1 leads the shell properly toward the peeling process, but also, it improves its yield limit.

4-1-2-2 Peeling force

Analytical methods

After the start of the peeling procedure the transmitted force through the device (which is the resistance of the device) remains constant. This force is an important parameter for the device and can be calculated approximately by the following method.

The relevant terms to the analysis are given as follows and are shown in figure 4-23.

y =The separated length of the peeling tube

M_p = Full plastic moment of peeling tube

τ = Peeling strength of adhesive

θ = The angle of rotation during failure.

δ = The failure elongation of the adhesive

R = Radius of curvature

t_g= thickness of the glue

t_t= thickness of tube

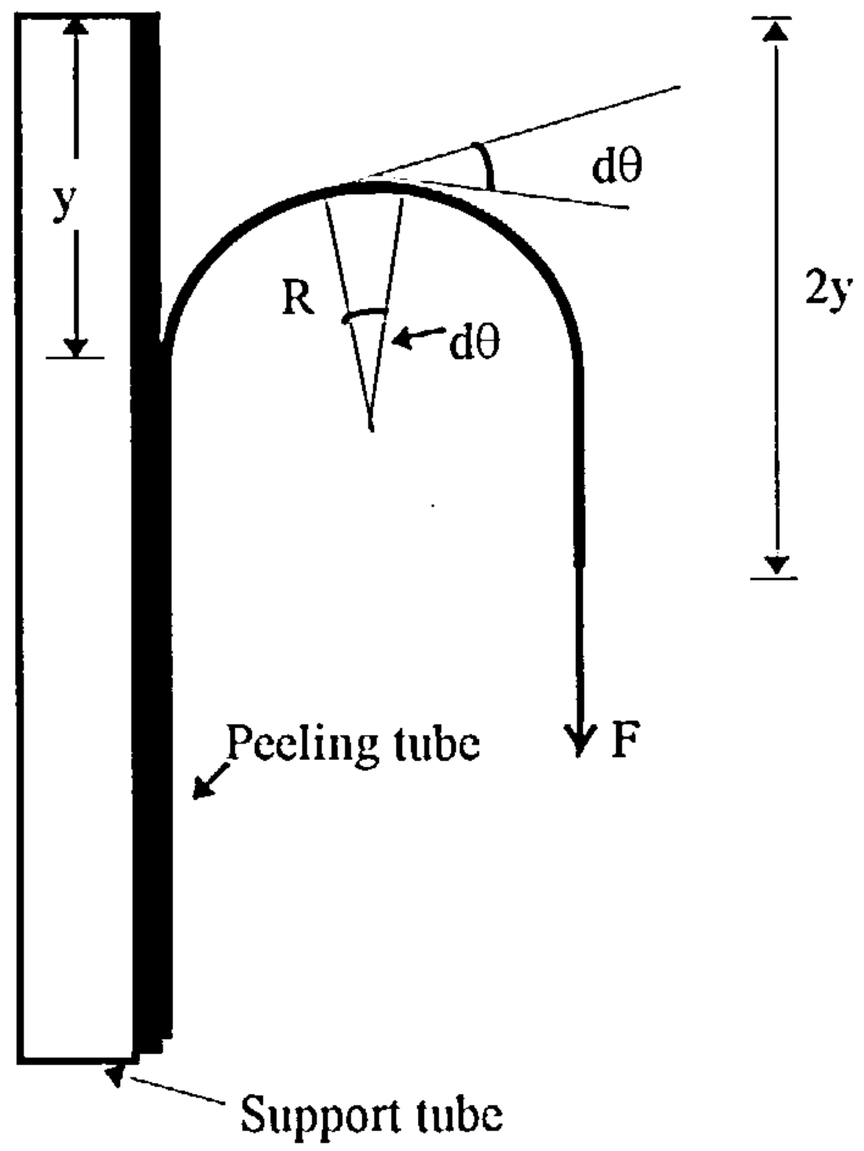

Fig 4-23

The dissipated energy during the peeling of tube at length y is given by:

$$0.5\ y\ 2\pi .R.t_g.\ \tau \quad + Mp\ \theta\ b + 0.5fi \qquad (4\text{-}1)$$

θ is the angle of rotation during failure and is calculated by the integration of an infinitely small length of the peeling tube over length y, which is:

$d\theta = dl/R$

$$\theta = 2\int_0^y dl\ /\ R = 2y\ /\ R \qquad (4\text{-}2)$$

(The coefficient 2 in the above equation is for the unbending effect of the tube.)

f_i is the work required to change the diameter of tube from $2R_1$ to $2R_2$.

Therefore the dissipated energy will be:

$$(\ 0.5t_g\tau + 2\ Mp\ /r)\ y2\pi R + fi \qquad (4\text{-}3)$$

The plastic moment, Mp, for a rectangular section with a unit width is $f_y\ t_s^2/\ 4$, in which f_y is the yield strength of the steel plate and t_s is the thickness of the tube. R_2 is the radius of the inverted tube and is equal to R_1 - 2R. Thus f_i is approximately equal to:

$$f_i = \{2(R_1\text{-}R_2)\pi /(2\pi R_1)\}(2\pi R_1 t_t)f_y = 4\pi R\ t_t\ f_y \qquad (4\text{-}4)$$

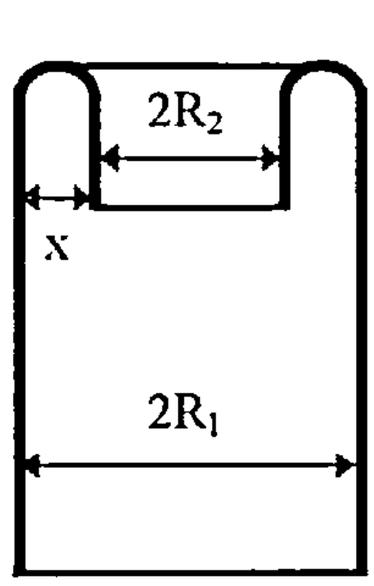

Fig 4-24

and the dissipated work will be:

$$(0.5t_g\tau + f_y t_t^2 /2R)\, y\, 2\pi R + 4\pi R\, t_t\, f_y \qquad (4\text{-}5)$$

This energy is equal to the external done work ,which is F(2y), therefore, the transmitted force will be:

$$F = 0.5\,(0.5\, t_g\tau + f_y t_t^2 /R\,)(2\pi R_1) + 2\pi R\, t_t\, f_y$$

$$F= 0.5\pi R_1\, t_g\tau + \pi f_y t_t(R_1 t_t/R + 2R) \qquad (4\text{-}6)$$

The following typical data is assumed to all forms of shell which have been considered:

Table 4-3

E	200000N/mm^2
m	7.8E-6Kg/mm^3
f_y	300 N/mm^2
R_1	60 mm
R	4.5 mm
t_g	0.5 mm
t_t	2 mm

Using these values, equation 4-6 gives:

$$F=0.5 \times \pi \times 30 \times 30 \times 0.5 + \pi \times 300 \times 2 \times (30 \times 2/4.5 + 2 \times 4.5) = 42076 \text{ N}$$

Numerical method:

In order to find the peeling force of the tube, the shell was analysed without connection part 1 and an extended support tube (Fig 4-25):

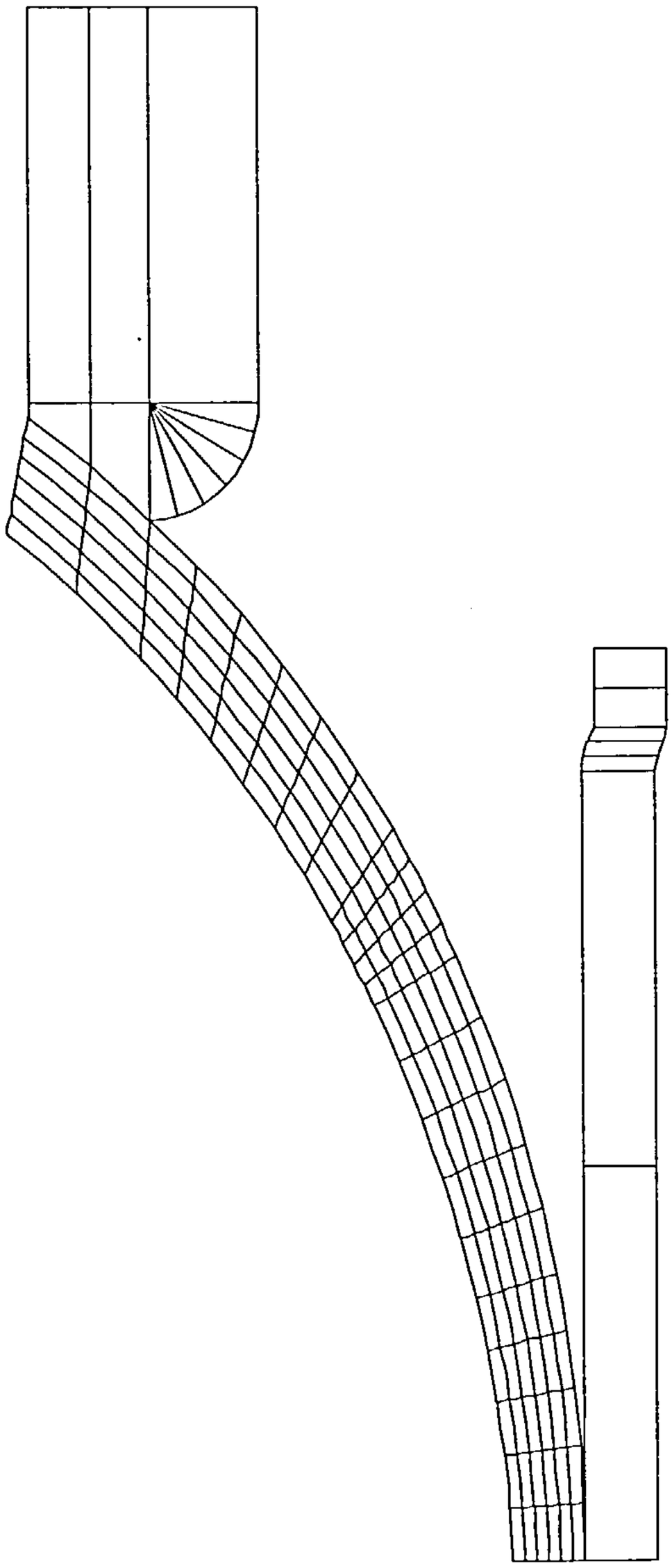

Fig 4-25: The finite element mesh to model the peeling phenomenon

The model of the device was loaded in a manner which has been described in section 4-1-1-1 and the result of the analysis is shown Fig 4-26 .

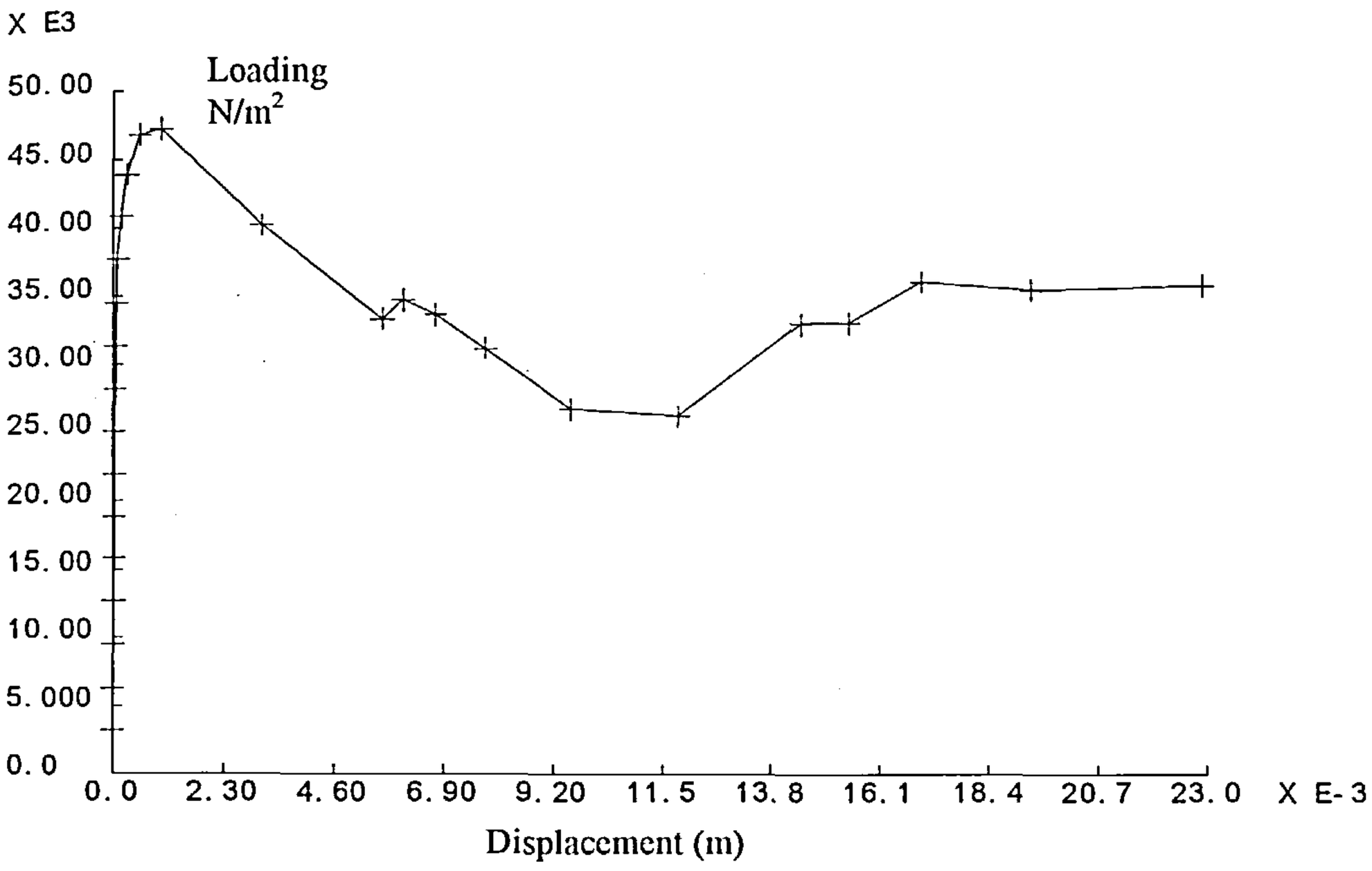

Fig 4-26: Load deflection curve for assessing peeling force

The final plateau for the load deflection can be seen to correspond to a load of 36000 N. It is obvious that by reducing R (the clearance between connection part 2 and the support tube) this load can be increased. In this model the effect of adhesive has not been considered, but it may be added to this result. This effect has been explained in the analysis of section 4-1-1-1. By adding the same amount to this result, the peeling force will be 36705N.

Figure 4-27 shows the deflection of the device in this case. The peeling process has been started and the tube is being inverted between the connection parts and the support tube. The shell in its contact region with the connection part 3 have experienced large strains and deformations. Therefore, it is advisable that the thickness of the shell in this region to be higher than the other regions.

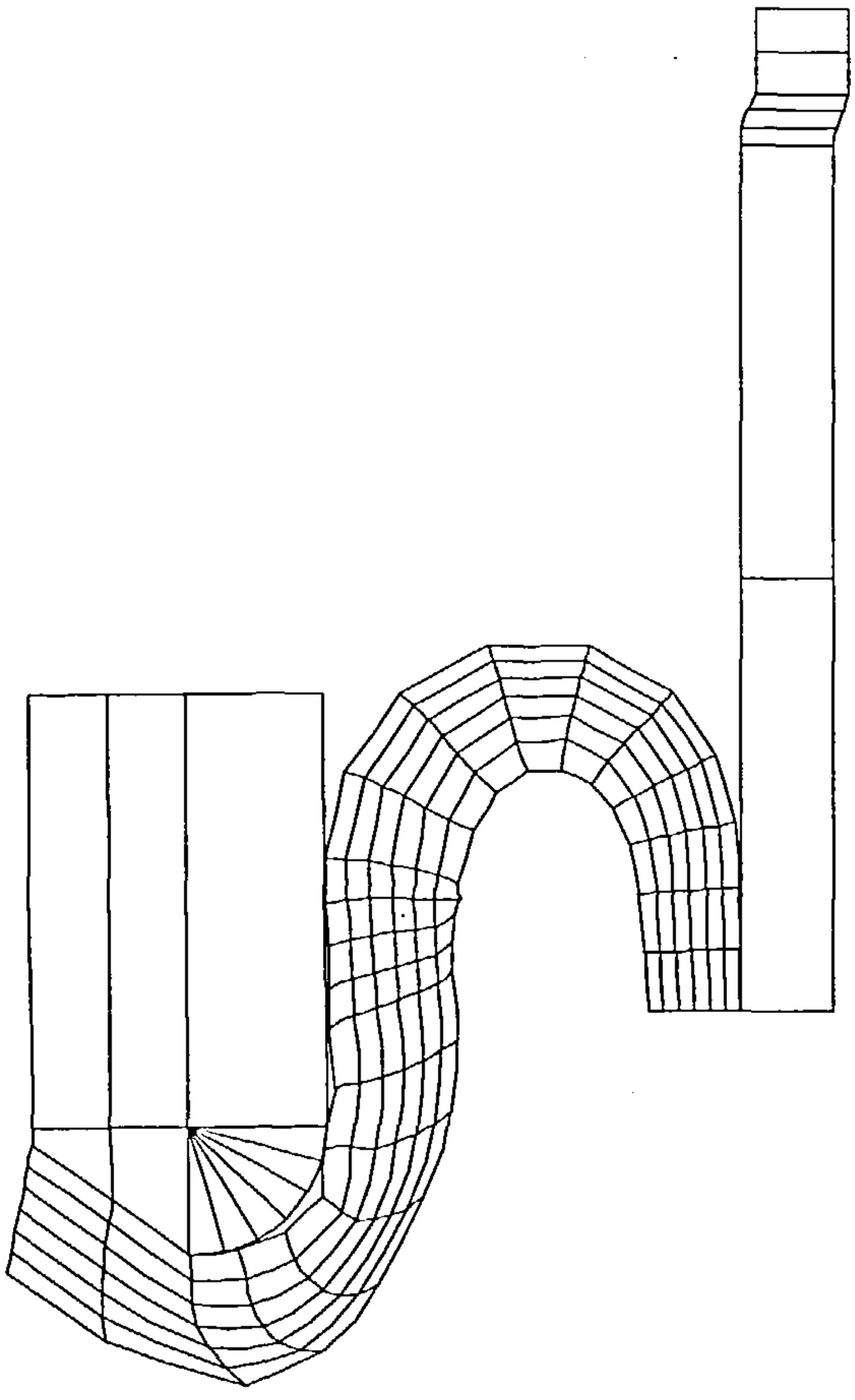

Fig 4-27: Deformed mesh of the shell during the peeling process

4-1-2-3 Buckling Analysis :

For the buckling analysis of the shell an initial Guyan Buckling analysis was run and then an eigenvalue control followed to improve the results. An elastic buckling analysis was executed by Lusas which had some modelling restrictions.

These restrictions will be explained for each case.

Feature definition

The Lusas program does not have a capability to carry out a buckling analysis when slide line or non-linear material are used . Therefore, for the buckling analysis of the shell, the following configuration has been used (Figure 4-28). In this arrangement, the support tube and the connection parts have been deleted and an elastic material has been considered.

Although this analysis involves some approximations, but their effects are in safety side. In the other words, if the analysis shows that there is no elastic buckling hazard

ith this configuration, it can be resulted that there will not be any buckling possibility in the original configuration.

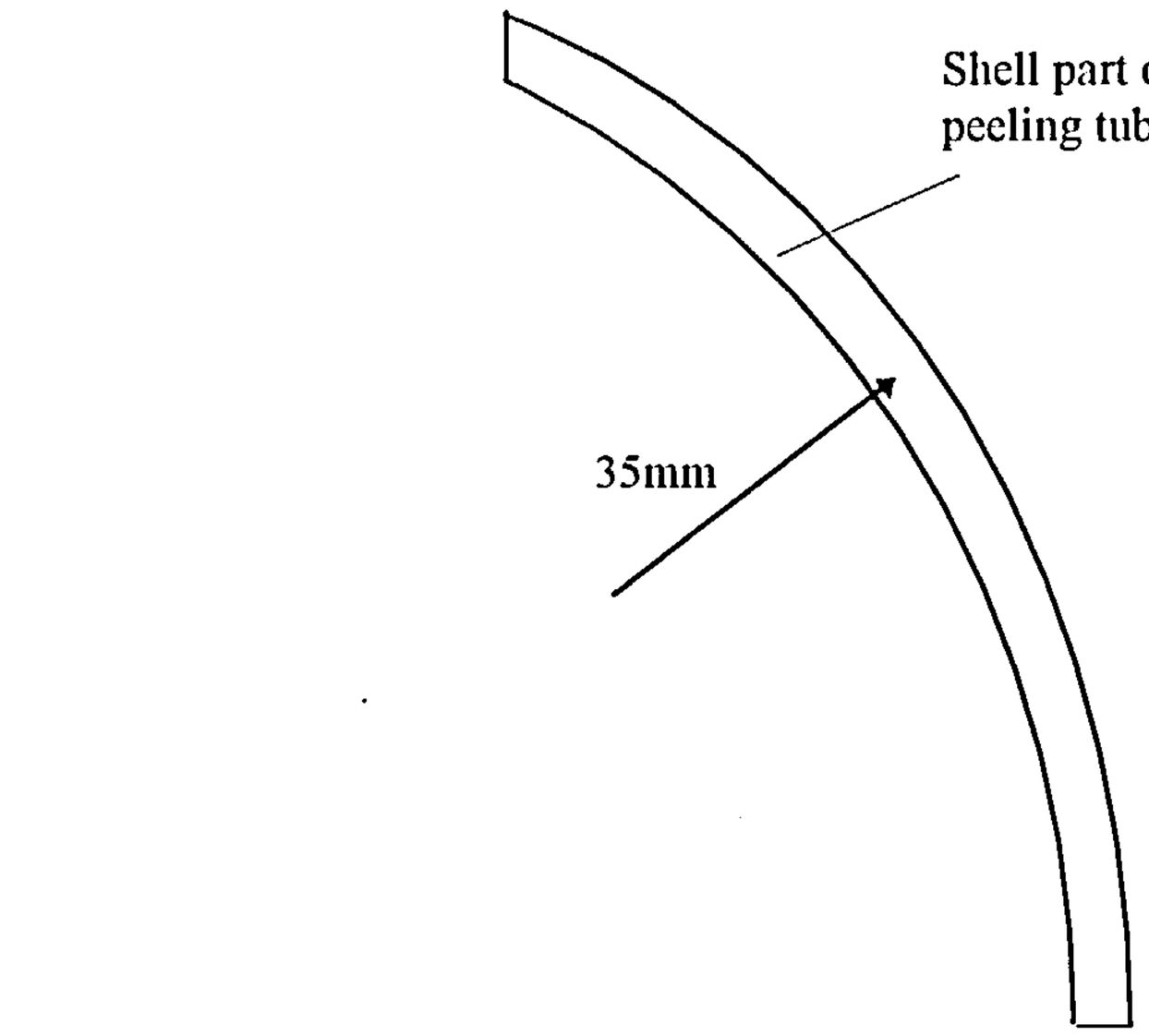

Fig 4-28: Detail of the shell for buckling analysis

By using the rotation facility of Lusas, a symmetrical shell was created for modelling.

Meshing: Three dimensional isoparametric solid continuum elements HX20 have been used for modelling the shell (Fig 4-29).

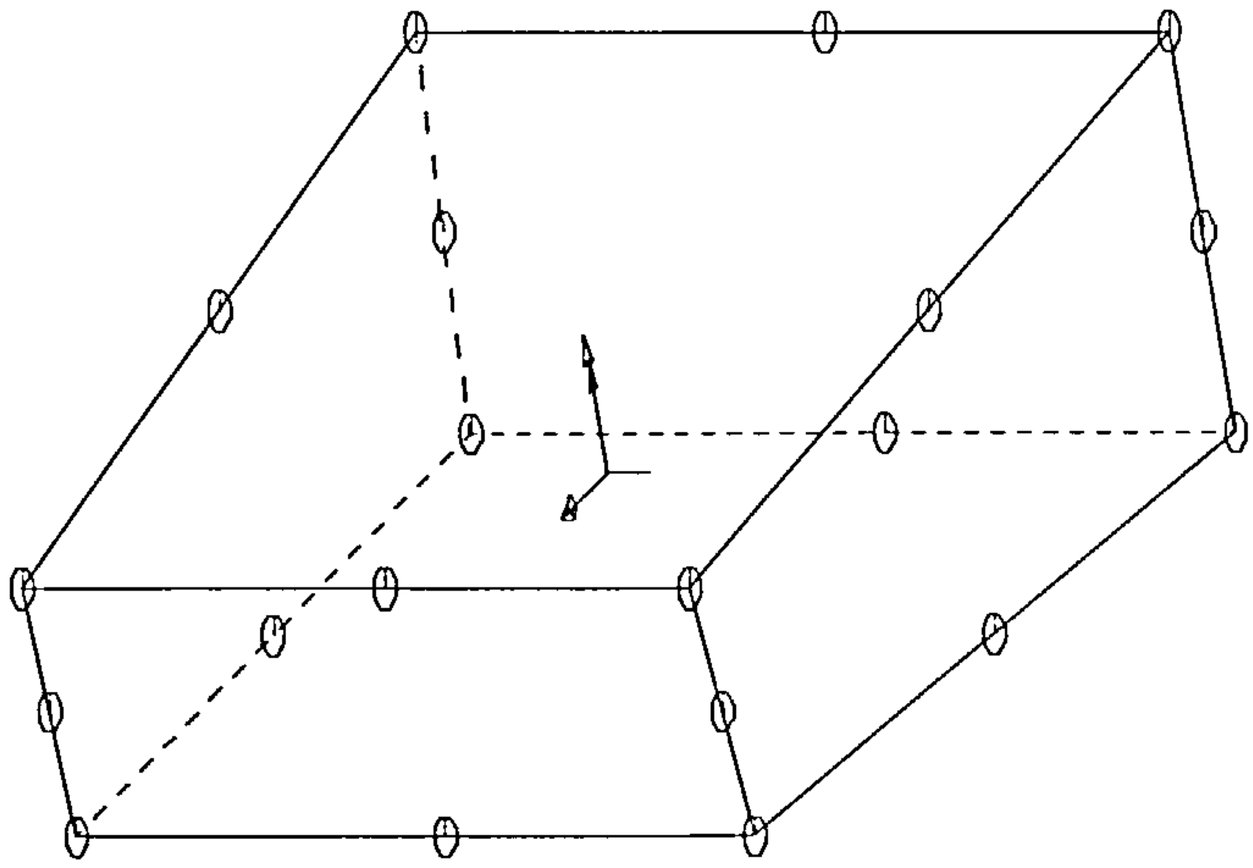

Fig 4-29: 3-dimentional continuum element, HX20

This element has the capability of modelling curved boundaries and is numerically integrated. It has three degrees of freedom, U, V, W at each node. No any geometric properties are assigned to this element.

The element mesh for the shell consists of 10 elements around the circumference and 20 along the surface (Fig 4-30).

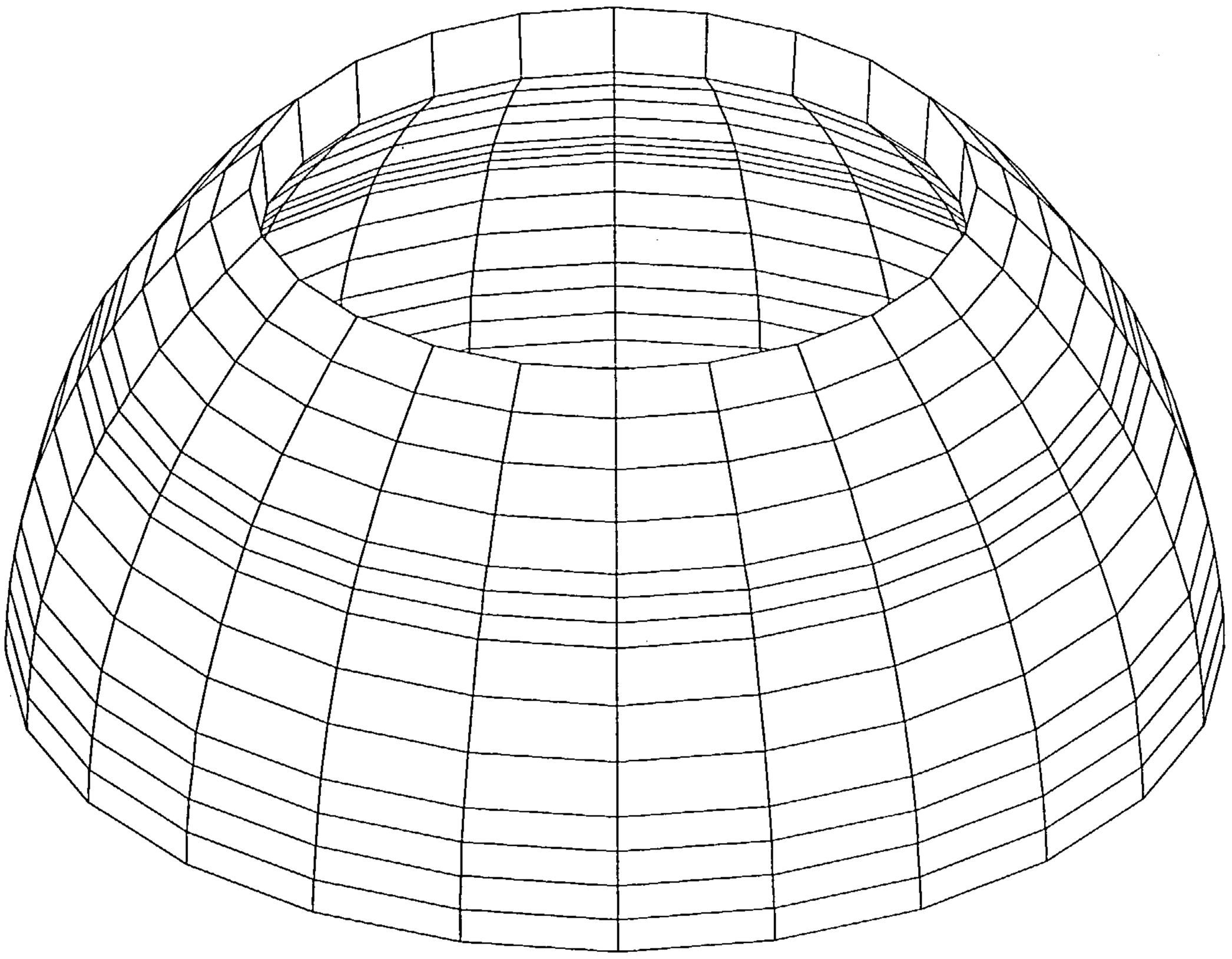

Fig 4-30: Meshing of the Shell

Material: Only elastic material properties have been considered for the shell. The typical values are shown in table 4-4.

Table 4-4

Elastic modulus E	2.0E11 N/m^2
Poisson Ratio ν	0.3
mass m	7800 Kg/m^3

Geometric Definition: A geometric definition is not required for this element.

Support conditions: All of the surfaces on the bottom edge are full restricted supports. For the top edge all degrees of freedoms except the translation in the Y and V directions are restricted.

Loading: A uniform loading of 1 N is assigned to the nodes of top edge. Therefore, the total loading of the shell will be 132 N (Fig 4-31).

By considering 1 N as loading in this analysis, the resulted load factors will be the loads on each node which causes the buckling of the shell.

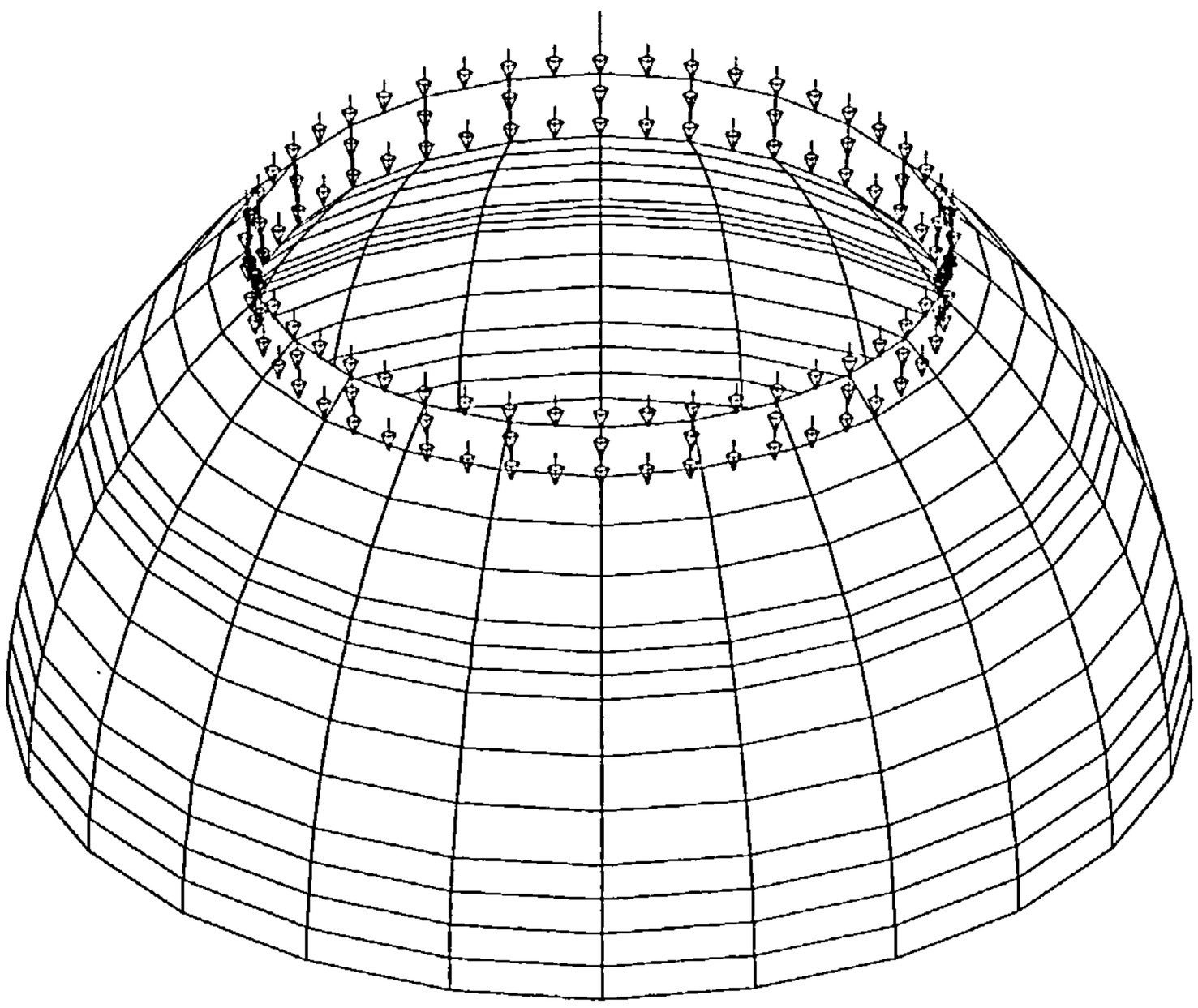

Fig 4-31: Loading of the Shell

Analysis control:

Eigenvalue buckling control has been used for this shell. Three buckling mode have been requested from the analysis. A generalised Jacobi method was chosen as the eigensolver and a Sturm sequence check was used with a maximum of forty iterations for the calculation.

Results: The results for three eigenvalues are shown in table 4-5:

Table 4-5

E I G E N V A L U E S		
MODE	EIGENVALUE	LOAD FACTOR
1	36796.6	36796.6
2	37722.5	37722.5
3	37722.6	37722.6

According to these result the minimum buckling load of the shell will be greater than 100KN. By comparing these results with the yield limit of the device, it is apparent that there is no elastic buckling possible for the shell.

The first and second buckling mode of the shell have been shown in Figures 4-32, 4-33.

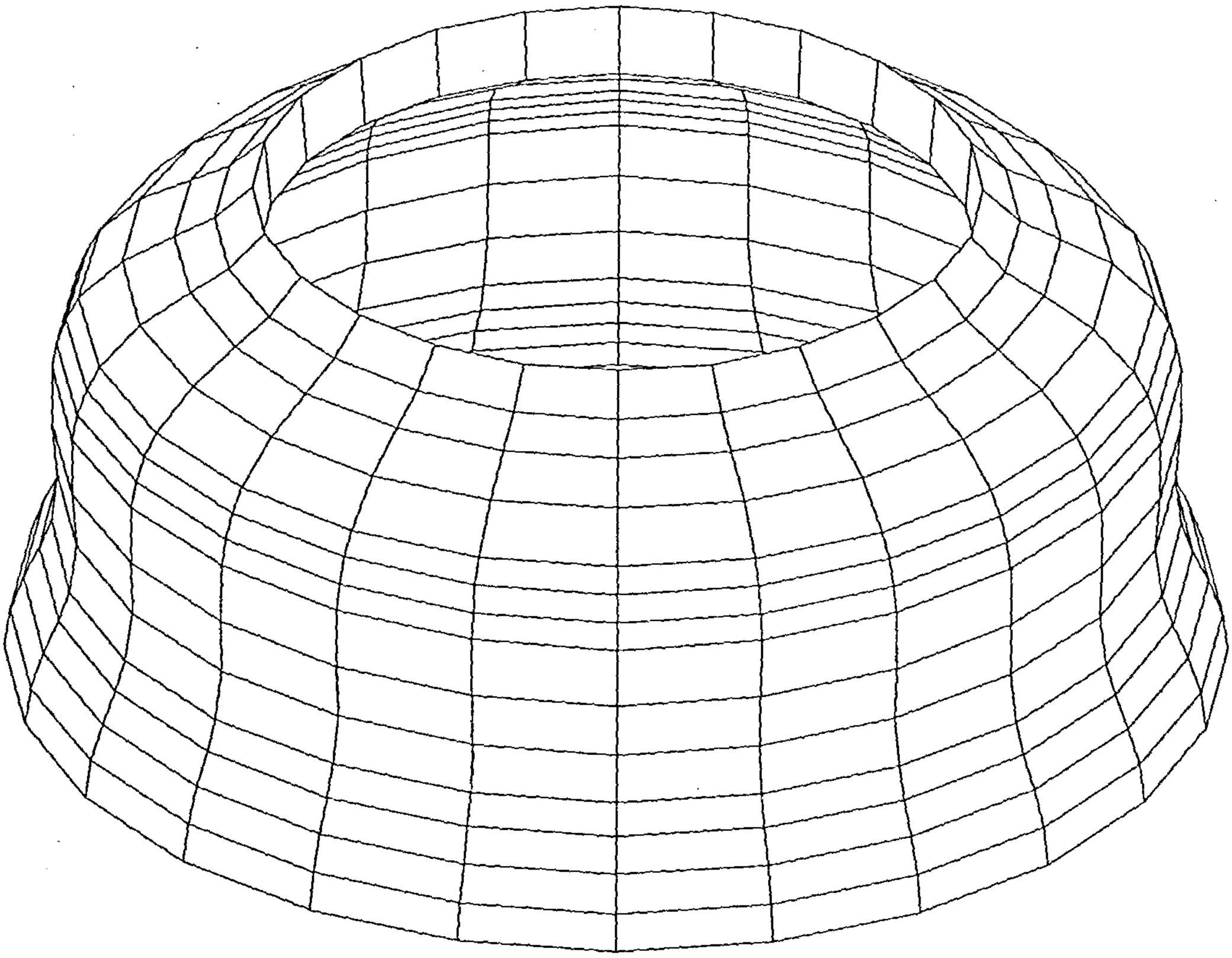

Fig 4-33: First buckling mode of the shell

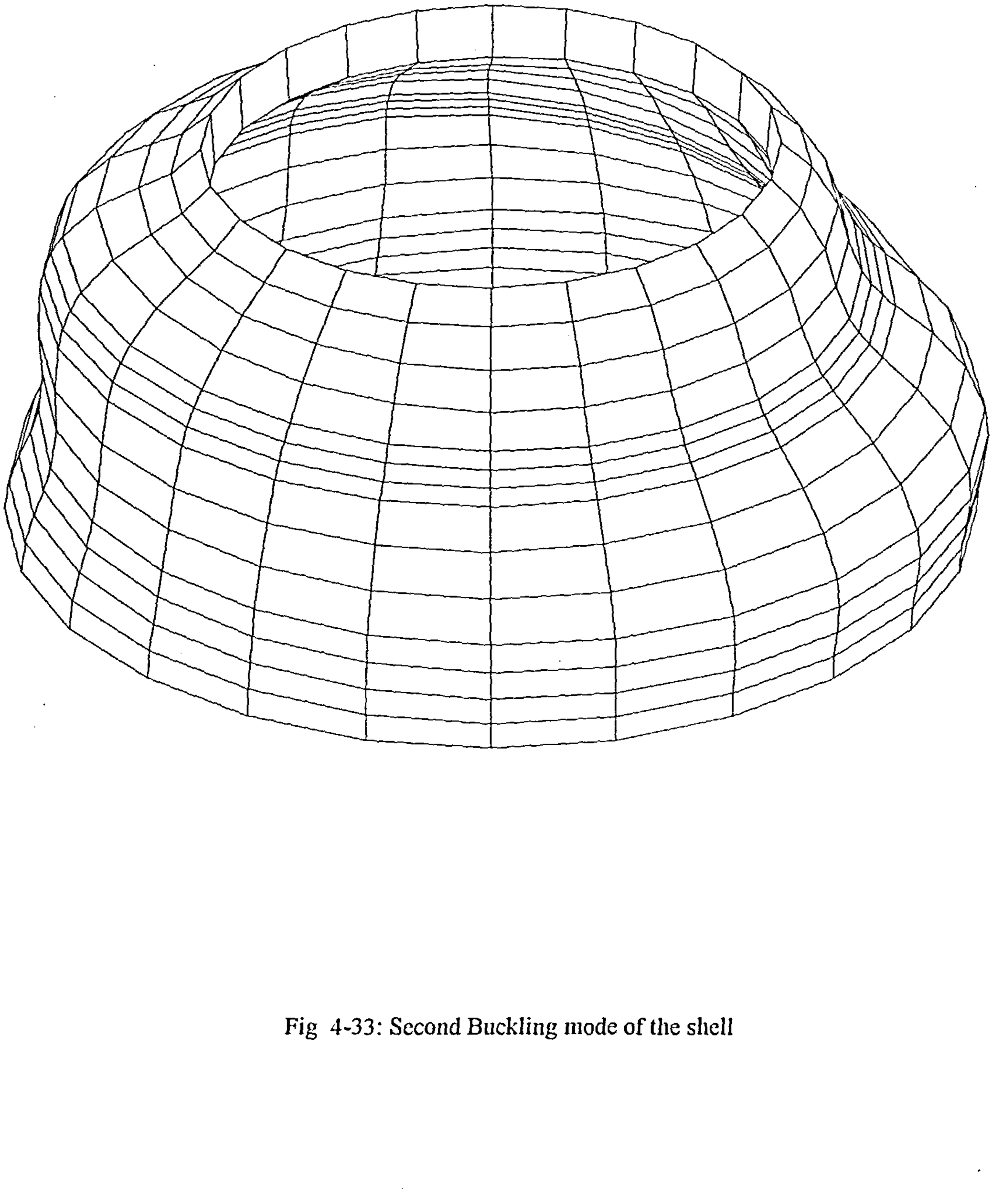

Fig 4-33: Second Buckling mode of the shell

4-1-3 Shell No 2- Two arcs for the shell

4-1-3-1 Nonlinear dynamic analysis

Two arcs are considered for the shell in Figure 4-34. Their details have been described in this figure. The other details are the same for the shells. The model has been analysed with the same data and modelling assumptions which were considered for the previous model. Therefore, only the results will be reported.

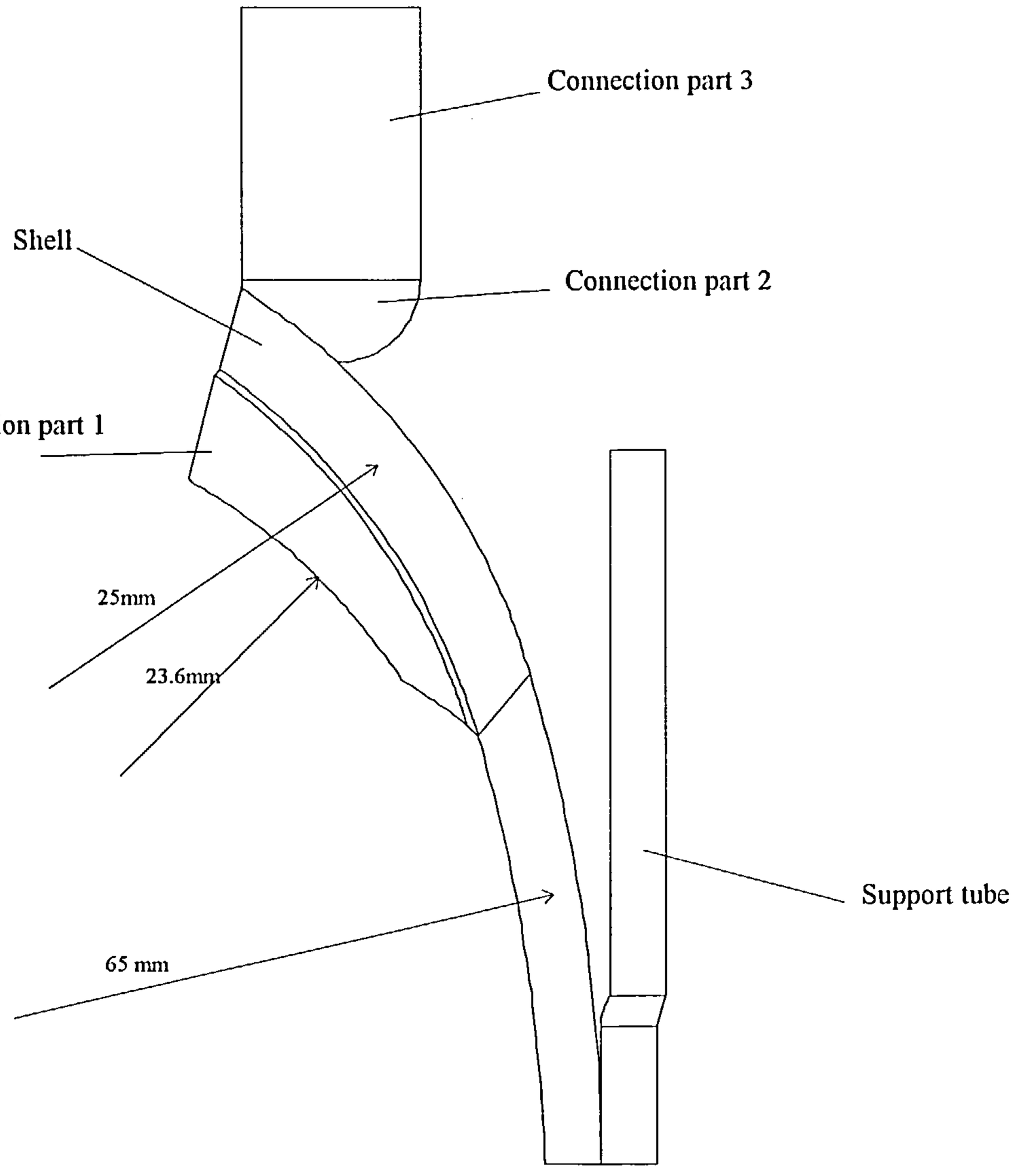

Fig 4-34: Feature definition of the second shell

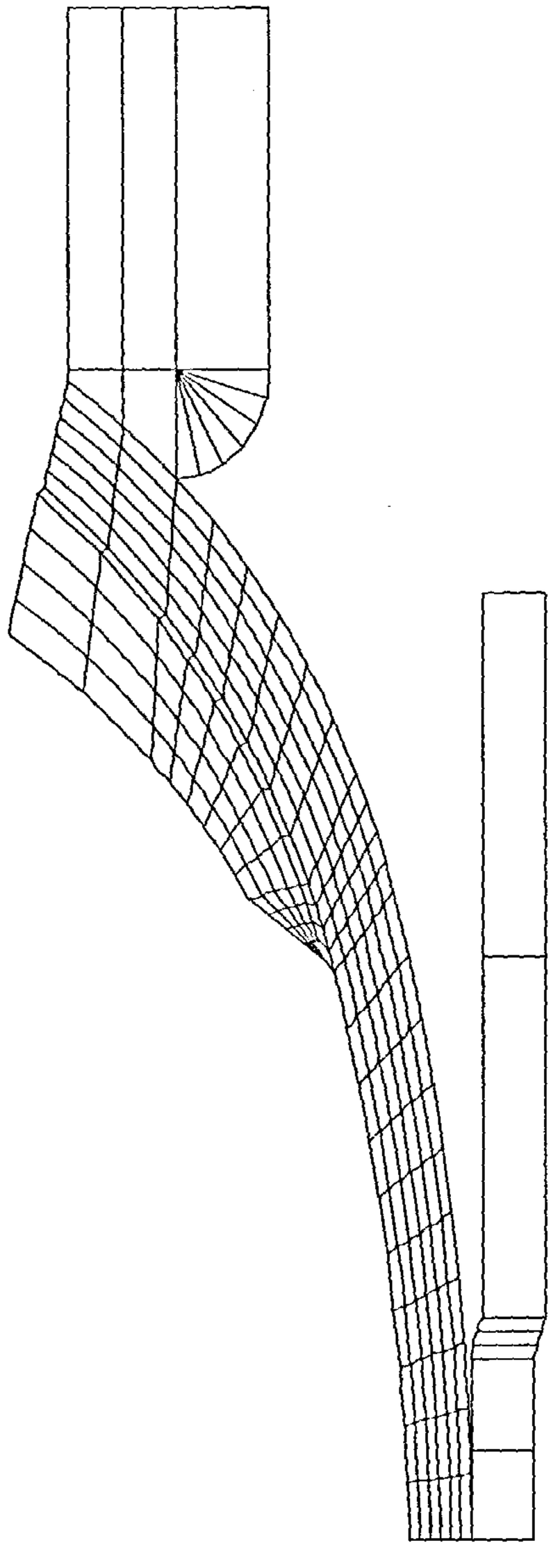

Fig 4-35: Finite element mesh of the shell

Results:

The load deflection curve of the device with the second shell has been shown in Figure 4-36 .

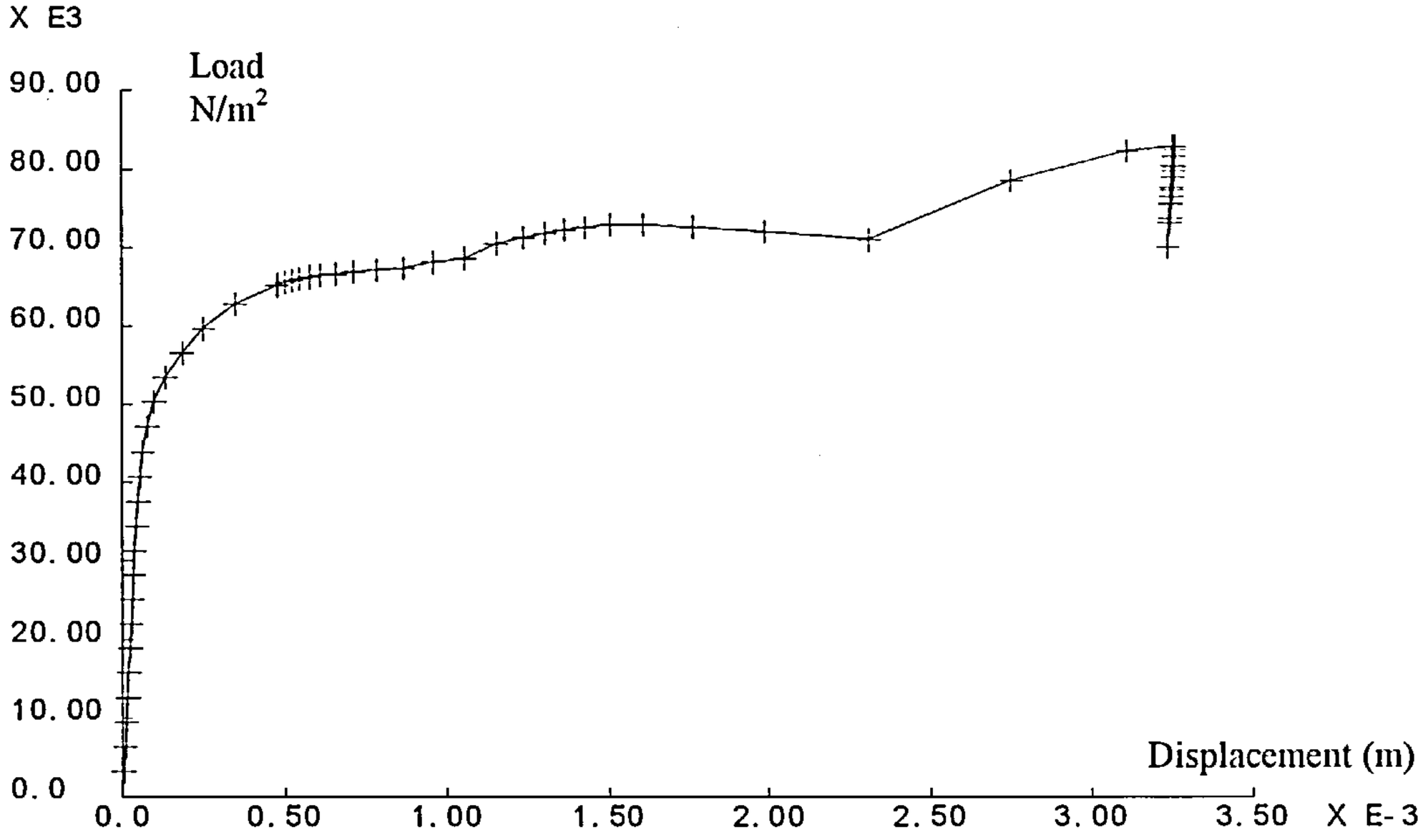

Fig 4-36: Load deflection curve of the device

By using two arcs for the shell the yield load has been raised by 10000 N. The adhesive fails immediately after yielding as in the previous case, and a sudden drop in load deflection curve is seen to occur. Separation of the connection part 1 and the shell has been shown in Figure 4-37.

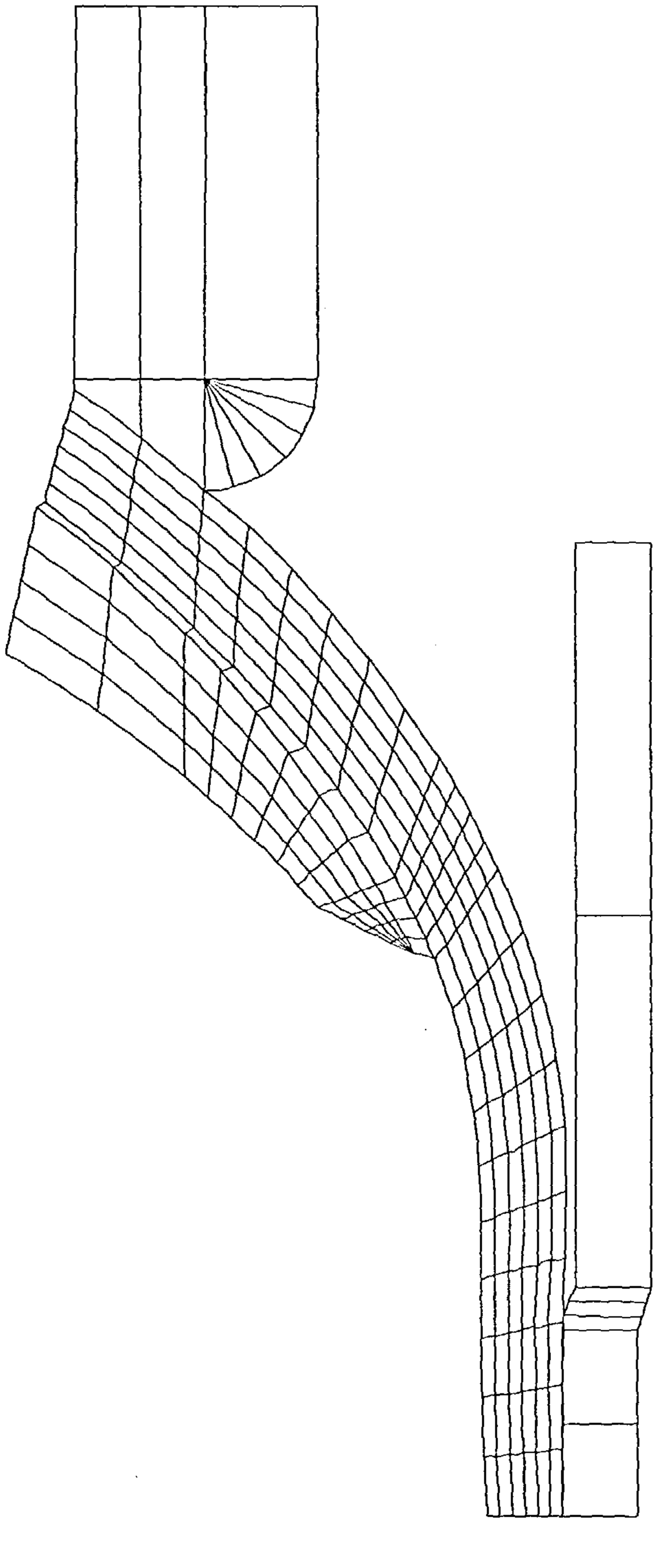

Fig 4-37: Separation of the peeling tube and the shell

This figure shows the end of interaction of the shell and the connection part one. After this stage the shell collapses and the peeling process starts. It is important to have smooth transfer from the collapse of the shell to the peeling process. The separation of connection part 1 and the shell imposes a proper mode on the collapse form of the shell and prevents from the high fluctuation of load at this stage.

The initiation of yielding in the shell and the connection part 1 have been shown in figures 4-38 and 4-39. These yielding have been occurred at load 32000N. The comparison of these figures with that of the single arc shell (Figures 4-17 and 4-18) shows that the yielded points in this case is less the previous example of the shell.

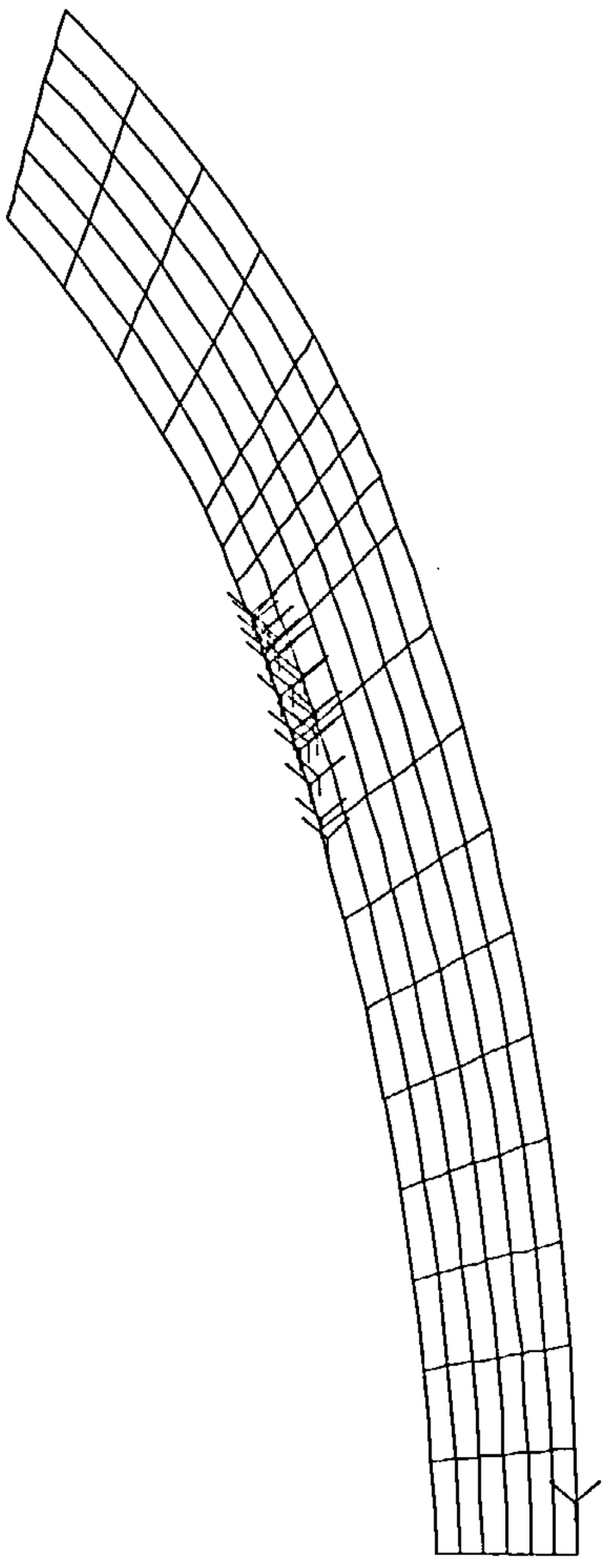

FIG 4-38: Initiation of yield points in the shell

The connection part one has been yielded at its tip. This indicates that there is concentration of stress between this part and the shell. The connection part one has the same material property as the shell.

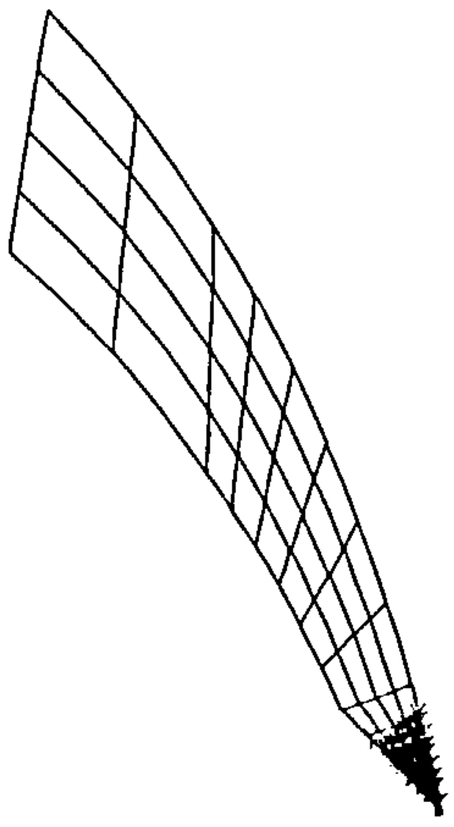

Fig 4-39: Initiation of yield points in the connection part 1

Load-response time curve of the device has been shown in Figure 4-40:

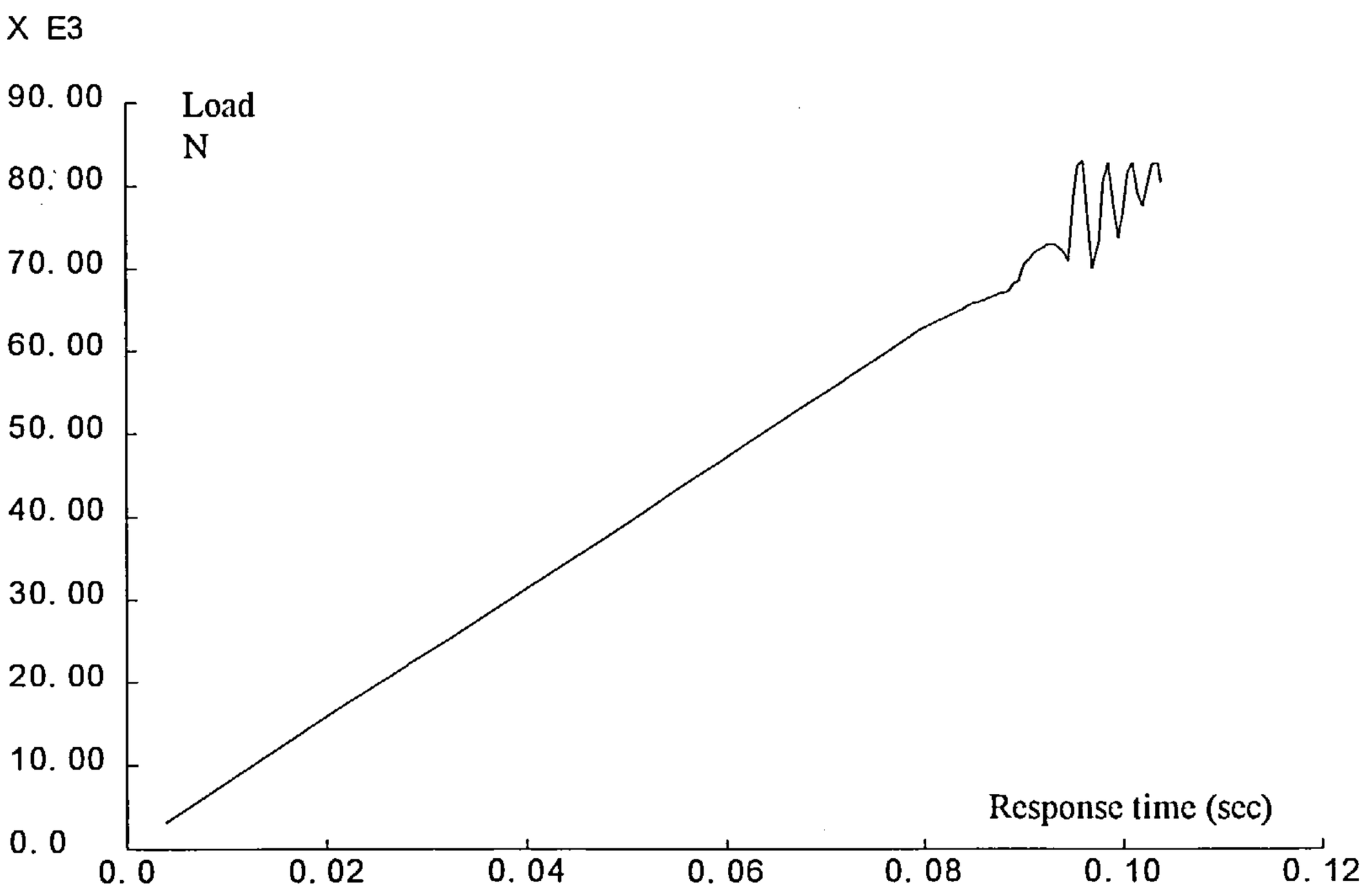

Fig 4-40: Load response time curve of the device

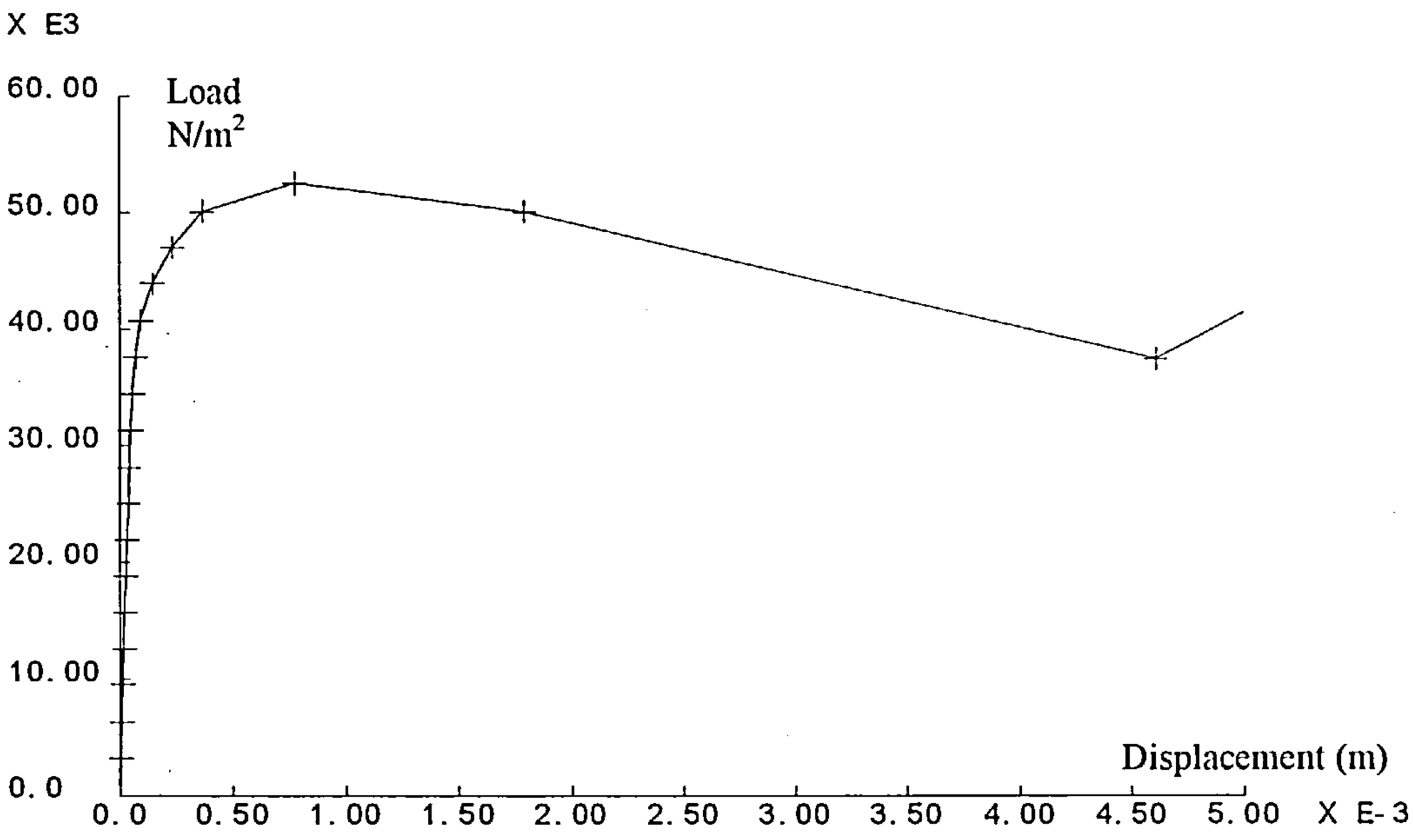

Fig 4-41: Load deflection curve of the device without connection part 1

Figure 4-41 shows the load-deflection curve for the numerical model of the energy absorbing device without the connection part 1. This curve is for estimating the peeling force of the shell.

The analytical method for calculating the peeling force in this shell is the same as the example of section 4-1-1-2. Therefore the analysis is not repeated for this shell.

4-1-3-2 Buckling analysis

For the same conditions as the previous case (section 4-1-1-3), buckling analyses were performed and the results are given in table 4-6:

Table 4-6

E I G E N V A L U E S		
MODE	EIGENVALUE	LOAD FACTOR
1	35421.8	35421.8
2	36134.1	36134.1
3	36135.1	36135.1

The first two buckling modes have been shown in Figures 4-42 and 4-43. The buckling modes of this shell are similar to the previous shell (section 4-1-1-3).

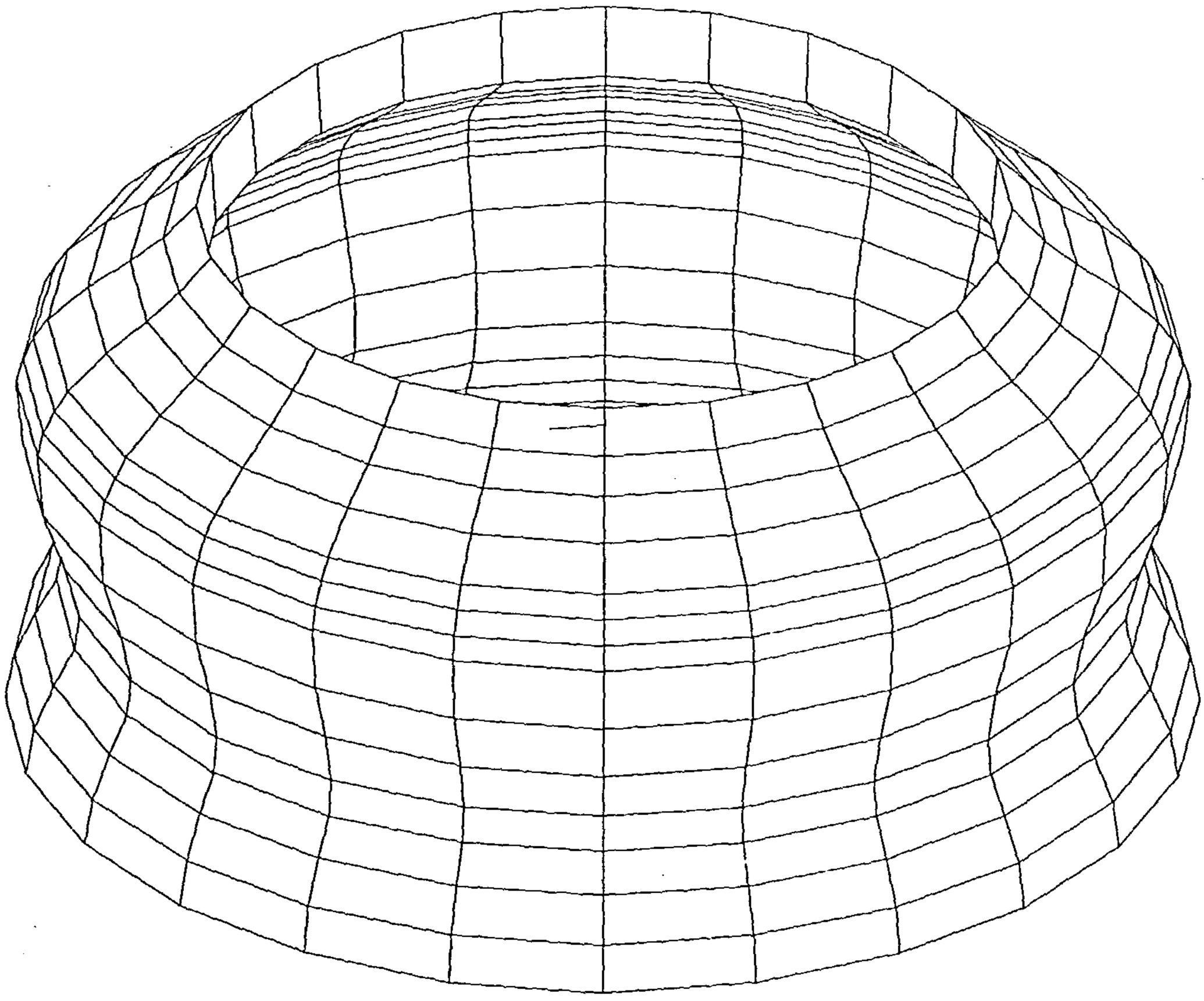

Fig 4-42: First buckling mode of the shell

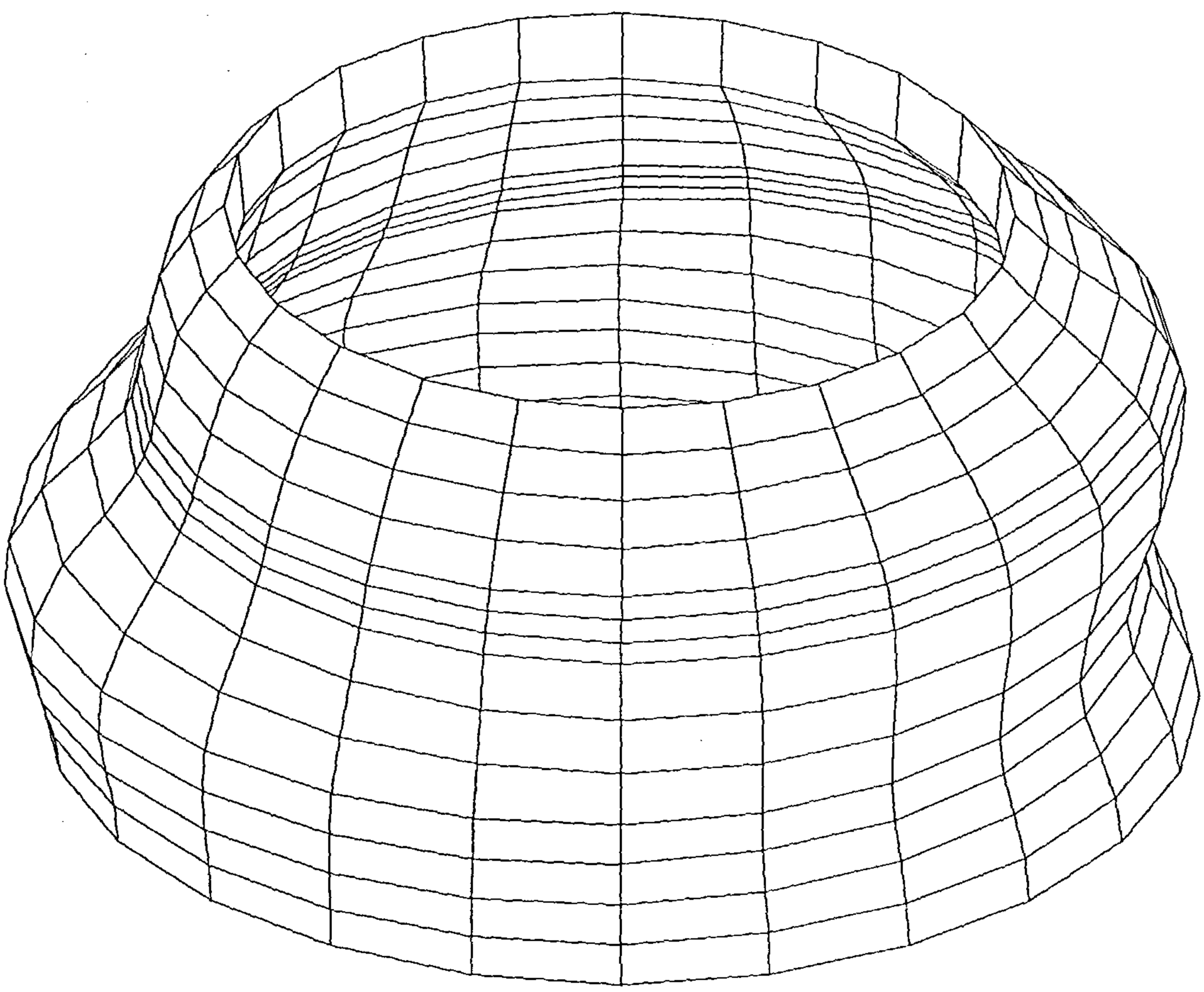

Fig 4-43: Second buckling mode of the shell

4-2 The connection set:

It is essential that an analysis of the wedges and the bar be carried out to determine the stresses in the teeth. For this purpose, a simple analytical solution can be carried out to obtain pre-design data. In the following section, we present this analysis.

4-2-1 Analytical method

The cross section of the connection set is shown in figure 4-44.

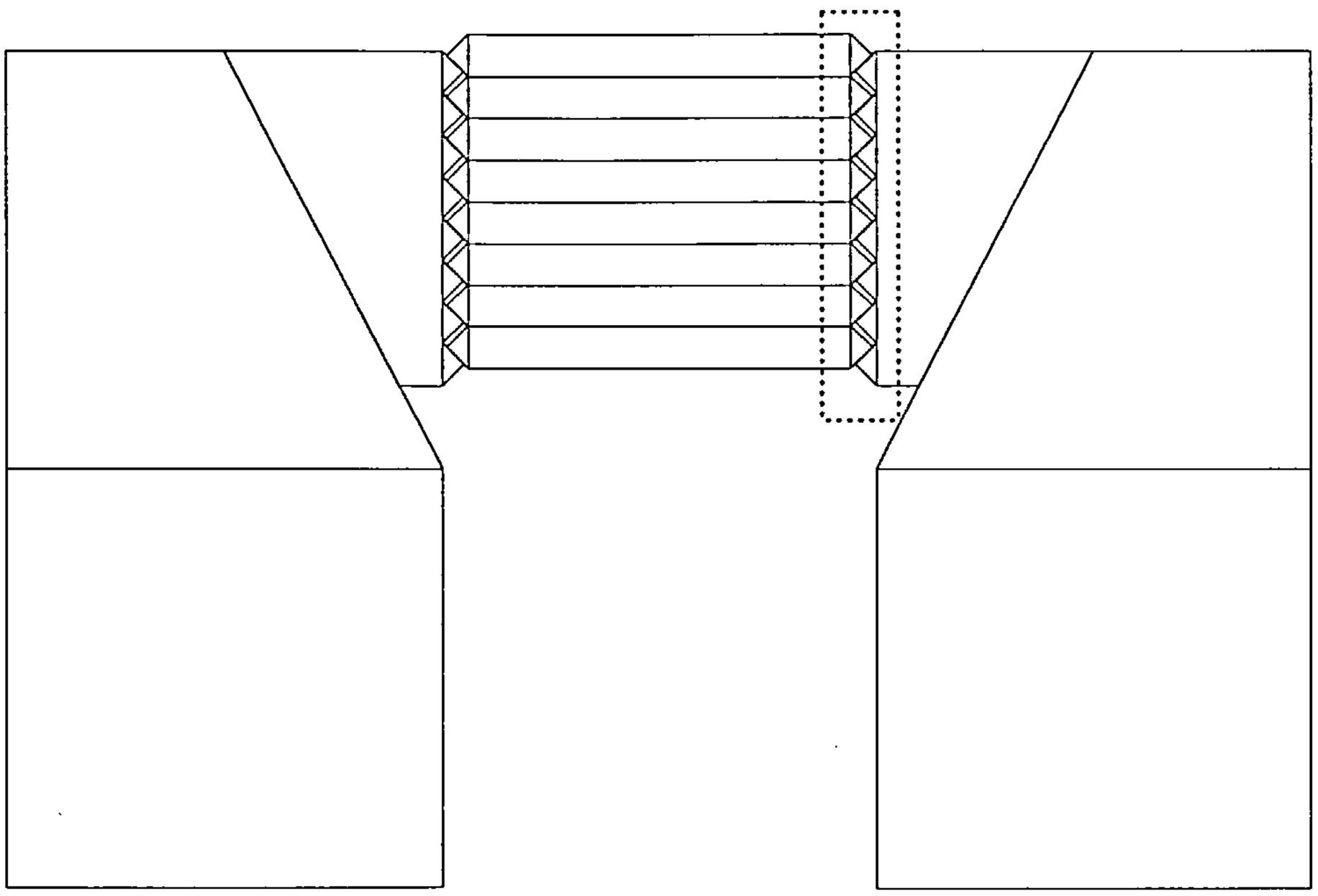

Fig 4-42: Cross section of the connection set

The stress in the teeth, can be calculated by the usual methods of solid mechanics.

Friction between surfaces is neglected in this calculation.

Figure 4-45 shows the free body description for the teeth.

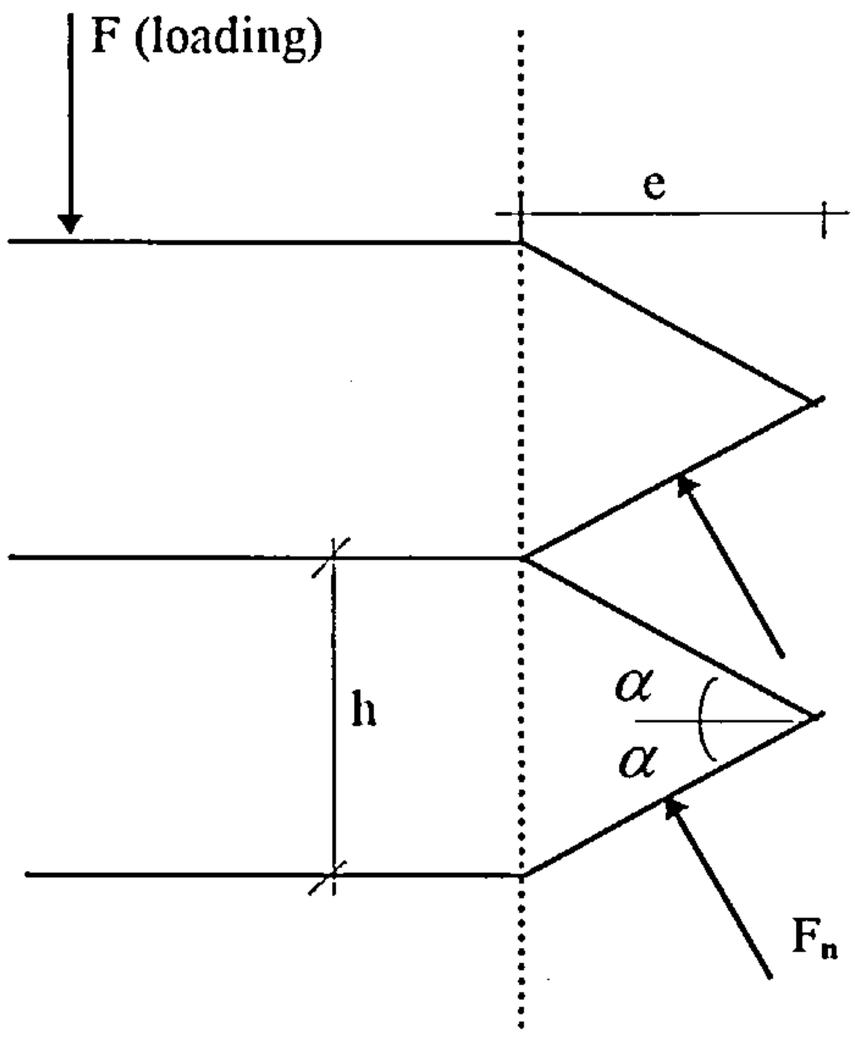

Fig 4-45: Teeth of the bar in close up

It is necessary to check the shear and bearing stresses in the cogs.

$arc(b)=R_b[2\arcsin(b/2R_b)]$

$$\tau_s=F/[2n.h.arc(b)] < \bar{\tau}_s \qquad (4\text{-}7)$$

In which, n is the number of teeth, h is its height, b is the cross width of the wedges Figures 4-39 and 4-40. $\bar{\tau}_s$ is the permissible shear stress.

For calculating the normal force:

$F_n=F/n\cos\alpha$

$$S_n=(e/\cos\alpha).arc(b) \quad , \quad \cos\alpha = e/\sqrt{(h/2)^2+e^2}$$

$$\sigma=F_n/S_n < \bar{\sigma} \qquad (4\text{-}8)$$

In which $\bar{\sigma}$ is the permissible normal bearing stress and R_b is the radius of the peeler bar.

The same relations are valid for the cogs of the wedges and the same design will be applied.

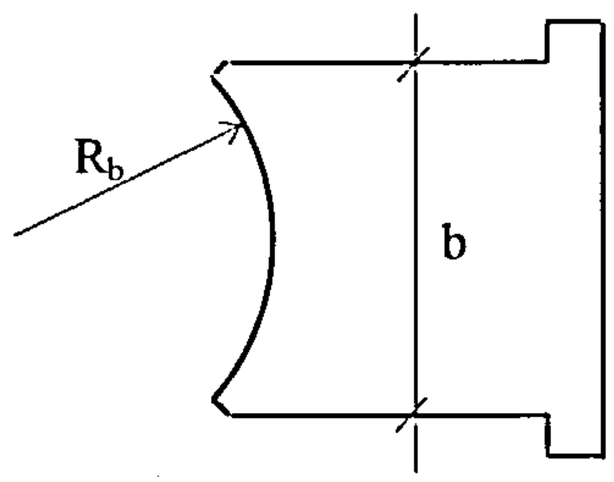

Fig 4-46: The wedge

As a numerical example, the following quantities is considered for the connection set.

Table 4-6

F	70000 N
$\overline{\sigma}$	400 N/mm^2
$\overline{\tau}_s$	200 N/mm^2
e	2 mm
h	4 mm
n	8
R_b	8.5 mm
b	12 mm

Therefore,

$arc(b)=R_b[2\arcsin(b/2R_b)]=8.5[2\times\arcsin(12/(2\times 8.5))]=13.3$ mm

$\tau_s=F/[2n.h.arc(b)]=70000/[2\times 8\times 4\times 13.3]=82.2$ N/mm^2 < 200 N/mm^2

$\cos\alpha = e/\sqrt{(h/2)^2+e^2} = 2/\sqrt{(4/2)^2+2^2} = 0.707$

$S_n=(e/\cos\alpha).arc(b)=(2/0.707)13.3=37.6$ mm^2

$F_n=F/n\cos\alpha=70000/(8\times 0.707)=12376.2$ N

$\sigma=F_n/S_n = 12376.2/37.6=329.1 < 400$ N/mm^2

4-2-2 Numerical Modelling

Having conducted the simple analytical method of section 4-2-1, numerical models are created for design of the set. Two models have been proposed to represent the connection set. The first is a two dimensional model, and the second a is three dimensional model. The two dimensional model uses plane stress elements. The results of this two dimensional model are then used as a starting point for a three dimensional analysis.

In order to save time, in the three dimensional analysis, only a quarter of the connection set has been modelled. In the two dimensional model only half of the cross section has been chosen for analysis. The effects of the other parts have been represented by appropriate boundary conditions.

4-2-2-1 Two dimensional modelling

Feature definition

The two dimensional analysis was performed by creating the following features for the connection set. From the cross section of Figure 4-44, only half of the connection was considered for the analysis, because of the symmetry. The effect of the other half was considered by assigning proper boundary conditions. Two surfaces were used to model the connection part 3. For the wedges, one surface and for each tooth an individual surface was used. The effect of the edges of the wedges have been simulated by two surfaces. The first surface has a common line with inclined line of the wedge and the second surface is in parallel with the first one and has fixed supports (Fig 4-47).

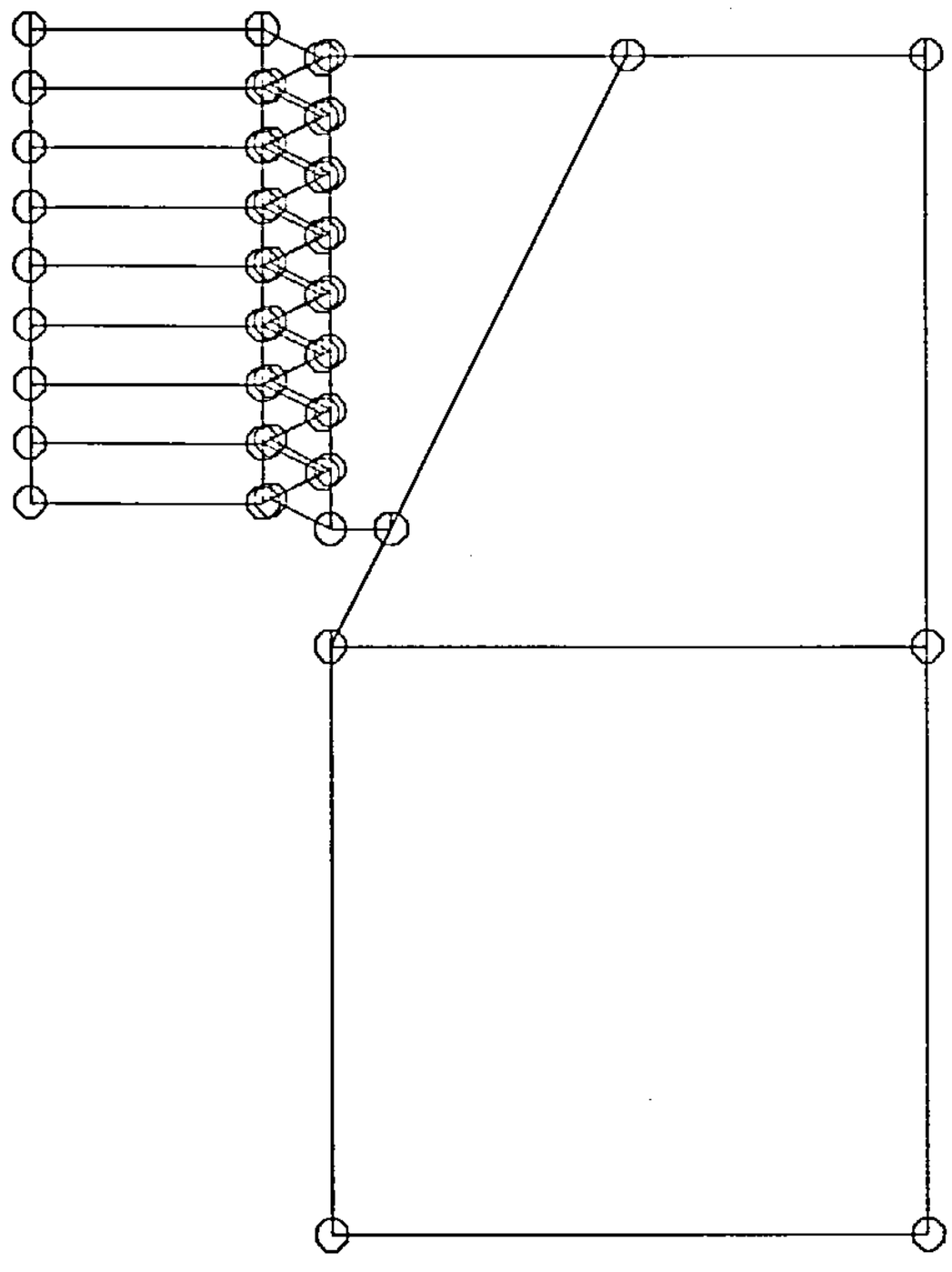

Fig 4-47: Feature definition for two dimensional analysis

Meshing

Quadrilateral and tetralateral plane stress elements QPM8 and TPM6 from the Lusas programme have been used for the meshing of the model (Fig 4-48).

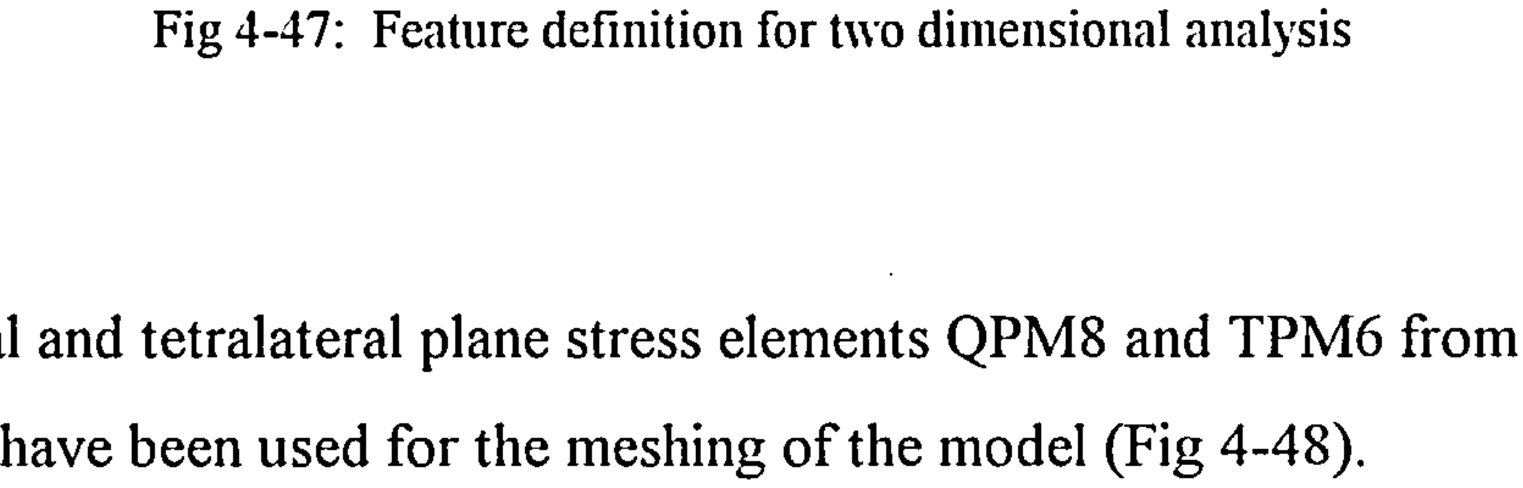

Fig 4-48: Plane Stress Quadrilateral QPM8 element

Each element has two degrees of freedom at each node and variable thickness could be applied to each node. This element also has a restriction for midside node centrality and for excessive element curvature which has been the case for the previous used elements.

The meshing is irregular for the wedges and for this purpose, a null line element has been defined and assigned to represent wedge lines. Figure 4-49 illustrates the mesh used in the numerical analysis.

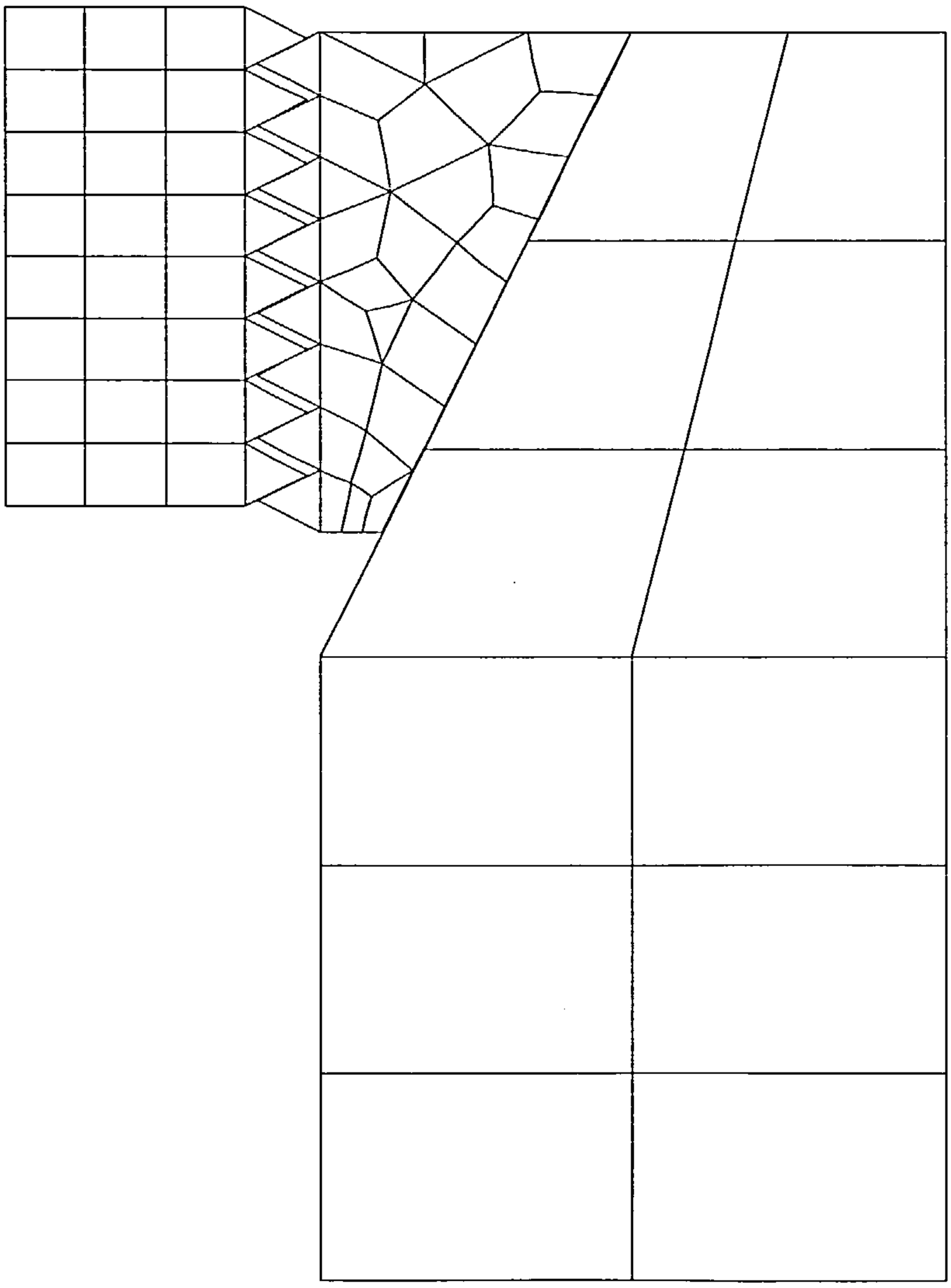

Fig 4-49: Two dimensional model meshing

Geometric definition:

A thickness of 30 mm was considered for all elements which is actually the width the of wedges.

Loading:

A concentrated uniform loading of 5000 N was applied on the lower line of the peeler bar (Fig 4-44). Therefore, the applied load on the set was 70000N which is the collapse load of the shell.

Support conditions:

Two support conditions exist for this model. One is to restrict all freedoms and the other to restrict the X direction displacement. The first condition has been assigned for all lower lines of the connection part 3. The second condition has been applied to the side lines of the connection part 3 These support and loading conditions have been shown in Fig 4-50.

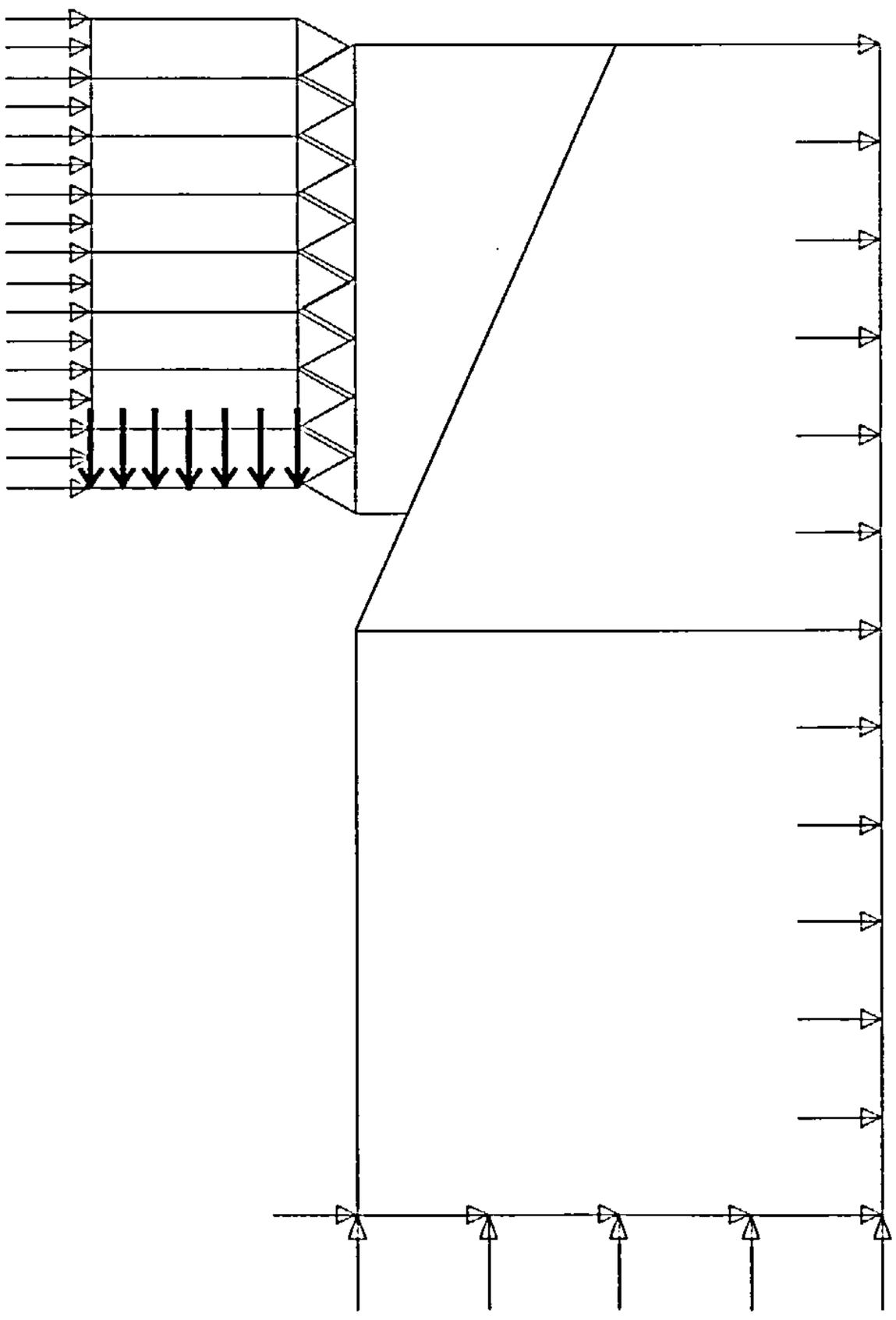

Fig 4-50: Support and Loading conditions

Material Definition:

Steel: For the steel material the following properties were assigned (table 4-6).

Table 4-7

E	2E11 N/m^2
ν	0.3
m	7800 kg/m^3
f_y	400000000 N/m^2

The plastic hardening gradient was considered zero. This plastic assignment is not in contradiction with the previous assumption for the connection parts. In fact in the peeling tube analysis, the rigidity of the connection set was higher than the peeling tube, so in that analyse, plasticity was not considered for these parts.

Slide line: Two slide lines have been considered for this connection set. The first is between the wedges and connection part 3 and the second between the teeth of the bar and the wedges. A high interface stiffness scale factor has been considered for the material of both the slave and master surfaces. For a convenient solution, connection part 3 and the teeth bar are considered as slave surfaces and the wedges as master surfaces. No pre contact has been assigned to the slide lines. A typical friction coefficient of 0.1 has been assigned to the teeth but no friction has been applied to other slide lines.

Geometric Nonlinearity: Total Lagrangian geometric nonlinearity has been chosen for this problem because of its stability and its validity for large displacements.

Load curve definition: Figure 4-51 shows definition of the time step coefficients which have been used in the analysis. This is the same load curve which was assumed in section 4-1-1-1 for the loading of the shell.

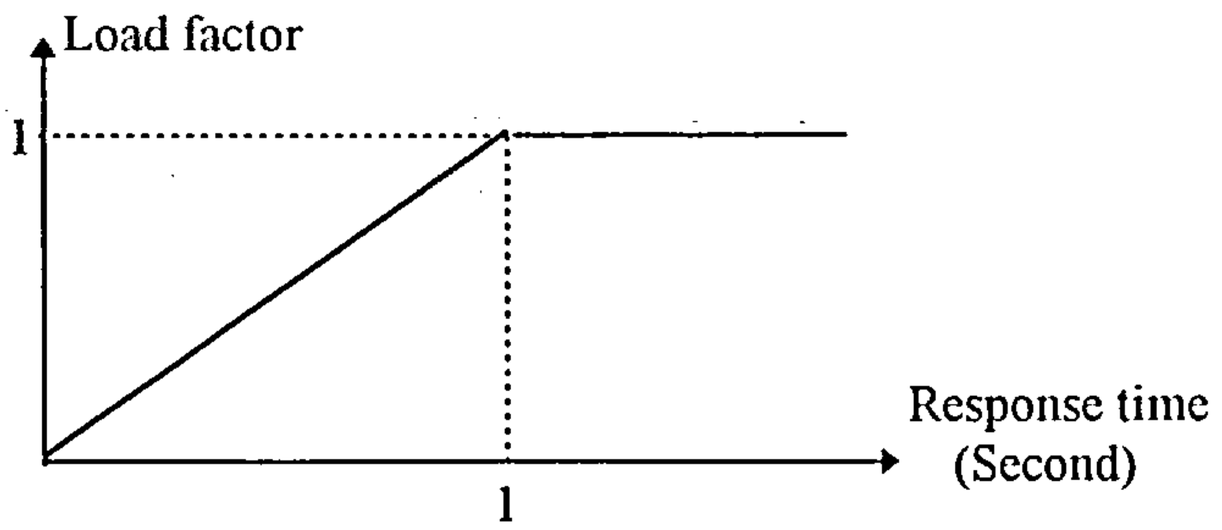

Fig 4-51: Load factor curve of the loading

Solution control: A nonlinear dynamic control was applied in this analysis. The time steps were 0.0001 second and a plot file was extracted from each of 5 steps. All other quantities were the same as were chosen in the previous models.

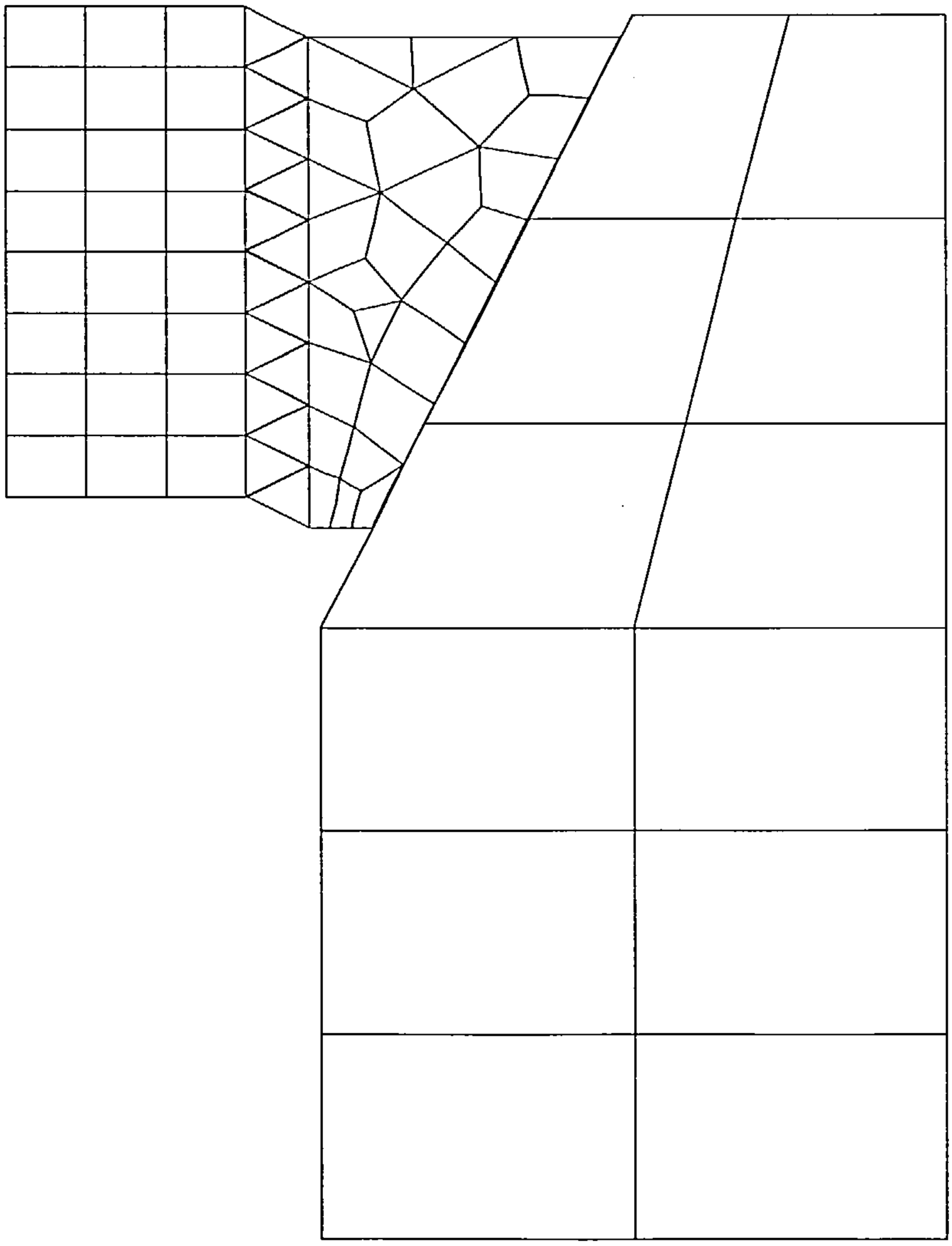

Fig 4-51: Deformed mesh of connection set

4-2-2-2 Three dimensional analysis:

A three dimensional model of the connection set has been created by using the rotation facility of Lusas. Only a quarter of the model has been analysed because the set has symmetry for Y and Z co-ordinates. This three dimensional model is useful for checking the design which has been resulted from the two dimensional analysis.

Meshing: Three dimensional isoparametric solid continuum elements HX20 have been used for modelling.

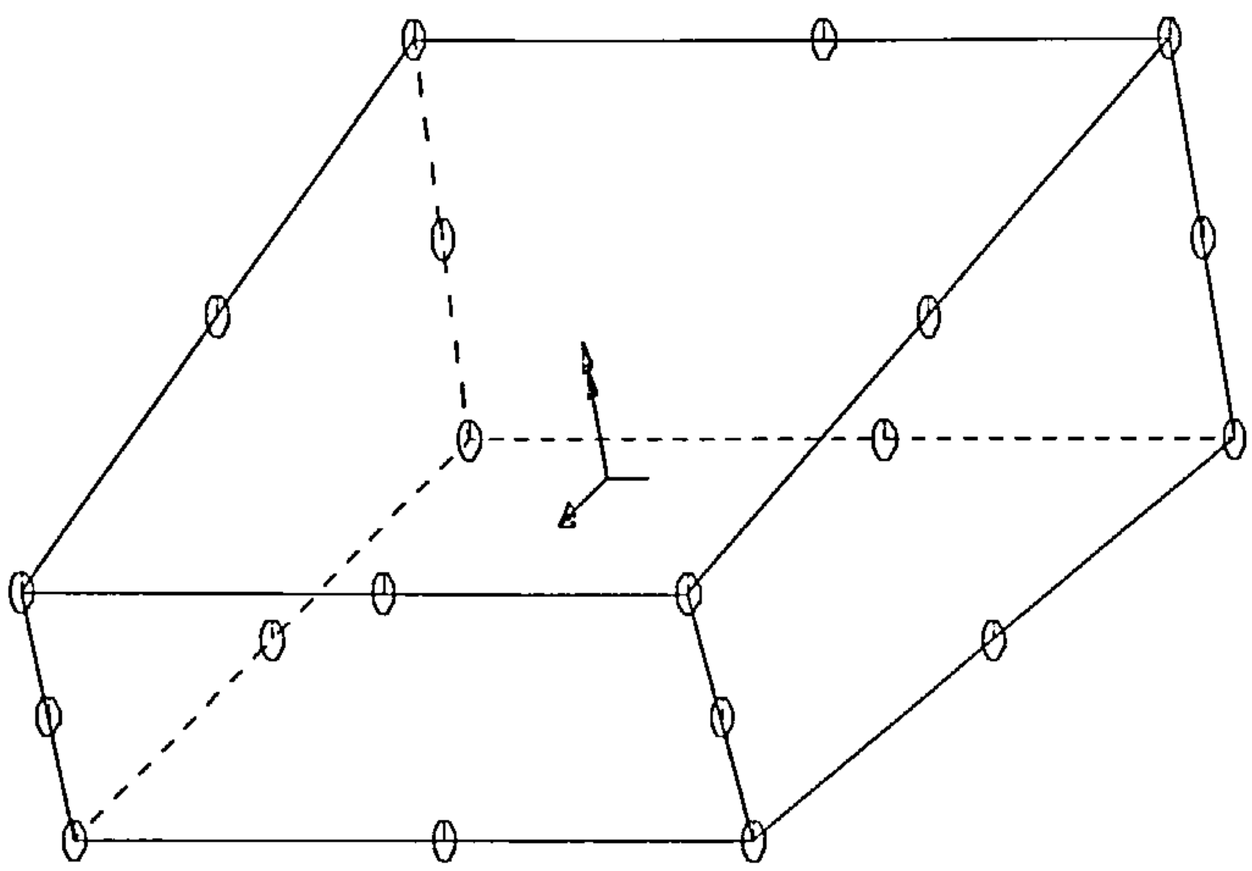

Fig 4-47: 3-dimensional continuum element, HX20

The finite element mesh of the connection set is shown in Figure 4-48.

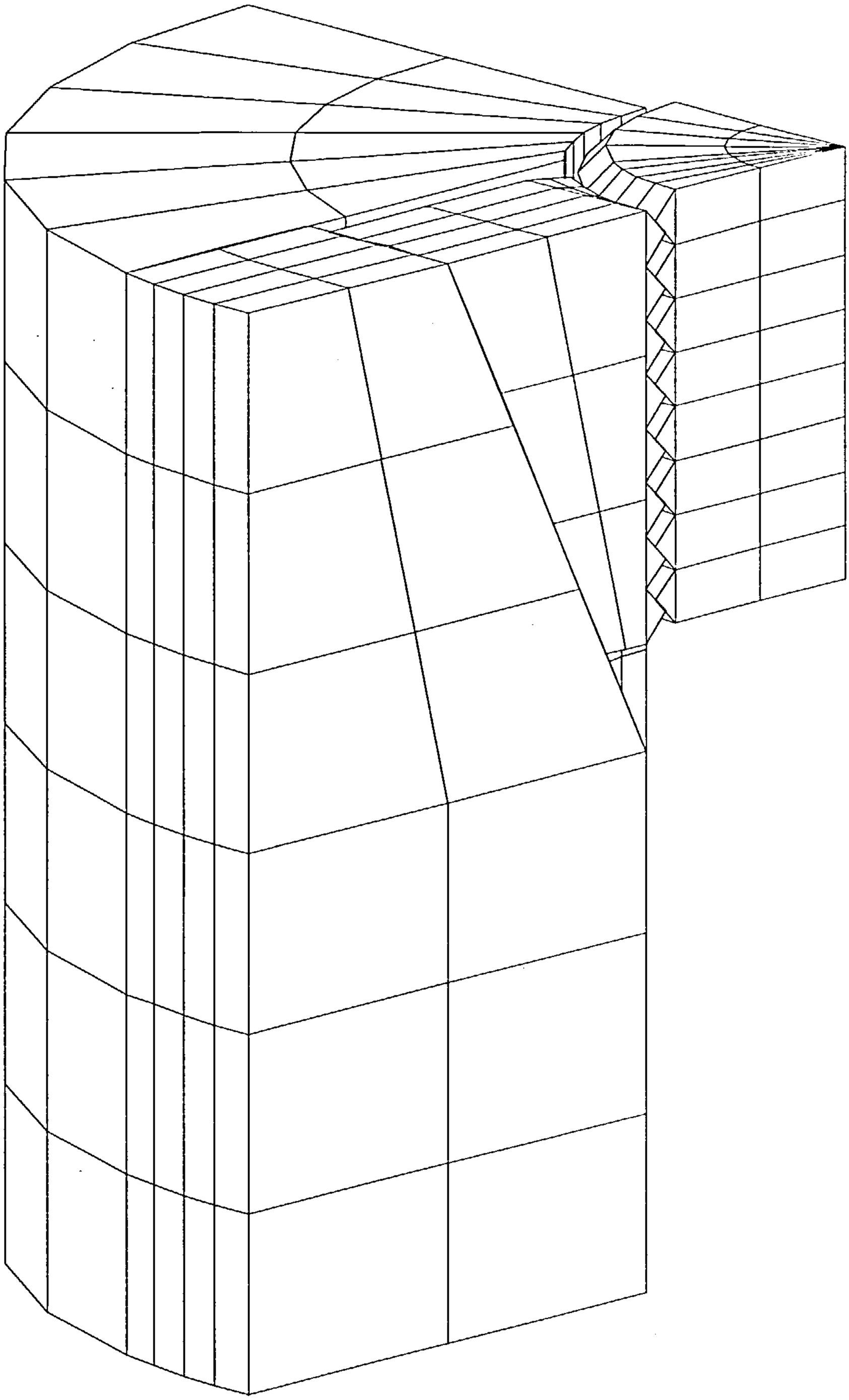

Fig 4-48: Meshing of the connection set

Loading and support conditions:

The same load condition as was used in the two dimensional model has been assigned for this model.

Solution control: A nonlinear dynamic control was applied in this analysis. The time steps were 0.0001 second and a plot file was extracted from each of 5 steps. All other quantities were the same as were chosen in the previous models.

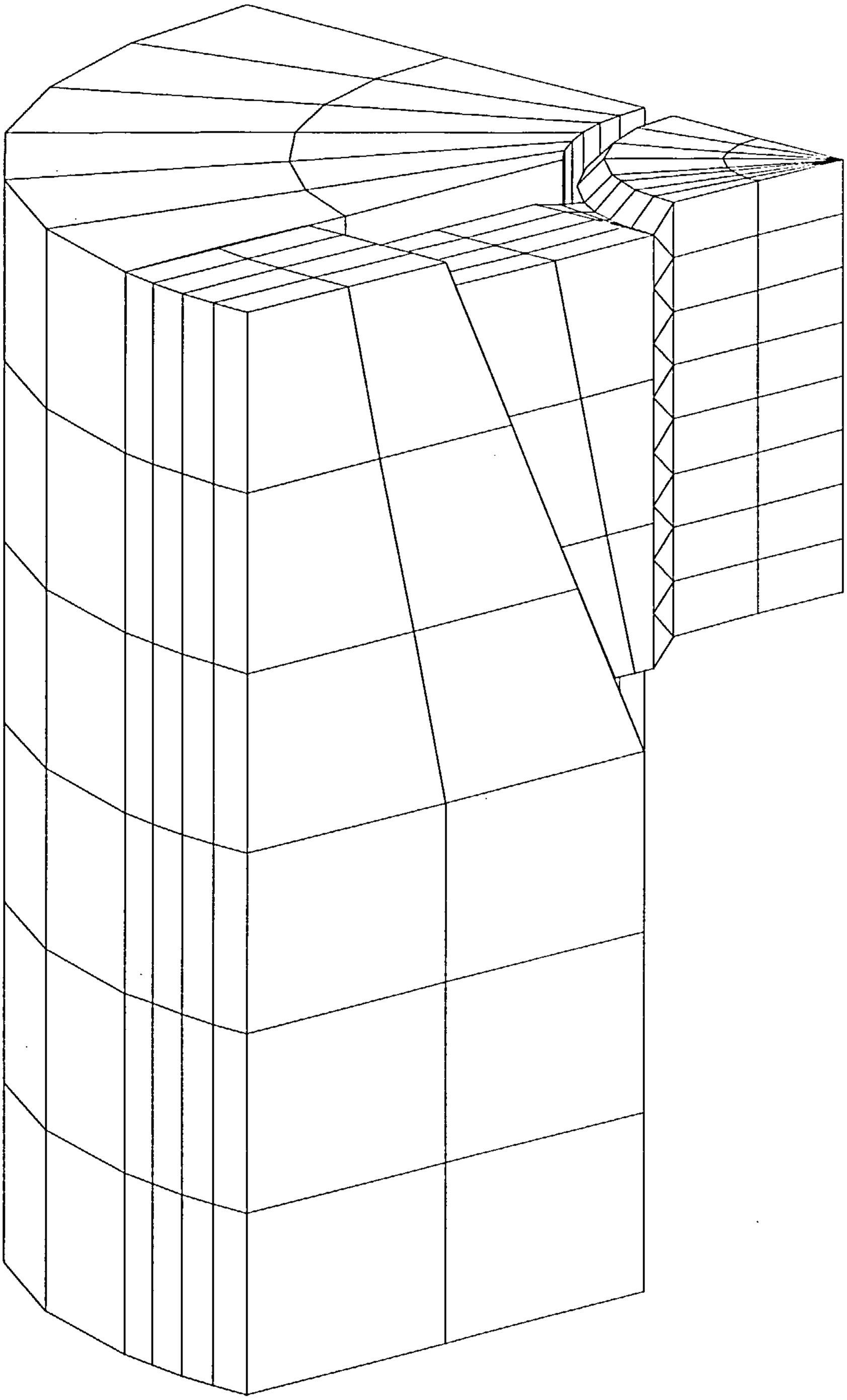

Fig 4-49: Deformed mesh of connection set

In this chapter the numerical modelling of the device was presented. These models were sufficient to design the device with any desired characteristics. In each case, a numerical example illustrated the proposed method and model. As well as the presented analytical methods, Lusas finite element program was the software which used in for the numerical analysis of this device.

In the next chapter, the use of this device will be examined in different kind of structures.

Chapter five: The application of the proposed energy absorbing device in structural engineering

The application of the novel energy absorbing device in different kinds of structures will be examined in this chapter. The improved capacity of structures, to absorb energy with the device, will be investigated.

The structures which will be discussed in this chapter are a framework, a single degree freedom structure and a multi-storey building. They will be analysed in two conditions which are:

i) when they are equipped with the energy absorbing device and

ii) when ordinary structural components have been used instead of the devices.

The comparison of the results of these two analyses will show the effectiveness of the device for improving the energy absorbing capacity of structures.

The material, which was used to model the device, will be discussed first. It is very suitable to use a bar element for the device in the modelling of the structures. It has been already mentioned in chapter 4 that there is a falling stage in the load deflection curve of the device, which is one of its important properties and should be considered properly in the response of the structure. The Lusas finite element programme has not a suitable material model with such variation, which can be assigned for a bar element. In the following section this matter will be discussed and a substructure which can be used in the modelling of structures to represent this device will be introduced.

5-1 Finite element model for the device

The concrete material model is the only available material model in the Lusas Program in which the degradation of strength has been considered in the behaviour. This model has been used as an element system to represent the degradation phenomena. It is used in Lusas to analyse the crack effects in concrete and is only applicable to plane stress elements. Therefore, a virtual substructure containing flat plate components, behaving in plane stress conditions, was designed to represent the device in the model of the structure. In the following, this substructure will be introduced.

5-1-1 Feature definition:

It has been already mentioned in chapter 3 that the device has a load deflection curve which can be divided into three stage, Figure 5-1.

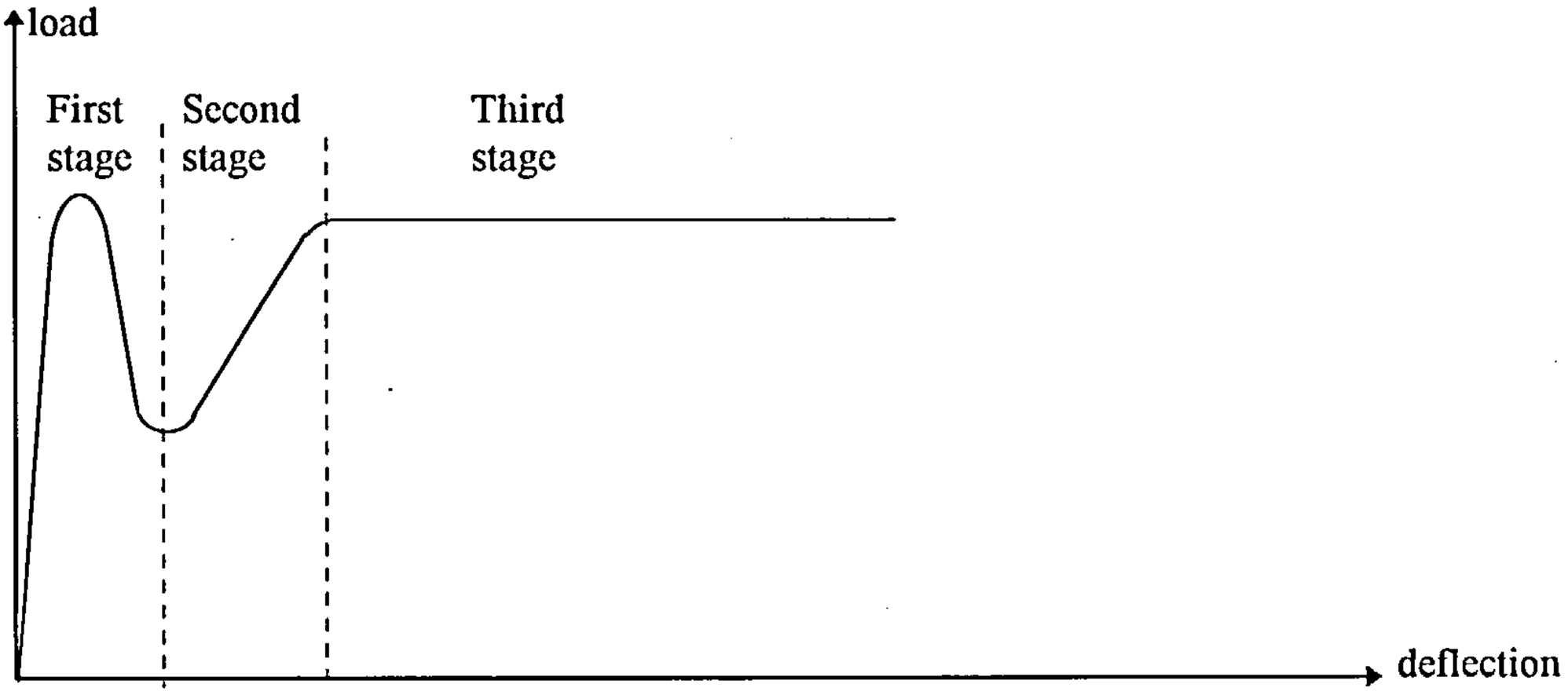

Fig 5-1: Load deflection curve of the device

An individual structure such as that shown in Figure 5-2, was designed and modelled to represent the device in the model of the structures and to respond to the applied load with the load-deflection variations of Figure 5-1.

This virtual substructure consisted of four flat plates and four bars. Plates 1 and 3 were used to create rigid supports to surfaces 2 and 4. In fact, they were effectively middle plates for connecting the bars and plates 2 and 4. A rigid material property was assigned to plates 1 and 3. All of these plates were represented in the plane stress condition.

Plate 2 created the falling part of the load deflection curve of the substructure. In fact the first stage of this load deflection curve was affected mostly by the properties of this element. The concrete material model in Lusas was used to assign material property for plate 2 and its applied values will be reported in section 5-3-1.

Plate 4 was important for the second stage of the load deflection curve and it created the rising part of load-deflection curve. This plate was coincident with plate 2 and was connected to it with tied slide lines. This plate was assigned with an elastic material model.

The bars, as well as connecting this substructure to the main structure, created the third stage of the load deflection curve. They were assigned with bilinear elastic-plastic material properties and the energy of impact was dissipated in these elements.

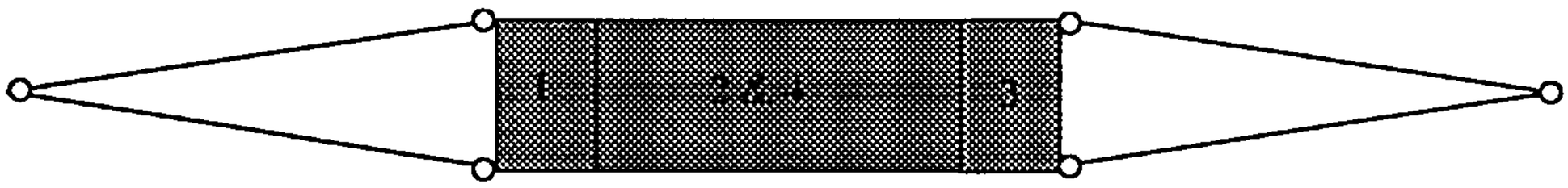

Fig 5-2: The substructure which represents the device

5-1-2 Mesh: Quadrilateral plane stress elements with a parabolic variation of displacements were used for the plates. These elements are denoted as QPM8 in the Lusas Finite Element program.

Two dimensional bar elements, denoted as BAR 2, were used to represent the bars. Elements 1 , 2 and 3 were directly in contact with each other having common border lines but element 4 was connected to the rest of the model by tied slide lines, which were assigned to adjacent lines with element 2.

5-1-3 Material Definition:

The LUSAS finite element programme has two models for considering the softening property of materials and these are linear decay and exponential decay, Figure 5-3.

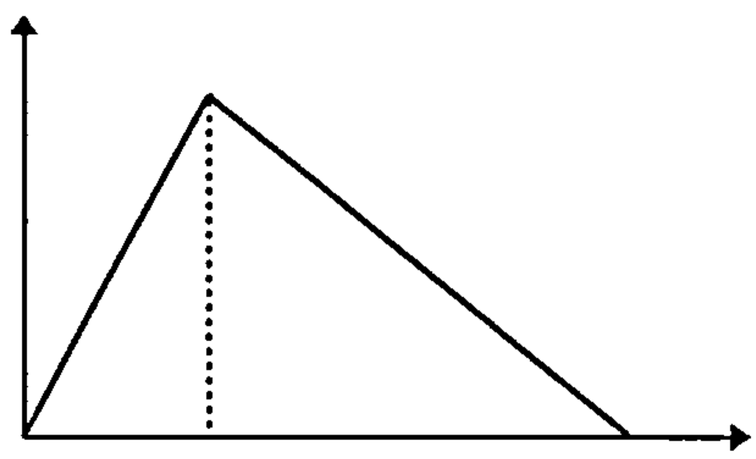

Linear decay

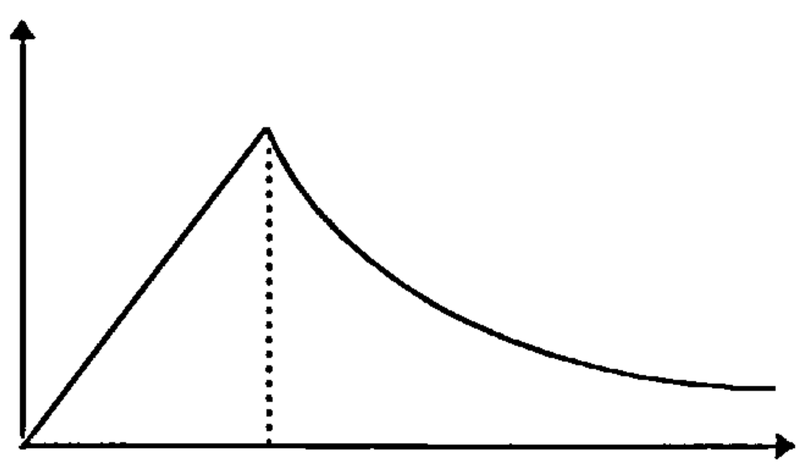

Exponential decay

Fig 5-3: Degradation of strength in LUSAS program

The associated representation of softening behaviour is provided by the concrete material model in Lusas. The material model with exponential decay was assigned to plate 2 because this form of softening could match better the falling stage of the load deflection curve.

The following material data (table 5-1) were assigned to plate 2.

Table 5-1

Elastic Modulus K N/m^2	1.2 E11
Poisson's Ratio	0.3
Mass Density KG/m^3	1.0
Compressive strength KN /m^2	2E8
Tensile Strength K N/m^2	2E8
Fracture Energy	3000 J

It should be noted that although the concrete material model in Lusas program has been used for plate 2, properties appropriate to steel values have been assigned. For example, a tensile strength of 2E8 KN/m^2 is never achieved in practice for concrete. The values in table 5-1 have been properly adjusted to obtain a response for this substructure similar to the proposed energy absorbing device.

Table 5-2 shows the properties assigned to the plates 1,3,4 and the bars.

Table 5-2

Component	Elastic Modulus K N/m^2	Poisson's Ratio	Mass Density KG/m^3	Yield limit K N/m^2
Plates 1& 3	2.0 E17	0.3	1.0	-
Bars	1.2 E11	0.3	1.0	2E8
Plate 4	6.0 E9	0.3	1.0	-

By considering these values for the material properties of the components, the yield load of the device was adjusted to 200KN. Because the cross section area of the bars was considered 0.001 m^2, therefore, the yield stress in the device was 2E8 N/mm^2. This is 30% less than the stresses which was considered for the other structural members (3E8 N/mm^2). This difference was as a safety factor.

5-1-4 Geometry definition: A thickness of 0.025 m was considered for all surface elements. For the bars, A= 0.001 m^2 was used. Therefore, the cross section of the

surfaces and the bars had equal areas and this made it easy to adjust the tensile strength of the device, only by defining the tensile strength of the components.

5-1-5 Support definition: Two hinge support were assigned to the bars. These hinge supports represented those hinges which are used to connect the device to the structure.

5-1-6 Loading definition: A point load of 2E6 N was applied to the bars as shown in Fig5-4. This load was sufficient for yielding the substructure.

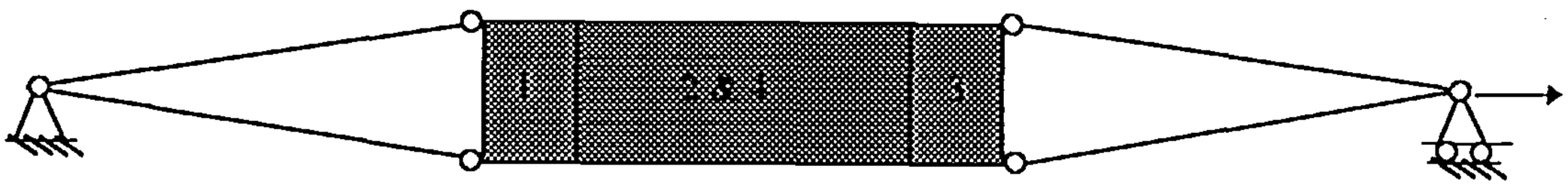

Fig 5-4:Loading and support conditions of the substructure

5-1-7 Curve definition: Figure 5-5 shows the variation of the load factor with time which was used for the applied load.

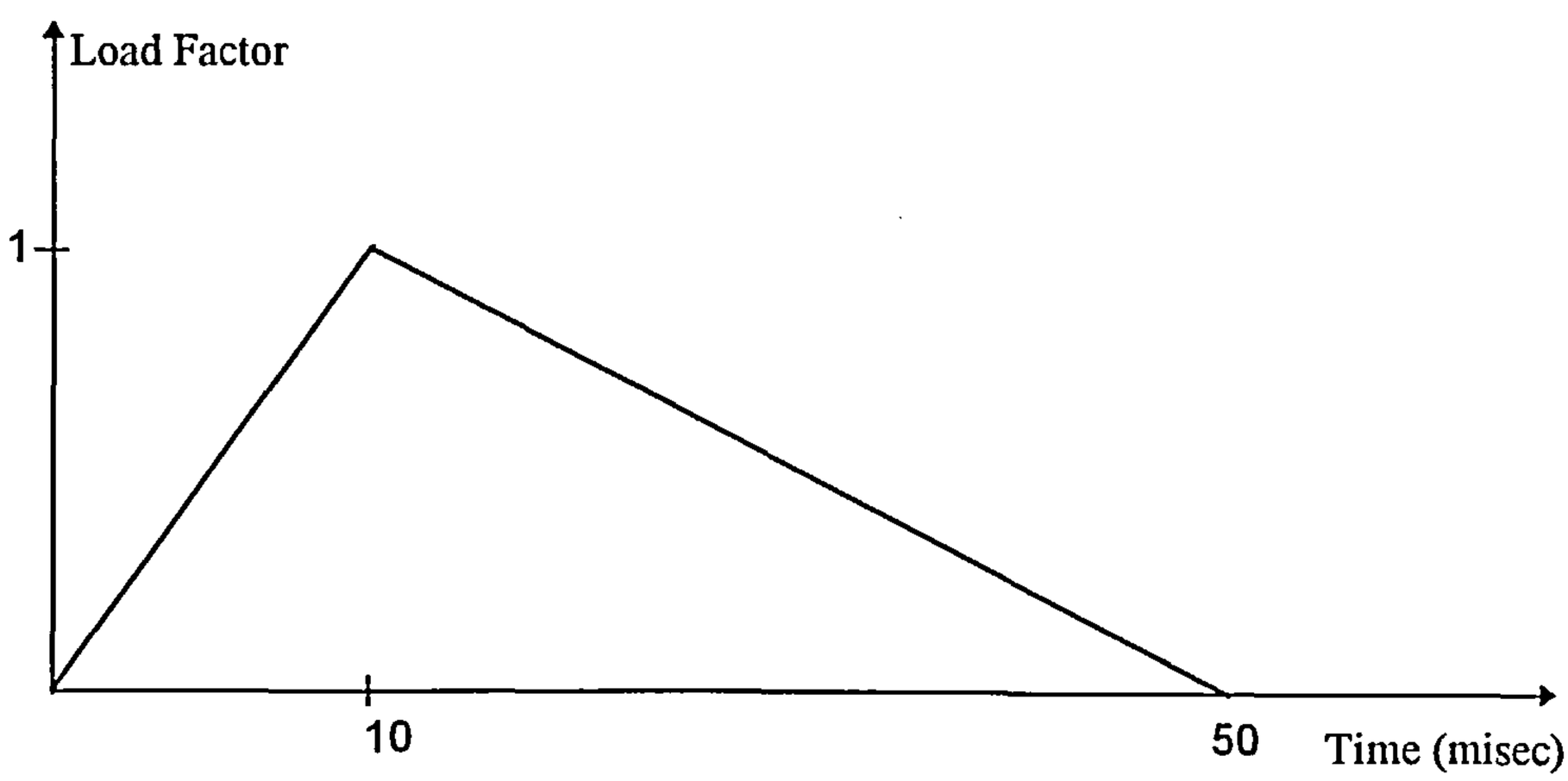

Fig 5-5: The Loading curve

5-1-8 Slide definition: A tied slide definition was used to connect plate 4 to the rest of model. This type of slide line is useful to model two adjacent components with different meshes (the definition of slide lines was given in chapter 4, section 4-1-1-1).

5-1-9 Control definition: The nonlinear dynamic analysis facility with the Total Lagrangian geometric nonlinearity option in the Lusas finite element programme was

used for the model. This type of geometric nonlinearity is a stable formulation and is valid where the rotational degrees of freedom are small.

5-1-10 Convergence criteria: The same criteria which was defined in section 4-1-1-1 was used for this analysis.

5-1-11 Result: Figure 5-6 is the load deflection curve of the substructure which was obtained as a result of the aforementioned numerical analysis.

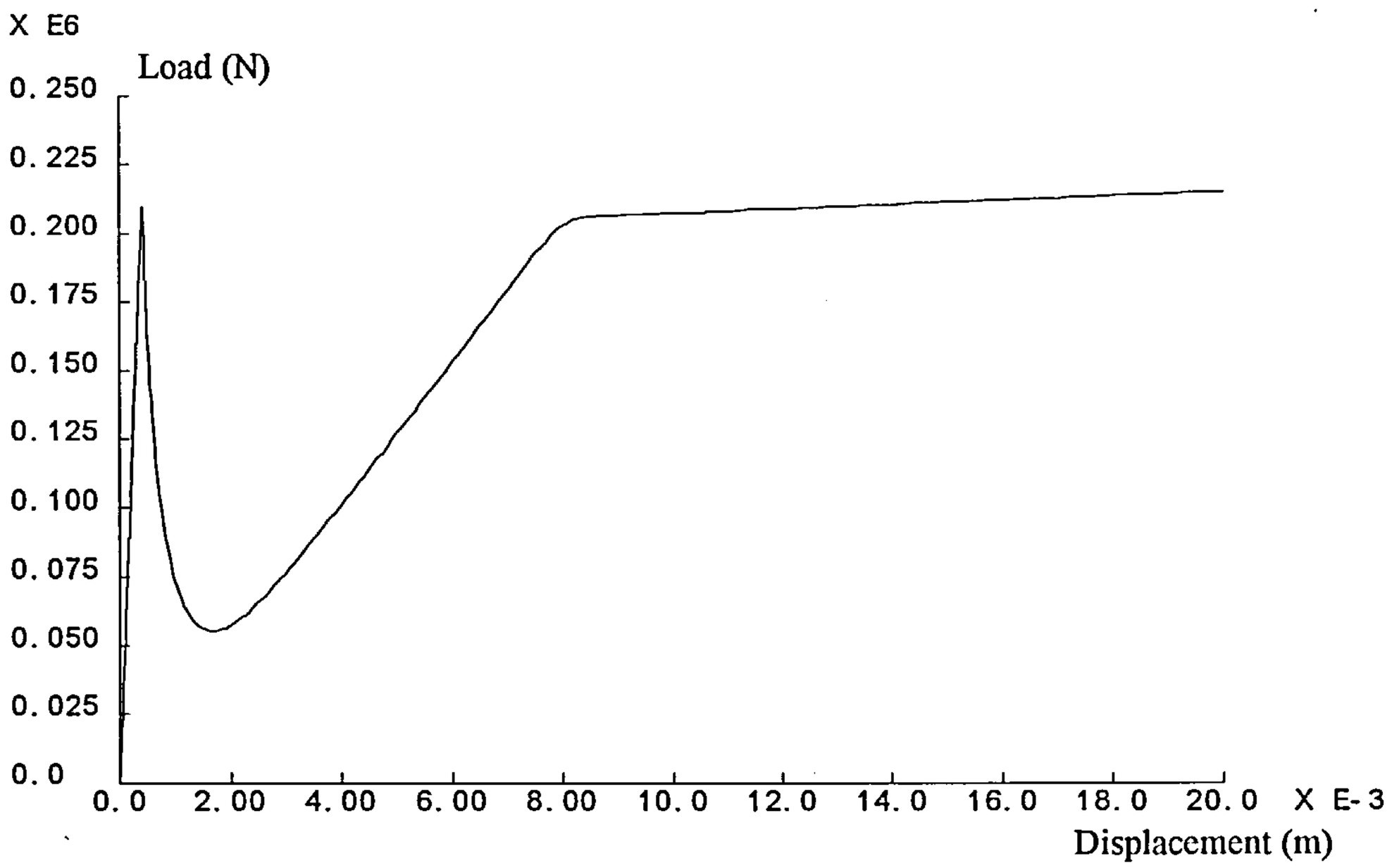

Fig 5-6: The response of the model

The amount of absorbed energy can be estimated from the confined area between the load deflection curve and the X axis of Fig 5-6

Practically, the device can deflect almost twice its original length. The deflected form of the device has been shown in Figure 5-7.

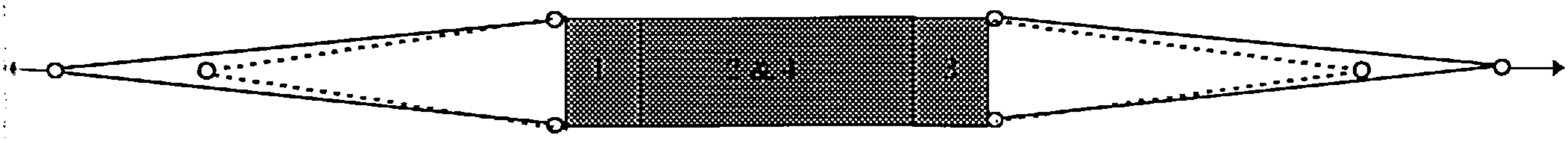

Fig 5-7: The deformed (full line) and undeformed (dash line) substructure

5-2 The response of Frameworks

In this section the response of a structural framework with and without the proposed energy absorber will be considered. The frame has been subjected to a blast loading. This loading will be defined in the following section.

5-2-1 The framework with the energy absorbing device

A frame work, shown in Figure 5-8 was chosen to be examined numerically when equipped with the energy absorbing device.

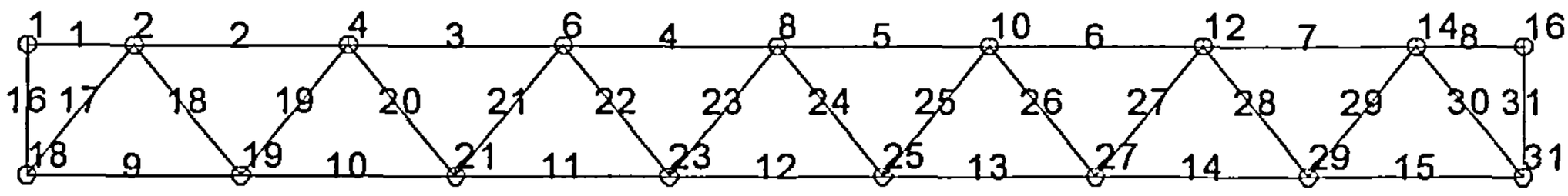

Fig 5-8: The framework

Figure 5-9 shows the frame in which member 12 has been replaced by the energy absorbing device.

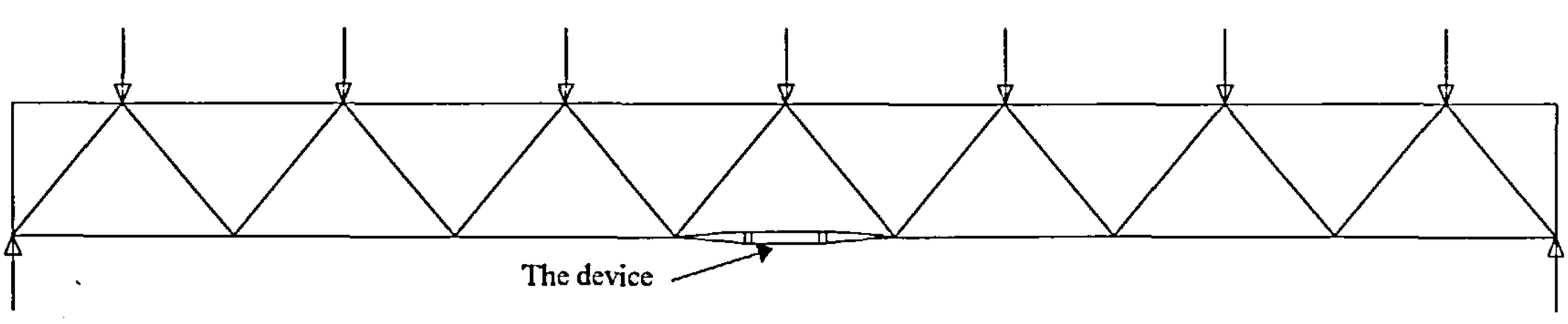

Fig 5-9: The framework which has been equipped with the energy absorbing device

The finite element modelling of the frame will be explained in the following:

Feature definition: The framework was modelled first and then the model of the energy absorbing device, which was created in the previous section, inserted in the overall model of the frame.

Mesh : Two dimensional BAR 2 elements were considered for the frame. The same mesh, which was discussed in section 5.1, was used to represent the energy absorber.

Material Definition:

The absorber had the same material properties which have been discussed in the previous section. Table 5-3 gives the values of the properties which were assigned to the material of bars of the frame.

Table 5-3

Elastic Modulus K N/m^2	1.2 E11
Poisson's Ratio	0.3
Mass Density KG/m^3	1.0
Yield Limit KN/m2	3E8

Geometry definition: An area of 0.001m^2 was considered for the all of bars.

Support definition: Two hinge supports at nodes 18 and 31 were applied to the framework.

Loading definition: A point load of 10000 KN was applied to each of the top nodes of the framework.

Curve definition: The definition of the loading curve for this model was the same as that used in the modelling of the device in the previous section, Fig 5-5. But in this case it was assigned with a load factor of 5 for this loading. This load factor was sufficient to develop ultimate condition in the framework.

Slide definition: The tied slide line definition shown in section 5-1 was used for modelling the device.

Control definition: Once again the nonlinear dynamic analysis with Total Lagrangian geometric nonlinearity option was used for the model. This is the same option which was used in section 5-1.

Convergence criteria: The convergence criteria of section 4-1-1-1 was used.

In the following figures, the load and strain variations with time in the bars have been shown. These curves show the responses in a period of 30 msec.

Figure 5-10 shows the load- response time curve in the upper members of the framework. Member no 2 has developed stress before than the other members but by approaching response time 5 msec, stress in member 4 has become dominant.

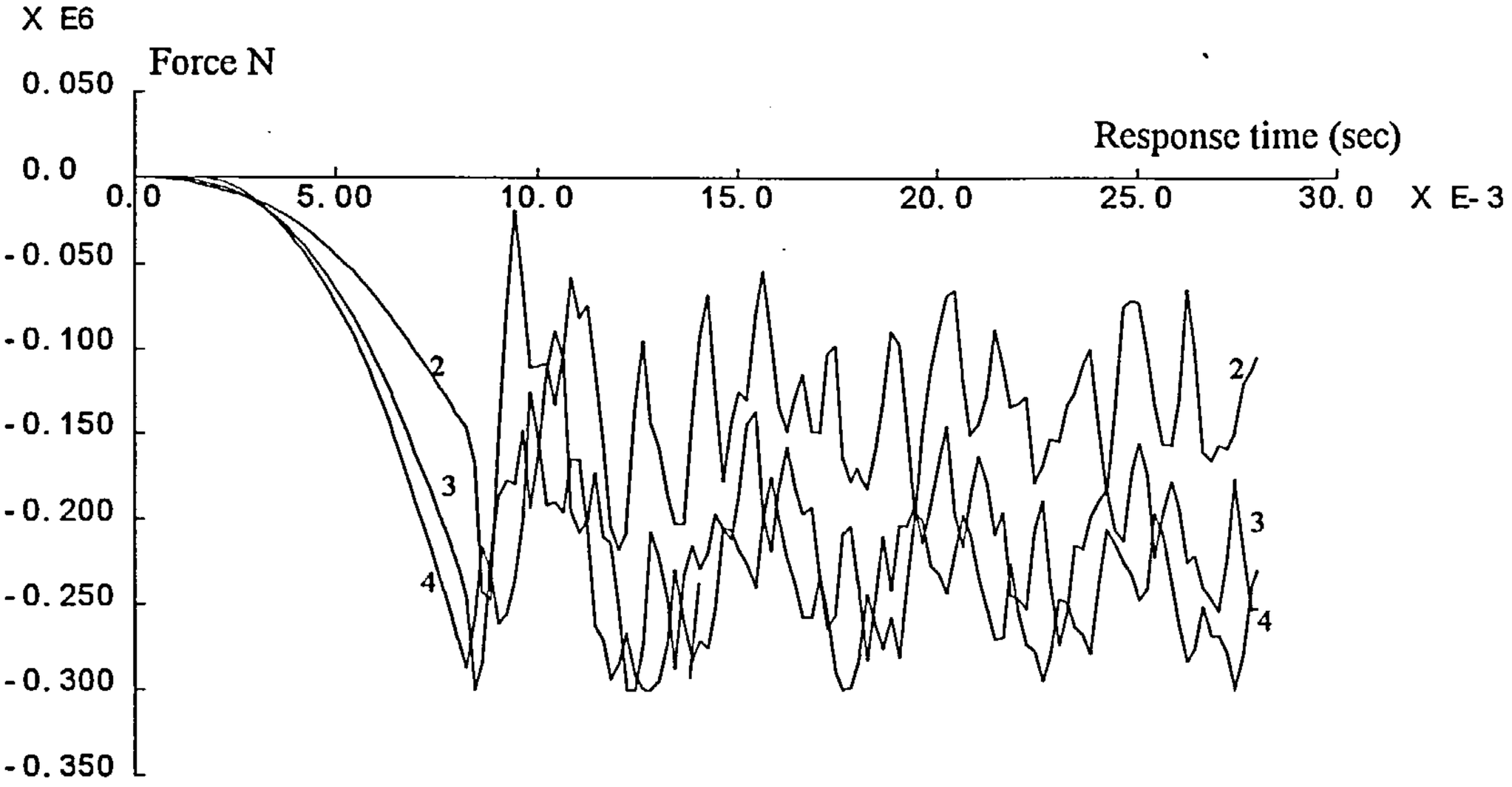

Fig 5-10: Load-response time curve for the top members of the framework (members no 2, 3& 4)

Figure 5-11 shows the load-response time curve for the bottom members of the framework. Member 10 has developed stress before than other members, but load in member 11 and the energy absorbing device have surpassed it.

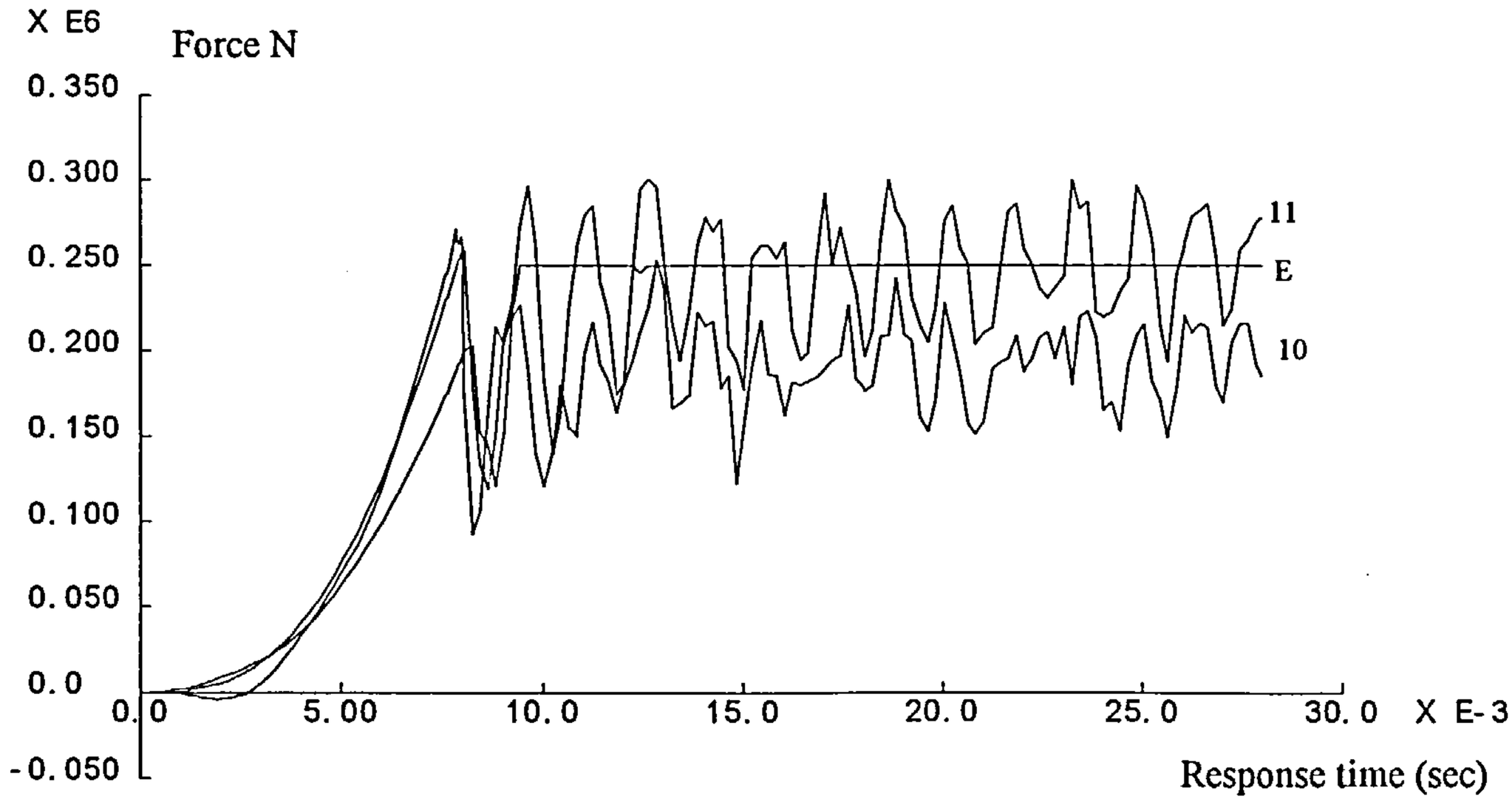

Fig 5-10: Load-response time curve for the bottom members of the framework
(members no 10,11& Energy absorbing device)

The results shown in Figures 5-10 and 5-11 demonstrate the effects of the falling part of the load deflection curve of the energy absorbing device (Fig 5-1) in the response of the framework.

The curves of Figures 5.12 and 5.13 show the strain- response time for the top and bottom members of the frame. It can be seen from these curves that there is no damage in the members of the framework except for the energy absorbing device.

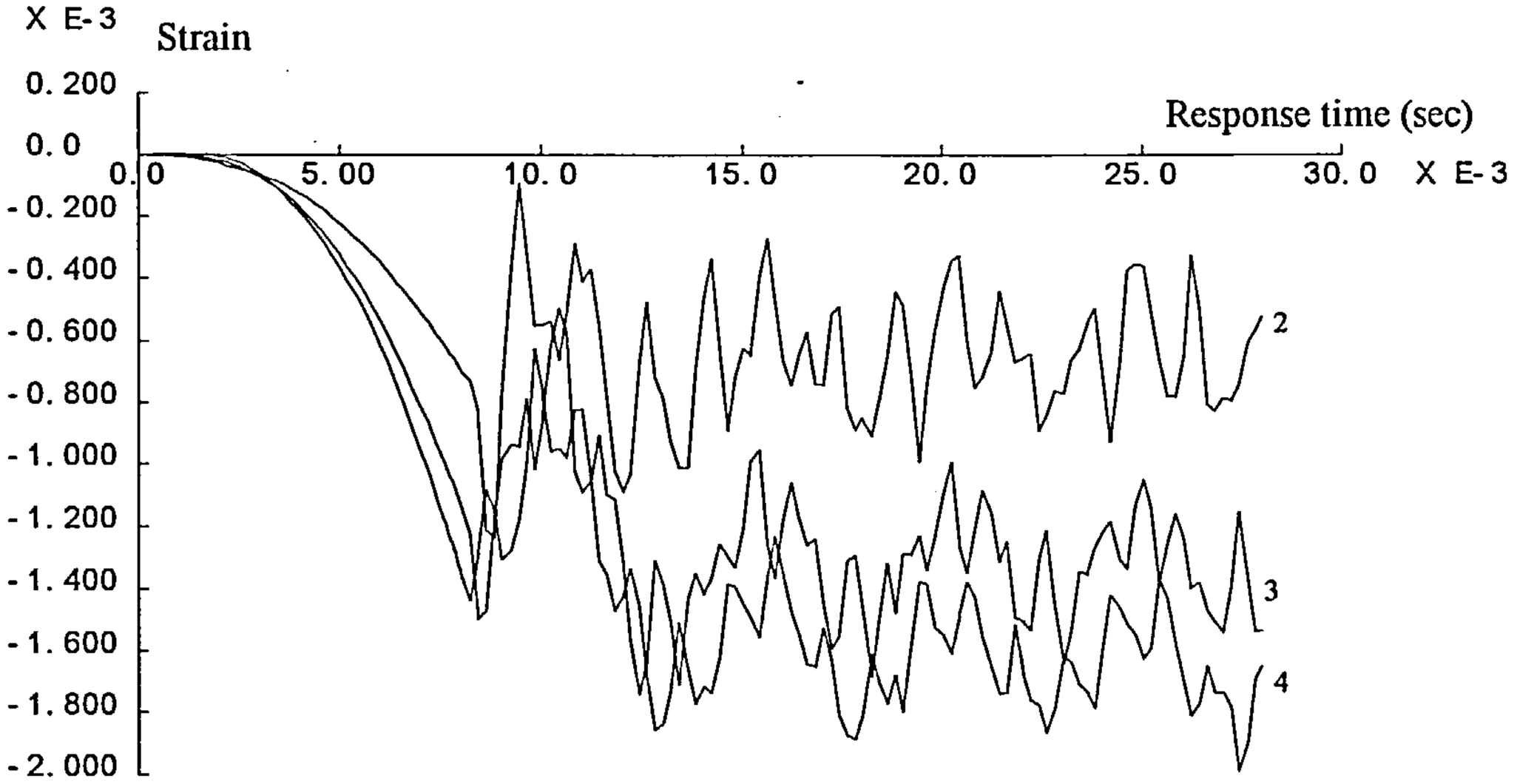

Fig 5-12: Strain-Response time curve for the top members of the framework (members 2, 3& 4). The strains are below than the yield strain of the considered steel material (0.002).

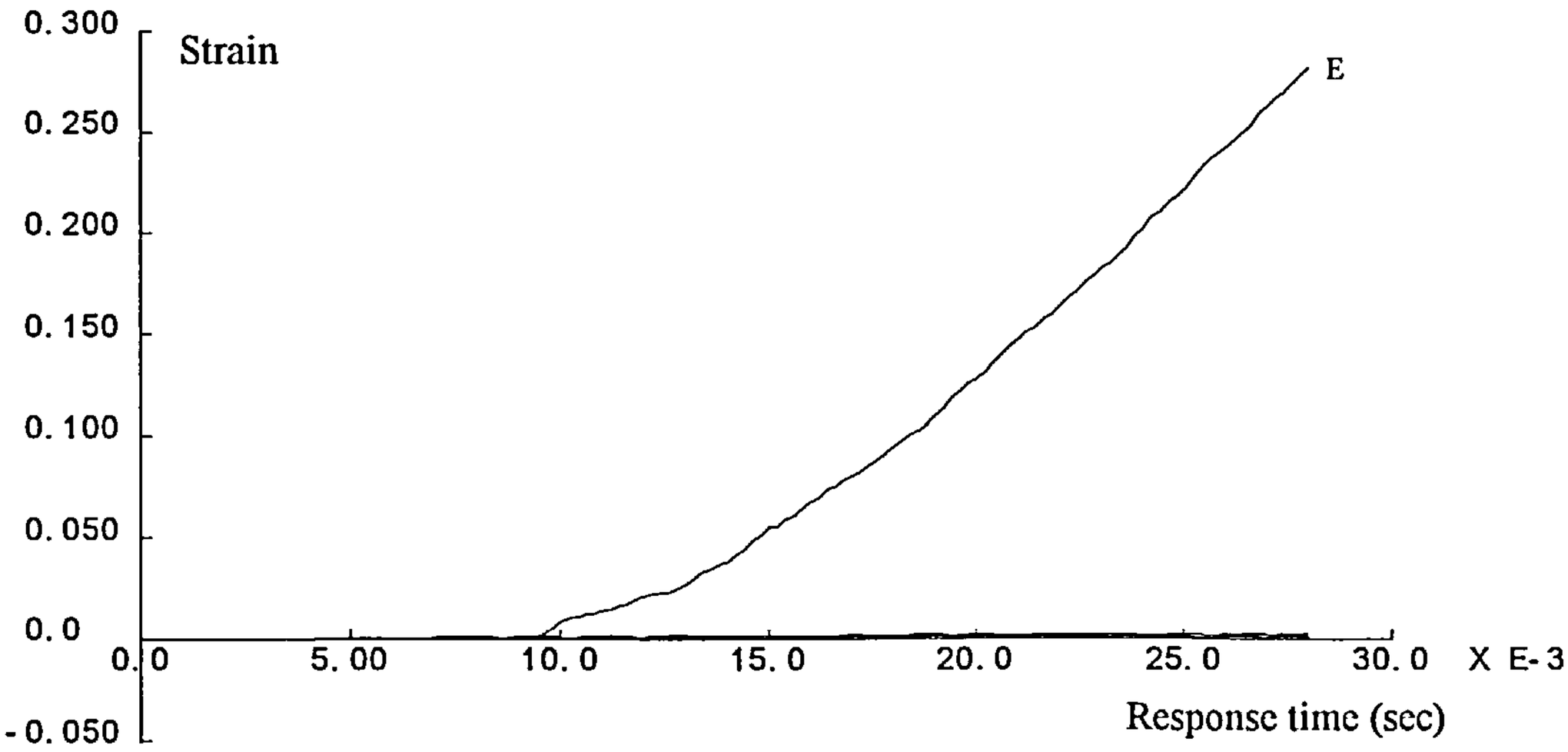

Fig 5-13: Strain-Response time curve for the bottom members of the framework and the energy absorbing device (E). Strains in the other members are negligible in comparison to the strain of the energy absorbing device and are almost coincident with the X axis

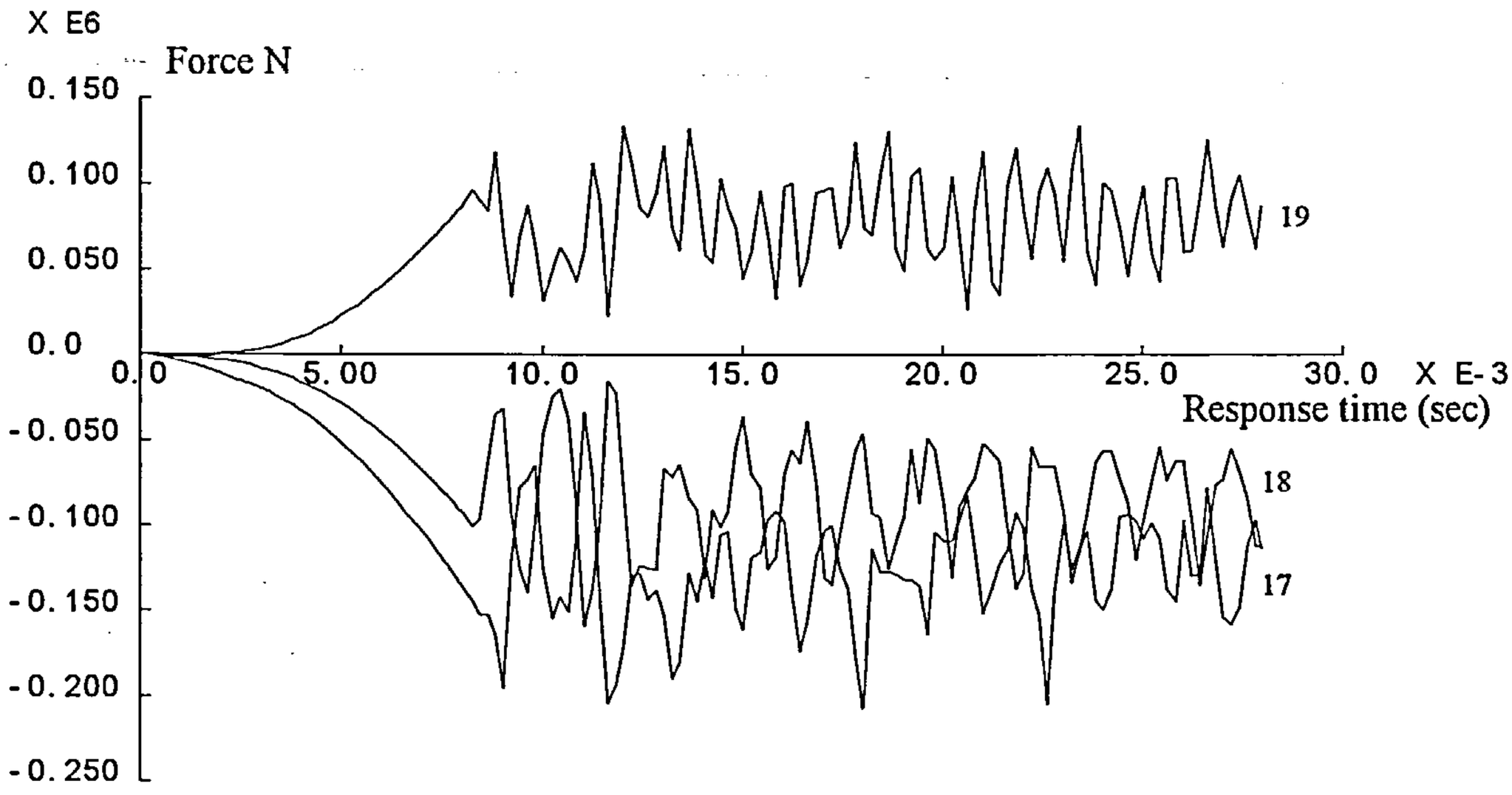

Fig 5-14: Load -response time curve for the diagonal members of the framework

Figure 5-14 shows the loads in the diagonal members. Stress in the member 17 is dominant in this figure.

Figure 5-15 is the strains in these members. According to this figure there is no damage in the diagonal members (Since they remain elastic).

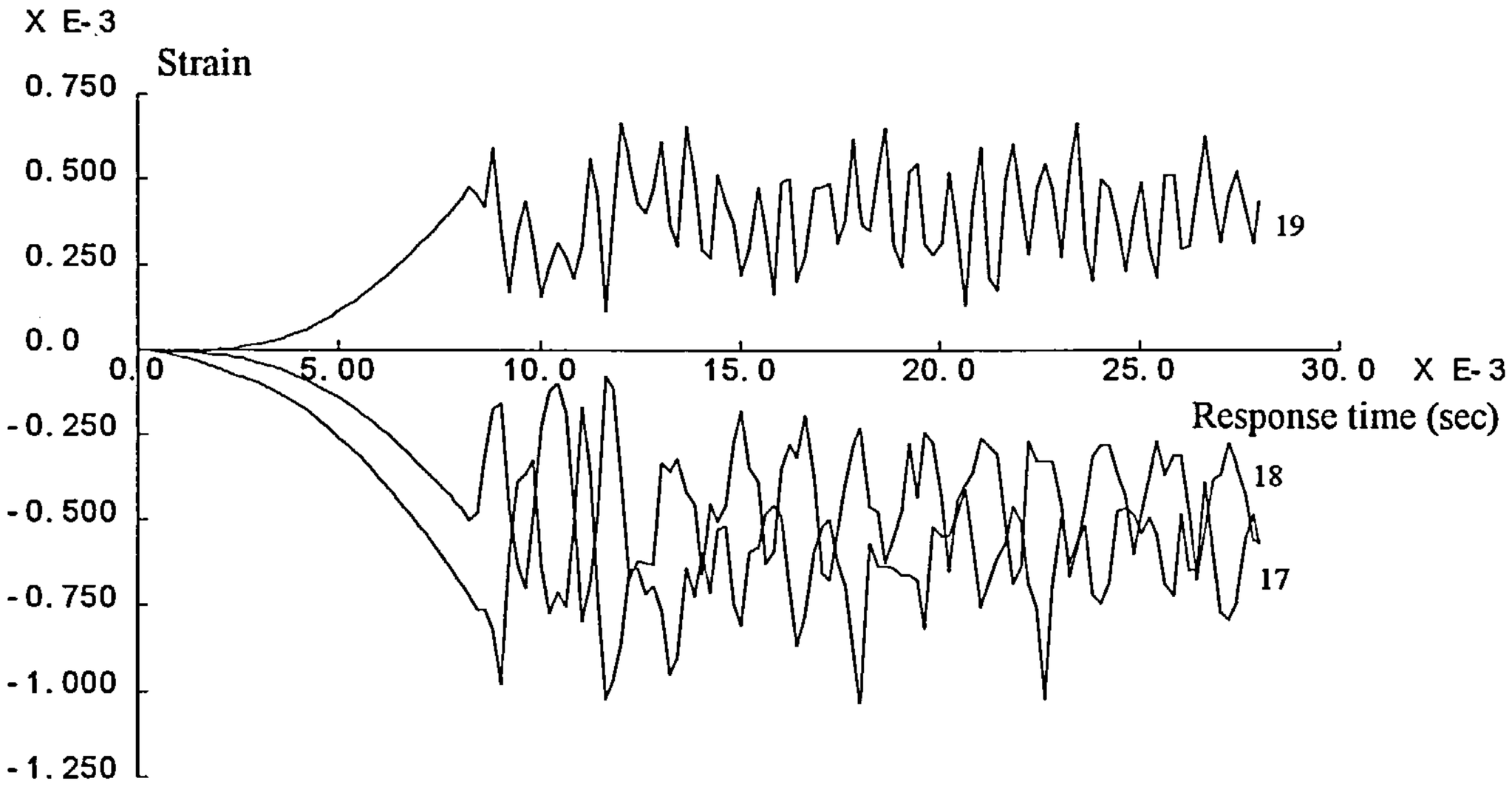

Fig 5-15: Strain -response time curve for the diagonal members of the framework

The analysis was carried out for a time response period of 60 msec and the result have been reported in the following figures.

Figure 5-16 is the load response time in this period. It shows that by approaching 60 msec, the loads in top members are reducing. They are less than the yield limit.

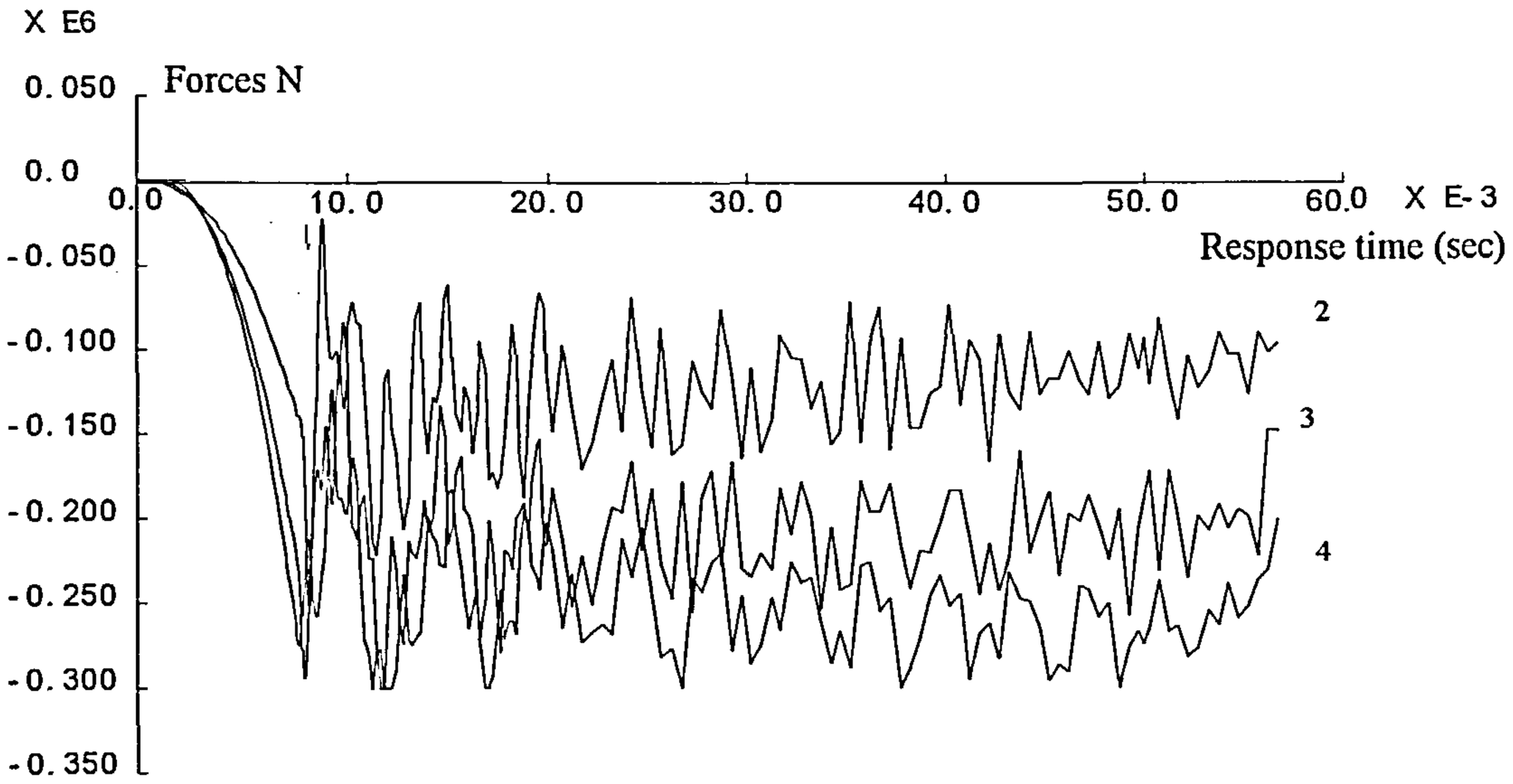

Fig 5-16: Load-Response time curve for the top members of the framework

Figure 5-17 shows the loads in the bottom members. The energy absorbing device has limited the loads in other members and has prevented from plastic deformation in these members.

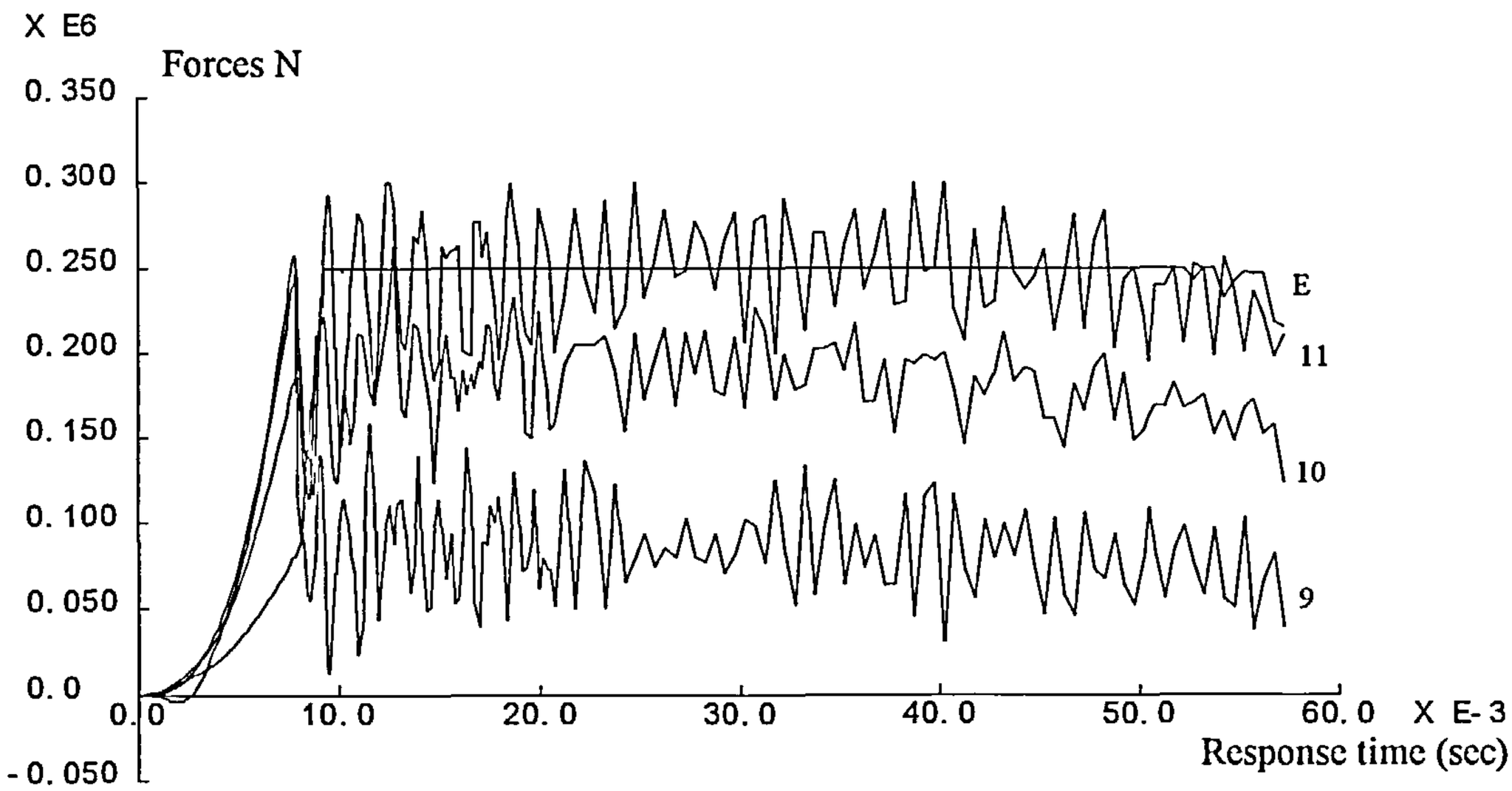

Fig 5-17: Load-Response time curve for the bottom members of the framework
(members 9, 10, 11 and the energy absorbing device E)

Figure 5-18 is the strain response time in 60 msec in the top members. The strains in all of these members are less than the plastic limit.

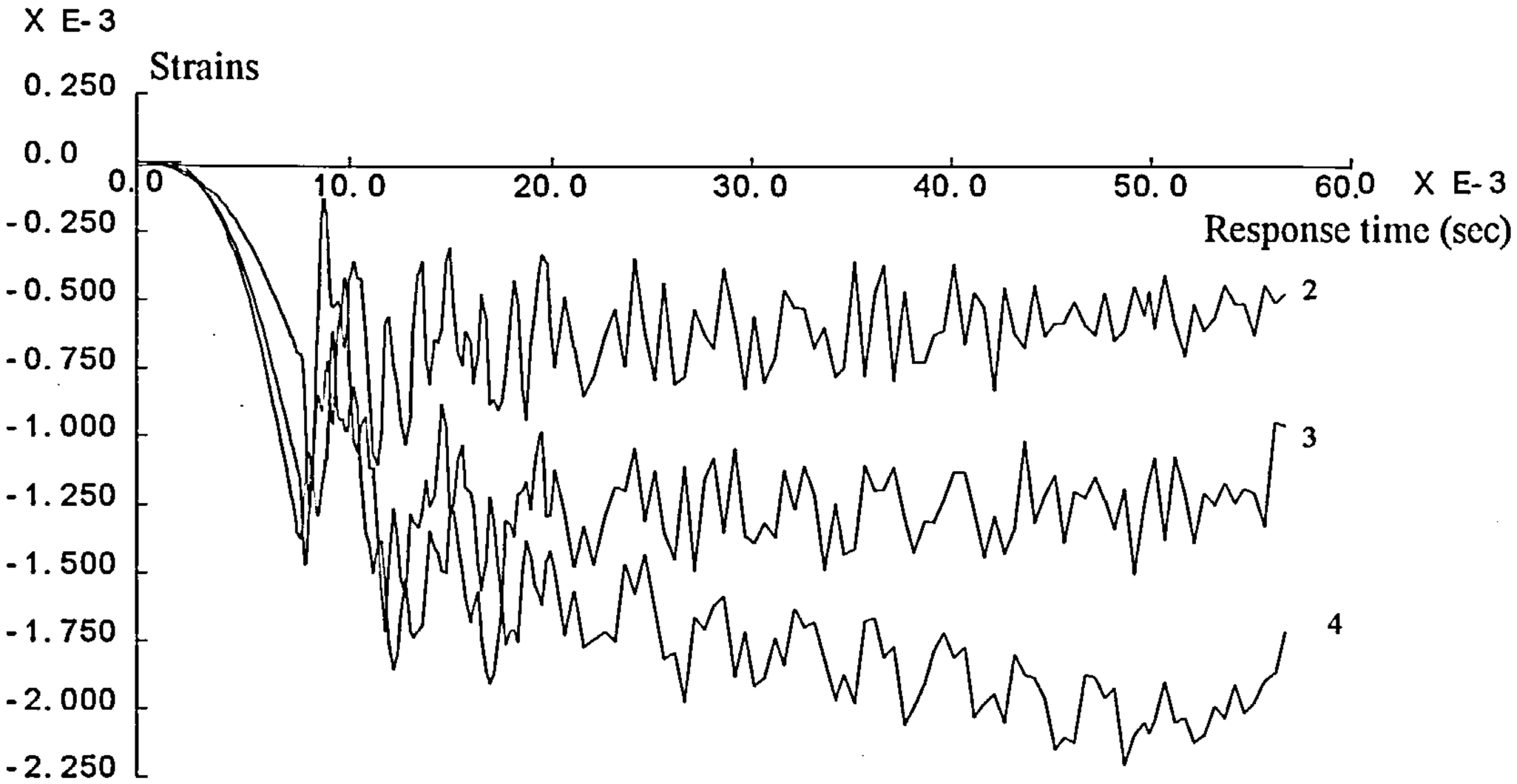

Fig 5-18: Strain-Response time curve for the top members of the framework (members 2, 3& 4)

Figure 5-19 shows the strain in the bottom members. Strain in the energy absorbing device is the predominant strain in this figure and the strains in other members are negligible in comparison to it.

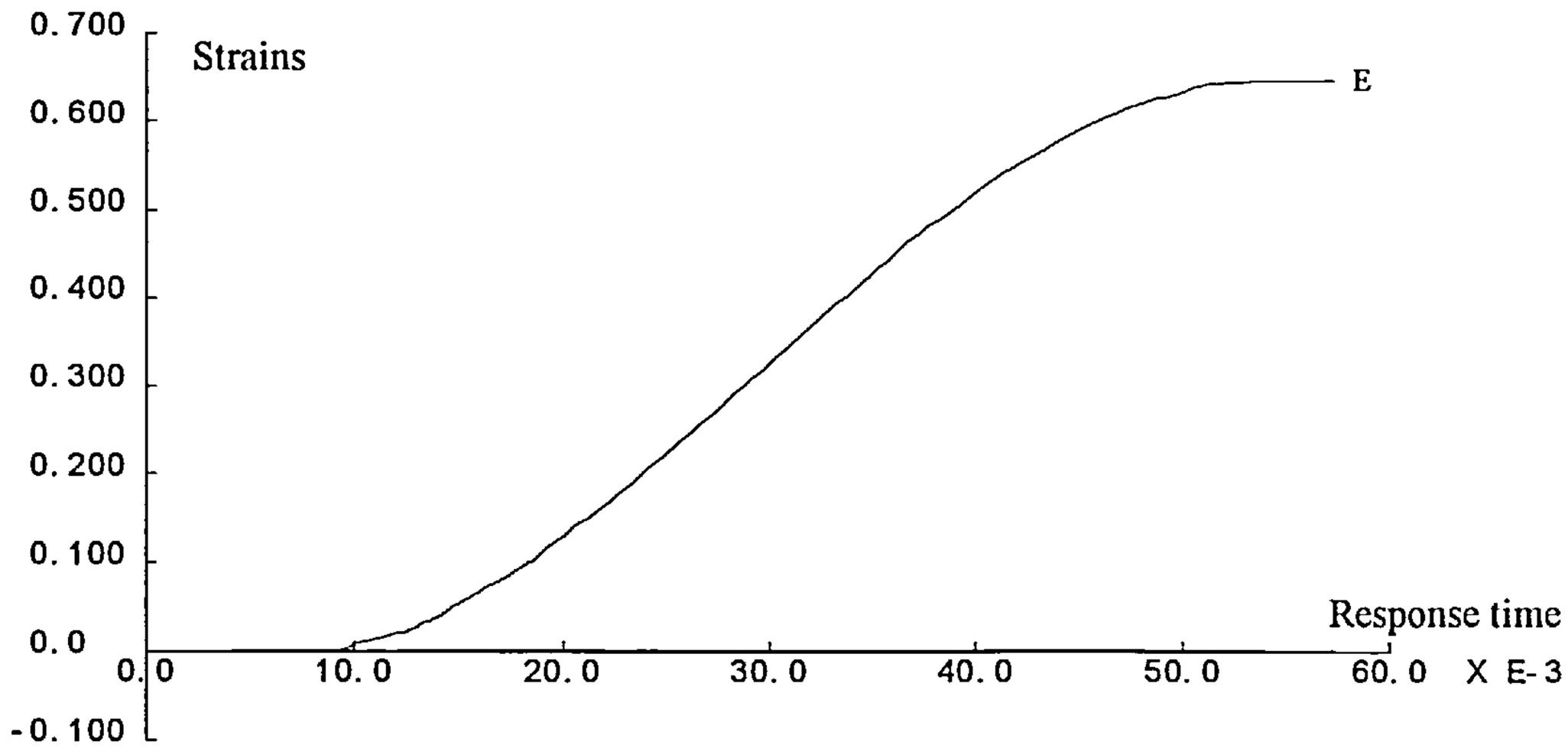

Fig 5-19: Strain-Response time curve for the bottom members of the framework and the energy absorbing device E. The strains in the other members are negligible in comparison to that of the energy absorbing device

The response during 60 (msec) also shows that there is no damage in the members except the energy absorbing device. The device has reached to a strain of 0.7 which is close to its final deflection. The other members have remained in the elastic range. Figure 5-20 is the deflection-response time of the central nodes of the framework. It shows that the deflection in these nodes are reducing by approaching 60 msec. This is the matter which was observed in Figures 5-16 and 5-17.

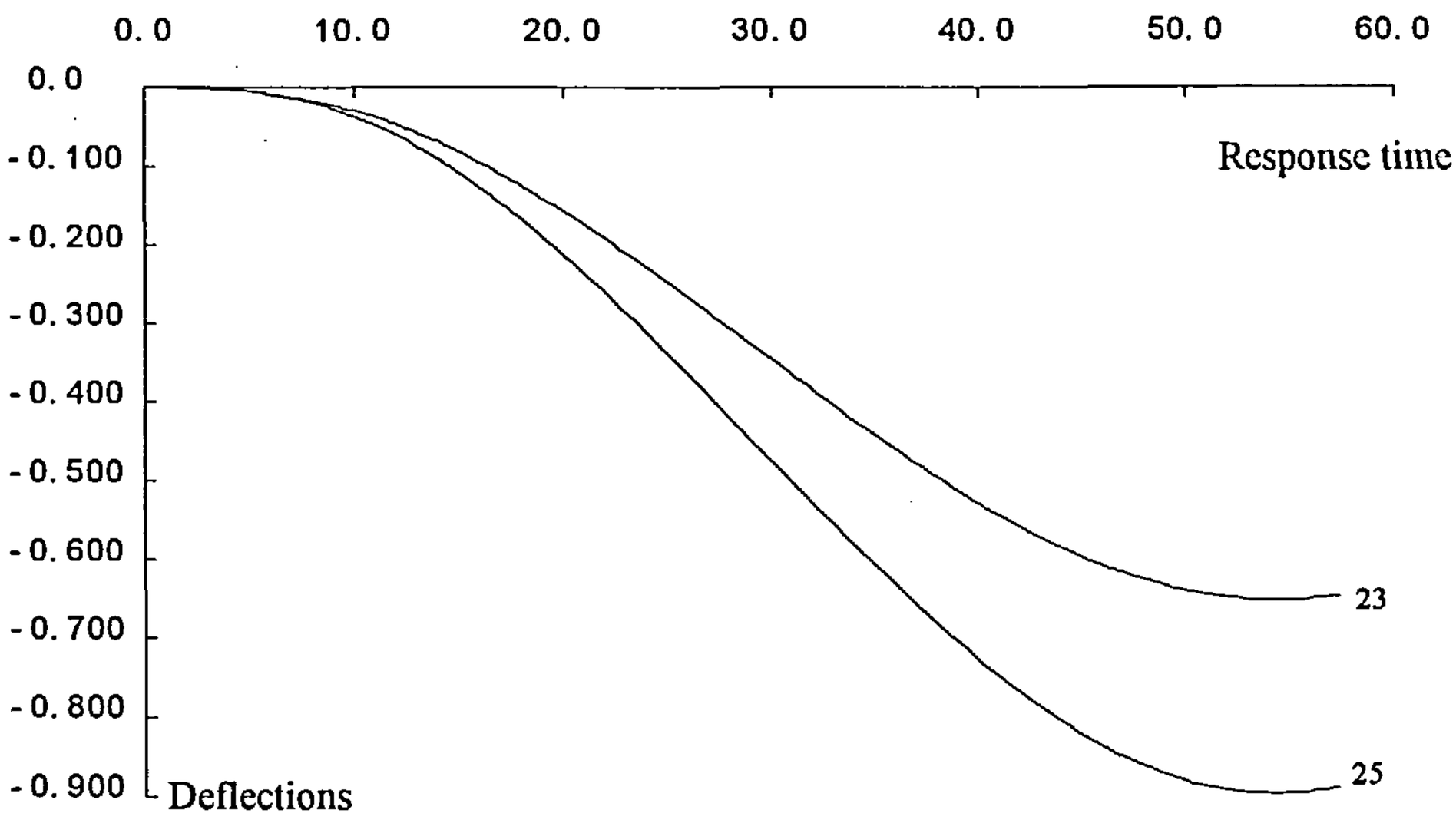

Fig 5-20: Deflection of the central nodes of the framework (nodes 23& 25)

The deflected form of the framework has been shown in figure 5 -21. This is the deflected form of the framework in the maximum deflection.

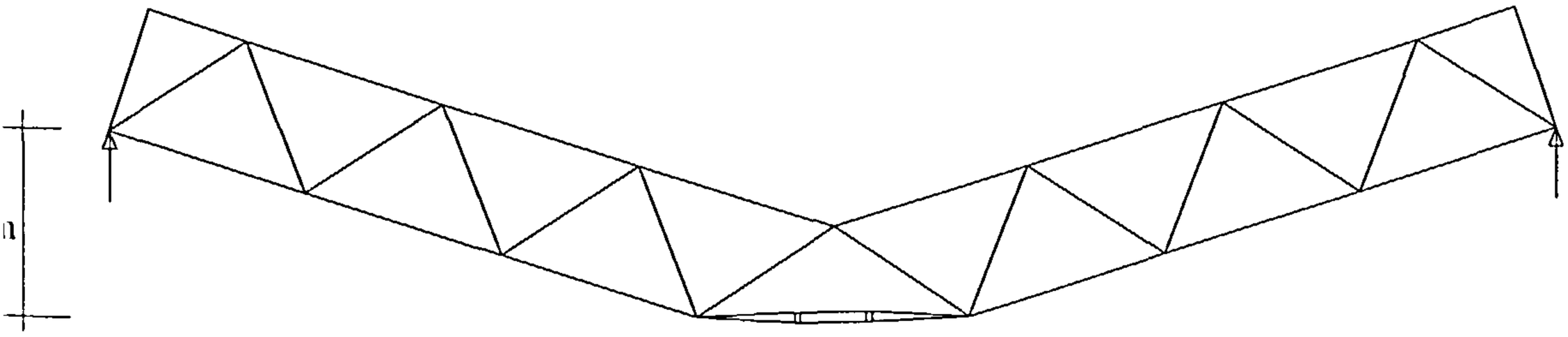

Fig 5-21: The deflected form of the framework. The maximum deflection of the framework is 0.9 m

It can be deduced from these graphs that the framework, when it is equipped with the energy absorbing device, has the capacity to accommodate the load factor of 5 without any damage to the individual structural members. The framework can be reused by repairing the energy absorbing device.

For a comparison, the response of the framework without the energy absorbing device will be examined.

5-2-2 Response of the framework without the energy absorbing device

In order to find how much the insertion of the absorber in a framework improves the impact strength of this structure, the response of the framework, described in section 5-2 but without the absorber, has been analysed. The applied load factor was 2.5 in this analysis which developed the ultimate strength state in the framework These results have been reported in Figures 5-22 to 5-27.

Results :

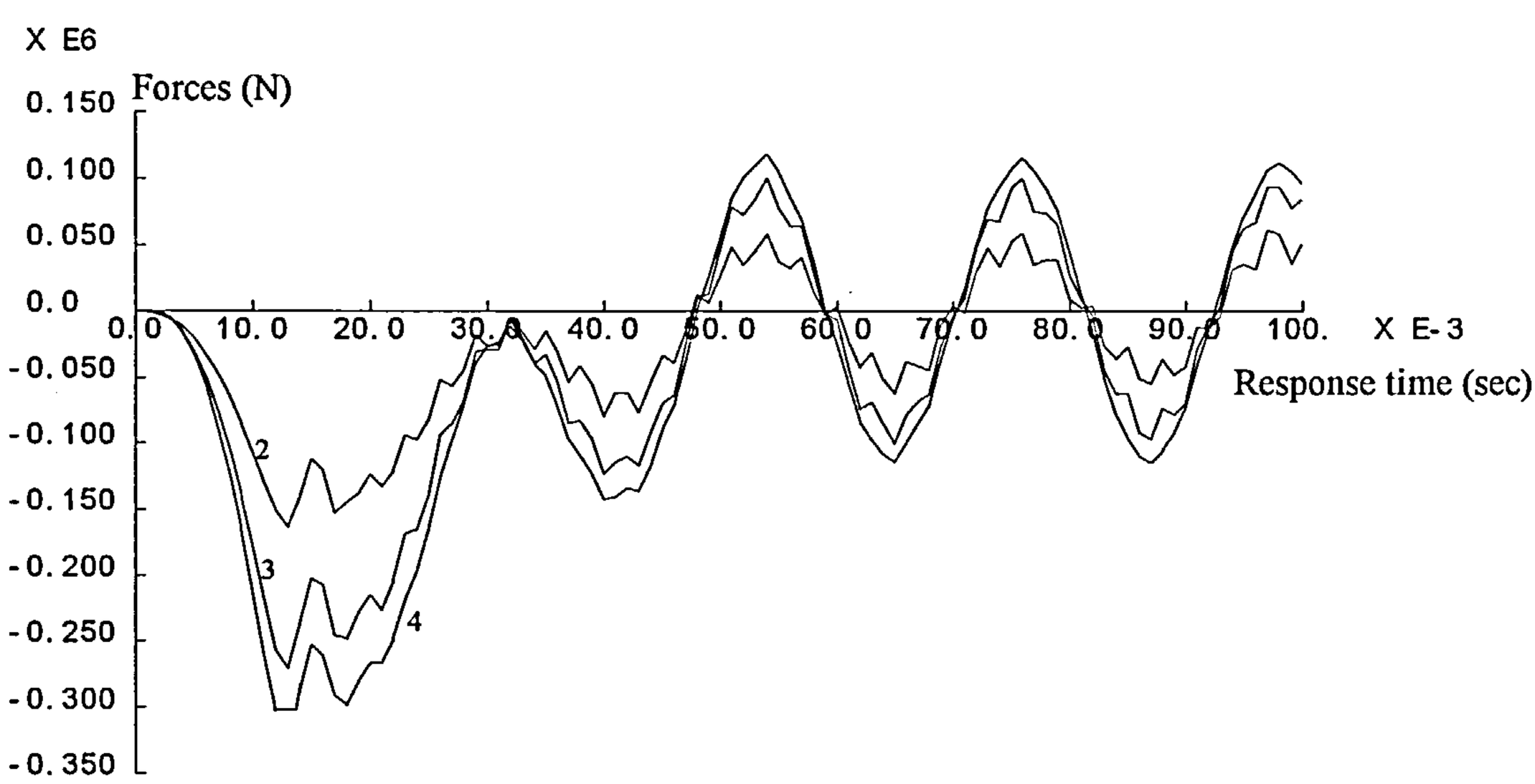

Fig 5-22: Load-response time curve for the top members of the framework without the absorber (members no 2, 3&4)

Figure 5-22 shows the loads in the top members of the framework. Stress in member 4 has reached the plastic limit.

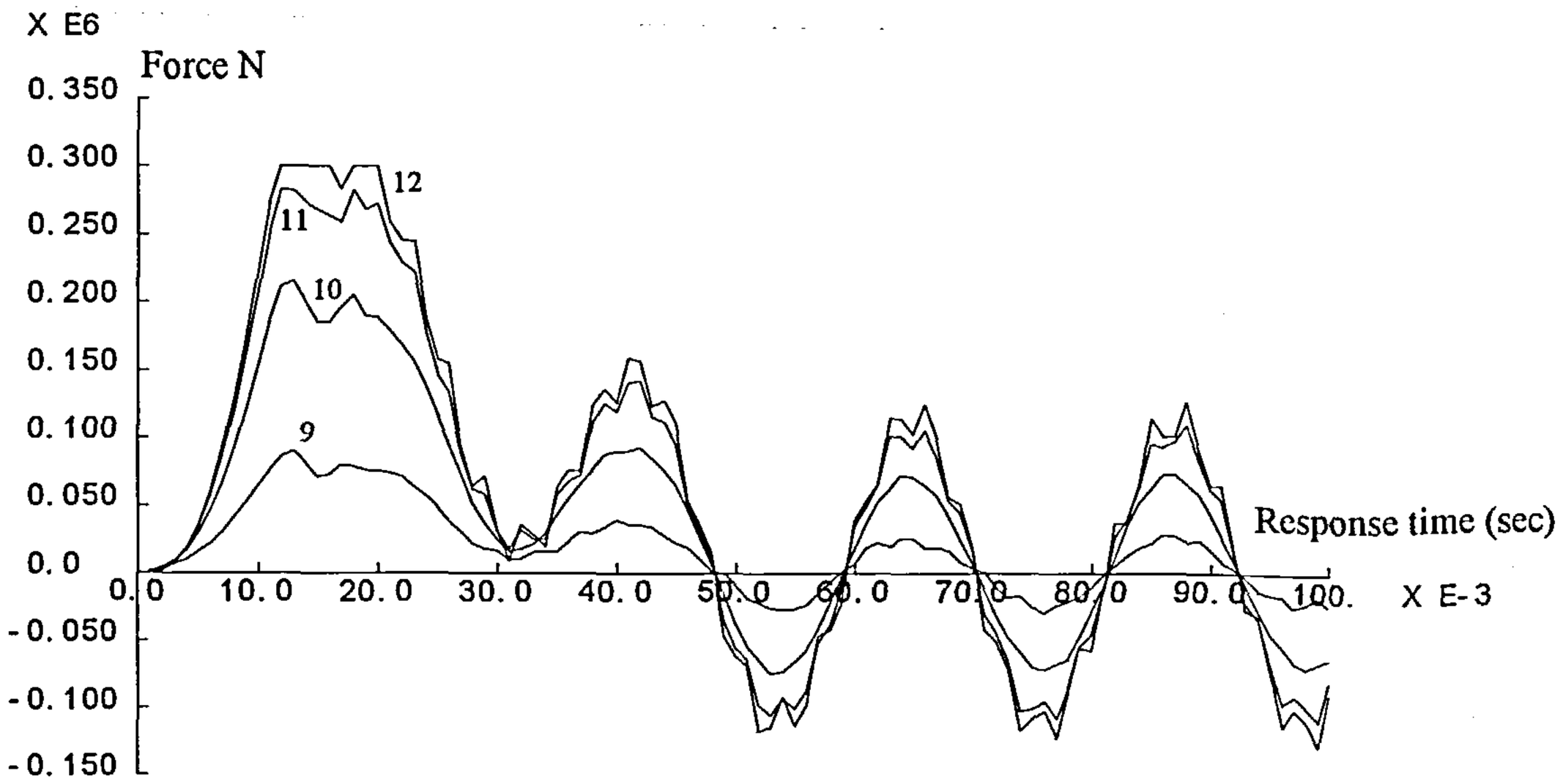

Fig 5-23: Load-response time curve of the bottom members of the framework (members no 9, 10, 11& 12)

Figure 5-23 is the load-response time in the lower members of the framework. It shows that member 12 has become significantly plastic. Load in member 11 is close to the plastic limit.

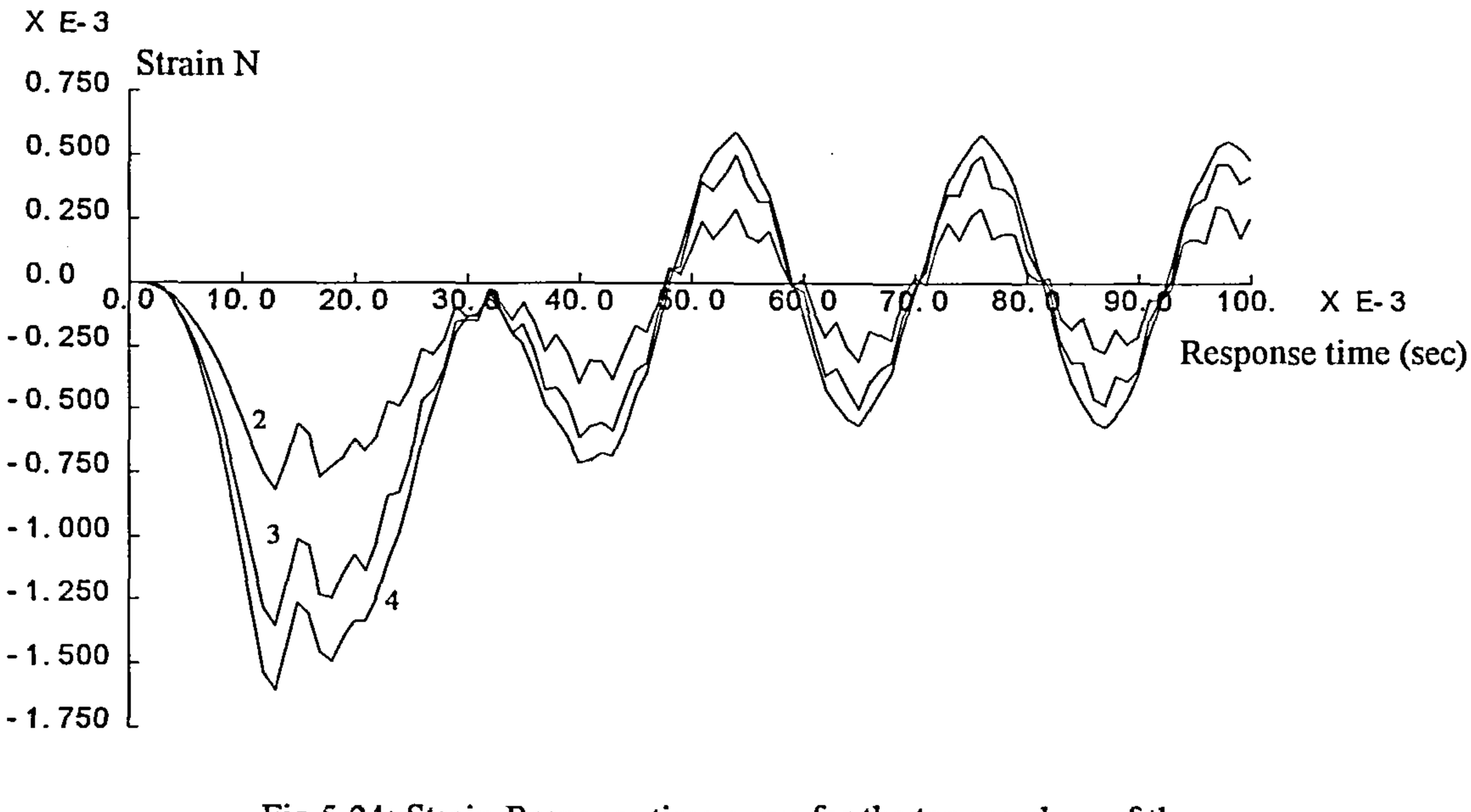

Fig 5-24: Strain-Response time curve for the top members of the framework (members 2, 3& 4)

Figure 5-24 is the strains in the top members. Strain in member 4 is dominant in this graph.

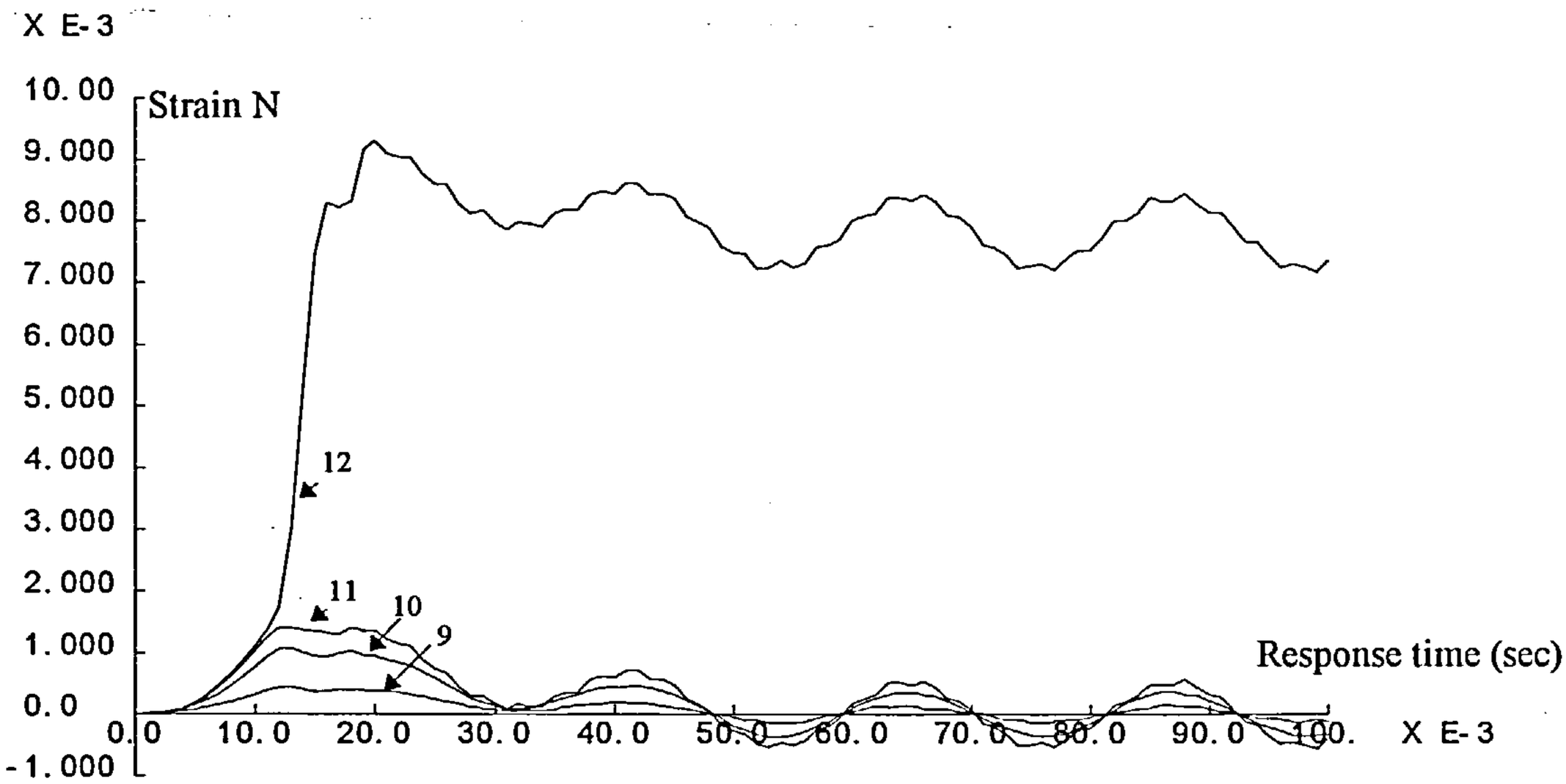

Fig 5-25: Strain-Response time curve for the bottom members of the framework (members no 9, 10, 11& 12)

Figure 5-25 is the strain-response time for the bottom members. The strain in member 12 has far exceeded the other members. It has some unrecoverable plastic deformations.

It is apparent from these results that by applying a load factor of 2.5 some members of the framework have become plastic and some unrecoverable damage has occurred in the bottom members. Therefore, by a comparison of these two analyses it has been demonstrated that the insertion of the absorber has increased the impact strength of the structure by the factor of more than two.

Figure 5-26 is the deflection-response time of the middle nodes. This figure shows that the deflection in this configuration is 40 mm at its peak value. In comparison with the previous configuration which the frame included the energy absorbing device, the vibration period of this framework is almost three times less than that of the frame with the absorber. Therefore, the inclusion of energy absorbing device in the structure has improved its period by the factor of three.

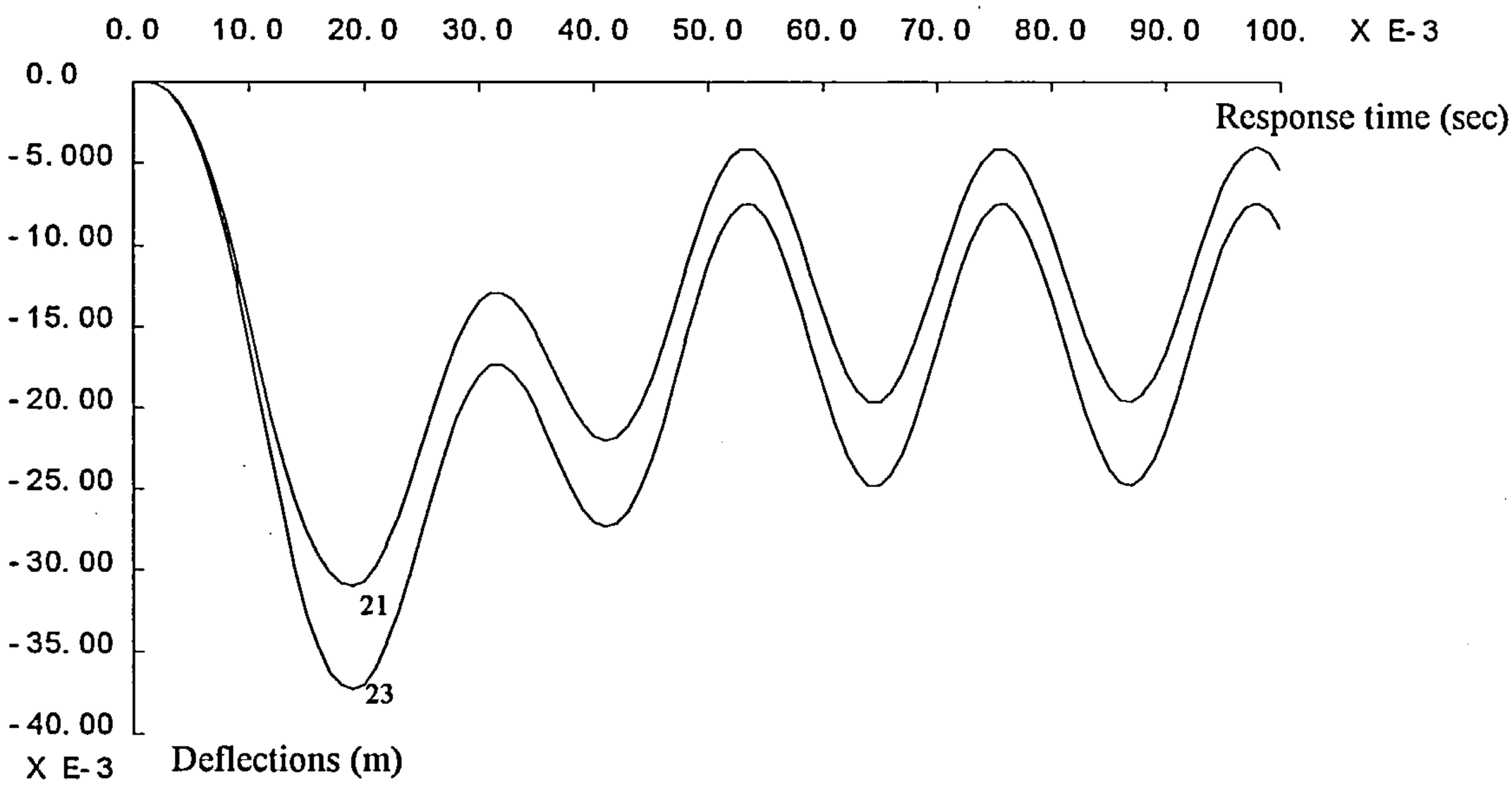

Fig 5-26: The deflections of the central nodes of the framework (nodes 21&23)

Figure 5-27 is the load response time for the diagonal members and indicates that there is no any damages in these members.

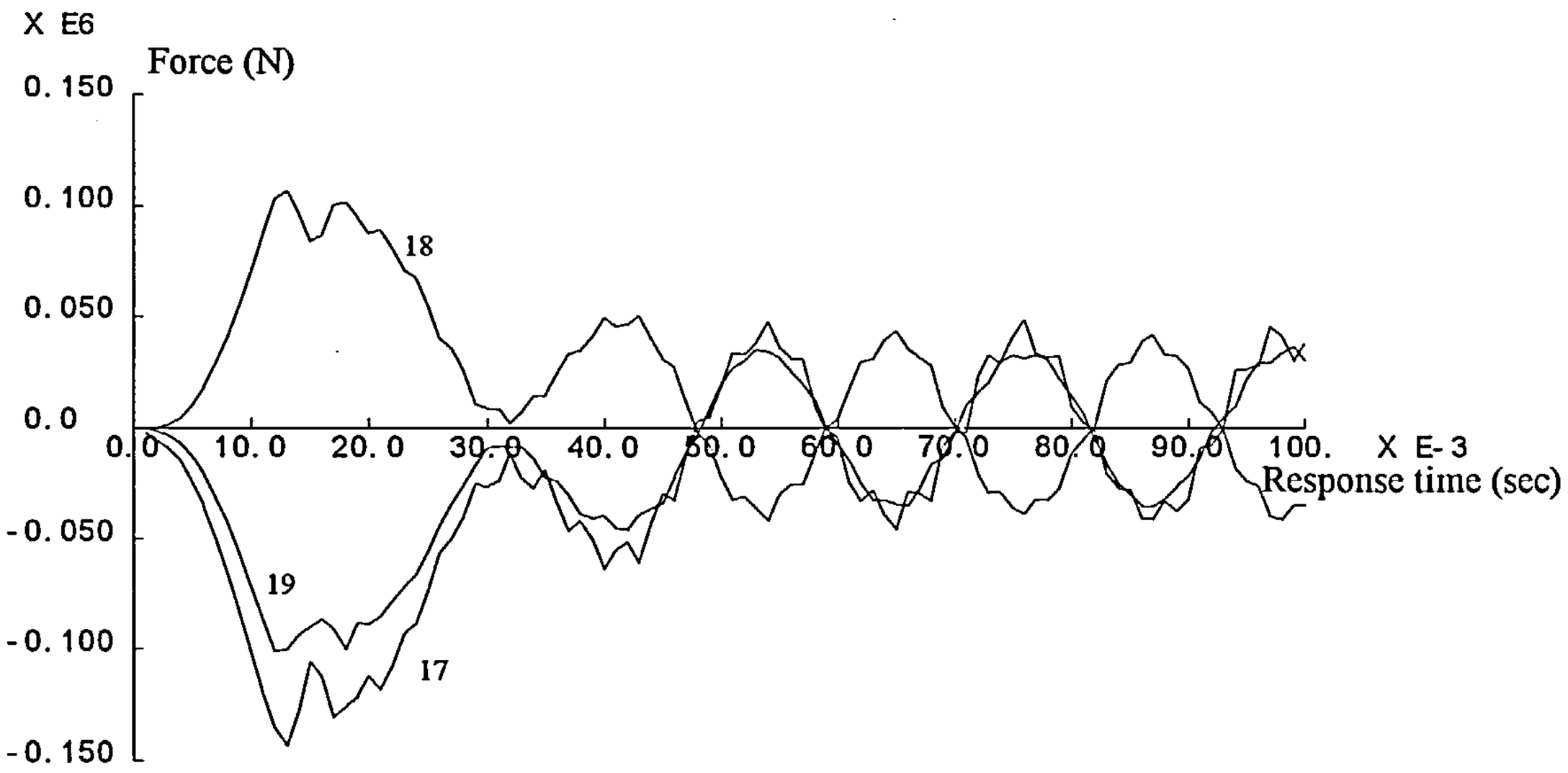

Fig 5-27: Load-Response time curve for the diagonal members of the framework (members no 17, 18& 19)

5-2-3 Natural frequency analysis:

An eigenvalue analysis was carried out for the framework to find the natural frequencies. This analysis was performed to ensure that the applied loading in the previous sections was not coincident with the natural frequency of the framework. The materials were considered elastic and an eigenvalue control was assigned to the model.

Control Definition:

Guyan eigenvalue control was assigned to the analysis with 10 automatically created master freedoms. In this method only those degrees of freedom are considered which contribute significantly the oscillatory structural behaviour. In a Guyan reduced eigenvalue extraction, the stiffness contribution of those freedoms whose inertia effect is considered insignificant (designated the slave freedoms), are condensed from the system. The reduced equation system is therefore dependent on those freedoms remaining (designated the master freedoms).

Three eigenvalues were requested from the programme. An eigenvalue control was then used to improve the results. The results and the first three natural frequency modes have been shown in table 5-4.

Table 5-4

EIGENVALUES FOR THE BRACED FRAME		
MODE	EIGENVALUE	FREQUENCY(HERTZ)
1	80097.6	45.0433
2	.102761E+07	161.337
3	.405689E+07	320.565

As shown in table, these natural frequencies are far away from that of the considered loading. Therefore, there was not any resonance phenomena in the response of the framework.

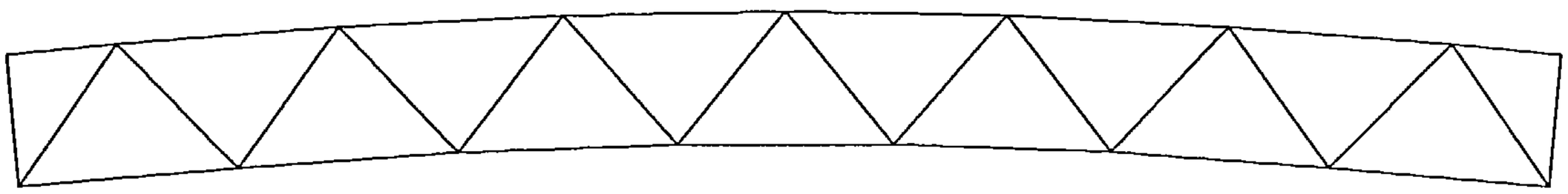

Fig 5-28: The first natural frequency mode of the framework

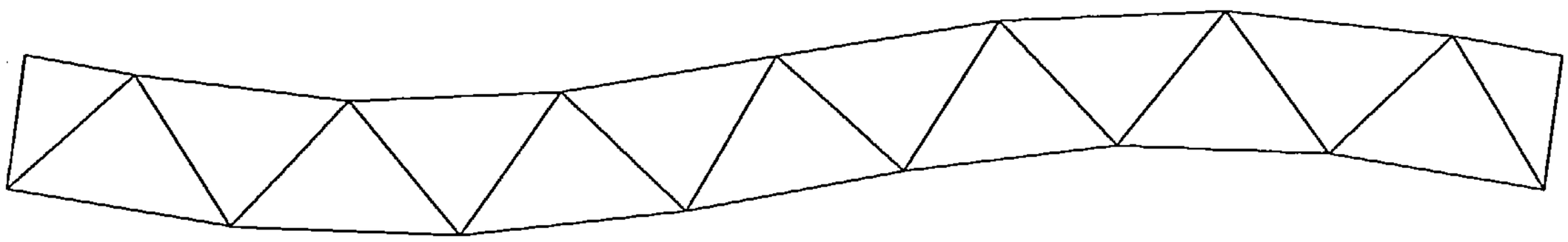

Fig 5-29: The second natural frequency mode of the framework

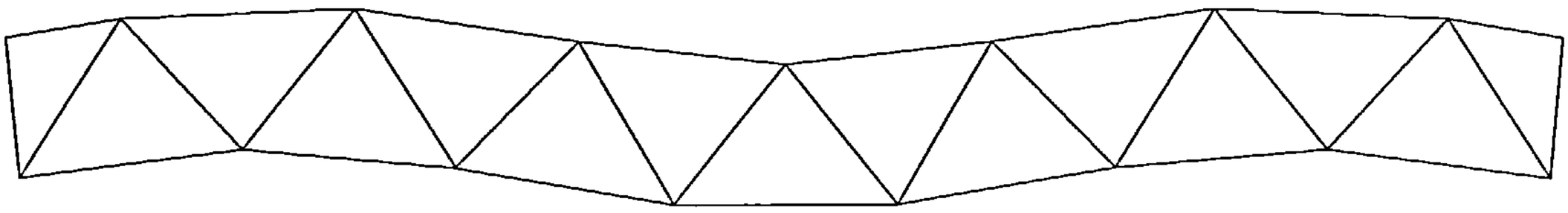

Fig 5-30: The third natural frequency mode of the framework

5-3 Single Degree Freedom Structure SDFS:

To demonstrate the application of the energy absorbing device in structures, the response of a SDFS to a base excitation was calculated and compared with the behaviour of the structure without the energy absorbing device as the second example.

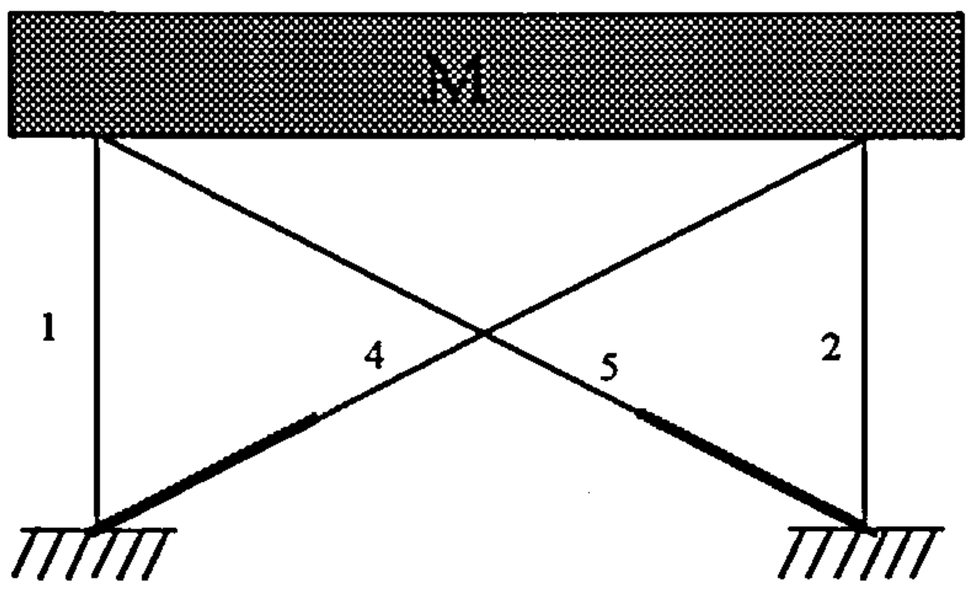

Fig 5-31: The SDFS equipped with the energy absorbing device

The structure consisted of a rigid mass M with two columns (1&2) and two braces (4&5). Their properties are described in the following sections. At first, the behaviour of the structure with the energy absorbing system in the cross members was calculated. This calculation was followed by the analysis of the SDFS without the absorbers. A comparison of the results of these two cases will show the effectiveness of the device in reducing shock acceleration.

5-3-1 The response of the SDFS with the energy absorbing system

Feature definition:

A frame with 3 m height and 4 m width was considered for this example. The beam was considered rigid and its mass was M=120 ton.

Mesh definition:

A thick beam element was used to represent the columns and beam Fig 5-32. This element is straight and includes shearing effects . The geometric properties are constant along the length. The element has 2 nodes with moment release end

conditions and the degrees of freedom are U,V, θ_z at each node. The element is referred to as the Engineering BEAM element in the Lusas Program.

BAR 2 elements from Lusas programme were used for the braces. This element has been already used for the framework of the previous section.

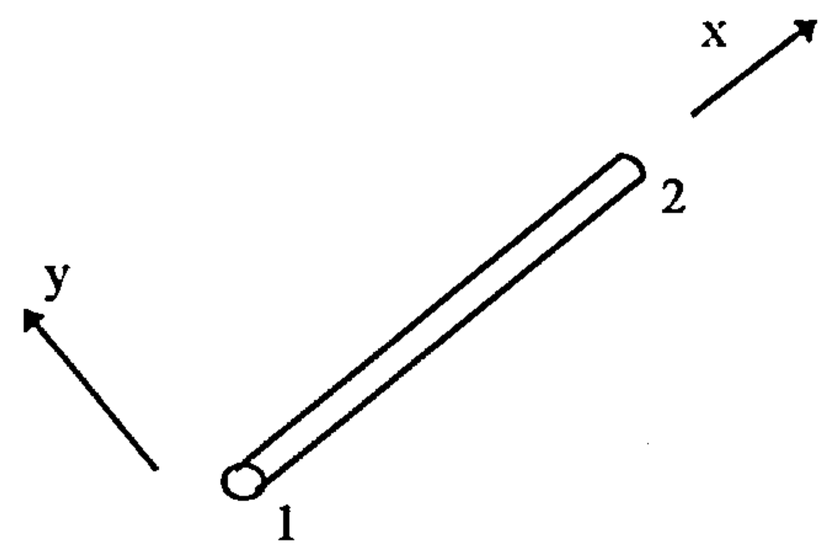

Fig 5-32: The Engineering BEAM element

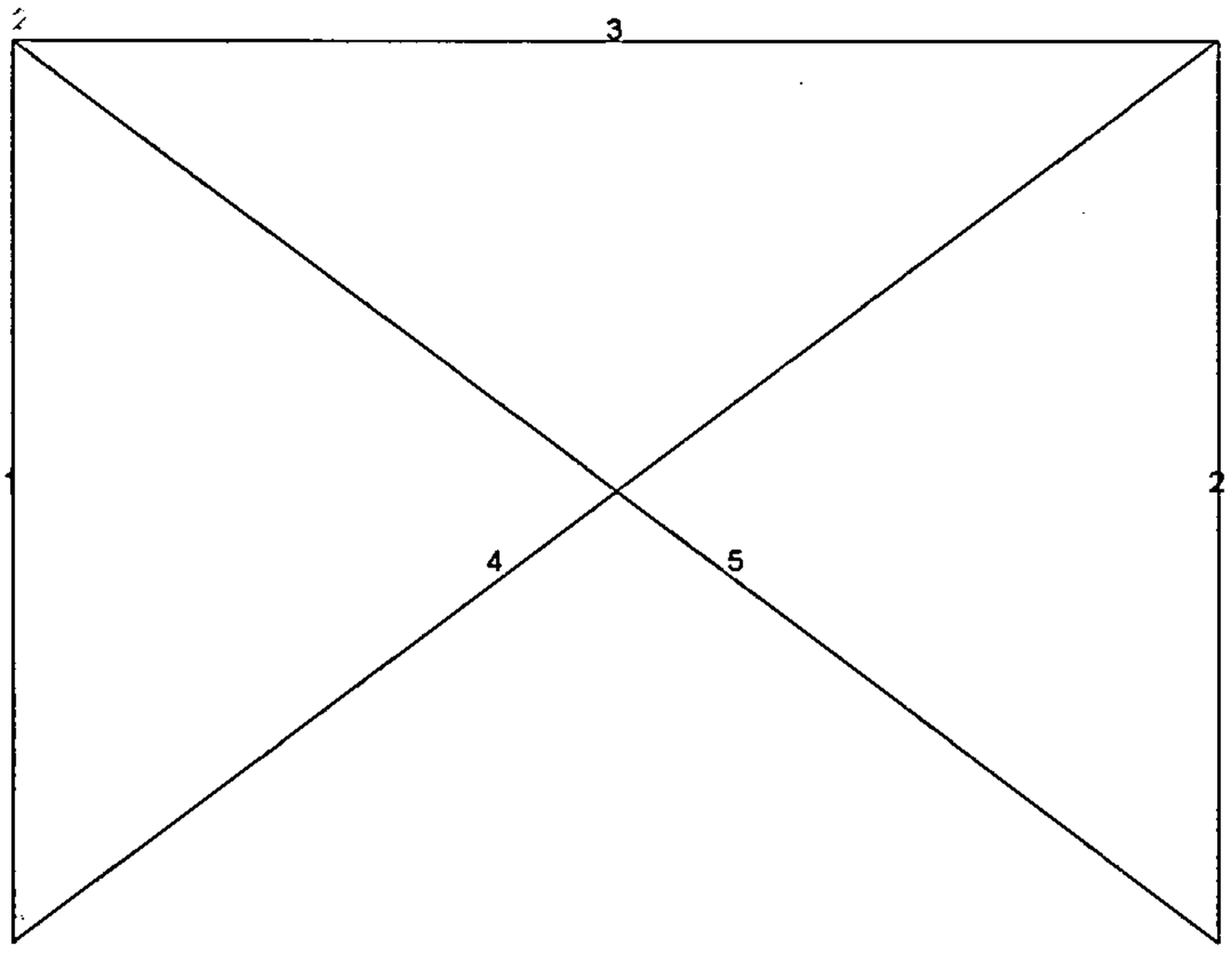

Fig 5-33: The finite element mesh of the framework

Geometric definition

A, I_{zz} , and A_s were the properties which were defined and assigned to the BEAM elements. For the BAR 2 elements, only A (area) was applied. Table 5-5 are the data which were used for the beam, columns and bars of this example.

For the columns:

Table 5-5

A	I_{zz}	A_s
0.00755 m^2	.525E-5 m^4	0.00755 m^2

For the beam:

The beam was considered to be rigid. The mass of this beam was M_a and this was applied in proportioned to the cross section and unit mass as an automatic feature in Lusas. Table 5-6 provides the values of A, Izz and A_z for the beam.

Table 5-6

A	I_{zz}	A_s
0.2 m^2	5.00E-1 m^4	0.2 m^2

Material definition

Engineering BEAM elements do not accept plastic material properties. Therefore, only an elastic material properties were assigned to this element. For BAR elements, a modified Von Mises material model was defined. In this analysis the falling stage in the load deflection curve of the device was disregarded. The effect of this falling stage is most crucial in high speed impacts like blast loading because it will produce an unloading shock wave and will reduce the stresses in the structural members quickly. In this periodic loading, which the loading speed is not high, the falling has not considerable effect on the reduction acceleration and therefore, has not been considered in the modelling.

Table 5-7

E (elastic modulus)	2.1 E11 KN/m^3
ν (Poisson ratio)	0.3
α (thermal coefficient)	0.0
m (mass density)	7800 KG/m^2
f_{yt} (tensile strength)	3.0E8 KN/m^2
f_{yc} (compressive strength)	1.0E2 KN/m^2

A low yield limit was considered for the compressive resistance of the device. This is the effect of connection set in the device (chapter 3) which releases the peeler bar under compressive loading.

Support definition

Fully restricted conditions were considered for the supports and these are shown in Figure 5-34. Rotations and displacements were suppressed in all directions in this fully fixed support.

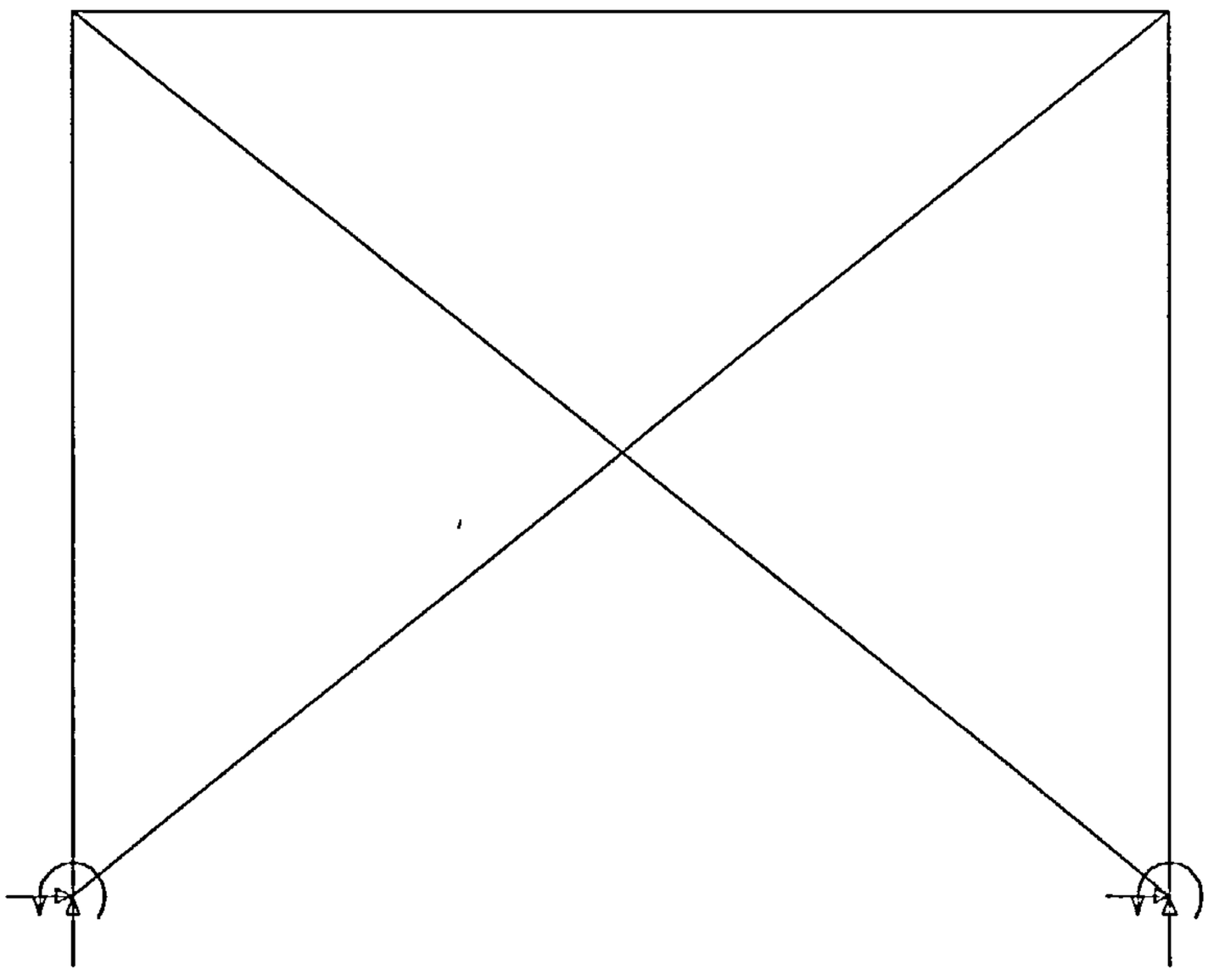

Fig 5-34: Support condition of the framework

Loading definition

A prescribed maximum acceleration of 50 m/sec^2 was defined as the loading of this example. This acceleration was high enough to create the ultimate condition in the frame. It was applied horizontally to the base of the frame and figure 5-35 shows the assumed variation with time.

Load curve

A cosine variation of load with time with an amplitude of 1 and frequency of 8 (Hertz) was defined as the load curve and assigned for the loading. This loading frequency has been applied because it was not coincident with the natural frequency of the frame (section 5-3-3).

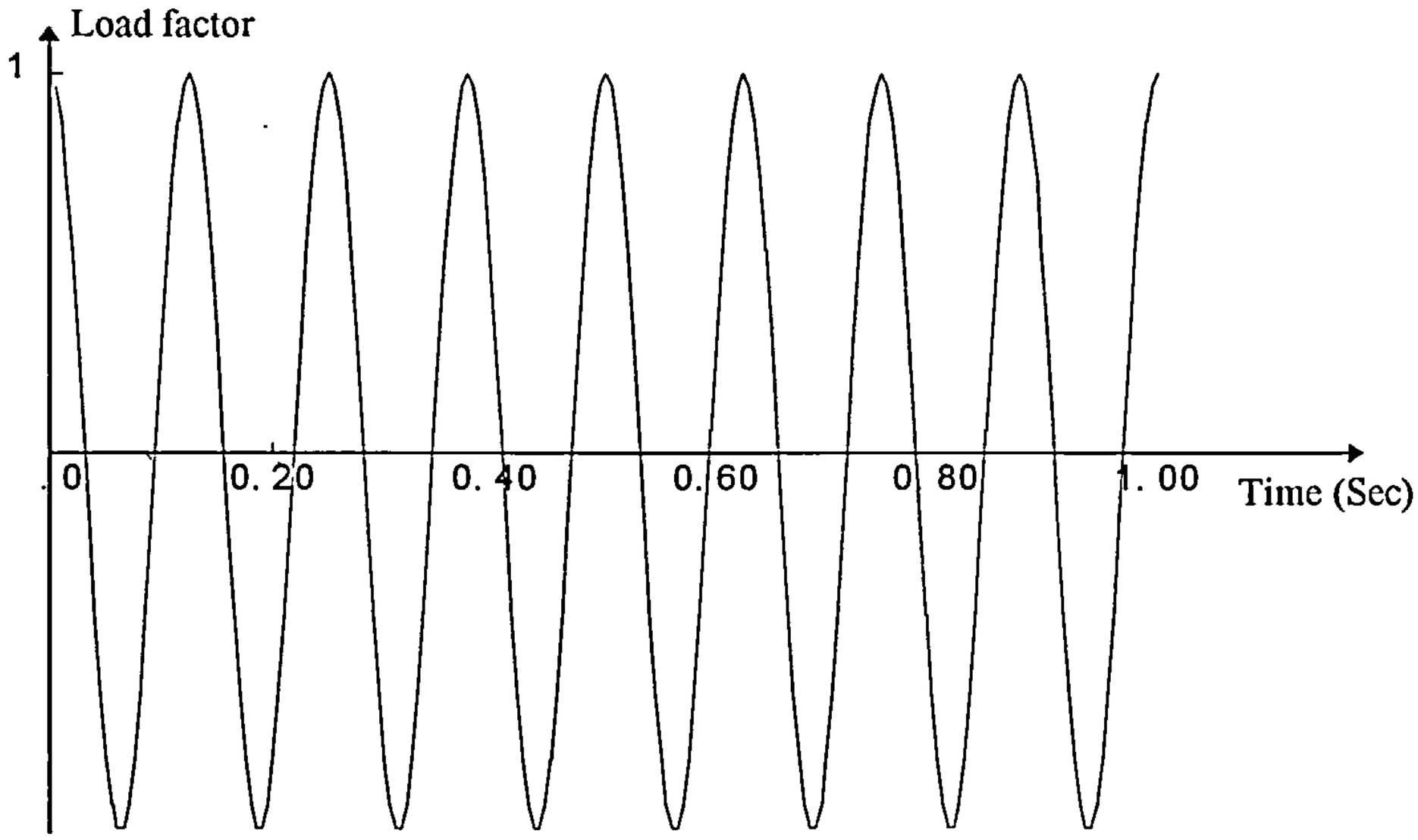

Fig 5-35: Load curve of the framework

Control definition

Once more, nonlinear dynamic control was assigned for this analysis with the time step of 0.001 sec. The quantities of section 4-1-1-1 were used for the convergence criteria.

Results: The results have been illustrated in Figures 5-36 to 5-45 for the structure with the energy absorbing device.

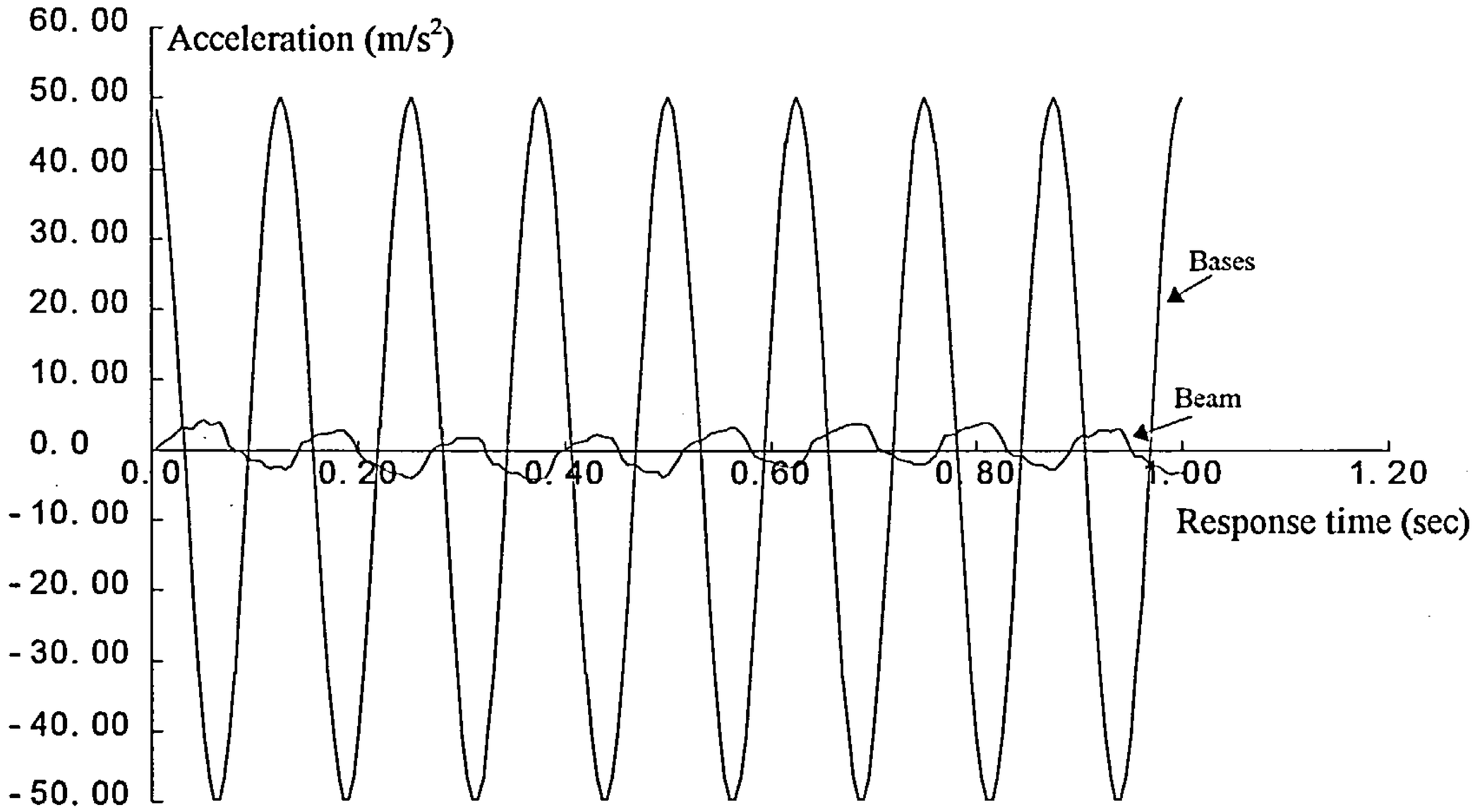

Fig 5-36: Accelerations of the base and the beam

It can be seen from figure 5-36 that the acceleration of the beam is only 10 percent of the basement acceleration. This is due to the dissipation of the energy by the absorbing device.

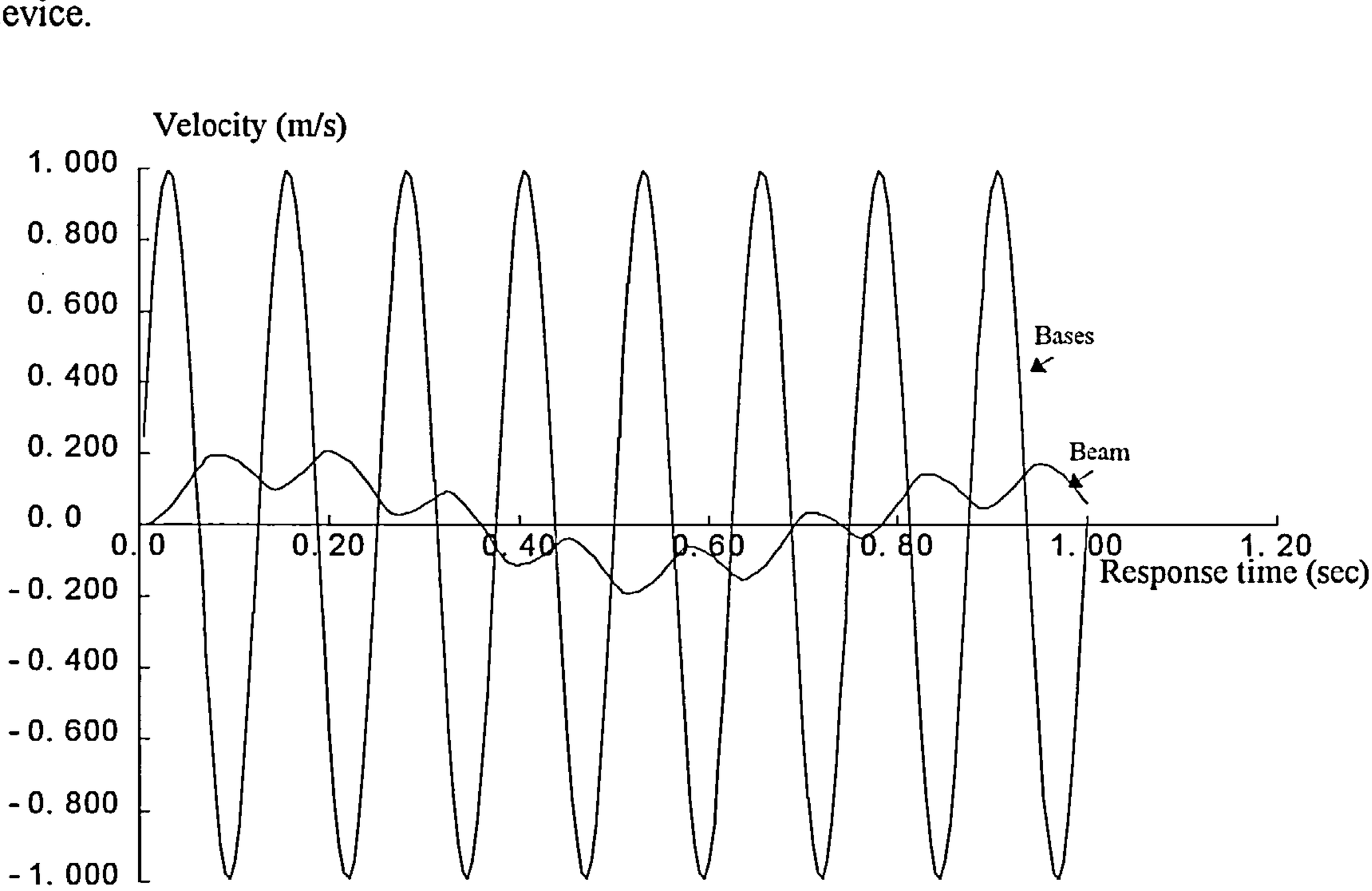

Fig 5-37: Velocities of the base and the beam

Figure 5-37 shows the velocities at the base and the beam. The peak velocity in the beam is only 20 percent of the basement's velocity.

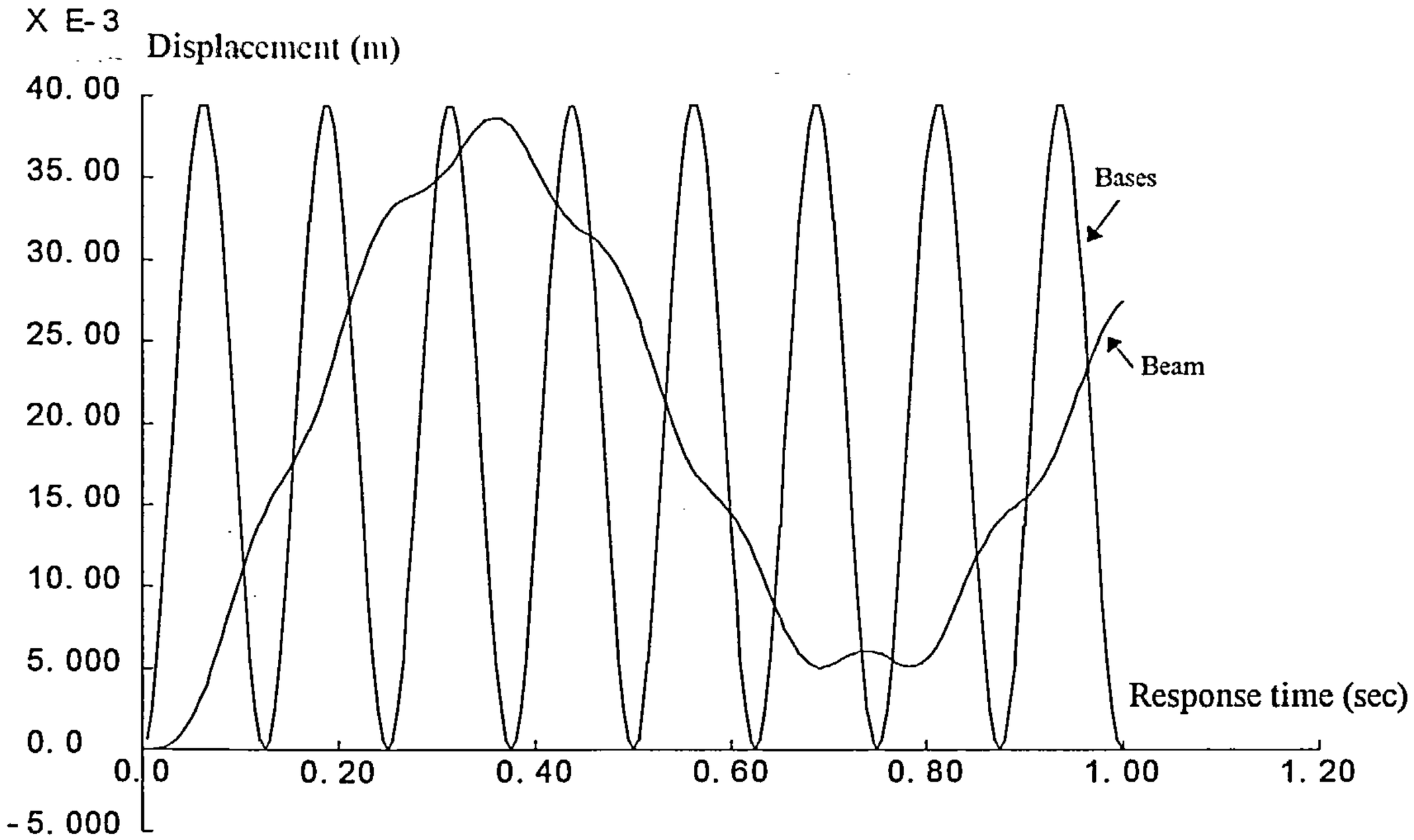

Fig 5-38: Horizontal displacement of the base and the beam

Figure 5-38 shows the displacement of the beam and the bases. It is seen that the period of vibration of the beam is almost six times that of the base.

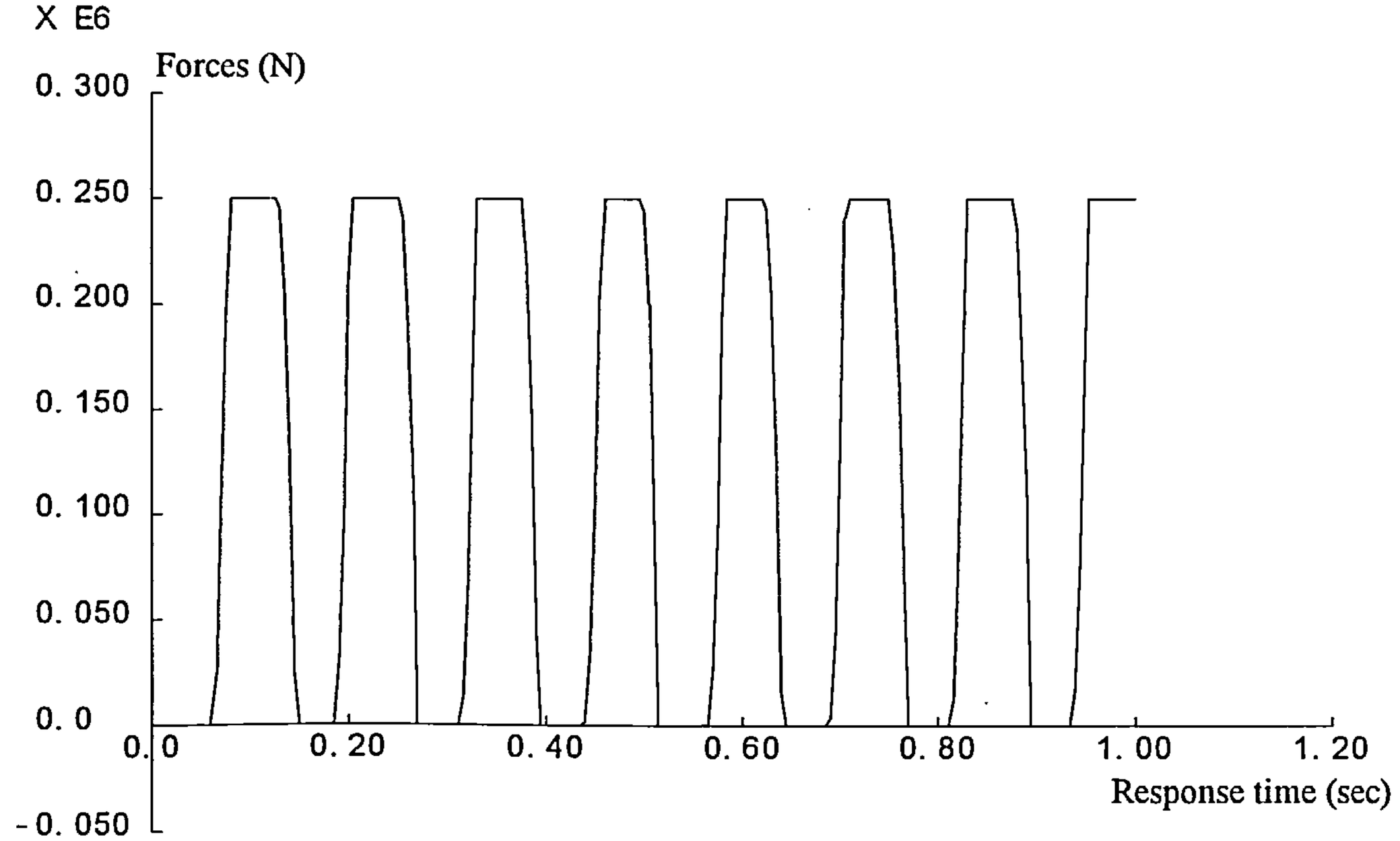

Fig 5-39: Forces in the brace no 4

Figure 5-39 is force-response time in brace no 4. The plastic deformation of this member can be observed in this figure. In each cycle, the energy absorbing device dissipates the energy of the applied load by undergoing plastic deformation.

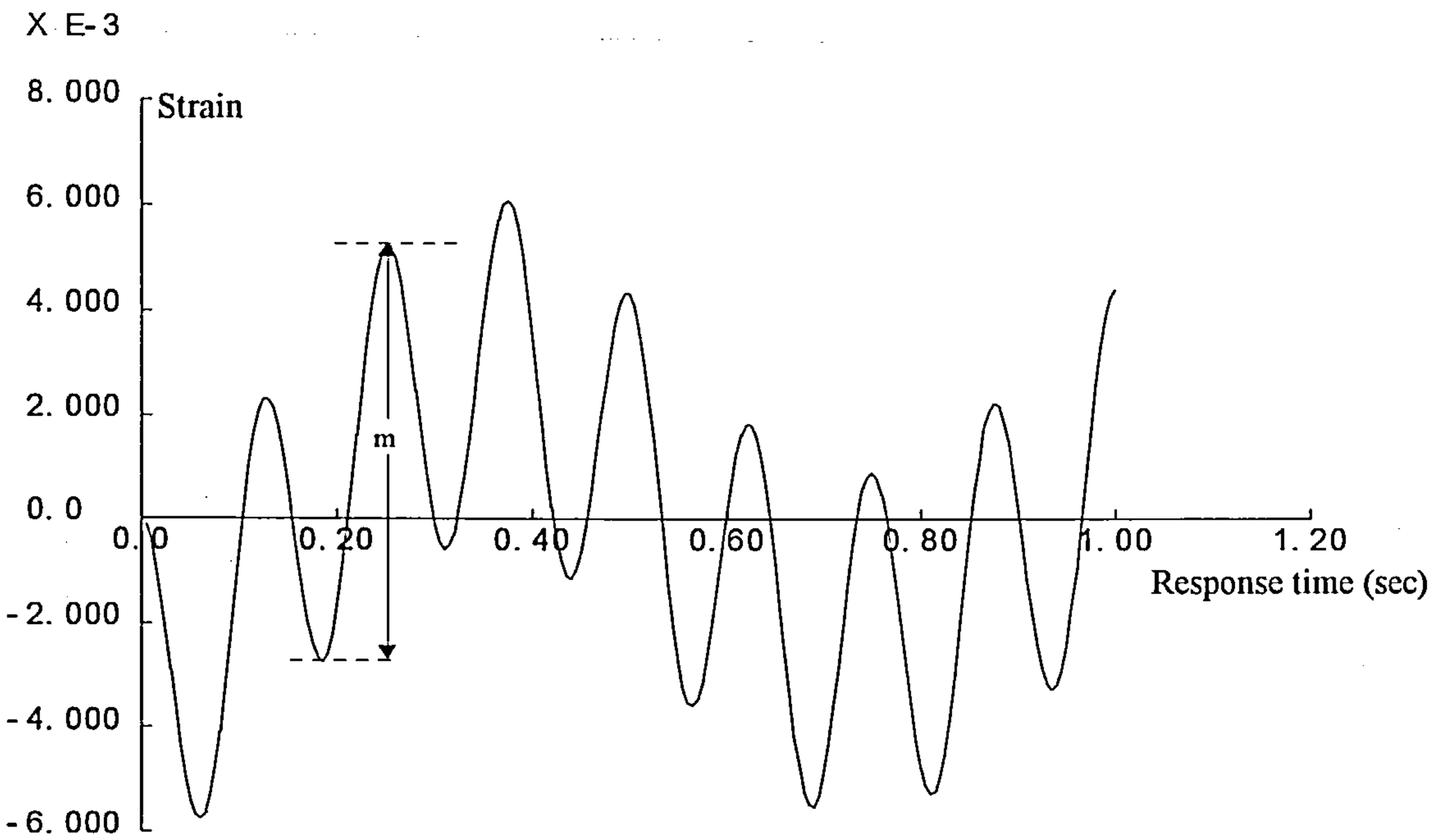

Fig 5-40: Strains in the brace no 4

For the computation of the absorbed energy Figure 5-40 should be considered. In this figure, the amplitude of the vibration is shown as 'm' (peak to peak) and is equal to 8000 micro strain. The length of a practical device will be about 1 metre. The devices have been applied in the braces in which their lengths in this frame are 5 metre.

Therefore, by accepting 0.8 strain as the maximum strain of the device, the permissible strain in the braces will be o.18 or 180000 micro strain.

In a one second period there is in average of 8 tensile amplitudes Figure 5-40, thus the device can tolerate the energy for almost 22 seconds before its absorbing capacity ends. It is obvious that by lengthening the device (in other words, increasing the energy absorbing capacity of the device) or by changing it yield limit, the maximum permissible time for such a severe vibration can be increased.

In the following, the axial and shear forces in the columns and their bending moment have been illustrated in Figures 5-41 to 43. It is seen from these figures that despite of the high rate of applied shock, the forces in these components are in acceptable ranges.

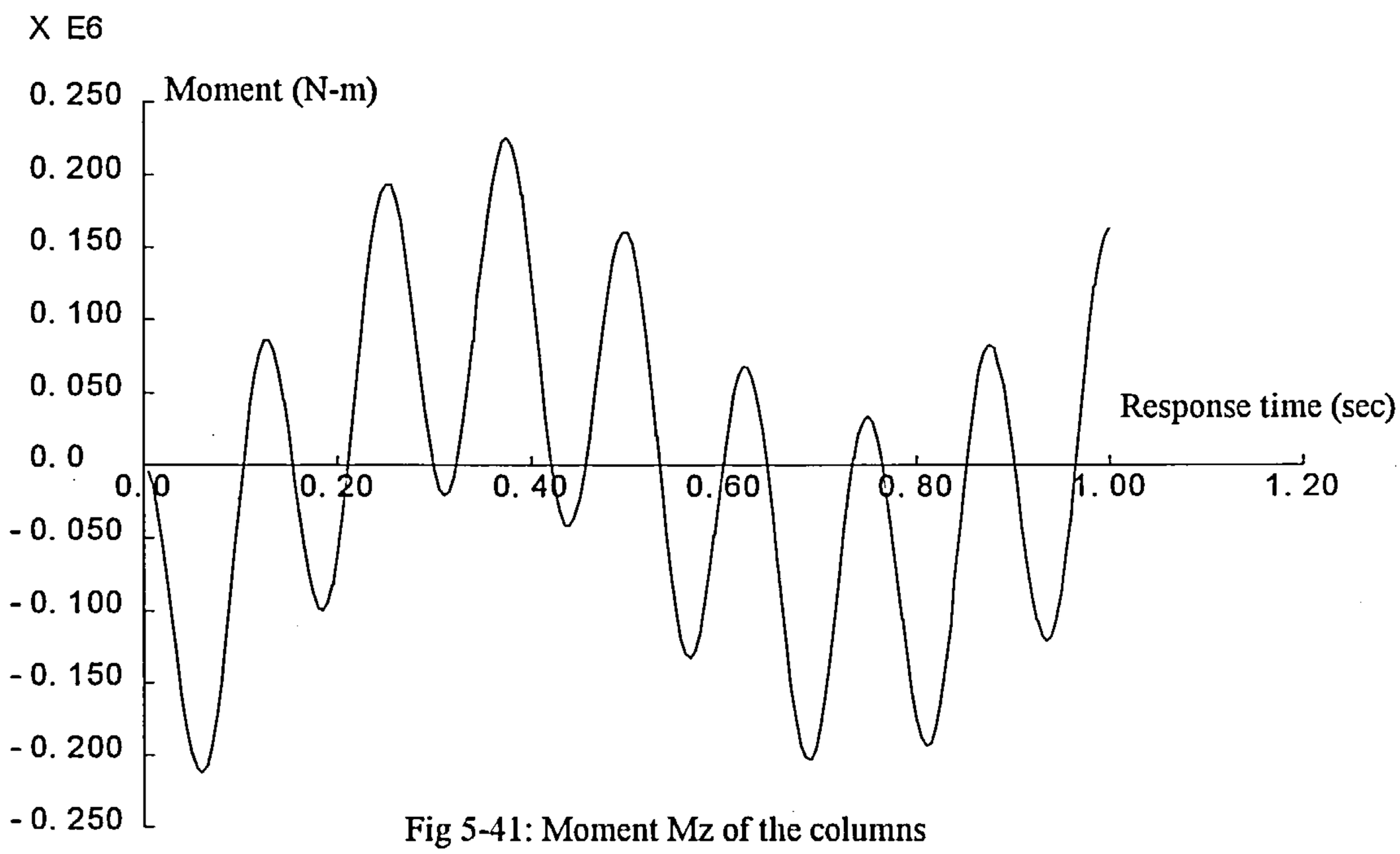

Fig 5-41: Moment Mz of the columns

Figure 5-41 shows the moment in the columns. The peak value in this figure in is 200KN-m which is a acceptable amount for these members.

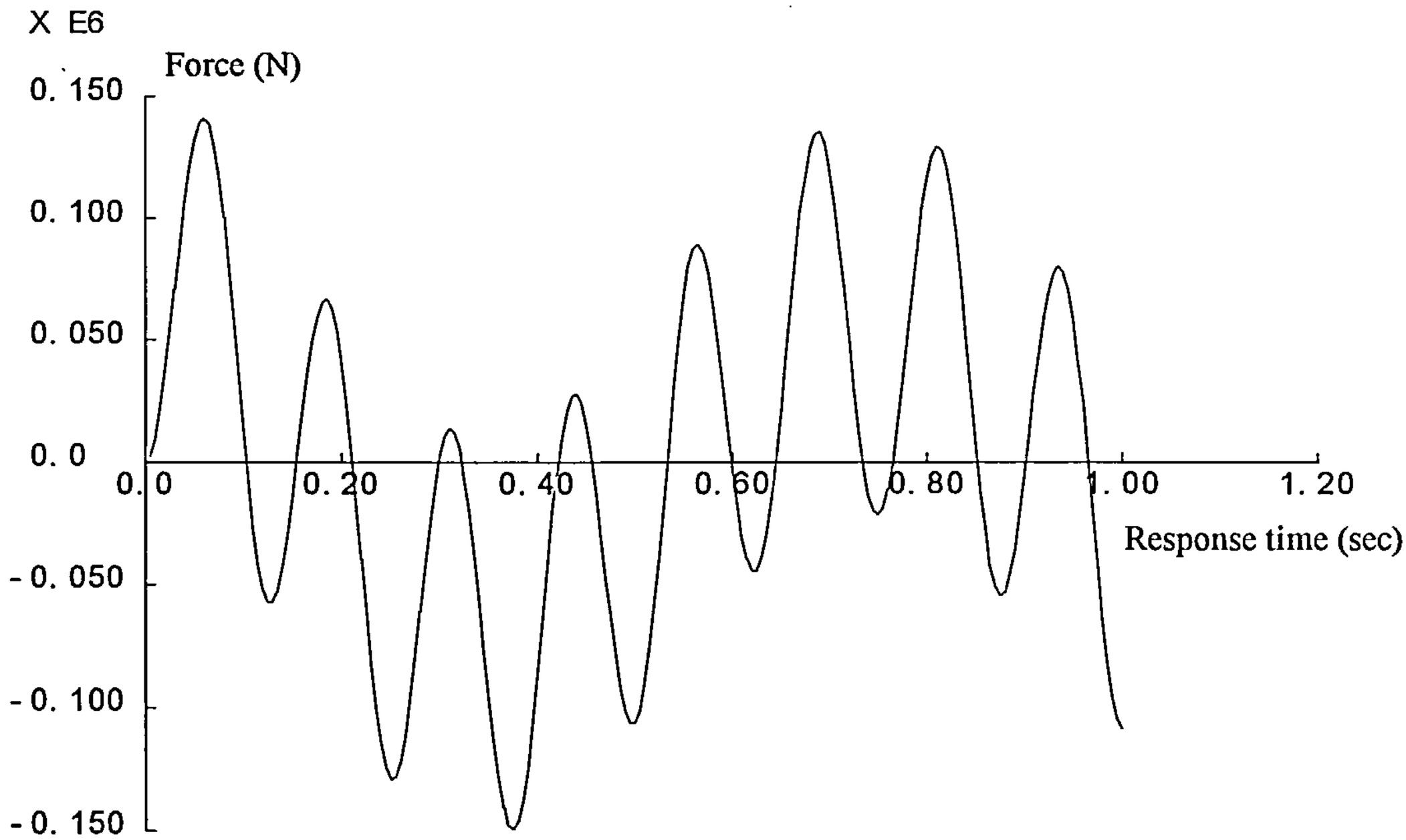

Fig 5-42: Axial forces of the columns

Figure 5-42 is the axial load in the columns. The peak value in this graph is 150KN is acceptable range for the columns.

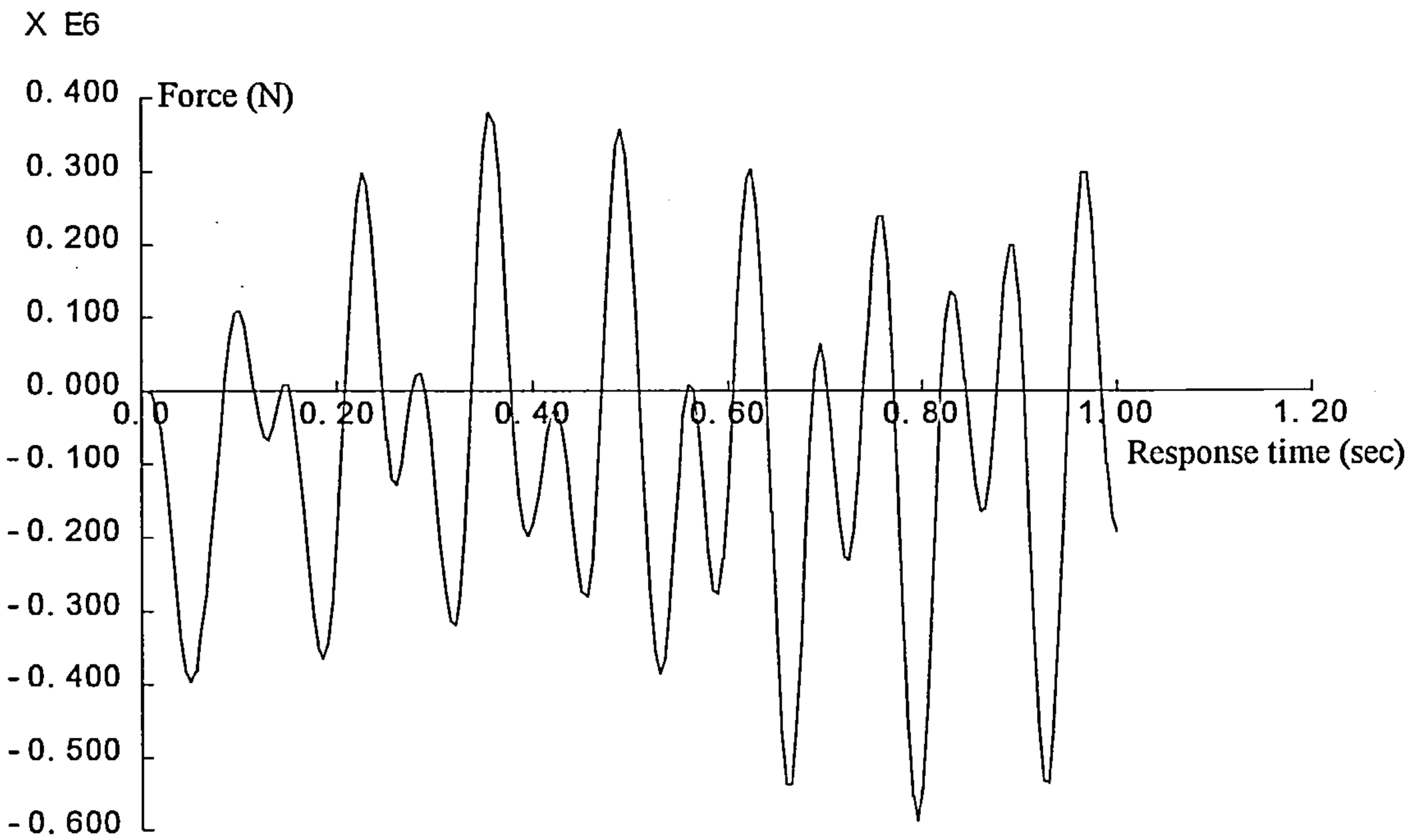

Fig 5-43: Shear forces of the columns

In this section, the behaviour of a SDFS, equipped with the energy absorbing device, was studied. It was noticed that a huge reduction in the acceleration, velocity in the beam is obtained when the absorbers included in the braces. In order to find importance of this arrangement, the behaviour this frame but without the absorbers, will be studied in the next section.

5-3-3 The response of SDFS without energy absorbing devices

For a comparison, the frame was analysed with the same loading and configuration as that in the previous section except that this frame did not include the energy absorbing devices. The results are reported in what follows.

Results:

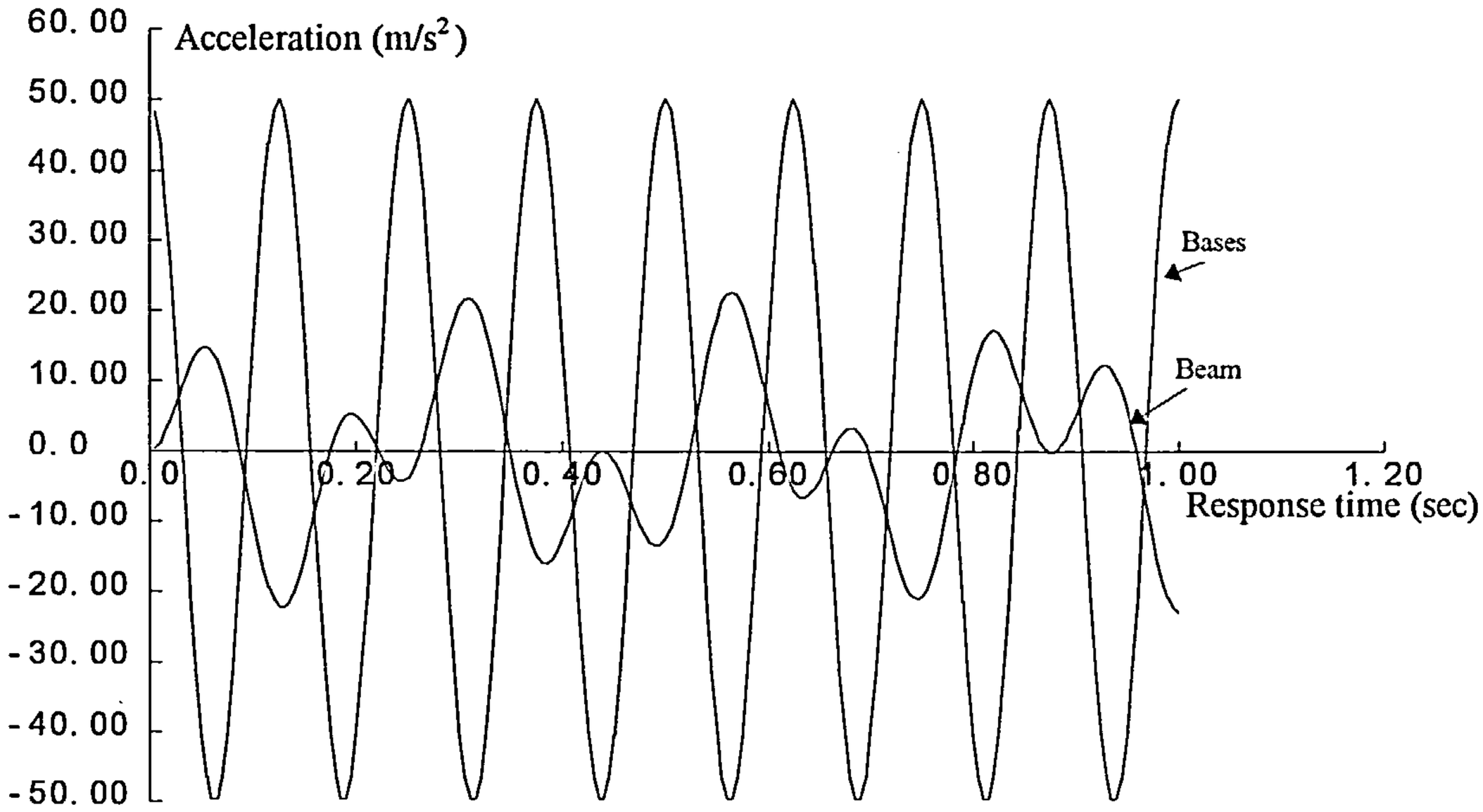

Fig 5-44: Accelerations of the base and the beam

Figure 5-44 shows the accelerations in the bases and the beam. It can be seen in this graph that the peak value for the acceleration of beam is 20 m/sec^2. It is 40 percent of the acceleration of bases.

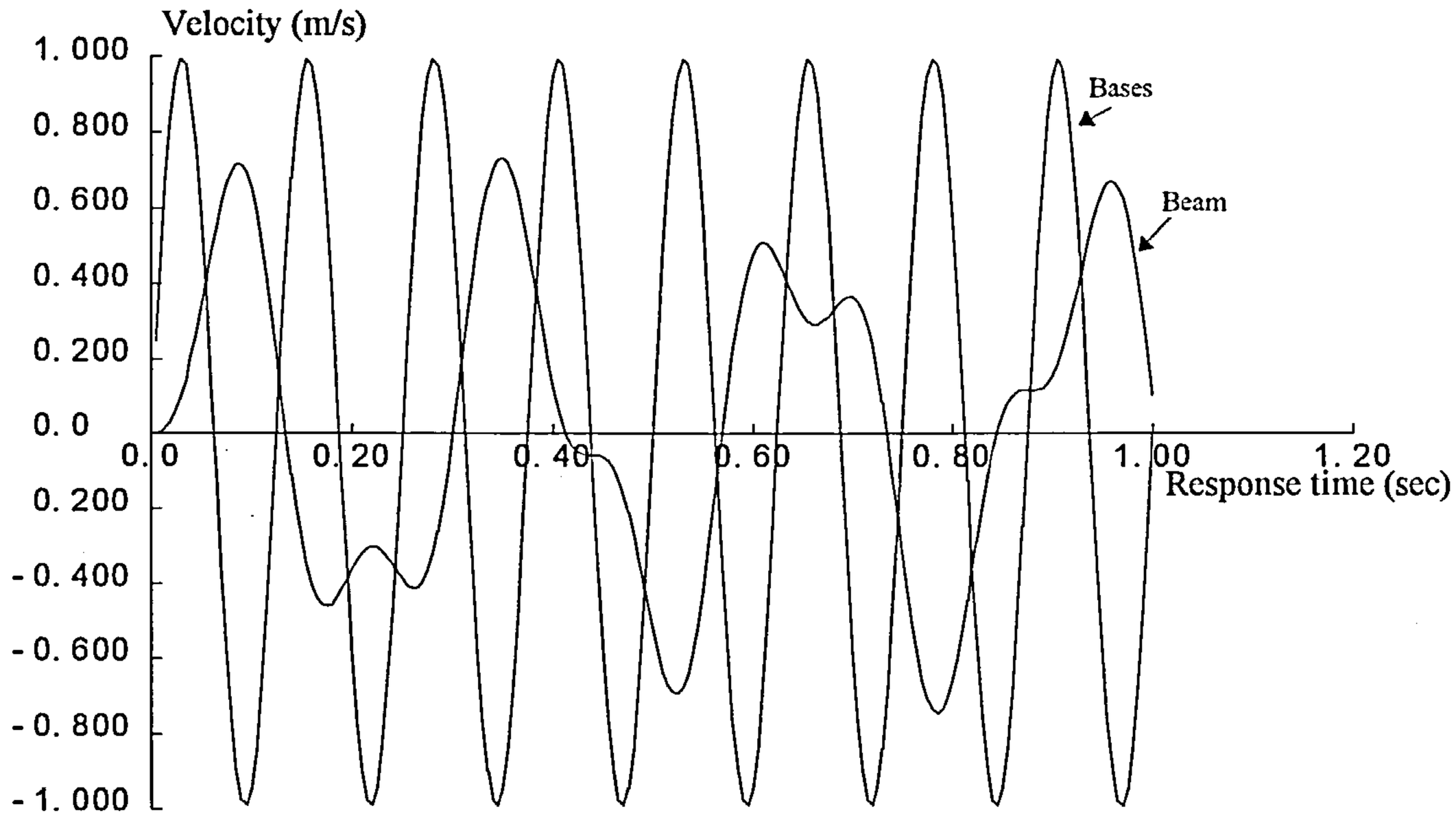

Fig 5-45: Velocity of the base and the beam

Figure 5-54 shows the velocities of the base and the beam. The peak value for the velocity of beam is 0.7 m/sec in this graph. It is 70 percent of the velocity of the base.

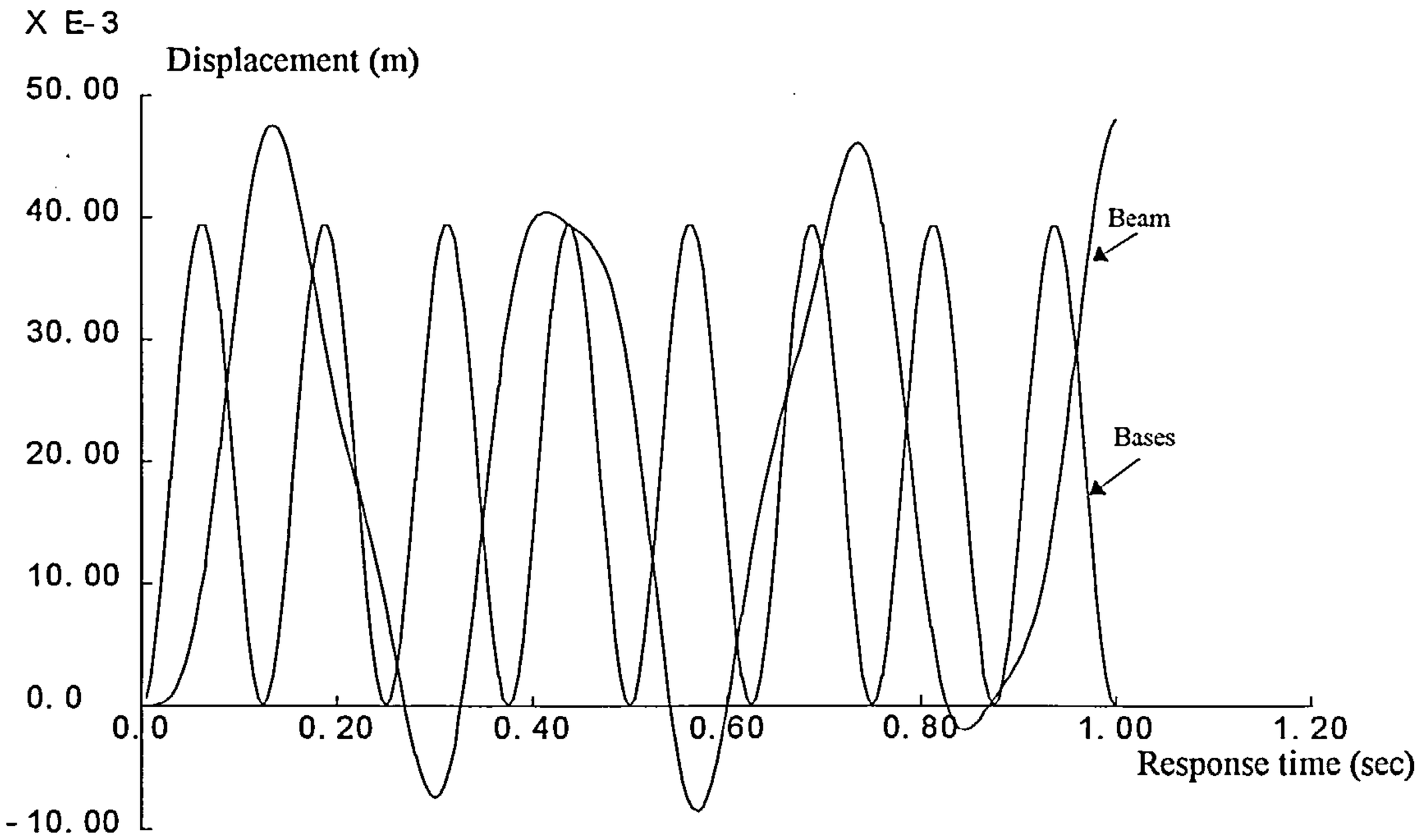

Fig 5-46: Displacements of the base and the beam

Figure 5-46 shows the displacement of the beam and bases during this cyclic loading. It is noticeable that the peak value for the displacement of beam is almost 20 percent more than that of the bases. Its period is twice of the loading period.

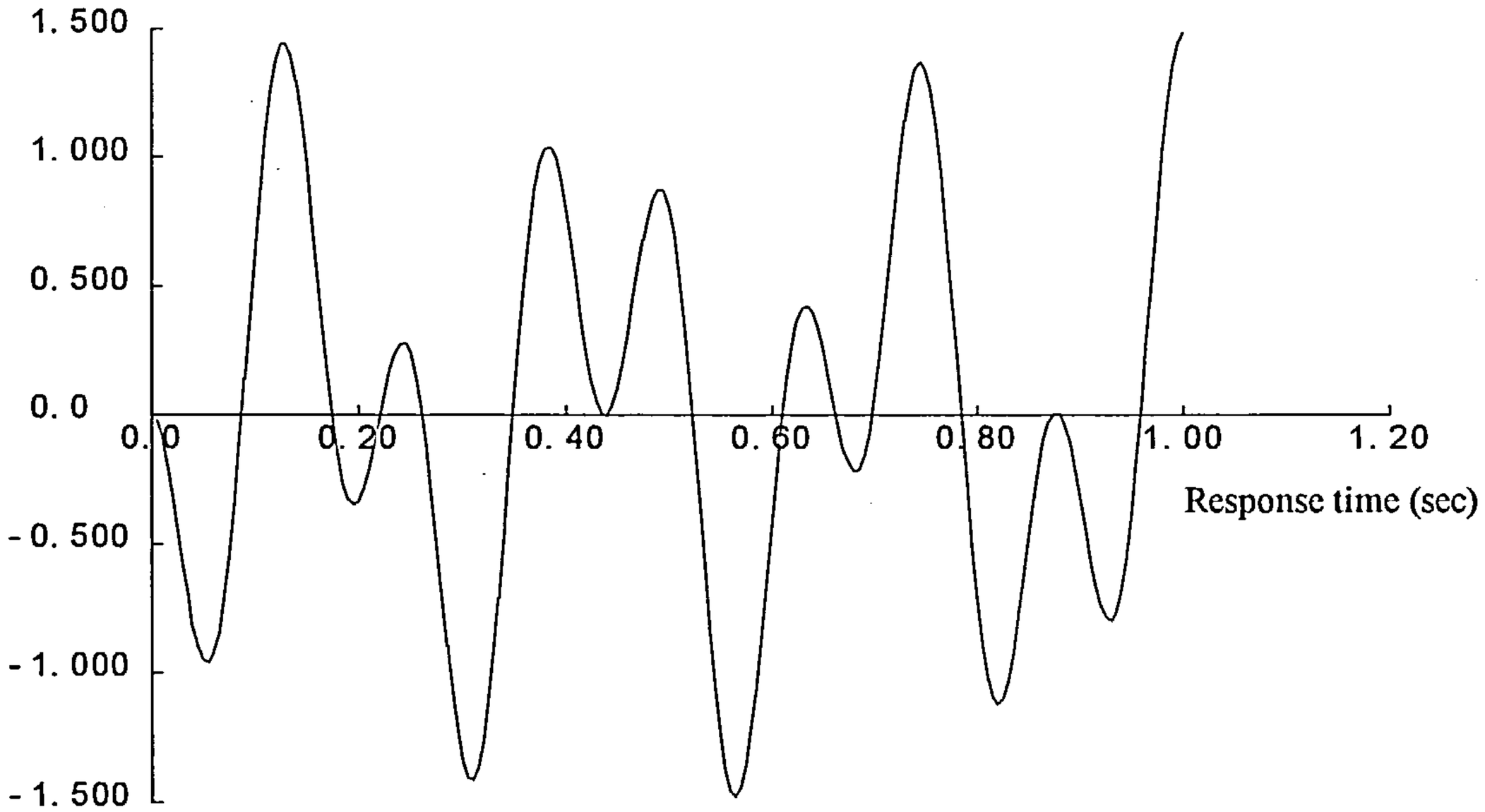

Fig 5-47: Forces in the braces

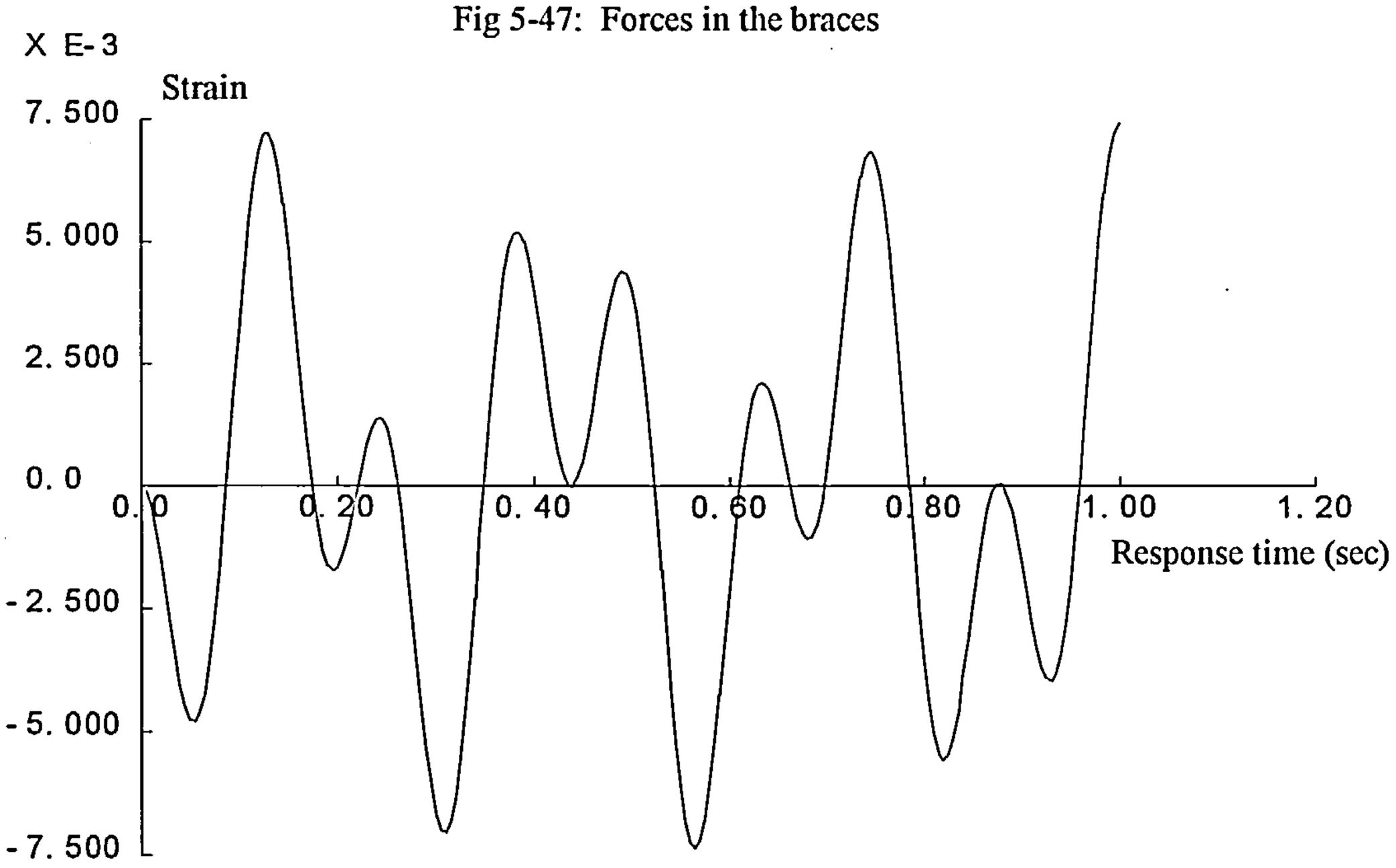

Fig 5-48: Strains in the braces

Figure 5-47 and 5-48 are the strains and forces in the braces, receptively. It can be seen from these graphs that the load in the braces have reached to a high value which are not permissible for these members. They should be redesigned and their cross section should be increased for such loading.

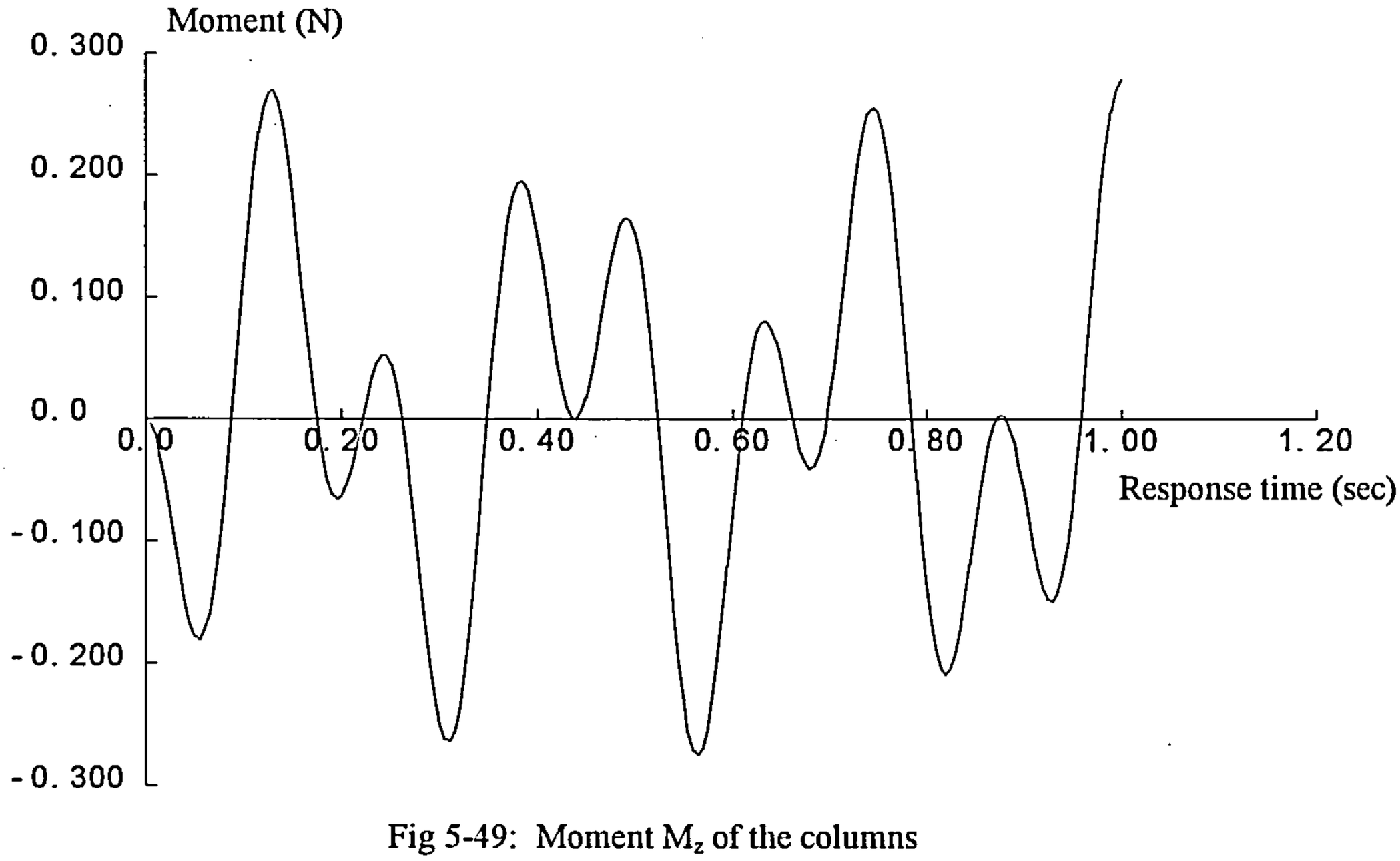

Fig 5-49: Moment M_z of the columns

Figure 5-49 is the moment in the columns. It shows that the bending moment has not changed significantly by removing the energy absorbing device from the system.

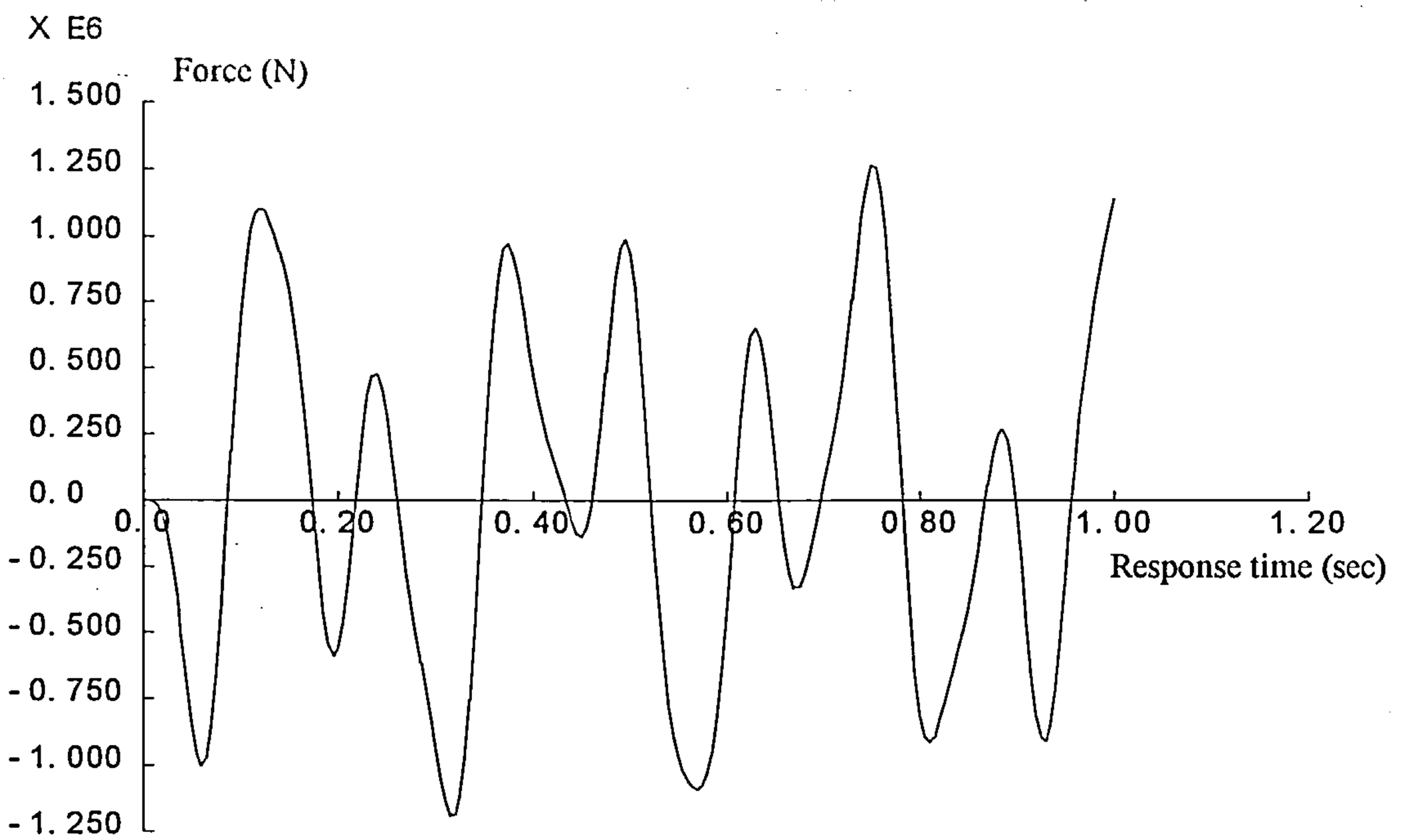

Fig 5-50: Axial forces of the columns

From Figure 5-50, it can be seen that the peak value in the axial force of the columns has reached to amount of 1500KN which is unacceptable for these columns. Therefore, an improvement in their cross section area is necessary to resist such loading.

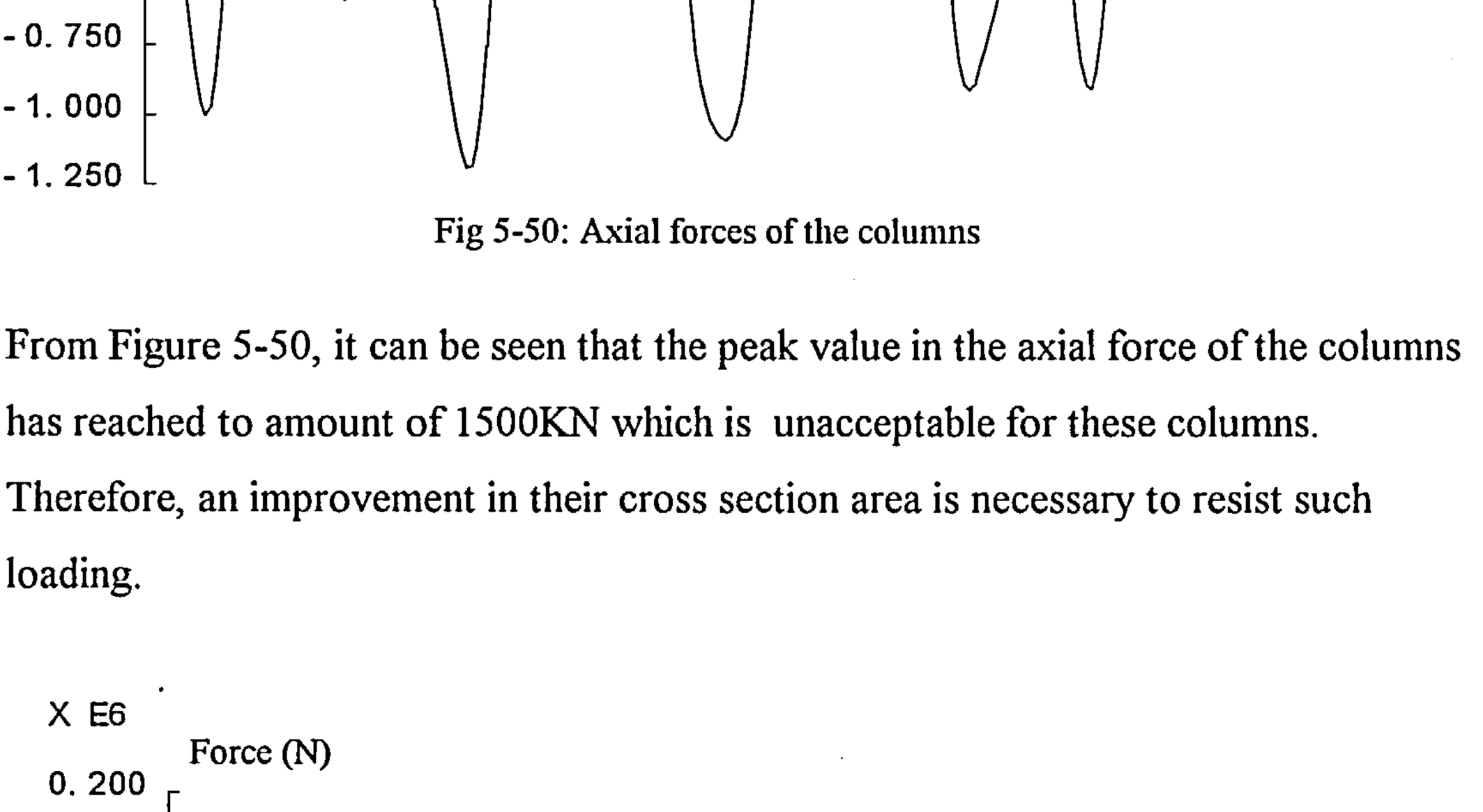

Fig 5-51: Shear forces of the columns

Figure 5-51 is the shear forces in the columns. Despite high increase in the axial load, its shear force has not been changed significantly by removing the energy absorbing device from the frame.

It can be seen from these graphs that when the energy absorbing devices are not used, the acceleration increases by a factor of 3 and the velocities by a factor of 4. For a comparison, the accelerations and velocities of the frame in these two cases, have been illustrated in Fig 5-52 & 53. The axial force also increases by three times but bending moments and shear forces have not changed significantly. The increase in axial force, implies that the frame should be redesigned and the section areas should be increased. This will result in a stiffer frame and consequently, the accelerations and velocities will increase.

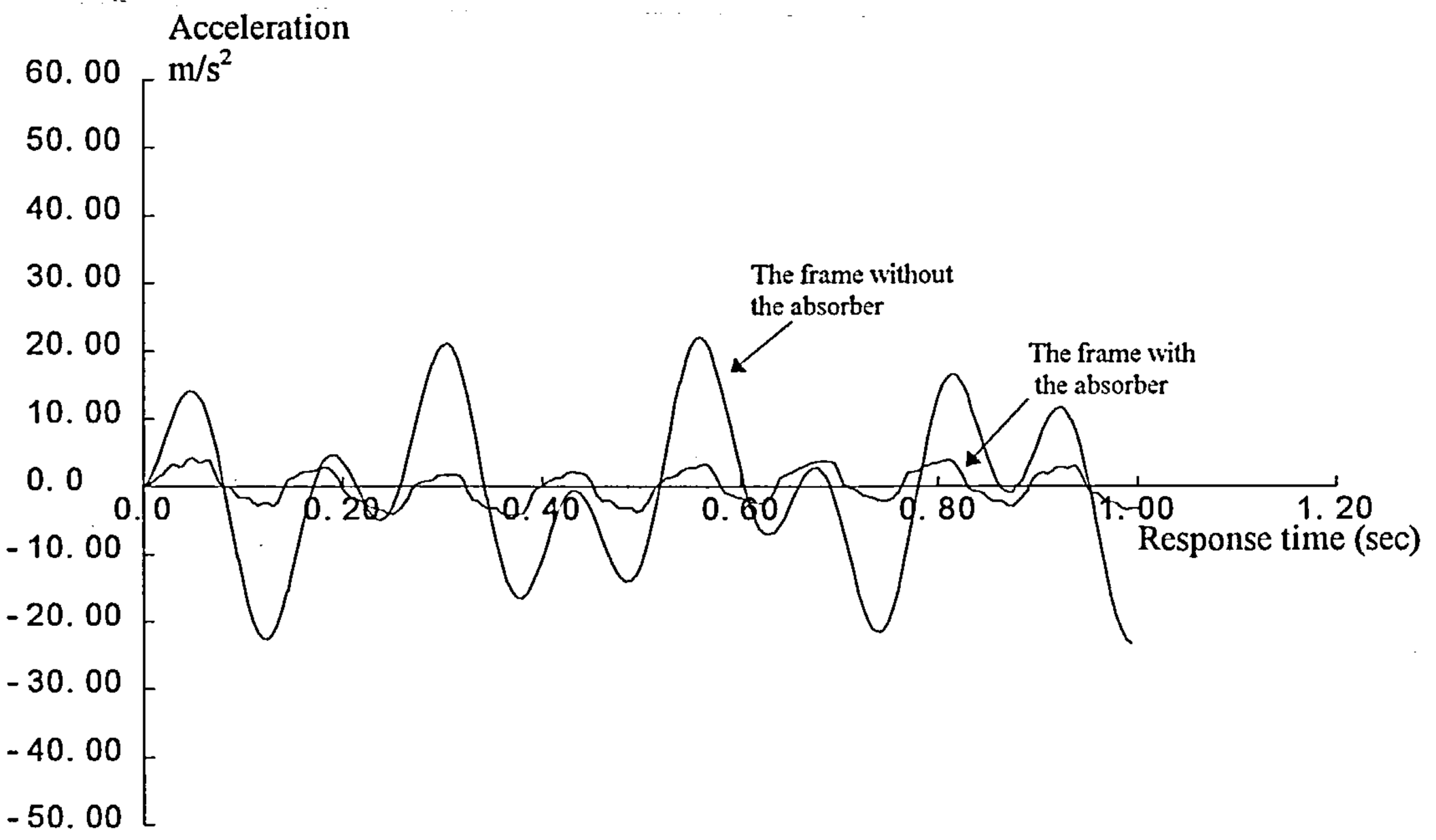

Fig 5-52: Acceleration of the frame with and without the energy absorbing device. The acceleration in the frame with the absorber is three times less than without the absorber

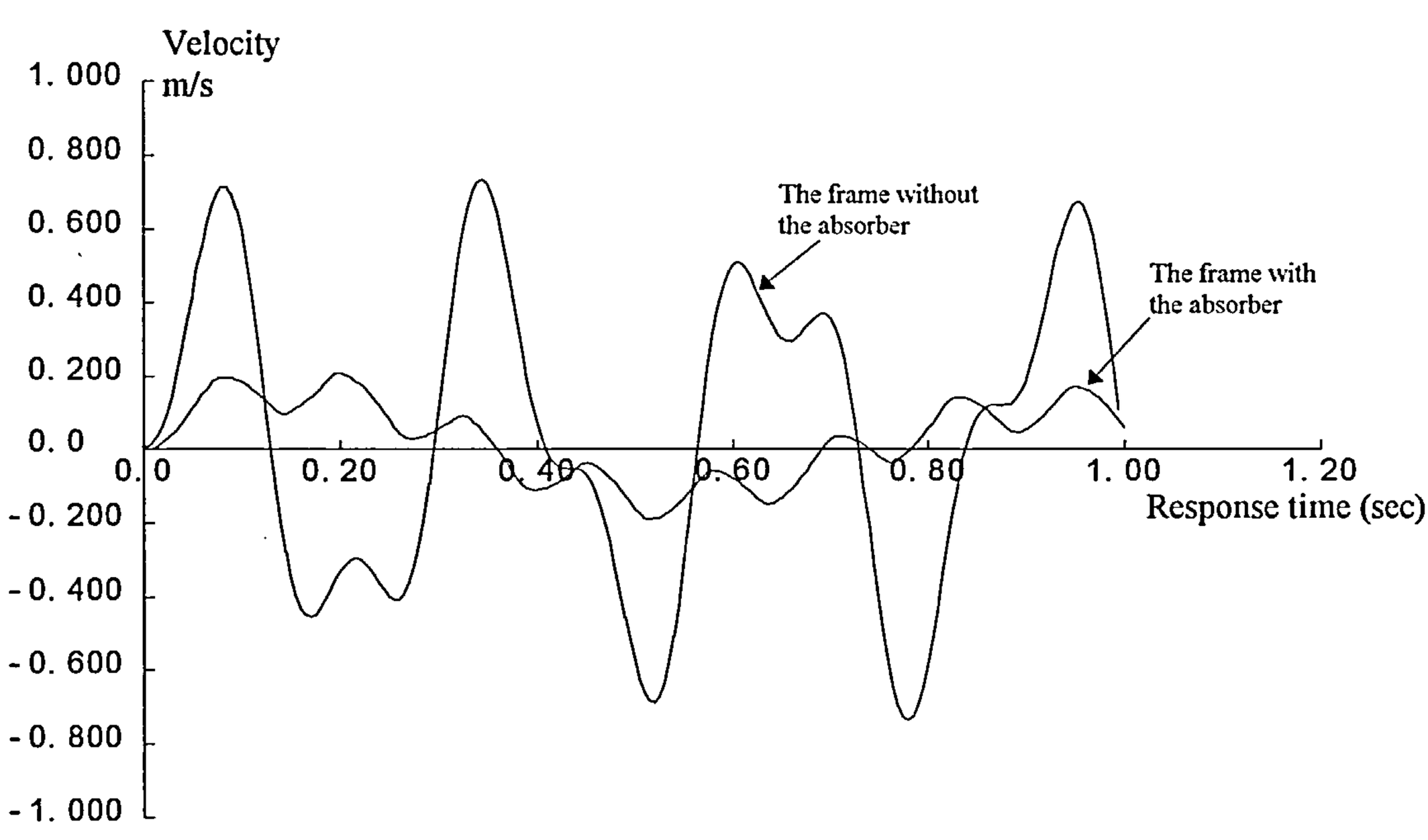

Fig 5-53: Velocity of the frame with and without the energy absorbing device. The velocity in the frame with the absorber is four time less than without the absorber.

5-3-3 Natural frequency analysis

A natural frequency analysis was carried out to find the modes of the frame. For this purpose, an eigenvalue control was assigned to the model. The natural frequencies of the frame were obtained from this analysis and compared with the applied loading frequency.

Control definition:

10 eigenvalues were requested from the analysis in this Eigenvalue control. The number of the starting iteration vectors was left zero in order to force LUSAS to find automatically a suitable amount. Normalisation was unity and a Generalised Jacobi was chosen as the solver. The results are shown in Table 5-8.

Table 5-8

EIGENVALUES FOR THE BRACED FRAME		
MODE	EIGENVALUE	FREQUENCY(HERTZ)
1	475.099	3.46906
2	8578.50	14.7410
3	9050.53	15.1411
4	340479.	92.8678
5	907243	151.594
6	997550.	158.960

From the result of this analysis it can be seen that the applied base acceleration in sections 5-3-1 and 5-3-2 was not coincident with the natural frequencies of the frame. This was important for avoiding a resonance situation in the vibration of the frame.

5-4 Multi-Degree Freedom Structure MDFS

In this section a multi degree freedom structure MDFS will be analysed which includes the energy absorbing device. The structural behaviour will be examined numerically.

5-4 -1 The response of a MDFS including the energy absorbing device

For this example the beams are considered to be rigid and high values have been assigned to the geometric properties of the beams (see the previous example of section 5-3). The section of the diagonal members in the upper storeys will be chosen strong enough to make the behaviour of building similar to a one degree freedom structure for the case of a high rate shock, which causes the absorbers to act. All of the properties of the model are the same as previous model and any change will be noticed. Two energy absorbing devices have been included in the first floor and these have been shown as thick lines in figure 5-54.

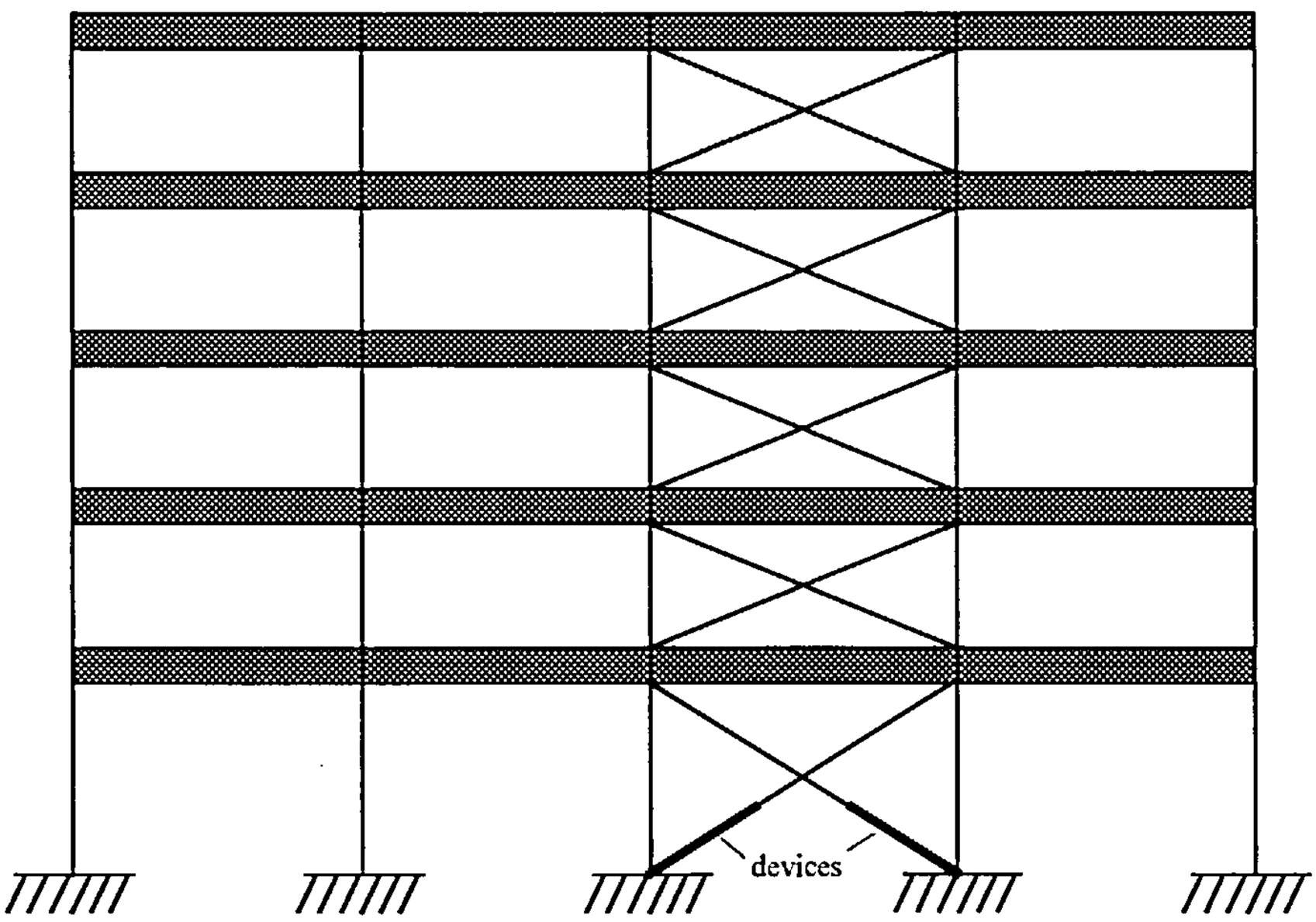

Fig 5-54: Multi- degree freedom structure

Geometric definition: An Area of A=0.005 m^2 was defined and assigned for all of the braces of the upper storeys of this example.

Load curve definition: A cosine load curve similar to the section 5-3 was defined with the frequency of 4 Hertz. This curve was assigned for the loading.

Mesh definition:

The same elements as those used for the SDFS of the previous section (5-3) were used for the finite element representation of this frame. The finite element mesh has been shown in figure (5-55).

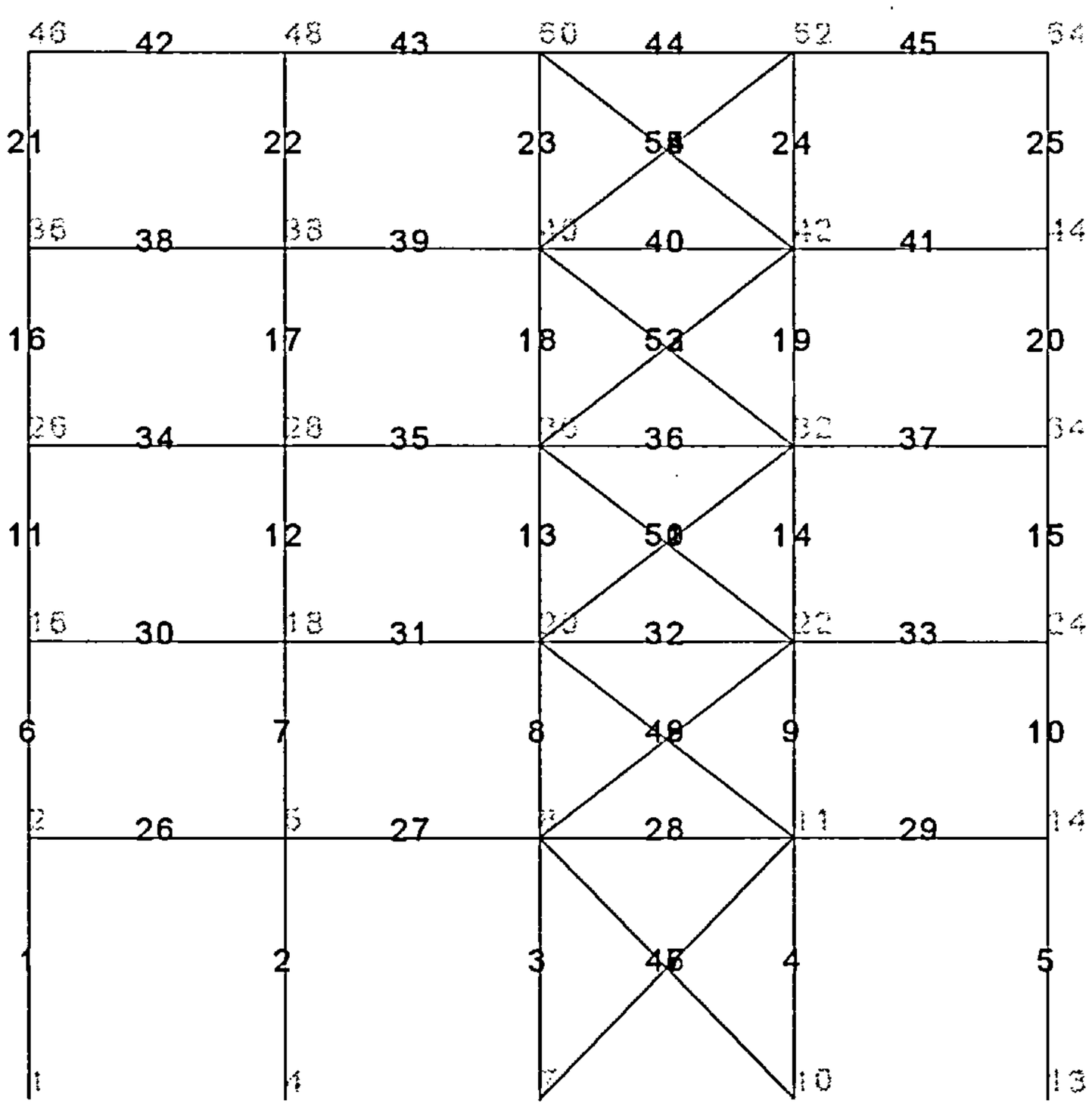

Fig 5-55: The finite element model of the multi degree freedom structure

Results:

In figures 5-56 to 5-58 the accelerations, velocities, displacements in the basement and in the level of the upper storeys are shown. The forces and moments in columns 4, which was the most critical position, have been shown in figures 5-61 to 5-63. In the next section these results will be compared with the case in which no energy absorbing devices were included in the structure.

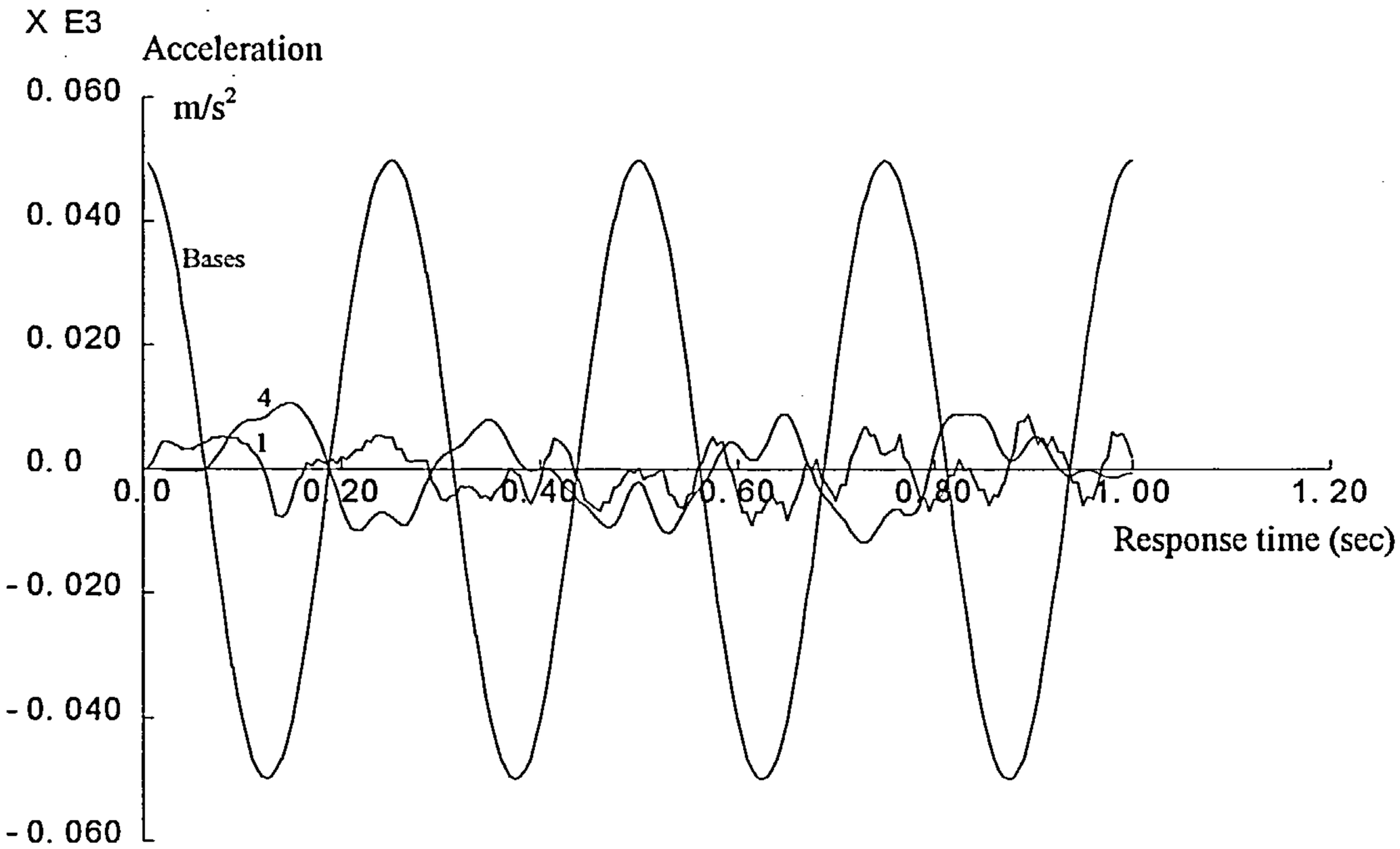

Fig 5-56: Acceleration of the bases, first floor and fourth floor

It is seen from figure 5-56 that the peak acceleration in the first floor is only 10 percent of the basement. The acceleration of the forth floor is also 20 percent the base. This is due to absorption of the energy by the absorbers.

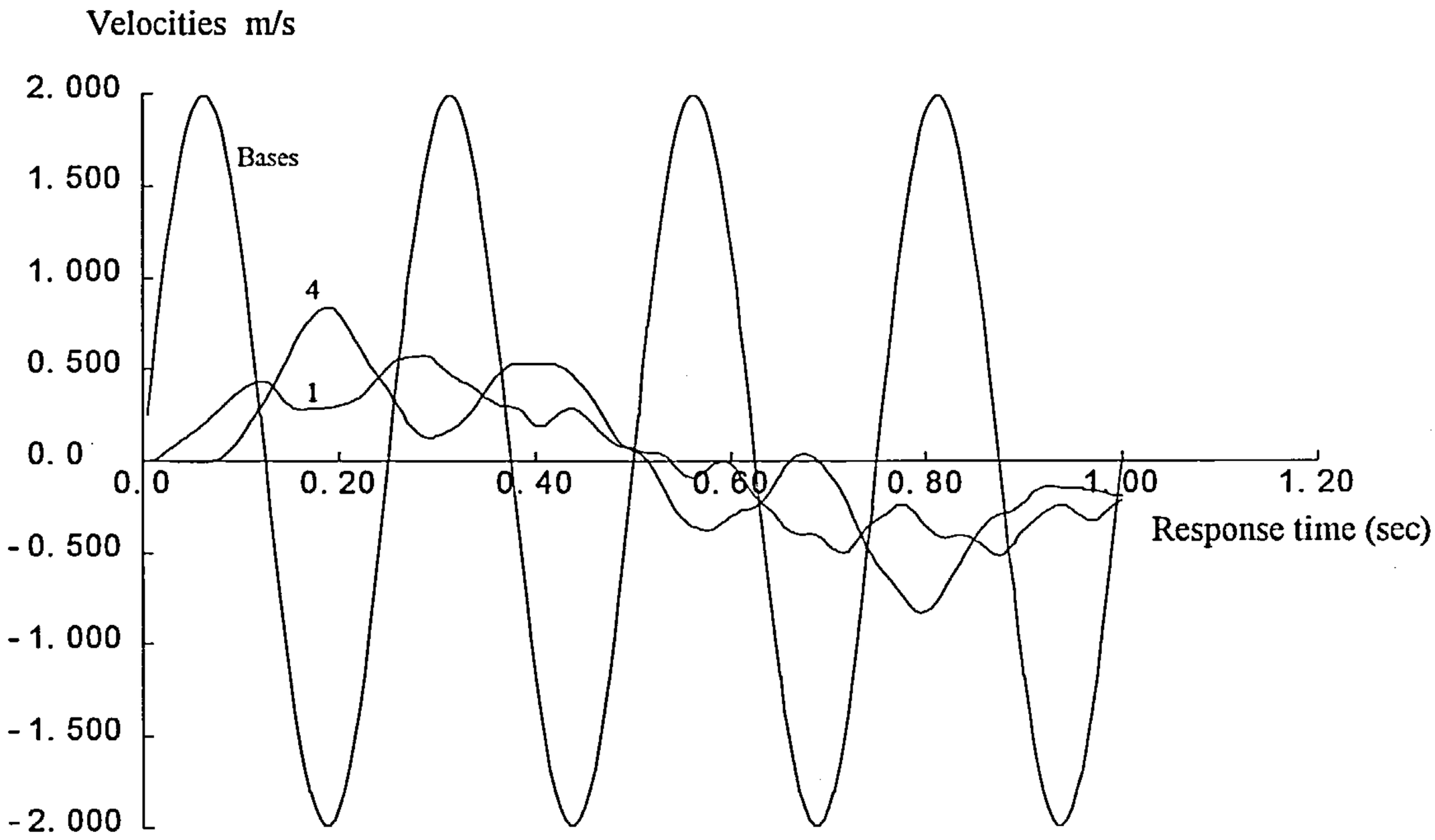

Fig 5-57: Velocities of the basement and floors 1&4

In figure 5-57, the velocities in the floors have been shown. This figure shows that the velocity in the fourth floor is about 40 percent of the base velocities and the velocity at first floor is less than one third of the base velocity.

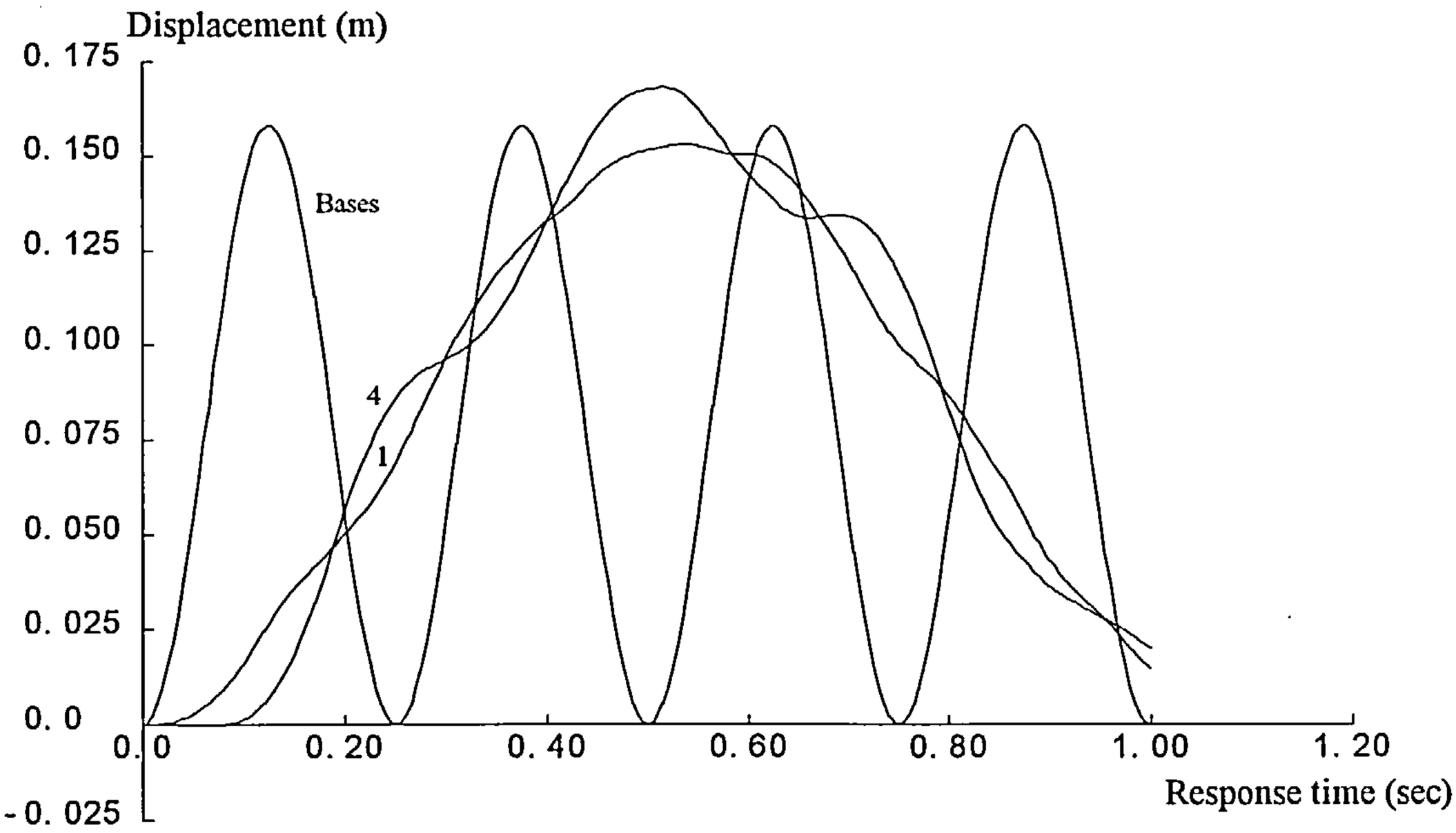

Fig 5-58: Displacement of the basement and floors 1&4

Figure 5-58 shows the displacements of the base, first floor and the fourth floor.
It can be seen from this figure that the behaviour of this building under such high rate excitation is very similar to that of the single degree freedom structure. The floors in this loading have almost the same displacements.

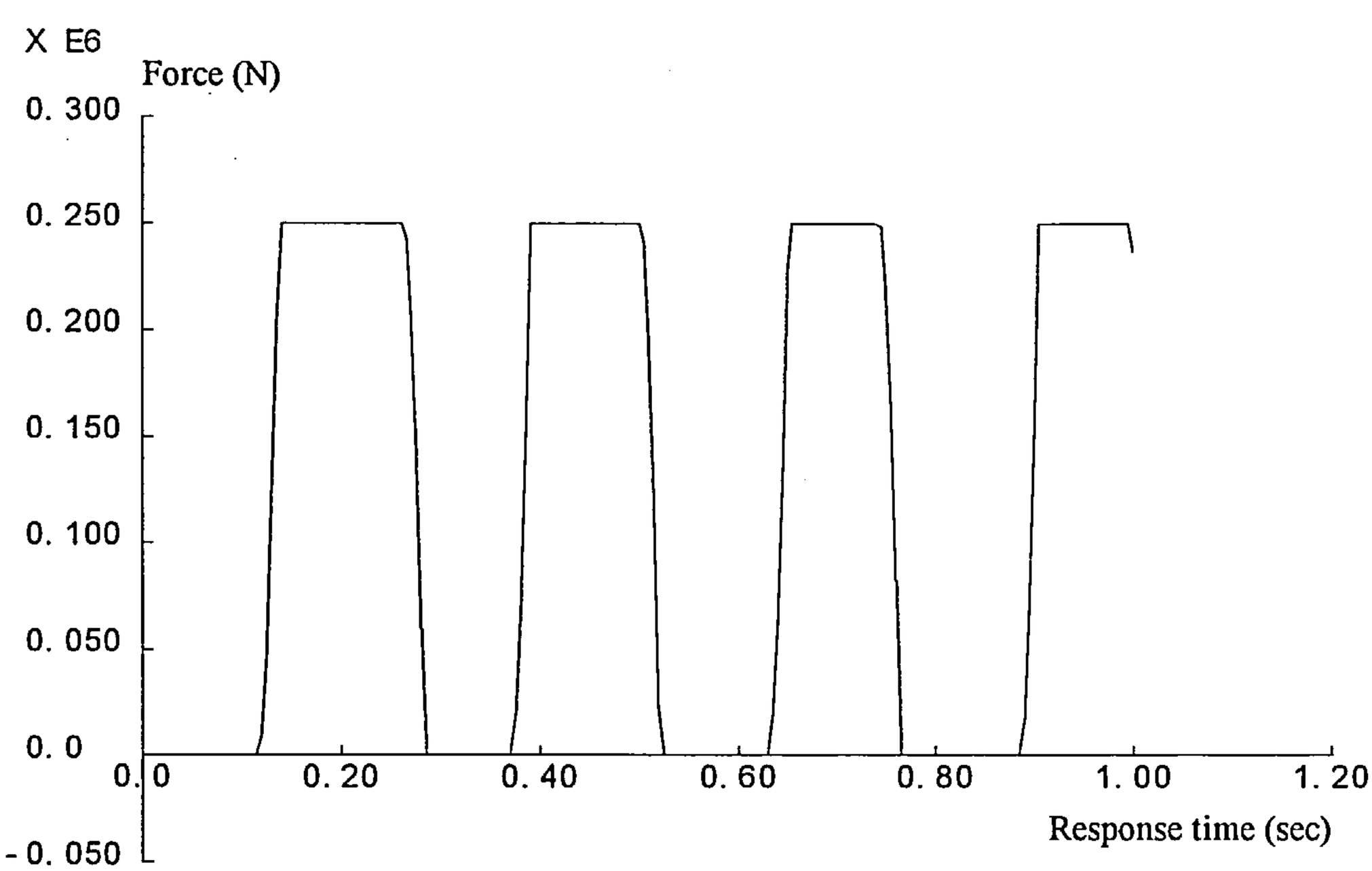

Fig 5-59: Forces in the braces in the basement (absorbers)

Figure 5-59 shows the forces in the absorbers. The loads in the devices have been limited to 250 KN. They are working in plastic range under this loading in the most of response time.

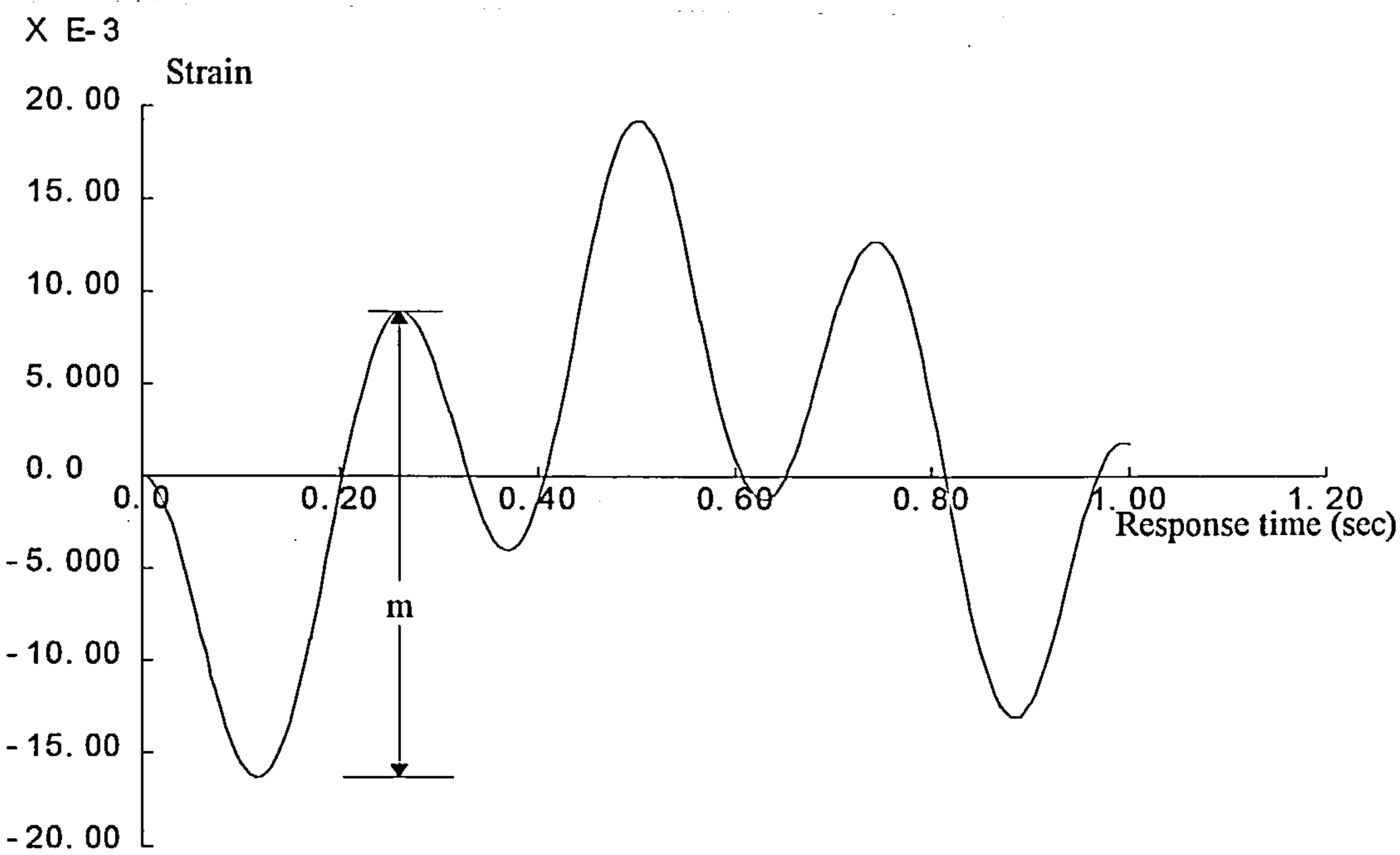

Fig 5-60: Strains in the braces in the basement (absorbers)

Figure 5-60 is the strain in the braces and can be used for calculation of the absorbed energy. If a total strain of 0.2 (200000 micro strain) is accepted for the braces of the basement (as was discussed in section 5-4-1), then it can be concluded that the frame can tolerate such excitement for almost 3 second, before the energy absorbing capacity the devices ends. As was mentioned in the previous section, this time can be increased by increasing the length of the device (in fact by increasing its absorbing capacity).

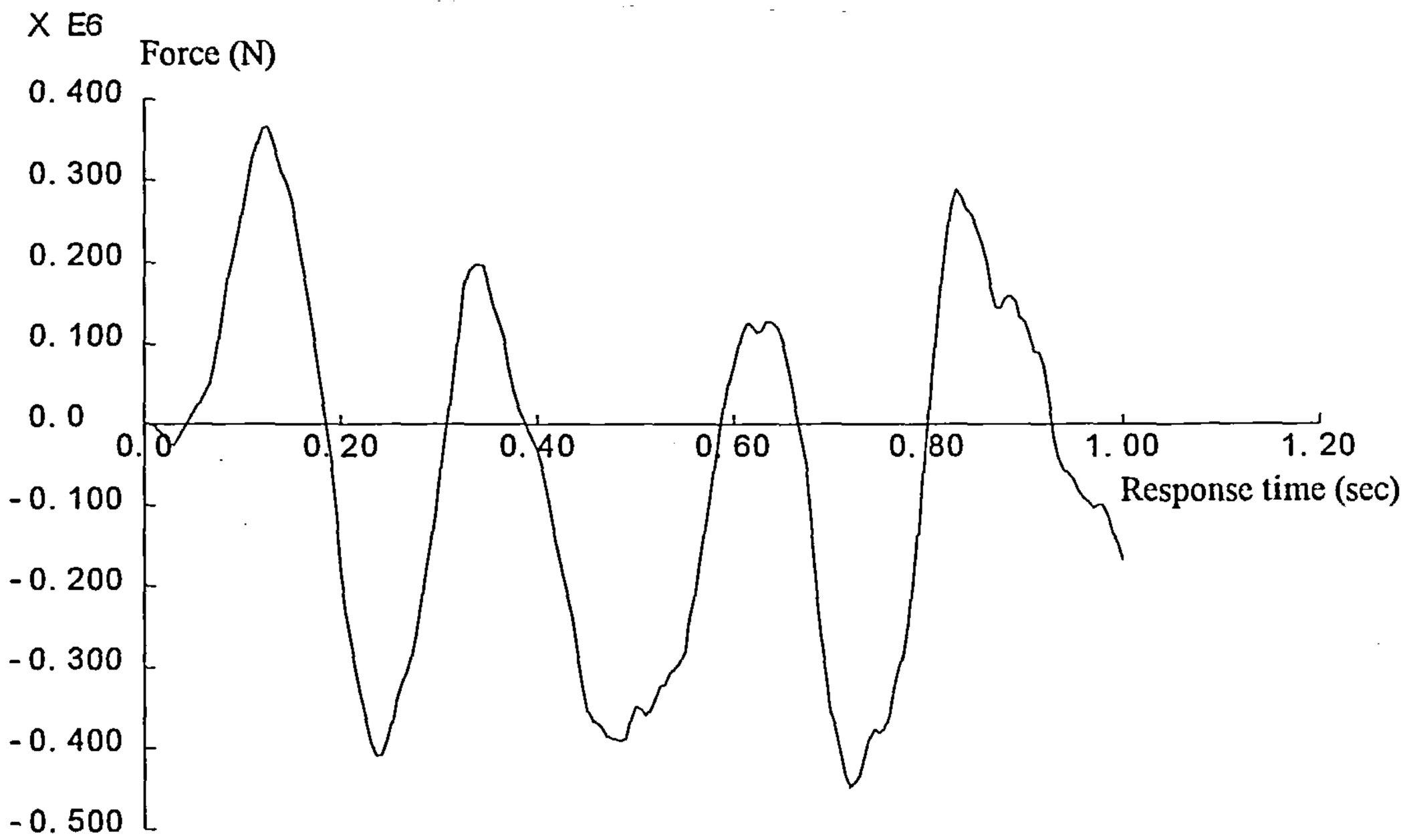

Fig 5-61: Axial force of the column 4

In Figure 5-61, the peak axial load is 400KN for the column 4, which is quite acceptable value for it. The shear force in the columns has been shown in Figure 5-62. Maximum shear forces in the columns are 220KN.

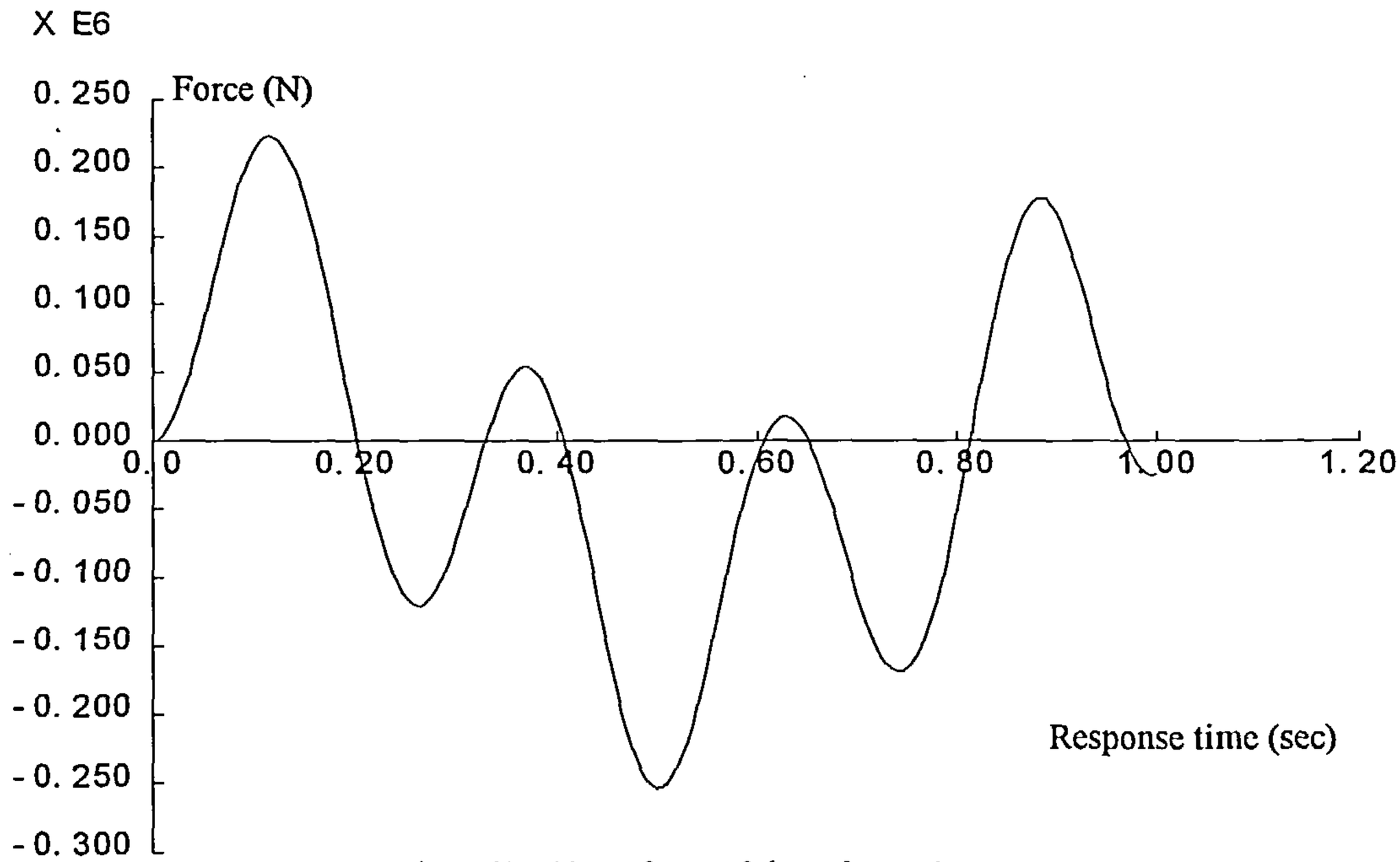

Fig 5-62: Shear force of the column 4

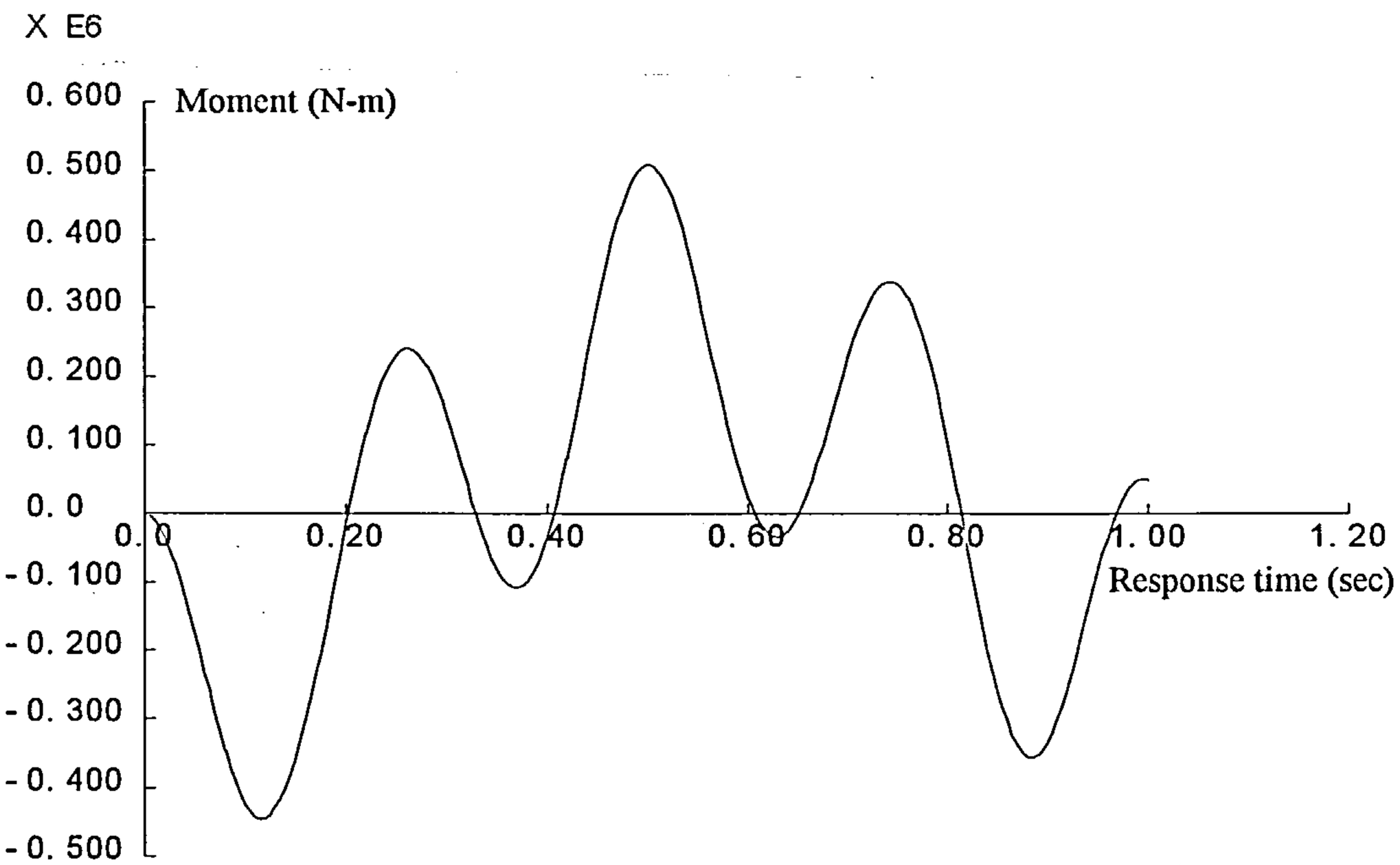

Fig 5-63: Moment Mz of the columns

Despite the high rate acceleration, which has been applied to the frame, it is seen from figure 5-61 to 5-63 that the forces and moments are still in the acceptable ranges. This is due to absorption of the energy by this novel energy absorbing device.

In the next section, the analysis of this frame will be carried out while the absorbers have been replaced by ordinary structural members. Their comparison will show the advantages of inclusion of the absorbers in structures.

5-4-2 The response of MDFS without the energy absorbing devices

The frame has been analysed without the energy absorbing devices and the result will be reported in this section. The same configuration and loading of the previous section (5-4-1) has been used for the frame, except that ordinary structural components were used instead of the energy absorbing devices.

Results:

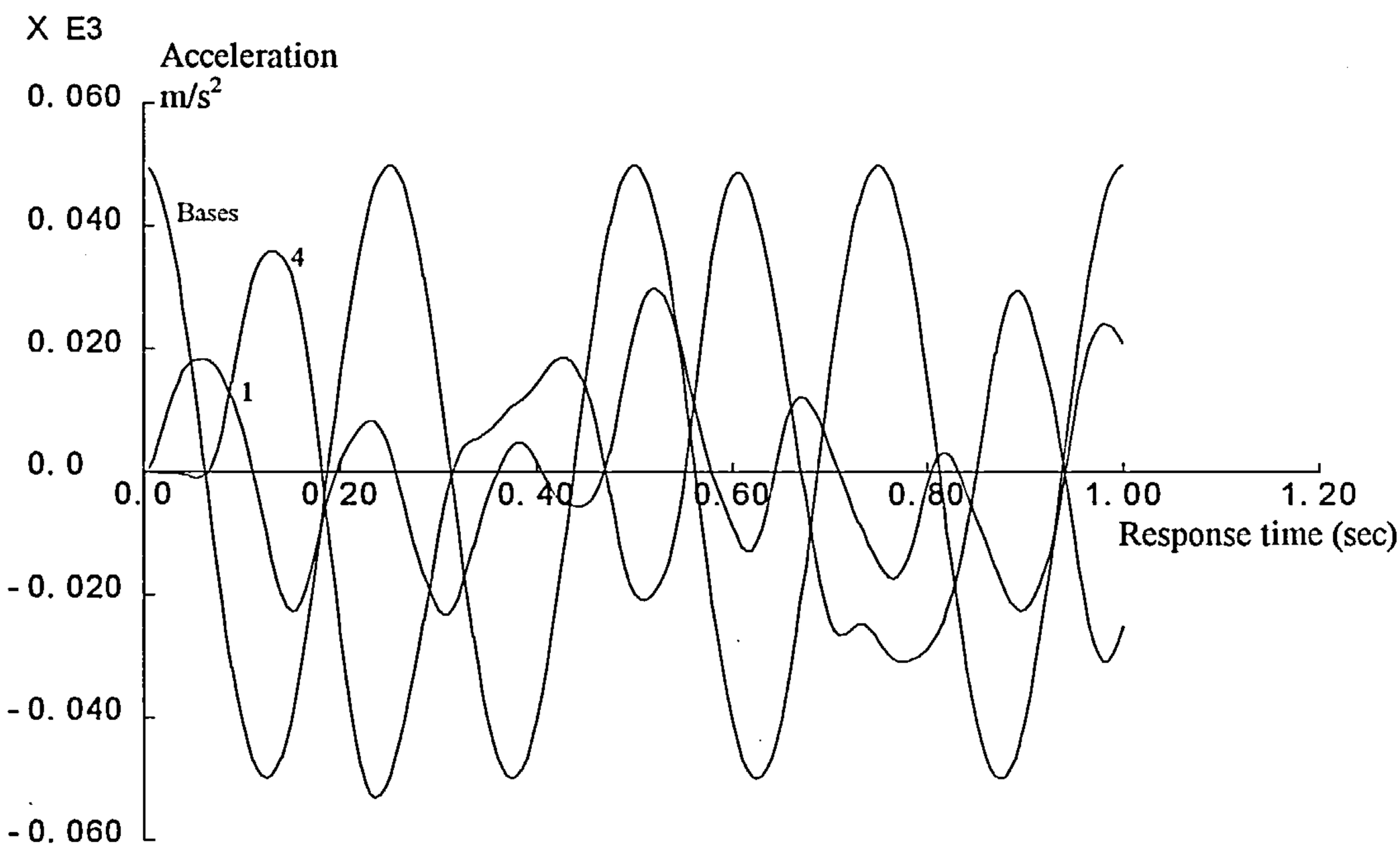

Fig 5-64: Acceleration of the basement and floors 1 &4

It is seen from Figure 5-64 that the acceleration in the top floor is of the same order as the basement acceleration and almost 5 times that of the result of the previous analysis which included the absorbers.

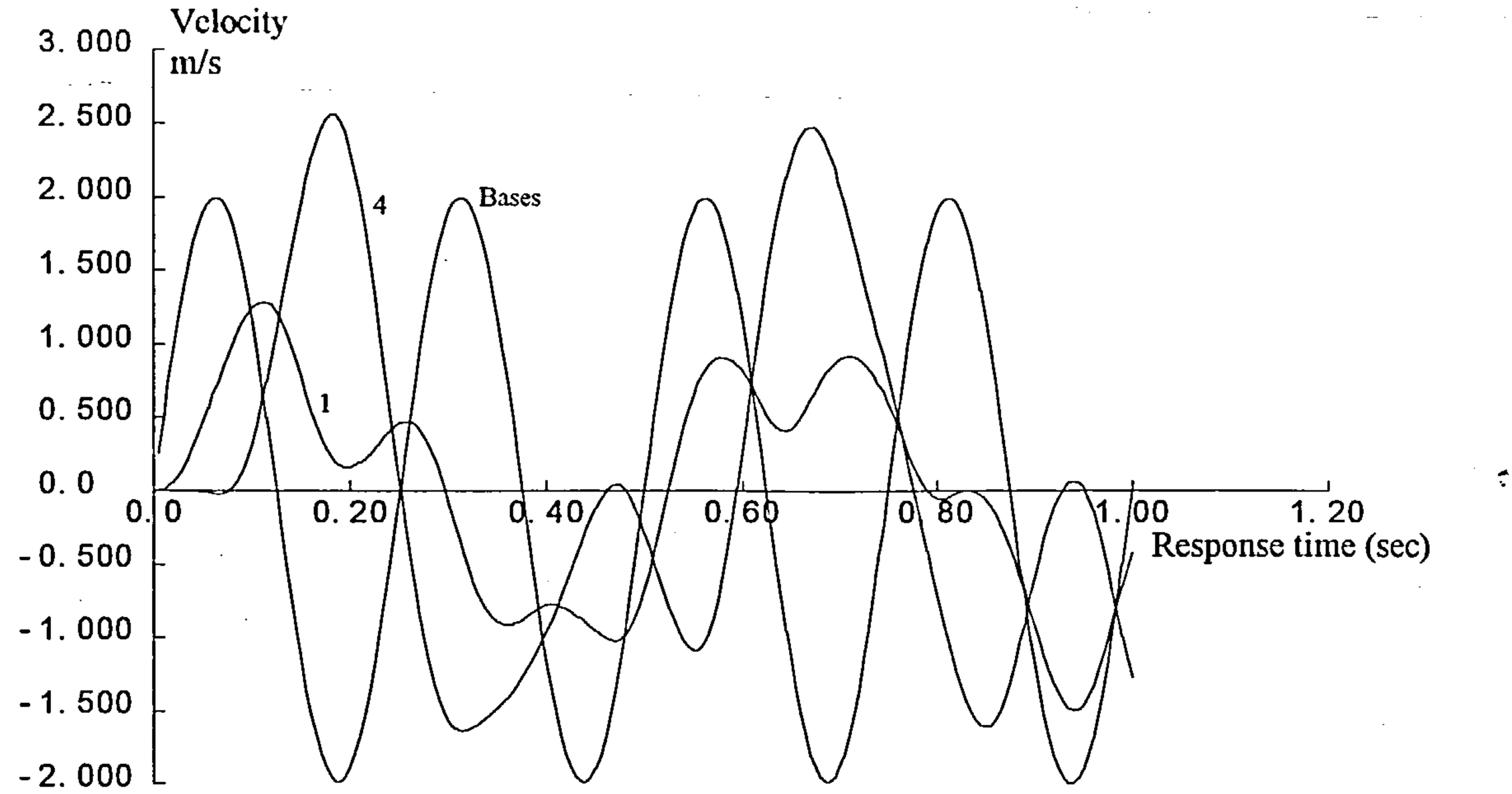

Fig 5-65: Velocities of the basement and floors 1&4

Figure 5-65 shows the velocities in the frame without the inclusion of the energy absorbing device. The velocity has been increased by a factor of three and is equal to the basement velocity.

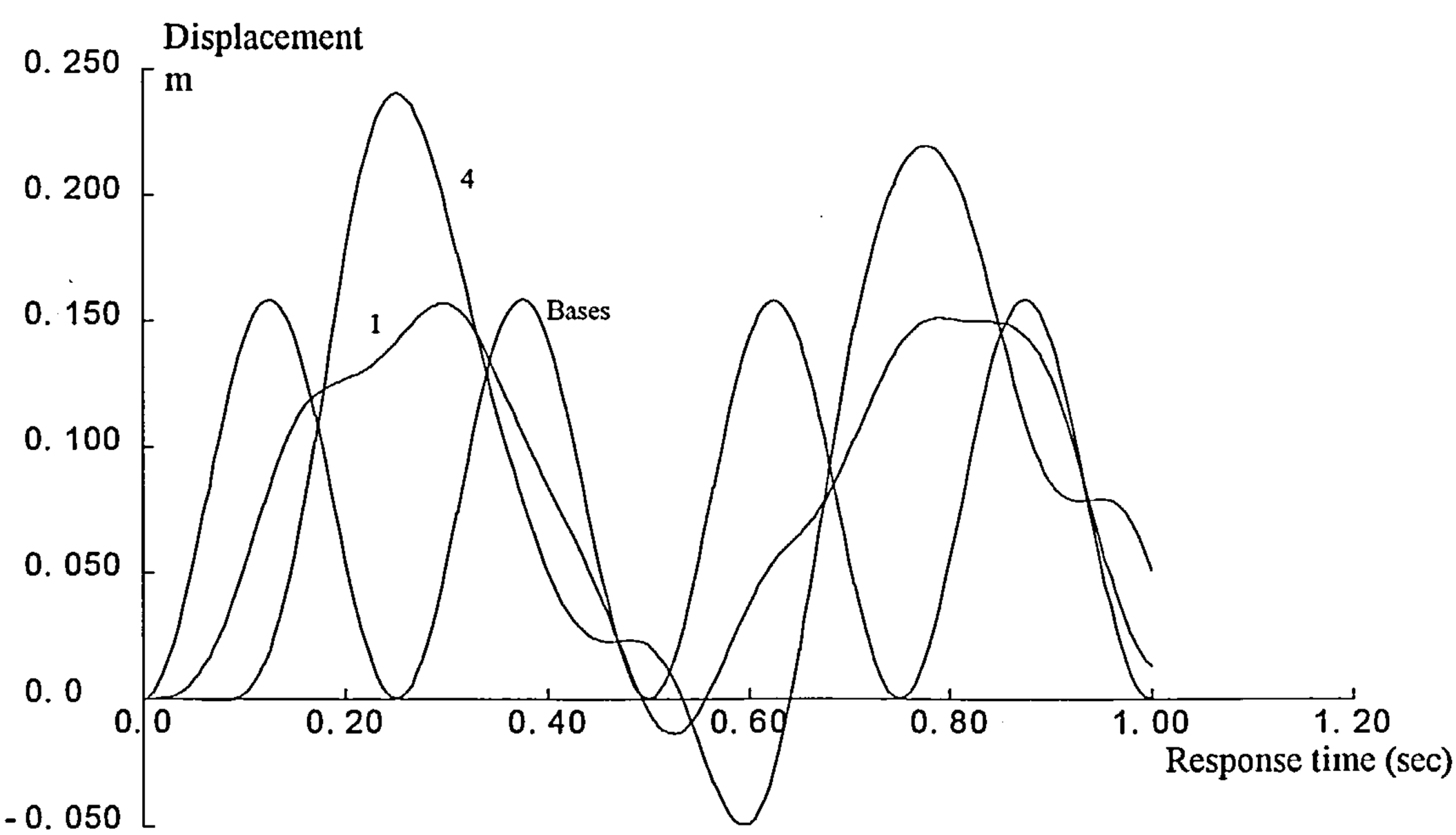

Fig 5-66: Displacement of the basement and upper floors

From Figure 5-66 it can be seen that the response of the building is not similar to that of single degree freedom any more. There is a significant difference between the displacement of the first and fourth floors.

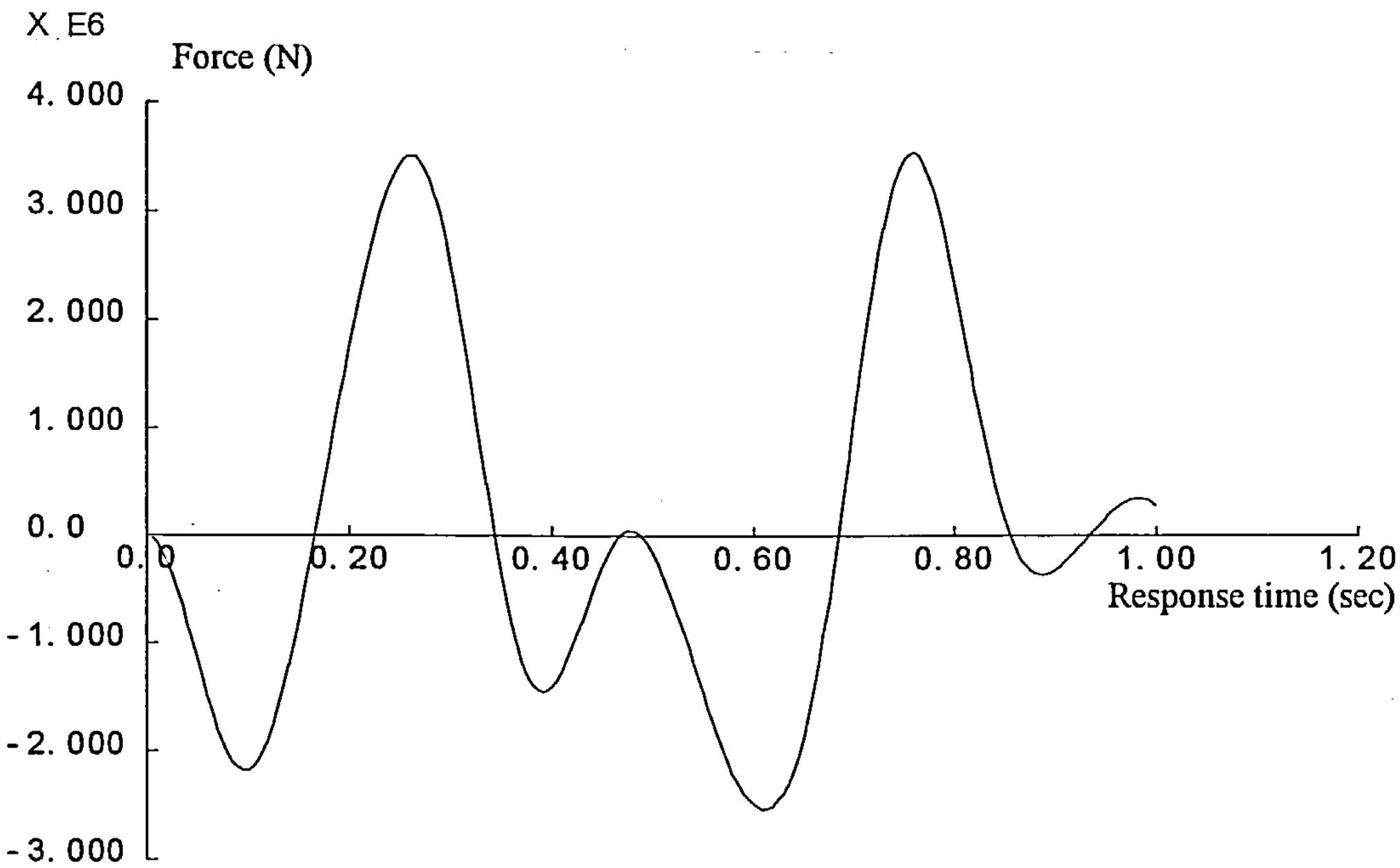

Fig 5-67: Forces in the braces of the basement

Figure 5-67 shows that there is a significant increase in the maximum load of the braces. It has been raised to 4000KN while was only 250KN for the frame with the energy absorbing devices.

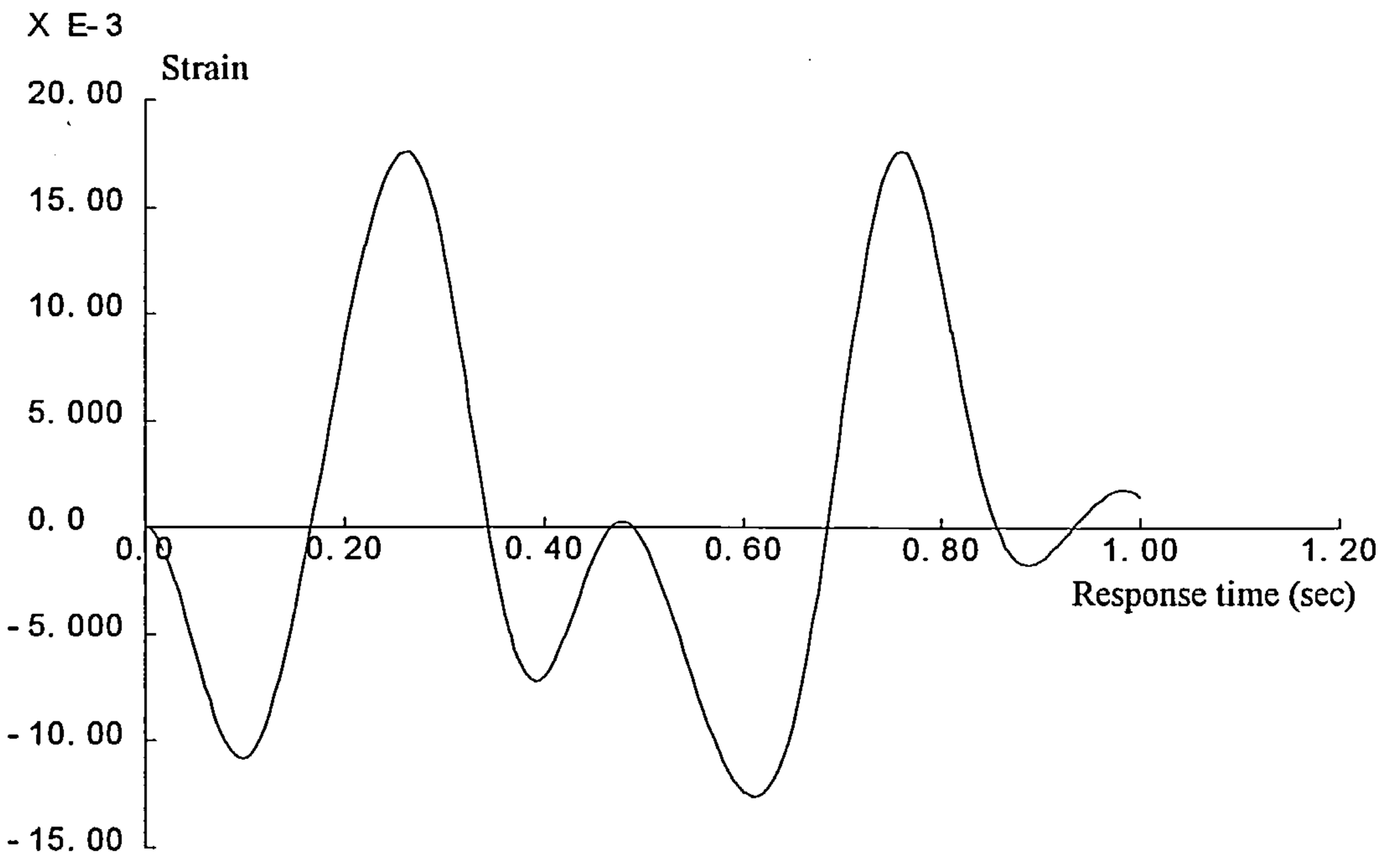

Fig 5-68: Strains in the braces of the basement

It is noticeable in Figures 5-67 and 5-68 that the loads in the braces have reached a large magnitude. A redefinition of the cross section areas of these members will be necessary.

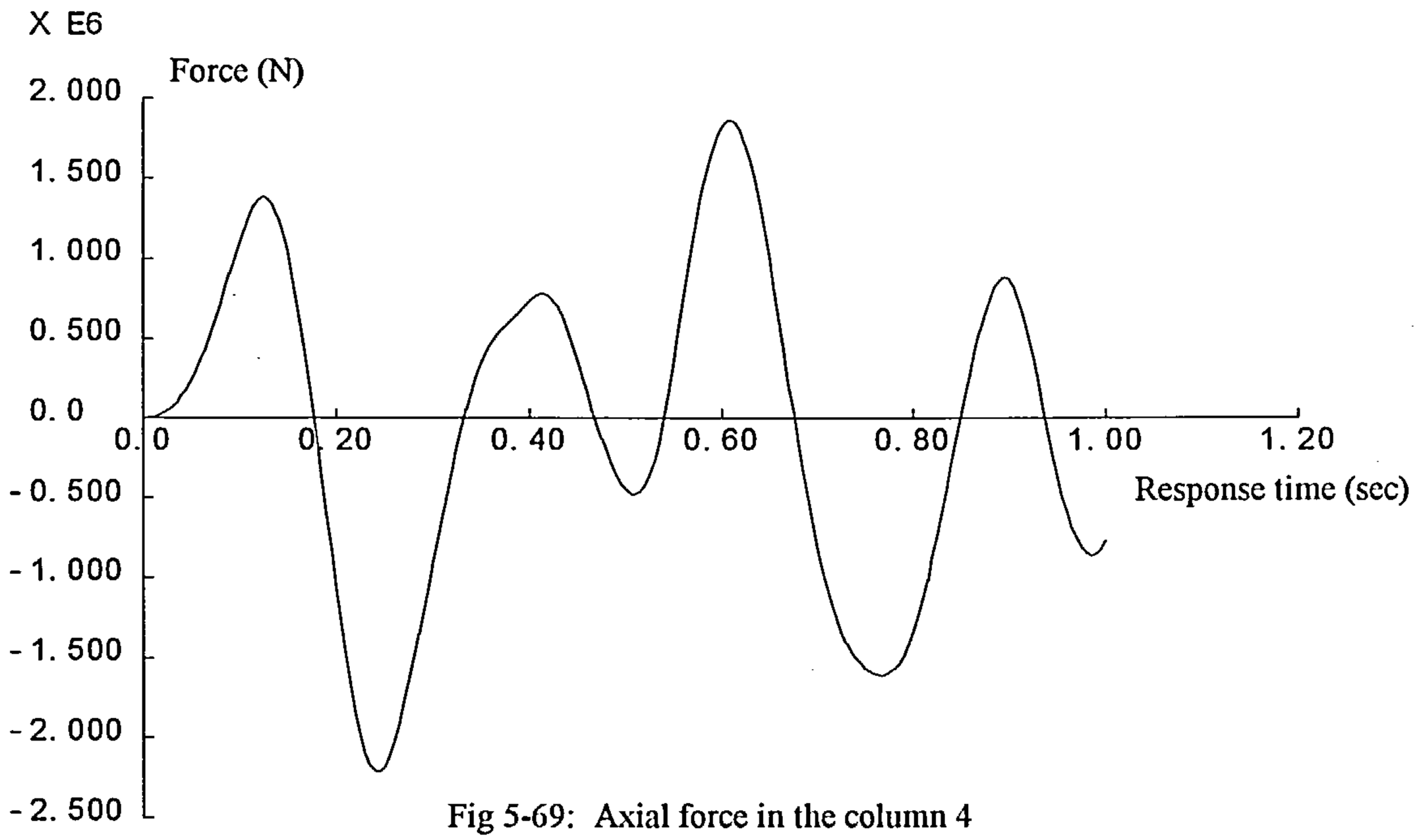

Fig 5-69: Axial force in the column 4

Figure 5-69 shows the axial force in column 4. The maximum load in this column has been increased to 2200KN whilst was only 400KN for the frame with the absorber.

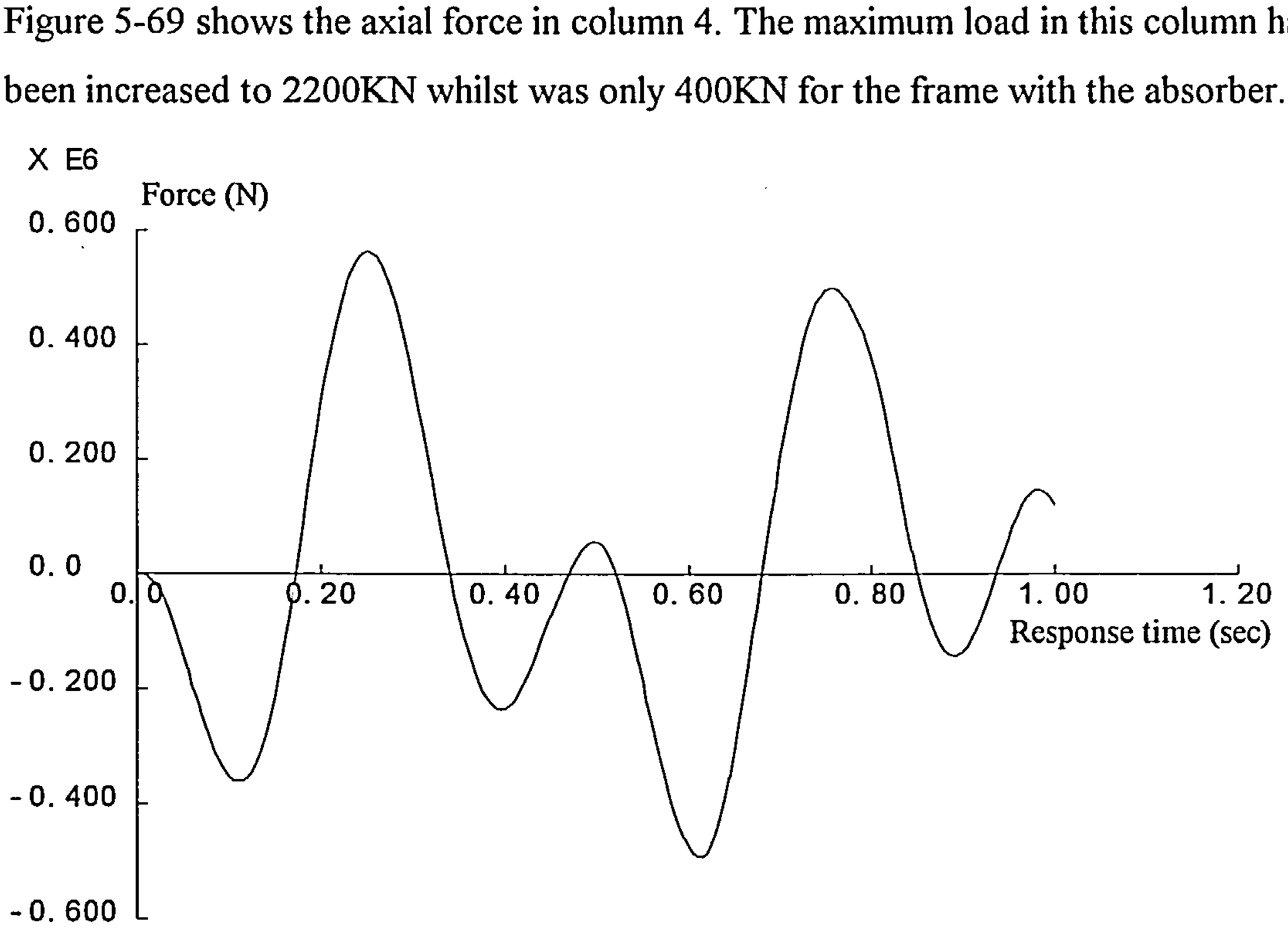

Fig 5-70: Shear force in the column 4

Maximum shear forces in figure 5-70, in column 4, is 600KN which is almost twice of the previous configuration of the frame which included the energy absorbing devices.

Figure 5-71 shows the variation of bending moment in the column 4 with time. The peak value in this graph is 500KN-m which was 280KN-m in the frame with the energy absorber.

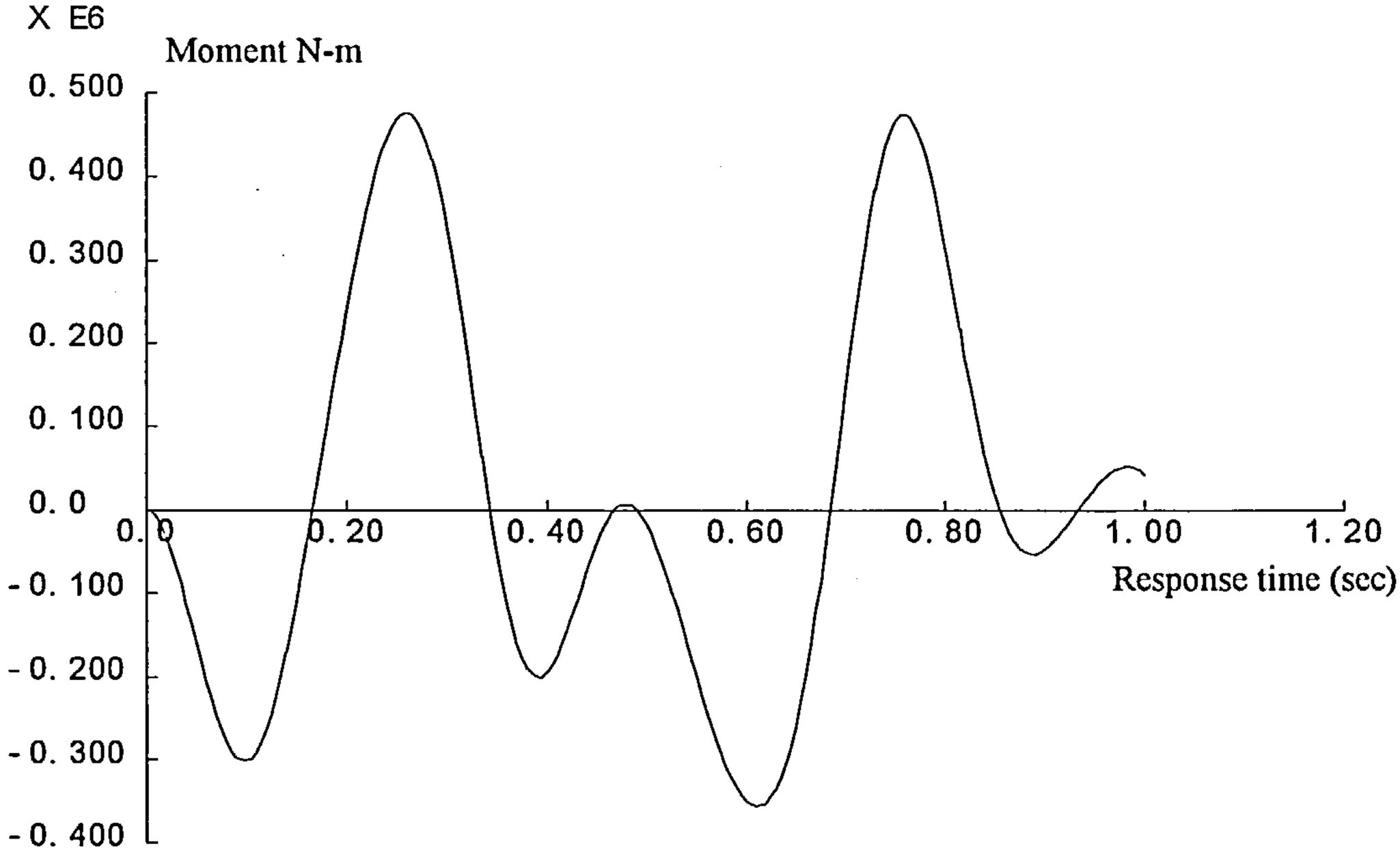

Fig 5-71: Moment Mz in the column 4

From these results the accelerations and velocities of the top floors have been increased. For a comparison, the accelerations and velocities of the frame in these two conditions have been illustrated in the Figures5-72 and 5-73. It is also obvious that the columns or beams cannot sustain such loads for the case of no absorber. Therefore, a subsequent increase in the sections will be inevitable. This will result in a further increase in the accelerations and velocities.

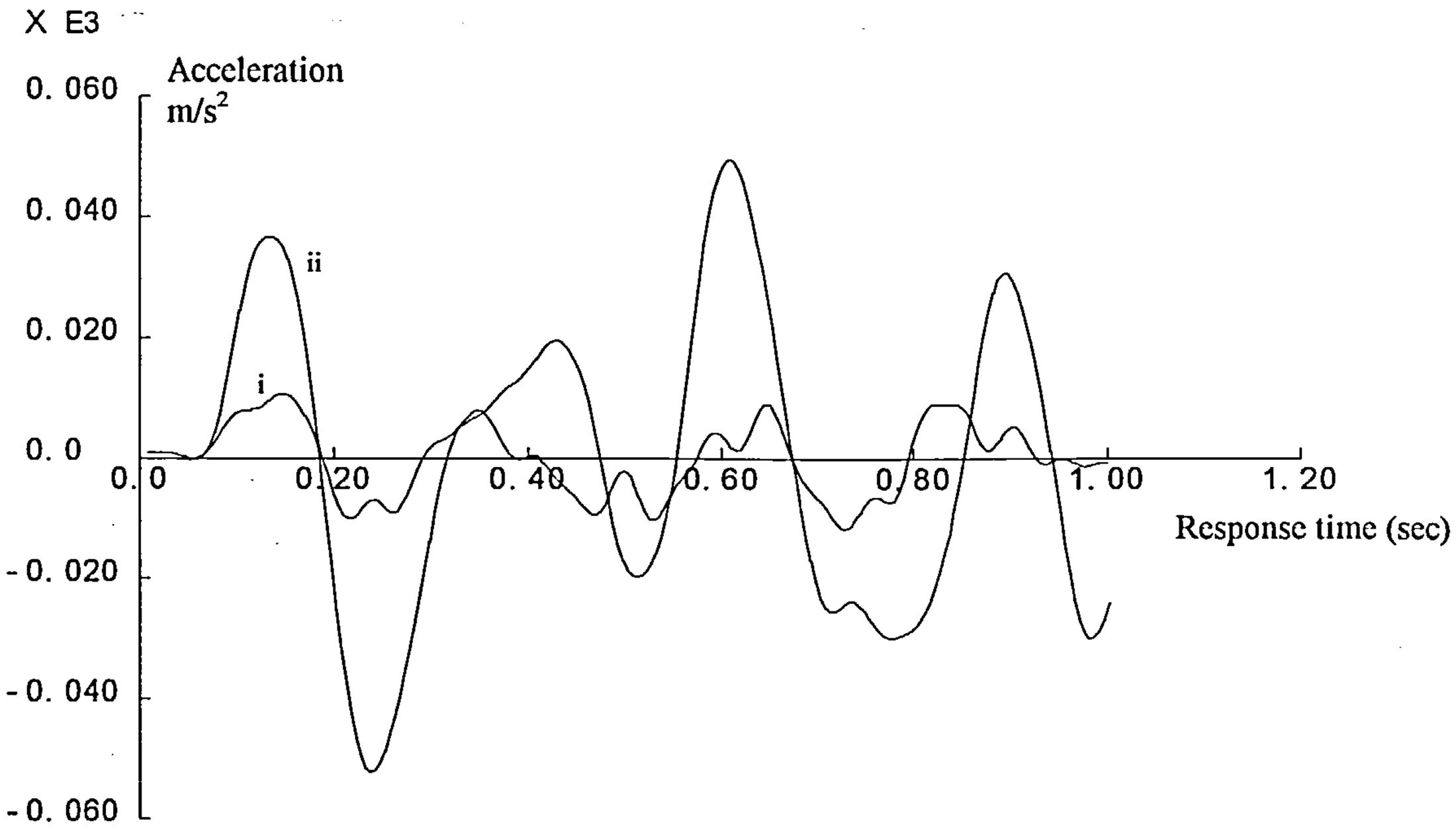

Fig 5-72: The acceleration of the fourth floor when the frame is
i) equipped with the energy absorbing device and
ii) without the energy absorber

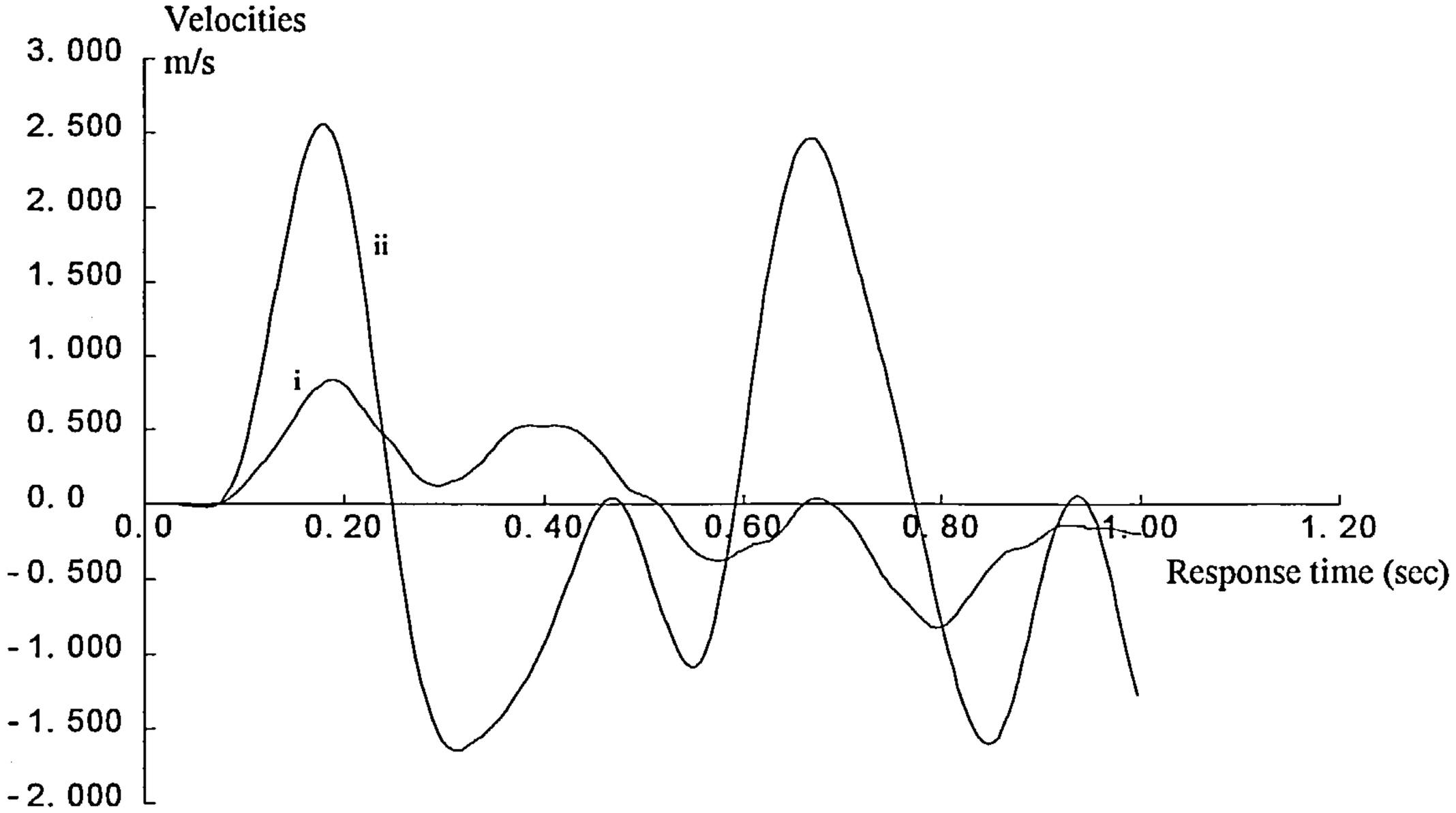

Fig 5-73: The velocity of fourth floor of the building when the frame is
i) equipped with the energy absorbing device and
ii) without the energy absorber

5-4-3 Natural frequency analysis:

An eigenvalue analysis has been carried out to find the natural frequencies and their modes. This ensured that the applied loading acceleration in the analysis of this framework was away from the natural frequencies of the frame and there was no resonance phenomenon in the vibrations. This analysis is the same as the natural frequency analysis of the SDFS with the same control definitions. Therefore, only the results are reported in table 5-9.

Results:

Table 5-9

EIGENVALUES FOR THE BRACED FRAME		
MODE	EIGENVALUE	FREQUENCY(HERTZ)
1	137.39	1.86551
2	1742.41	6.64348
3	3838.61	9.86068
4	6521.77	12.8530
5	8093.54	14.3182
6	14528.3	19.1835
7	20104.4	22.5666
8	32789.3	28.8195
9	44741.9	33.6649
10	81617.2	45.4685

From the result of this analysis it is seen that the applied base acceleration in sections 5-4-1 and 5-4-2 is not coincident with the natural frequencies of the frame.
This was important for an acceptable comparison between the results of these two analyses.
The first five modes have been shown in the figures 5-74 to 5-78.

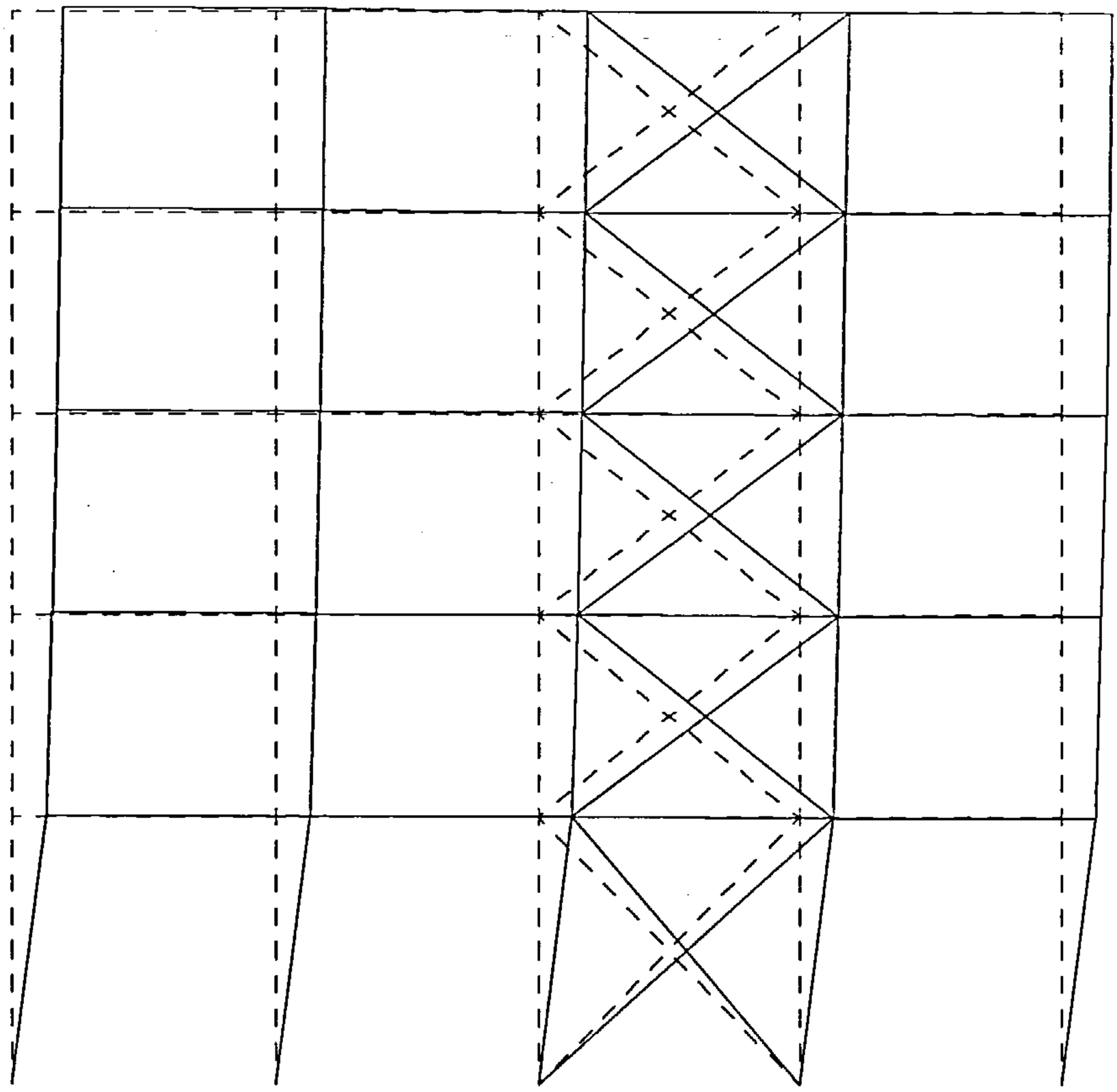

Fig 5-74: The first mode of the frame

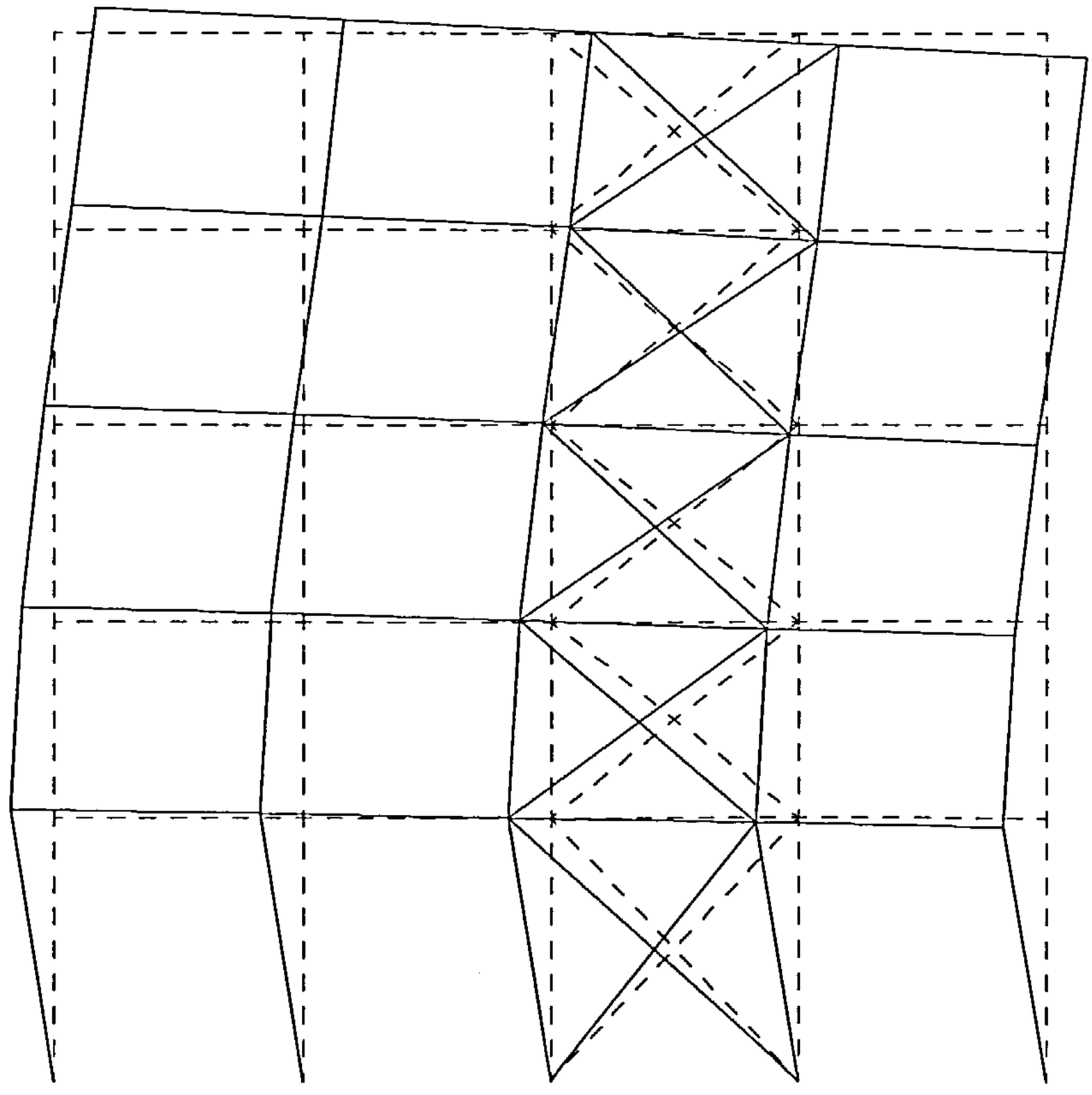

Fig 5-75: The second mode

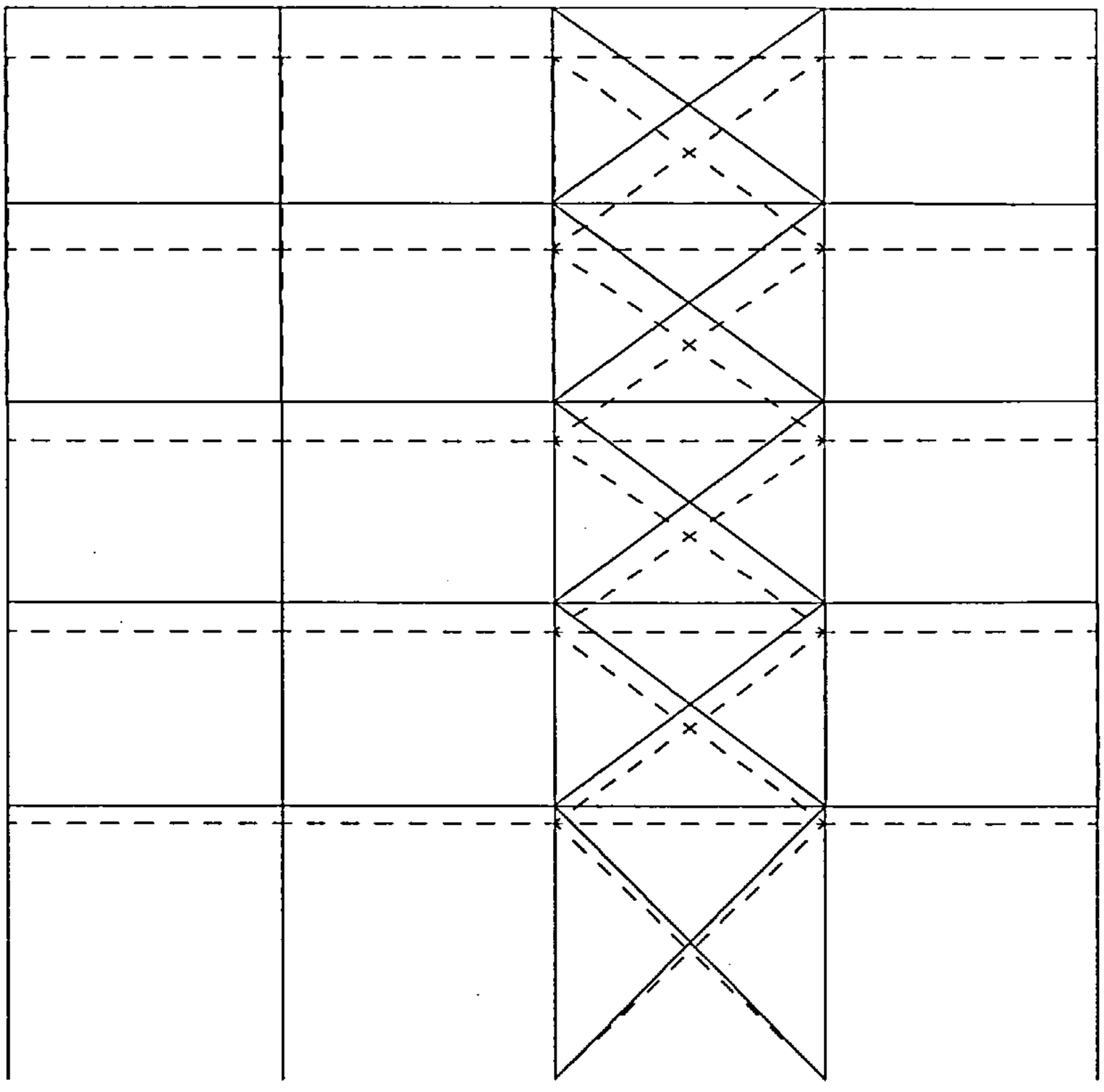

Fig 5-76: The third mode

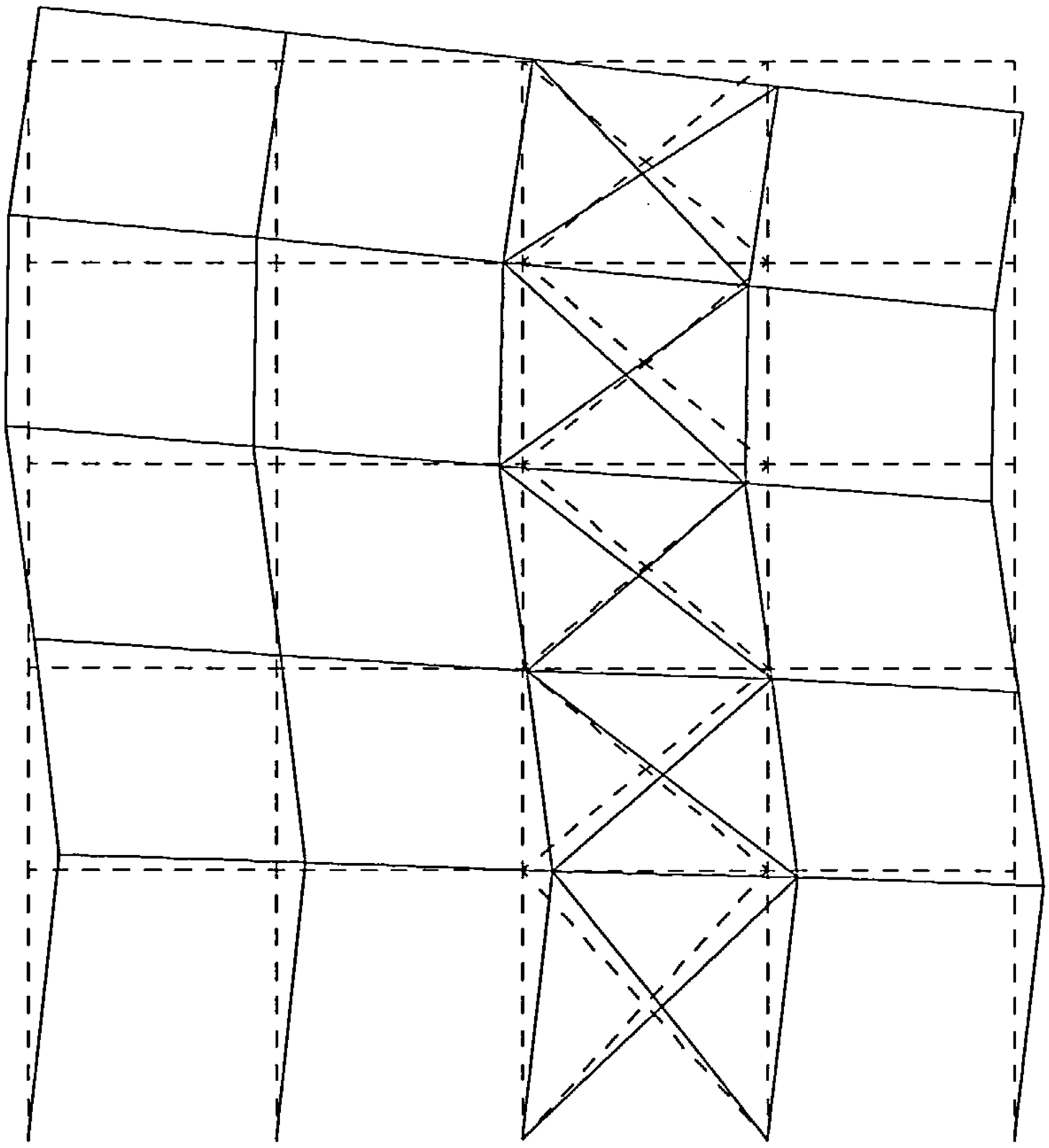

Fig 5-77: The fourth mode

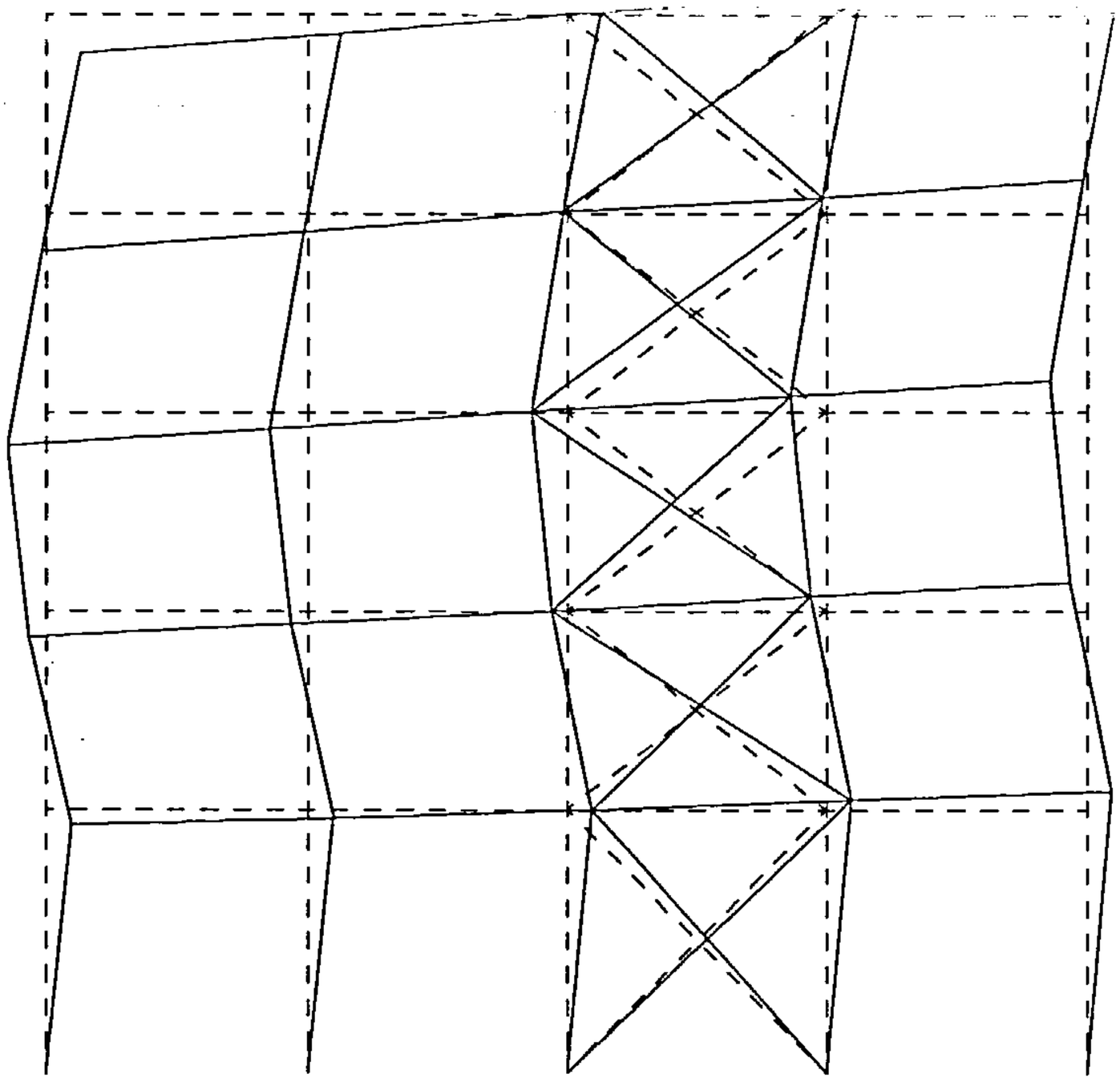

Fig 5-78: The fifth mode

In this chapter the application of the device inside in structures was investigated.

In all these examples, it was noticed that a huge reduction in the acceleration and the velocities are achieved when the absorbers are included in the structure. The reduction in the forces of the columns and braces is another outcome of this arrangement.

Chapter Six: General Conclusions

6-1 Summary of Work

Energy absorbing devices, were considered as matter of research in this thesis. The available devices were briefly explained and it was noticed that all of them suffer from some disadvantages which can not be used as structural members and high capacity energy absorbing devices simultaneously.

This restriction caused to look for a new energy absorbing device with the properties which are proper for being a load carrying member. For this reason the peeling and inverting of a tube were used as energy absorbing phenomena and a new energy absorbing device was created in the framework of this thesis.

It was noticed that this device has predominant advantages in comparison to the other devices. It is based on peeling and inverting of a tube and has more energy absorbing capacity than pure tube inverting devices. A high and adjustable yield limit is also a important character for this energy absorbing device.

By application of a special mechanism in this device, the device was able to shorten under compressive forces. This is a unique property for the device and makes it able to compensate its lengthening during the absorbing process. It was observed that by this mean the braces of a frame, which have been equipped with this energy absorbing device, will get taut again after experiencing a high tensile load and become ready for absorbing further energy in the next cycles.

It was also noticed that the device has uniform rectangular response for the applied tensile load until the end of its absorbing capacity. After this final point the device works like an ordinary structural bar.

The device was designed properly to change easily the absorbing set and therefore to recharge the device.

The work, which has been explained in the thesis for the design of this novel energy absorbing device, has involved the following developments:

1) -Introducing the technical details of the device.
2) -Creating numerical models for its design.

3) -Assessing numerically the behaviour of several kinds of structures when they are equipped with this new energy absorbing device.

As well as performing analytical computation for the analysis of the behaviour of the device, numerical modelling was also carried out in each stage. The necessary models were created and Lusas Finite Element programming was chosen as solver of these finite element models. It was also noticed that in some cases, this software suffered from some disadvantages. For improving this defect, some additional models were created. The shell part of the peeling device was the important part in the behaviour of the device. Therefore, the computation of the device was started by numerical modelling of this shell and proper forms were suggested for it. In this regard it was noticed that connection part 1 plays an important role for load deflection curve of the shell and it was explained that how it affects the response of the device.

Behaviour of the connection set was investigated exclusively in a separate section of this thesis. The numerical and analytical methods for its analysing and designing was reported. In this regard two numerical models was created, the first one was a two dimensional plane stress model and the second one was a three dimension model. It was explained that because very short steps should be taken in the analysis, at first a two dimensional analysing is carried out to find a pre-design data, and then the final details could be obtained from three dimensional analysing.

The response of structures, when equipped with this energy absorbing device, has been discussed in chapter 5. Two kinds of structures were chosen for this investigation: a framework and a concentrically braced moment resistant frame.

The framework was studied for two cases, when it is equipped with the energy absorbing device and second without the device. In both cases, triangular explosive loading was applied to the framework. It has been shown that by using only one device in the framework, the impact resistance is improved by more than twice when compared with the case of no device. It was noticed that by including the device, the impact load was more than twice the value of that which cause the frame without the device to collapse. At this load the frame with the device was still undamaged. These analysis were carried out by using the Lusas finite element program.

A single degree freedom structure was the second case which was studied in chapter 5.

By creating suitable models, the response of this frame was analysed in two cases, first by using the energy absorbing devices in the braces of the frame and second, without using the device. In both cases, the same base excitation was the applied loading.
It was resulted that in the unequipped frame, accelerations and velocities in the first floor is almost three times of the equipped frame. The axial forces in the columns were almost three times of the equipped frame. This means that a correction in the cross sections of columns was inevitable for this frame and therefore an additional increase in the acceleration was expected for the unequipped frame.
The final structure which was studied in chapter 5, was a multi-storey building. The same as single degree freedom structure, this multi storey frame was considered in two case, when it was equipped with the energy absorbing device and without it. In both cases, the same base excitations were applied to the frame.
The comparison between these two conditions of the frame resulted that the acceleration and velocities in the equipped framework were much lower than unequipped one. It was observed that the forces in the columns of equipped frame is almost three times less than the other one. In this design it had been tried to make this Multi Degree Freedom Structure much similar to one degree freedom one and for this reason the beams were selected from rigid section. For braces of other floors a sufficient areas were assigned to create enough stiffness in these floors.

6-2 The works for future

The most important work, which has been left for the future, is the experimental tests of this novel energy absorbing device. Because of the absence of necessary equipment we couldn't do any test in this regard and they are left for the future. The following steps must be taken to perform these tests:

1) The device should be made in several specimens and should be tested to validate the numerical models of the device.

2)- After obtaining the final design of the device, it should be tested in the structures. As was described in chapter 5, the best structures for the application of this device are frameworks and CBMRF. Advanced equipment will be necessary for application of an explosive load on the framework. For the frames, a shaking table is necessary.

References

1) Aguirre M, Sanchez A R, 'STRUCTURAL SEISMIC DAMPER' *JOURNAL OF STRUCTURAL ENGINEERING,* ASCE, 1992, Vol. 118 No 5 pp. 1158-1171

2) Aristizabal-Ocho J D 'DISPOSABLE KNEE BRACING: IMPROVEMENT IN SEISMIC DESIGN OF STEEL FRAMES.' *JOURNAL OF STRUCTURAL ENGINEERING,* ASCE , 1986, No 7 pp. 1544-152

3) Arnold C. 'SOFT FIRST STORIES: TRUTH AND MYTH', *PROC. 8TH WORLD CONF. ON EARTHQUAKE ENG , SANFRANCISCO; 1984, Vol.* V, 943-9

4) Bailey T, Semercigil SE, 'A PASSIVE CONTROLLER FOR FLEXIBLE L-STRUCTURES' *JOURNAL OF SOUND AND VIBRATION,* 1994, Vol.173, No.1, pp.131-136

5) Balendra T, Lim EL, Lee SL, 'DUCTILE KNEE BRACED FRAMES WITH SHEAR YIELDING KNEE FOR SEISMIC RESISTANT STRUCTURES' *ENGINEERING STRUCTURES,* 1994, Vol.16, No.4, pp.263-269.

6) Beck J. L. , Skinner R. I., 'THE SEISMIC RESPONSE OF A REINFORCED CONCRETE BRIDGE PIER DESIGNED TO STEP' *EARTHQUAKE ENGINEERING AND STRUCTURAL DYNAMICS,* 1974, Vol. 2, 343-58.

7) Boardman P. R. , Wood B. J. , Carr A. J., ' UNION HOUSE-CROSS BRACED STRUCTURE WITH ENERGY DISSIPATORS' *BULL. NZ NAT. SOC. FOR EARTHQUAKE ENGINEERING,* 1983, Vol. 16, No. 2 , pp 83-97.

8) Bourahla N, 'KNEE BRACING SYSTEM FOR EARTHQUAKE RESISTING STEEL FRAMES' PHD *THESIS,* University of Bristol, 1990.

9) Carney J. F. , Veillette J. R. , 'IMPACT RESPONSE AND ENERGY DISSIPATION CHARACTERISTICS OF STIFFENED METALLIC TUBES'

PROCEEDING OF THE INTERNATIONAL CONFERENCE ON STRUCTURAL IMPACT AND CRASHWORTHINESS, London, 1984, Vol. 2, p 264

10) Chen SJ, Yeh CH, Chu JM, 'DUCTILE STEEL BEAM-TO-COLUMN CONNECTIONS FOR SEISMIC RESISTANCE', *JOURNAL OF STRUCTURAL ENGINEERING*,ASCE, 1996, Vol.122, No.11, pp.1292-1299.

11) Chopra A K., Clough D P, Clough R W, 'EARTHQUAKE RESISTANCE OF BUILDINGS WITH SOFT FIRST STOREY' , *EARTHQUAKE ENGINEERING AND STRUCTURAL DYNAMICS,* 1973, Vol. 1, No4, pp 347-55.

12) Dowrick, David J ' EARTHQUAKE RESISTANT DESIGN FOR ENGINEERS AND ARCHITECTS' 2nd ed., Wiley, 1987.

13) Ezra A. A. , Fay R. J. 'AN ASSESSMENT OF ENERGY ABSORBING DEVICES FOR PROSPECTIVE USE IN AIRCRAFT IMPACT SITUATIONS' *DYNAMIC RESPONSE OF STRUCTURES*. P 225 eds. G.Herrmann and N. Perrone, Pergamon Press oxford, (1972)

14) Filiatrault A, Tremblay R, Kar R, 'PERFORMANCE EVALUATION OF FRICTION SPRING SEISMIC DAMPER' *JOURNAL OF STRUCTURAL ENGINEERING,ASCE*, 2000, Vol.126, No.4, pp.491-499.

15) Filiatrault A, Cherry S. , 'PERFORMANCE EVALUATION OF FRICTION DAMPED BRACED STEEL FRAMES UNDER SIMULATED EARTHQUAKE LOADS' *ARTHQUAKE SPECTRA*, 1987, Vol. 3 No1, p 57

16) Ghobarah A, Ramadan T, 'SEISMIC ANALYSIS OF LINKS OF VARIOUS LENGTHS IN ECCENTRICALLY BRACED FRAMES', CANADIAN *JOURNAL OF CIVIL ENGINEERING*, 1991, Vol.18, No.1, pp.140-148

17) Ciba polymers 'USER'S GUIDE TO ADHESIVE', 1995

18) Constrado 'STEEL DESIGNER'S MANUAL' *FORTH EDITION*, Collins, 1983.

19) Harris JA, Adams RD, 'AN ASSESSMENT OF THE IMPACT PERFORMANCE OF BONDED JOINTS FOR USE IN HIGH-ENERGY ABSORBING STRUCTURES' *PROCEEDINGS OF THE INSTITUTION OF MECHANICAL ENGINEERS PART C- JOURNAL OF MECHANICAL ENGINEERING SCIENCE,* 1985, Vol.199, No.2, pp.121-131.

20) Hsu S. Y., Fafitis A., 'SEISMIC ANALYSIS OF FRAMES WITH VISCOELASTIC CINNECTIONS' *JOURNAL OF STRUCTURAL ENGINEERING,* ASCE, Vol. 118, No 9, Sep. 1992.

21) Hull D. 'AXIAL CRUSHING OF FIBRE REINFORCED COMPOSITE TUBES' *FIRST INTERNATIONAL SYMPOSIUM ON STRUCTURAL CRASHWORTHINESS,* Liverpool, 1983.

22) Jangid RS, Datta TK,'DISSIPATION OF HYSTERETIC ENERGY IN BASE ISOLATED STRUCTURE', *SHOCK AND VIBRATION*, 1996, Vol.3, No.5, pp.353-359 IS: 1070-9622.

23) Johnson W, 'IMPACT STRENGTH OF MATERIALS; Edward Arnold, 1972.

24) Johnson W. , Reid S. R. , 'THE COMPRESSION OF CROSSED LAYER OF THIN TUBES' *INTERNATIONAL JOURNAL OF MECHANICAL SCIENCES*, 1977, Vol. 19, p423.

25) Johnson W. , Reid S. R, 'METALLIC ENERGY DISSIPATING SYSTEMS' *APPLIED MECHANICS REVIEWS*, 1978, Vol. 31, p277.

26) Jones A. Zukas ' IMPACT DYNAMICS' New York ; Chichester : Wiley, 1982.

27) Jurukovski D ,Petkovski M, Rakicevic Z, 'ENERGY ABSORBING ELEMENTS IN REGULAR AND COMPOSITE STEEL FRAME STRUCTURES' *ENGINEERING STRUCTURES,* 1995, Vol. 17, No 5, pp 319-333.

28) Jurukovski D. , Simenov, B. , Trajkovski, V. , Petkovski M. , 'DEVELOPMENT OF ENERGY ABSORBING ELEMENTS' *IZIIS REPORT* 94-88m-, May 1988

29) Kecman D, 'ANALYSIS OF FRAMEWORK-TYPE SAFETY STRUCTURES IN ROAD VEHICLES' *STRUCTURAL CRASHWORTHINESS*, Ed. N Jones and T Weirzbicki, butterworth & Co Ltd, 1983

30) Keel C. J., Mahmoodi P., 'DESIGN OF VISCOELASTIC DAMPERS FOR THE COLUMBIA CENTRE BUILDING' *BUILDING MOTION IN WIND*, (eds N.Isumove and Tschanz) ASCE, New York, 1986, pp 66-82

31) Kellv G. M. , Skinner R.I., Heine A. J. 'MECHANISM OF ENERGY ABSORPTION IN SPECIAL DEVICES FOR USE IN EARTHQUAKE RESISTANT STRUCTURES' *BULL. NZ NAT. SOC. FOR EARTHQUAKE ENGINEERING,* 1972, Vol. 5, No. 3 , pp 63-88.

32) Kelly J.M., R.I. Skinner and A.J. Heine 'MECHANISMS OF ENERGY ABSORPTION IN SPECIAL DEVICES FOR USE IN EARTHQUAKE RESISTANT STRUCTURES', *BULL. N.Z. SOCIETY OF EARTHQUAKE ENGINEERING* 1972, Vol. 5, No 3, pp63-88.

33) Kurokawa Y, Sakamoto M, Yamada T, Kurino H, Kunisue A,'SEISMIC DESIGN OF A TALL BUILDING WITH ENERGY DISSIPATION DAMPER FOR THE ATTENUATION OF TORSIONAL VIBRATION' *STRUCTURAL DESIGN OF TALL BUILDINGS*, 1998, Vol.7, No.1, pp.21- 32.

34) Li WQ, Tsai CS, 'SEISMIC MITIGATION OF STRUCTURES BY USING VISCOELASTIC DAMPERS' *NUCLEAR ENGINEERING AND DESIGN*, 1994, Vol.147, No.3, pp.263-274.

35) Macaulay, M ' INTRODUCTION TO IMPACT ENGINEERING' *CHAPMAN AND HALL*, 1987.

36) Makris N, Constantinou MC, 'SPRING VISCOUS DAMPER SYSTEMS FOR COMBINED SEISMIC AND VIBRATION ISOLATION' *EARTHQUAKE ENGINEERING & STRUCTURAL DYNAMICS*, 1992, Vol.21, No.8, pp.649-664.

37) Mahmoodi P., 'STRUCTURAL DAMPERS', *JOURNAL OF STRUCTURAL DIV.*, ASCE, 1972, 95 (ST8), 1661-1672.

38) Mahmoodi P, .Keel C. J., 'PERFORMANCE OF VISCOELASTIC STRUCTURAL DAMPERS FOR THE COLUMBIA CENTRE BUILDING' *BUILDING MOTION IN WIND*, (eds N.Isumove and Tschanz) ASCE, New York, 1986, pp 83-106.

39) Megget L. M., 'THE DESIGN AND CONSTRUCTION OF A BASE ISOLATED CONCRETE FRAME BUILDING IN WELLINGTON, NEW ZEALAND' PROCEEDING OF 8TH WORLD CONFERENCE ON EARTHQUAKE ENGINEERING, San Francisco, 1984, Vol. V, 935-42.

40) Mo Y L, Chang Y F 'EFFECT OF FIRST STOREY SHEARWALLS WITH TEFLON SLIDERS ON EARTHQUAKE RESISTANT BUILDINGS', *MAGAZINE OF CONCRETE RESEARCH, 1993, Vol.45, No 165, pp. 293-300.*

41) Murray N W, 'THE STATIC APPROACH TO PLASTIC COLLAPSE AND ENERGY DISSIPATION IN SOME THIN WALLED STRUCTURES' *STRUCTURAL CRASHWORTHINESS*, Ed. N Jones and T Weirzbicki, butterworth & Co Ltd, 1983.

42) Mutto K. , 'EARTHQUAKE RESISTANT DESIGN OF 36 STOREY KASUMIGASEKI BUILDING' , PROCEEDING OF 4TH WORLD CONFERENCE ON EARTHQUAKE ENGINEERING, Chile, 1969, Vol. III, J4, pp15-33.

43) Naiem F. , Kelly J. M. 'DESIGN OF SEISMIC ISOLATED STRUCTURES' John Wiley & Sons, INC 1999,

44) Ohashi Y. , Murakami S. , 'ELASTO-PLASTIC BENDING OF A CLAMPED THIN CIRCULAR PLATE ' PROCEEDING OF 11TH INTERNATIONAL CONGRESS OF APPLIED MECHANICS, 1964.

45) Oledzki AA, Siwicki I, Wisniewski J, 'IMPACT DAMPERS IN APPLICATION FOR TUBE, ROD AND ROPE STRUCTURES', *MECHANISM AND MACHINE THEORY*, 1999, Vol.34, No.2, pp.243-253.

46) Oliver J. and Onate E. 'A TOTAL LAGRANGIAN FORMULATION FOR THE GEOMETRICALLY NONLINEAR ANALYSIS OF STRUCTURES USING FINITE ELEMENTS' *INTERNATIONAL JOURNAL FOR NUMERICAL METHODS IN ENGINEERING*, 1984, Vol 20, p 2253-2281.

47) Pafitis DG, Hull D, 'DESIGN OF FIBER COMPOSITE CONICAL COMPONENTS FOR ENERGY ABSORBING STRUCTURES' *SAMPE JOURNAL*, 1991, Vol.27, No.3, pp.29-34.

48) Pall A S, Marsh C, 'RESPONSE OF FRICTION DAMPED BRACED FRAMES' *J. STRUCTURAL DIVN*, ASCE, 1982, Vol. 108 No ST6, 1313-23.

49) Pall A. S. 'RESPONSE OF FRICTION DAMPED BUILDINGS' *PROC. 8TH WORLD CONF. ON EARTHQUAKE ENG.*, Sanfrancisco, 1984, Vol.V, pp 1007-14.

50) Pekcan G, Mander JB, Chen SS, 'EXPERIMENTS ON STEEL MRF BUILDING WITH SUPPLEMENTAL TENDON SYSTEM', *JOURNAL OF STRUCTURAL ENGINEERING-ASCE, 2000*, Vol.126, No.4, pp.437-444.

51) PINELLI_JP, CRAIG_JI, GOODNO_BJ, 'ENERGY-BASED SEISMIC DESIGN OF DUCTILE CLADDING SYSTEMS' *JOURNAL OF STRUCTURAL ENGINEERING*-ASCE, 1995, Vol.121, No.3, pp.567-578.

52) Pong WS, Tsai CS, 'SEISMIC STUDY OF BUILDINGS WITH VISCOELASTIC DAMPERS' *EARTHQUAKE ENGINEERING & STRUCTURAL DYNAMICS*, 1999, Vol.28, No.9, pp.941-955.

53) Rai DC, ' SUPPLEMENTAL DAMPING FOR SEISMIC STRENGTHENING: A CASE STUDY' *ENGINEERING STRUCTURES*, 1999, Vol.21, No.7, pp 603-614.

54) Rai DC, Wallace BJ, 'ALUMINIUM SHEAR-LINKS FOR ENHANCED SEISMIC RESISTANCE' *EARTHQUAKE ENGINEERING & STRUCTURAL DYNAMICS*, 1998, Vol.27, No.4, pp.315-342.

55) Rasmussen E. 'DAMPERS HOLD SWAY' *CIVIL ENGINEERING*, 1997, Vol.67, No.3, pp.40-43.

56) Reddy T. Y. , Reid S. R. , 'LATERAL COMPRESSION OF TUBES AND TUBE SYSTEMS WITH SIDE CONSTRAINTS' *INTERNATIONAL JOURNAL OF SOLIDS AND STRUCTURES*, 21, 187 (1979).

57) Redwood R. G., 'DISCUSSION OF CRUSHING OF A BETWEEN RIGID PLATES' *JOURNAL OF APPLIED MECHANICS,* ASME, 31, 357 (1964)

58) Reid S.R. 'LATERALLY COMPRESSED METAL TUBES AS IMPACT ENERGY ABSORBERS' *FIRST INTERNATIONAL SYMPOSIUM ON STRUCTURAL CRASHWORTHINESS,* Liverpool, 1983.

59) Reid S. R. , Bell W. W. , 'INFLUENCE OF STRAIN HARDENING ON THE DEFORMATION OF THIN RINGS SUBJECTED TO OPPOSED CONCENTRATED LOADS' *INTERNATIONAL JOURNAL OF SOLIDS AND STRUCTURES*, 1982, Vol 18, p 643.

60) Reid S. R, Austin C. D. , Smith R. , 'TUBULAR RINGS AS ENERGY ABSORBERS' *PROCEEDING OF THE INTERNATIONAL CONFERENCE ON STRUCTURAL IMPACT AND CRASHWORTHINESS, London, 1984 vol. 2*

61) Robinson W H, Greenbank L R, 'PROPERTIES OF AN EXTRUSION ENERGY ABSORBER' , *BULL. NZ NAT. SOC. FOR EARTHQUAKE ENGINEERING,* 1975, Vol. 8, No. 3 , pp 187-91.

62) Roeder CW, Schineider SP, Carpenter JE, 'SEISMIC BEHAVIOR OF MOMENT-RESISTING STEEL FRAMES - ANALYTICAL STUDY', *JOURNAL OF STRUCTURAL ENGINEERING*,ASCE, 1993, Vol.119, No.6, pp.1866-1884.

63) Roger E Schol, 'AN ALTERNATIVE STRUCTURAL SYSTEM FOR IMPROVING THE EARTHQUAKE PERFORMANCE OF THE BUILDINGS' *EIGHTH WORLD CON. ON EARTHQUAKE ENG.*, 1984, Vol. V pp1015-1022.

64) Romero EM, 'SUPPLEMENTARY ENERGY DISSIPATORS FOR MAXIMUM EARTHQUAKE PROTECTION OF TALL BUILDING STRUCTURES', *STRUCTURAL DESIGN OF TALL BUILDINGS*, 1995, Vol.4, No.1, pp.91- 101.

65) Runtz J.A, Hodge P. G. ' CRUSHING OF A TUBE BETWEEN RIGID PLATES' *JOURNAL OF APPLIED MECHANICS,* ASME, 1963, Vol.30,p 391.

66) Sam MT, Balendra T, Liaw CY, 'EARTHQUAKE-RESISTANT STEEL FRAMES WITH ENERGY DISSIPATING KNEE ELEMENTS' *ENGINEERING STRUCTURES*, 1995, Vol.17, No.5, pp.334-343.

67) Samali B, Kwok K C S, 'USE OF VISCOELASTIC DAMPERS IN REDUCING WIND AND EARTHQUAKE INDUCED MOTION OF BUILDING STRUCTURES' *ENGINEERING STRUCTURES,* 1995 Vol. 17, No 9 pp 639-654.

68) Skinner RI, Beck JL, Bycroft GN, 'A PRACTICAL SYSTEM FOR ISOLATING STRUCTURES FROM EARTHQUAKE ATTACK' *EARTHQUAKE ENGINEERING AND STRUCTURAL DYNAMICS,* 1975, Vol. 3, No 3, 297-309.

69) Skinner RI, McVerry, GH , 'BASE ISOLATION FOR INCREASED EARTHQUAKE RESISTANCE OF BUILDINGS' *BULL. NZ NAT. SOC. FOR EARTHQUAKE ENGINEERING,* 1975, Vol. 8, No. 2 , pp 93-101.

70) Skinner RI, Robinson WH, Mcverry GH, 'SEISMIC ISOLATION IN NEW-ZEALAND' *NUCLEAR ENGINEERING AND DESIGN,* 1991, Vol.127, No.3, pp.281-289.

71) Shen KL, Soong TT, Chang KC, Lai ML, 'SEISMIC BEHAVIOR OF REINFORCED-CONCRETE FRAME WITH ADDED VISCOELASTIC DAMPERS' *ENGINEERING STRUCTURES*, 1995, Vol.17, No.5, pp.372-380.

72) Sheng-Yung Hsu, Apostolos Fafitis, ' SEISMIC ANALYSIS DESIGN OF FRAMES WITH VISCOELASTIC CONNECTIONS' *JOURNAL OF STRUCTURAL ENGINEERING*, 1992, Vol. 118 No 9.

73) Shrive N. G., K.R.F. Andrews, G. L. England 'THE IMPACT ENERGY DISSIPATION OF CYLINDRICAL SYSTEMS' *PROCEEDING OF THE INTERNATIONAL CONFERENCE ON STRUCTURAL IMPACT AND CRASHWORTHINESS,* London, 1984 vol. 2.

74) Silbar A, 'OPTIMIZED PASSIVE SAFETY AND CRASHWORTHINESS OF THE PASSENGER CAR' VEHICLE SYST DYN , 1992, Vol. 20, 596-607.

75) Steimer S. F., Chow F.L. , 'CURVED PLATE ENERGY ABSORBERS FOR EARTHQUAKE RESISTANT STRUCTURES', *PROC. 8TH WORLD CONF. ON EARTHQUAKE ENG.* , Sanfrancisco, 1984, Vol. V, pp967-74.

76) Stronge W J, T.X YU, W Johnson 'ENERGY DISSIPATION BY SPLITTING AND CURLING TUBES' *PROCEEDING OF THE INTERNATIONAL CONFERENCE ON STRUCTURAL IMPACT AND CRASHWORTHINESS,* London, 1984 vol. 2, pp 576-587.

77) Shustov V, 'ENERGY ABOSORBING TEQNIQUE: CHALLENGE OF PROPORTIONING' STRUCTURES UNDER SHOCK AND IMPACT III' *THIRD INTERNATIONAL SYMPOSIUM ON STRUCTURAL CRASHWORTHINESS,* Madrid, Spain, 1994, p 479-483.

78) Tsai CS, Lee HH, SEISMIC MITIGATION OF BRIDGES BY USING VISCOELASTIC DAMPERS' *COMPUTERS & STRUCTURES,* 1993, Vol.48, No.4, pp.719-727.

79) Tsai CS, Lee HH , 'APPLICATIONS OF VISCOELASTIC DAMPERS TO HIGH-RISE BUILDINGS', *JOURNAL OF STRUCTURAL ENGINEERING*-ASCE, 1993, Vol.119, No.4, pp.1222-1233.

80) Tsai CS, Tsai KC, 'TPEA DEVICE AS SEISMIC DAMPER FOR HIGHRISE BUILDINGS', *JOURNAL OF ENGINEERING MECHANICS*,ASCE, 1995, Vol.121, No.10, pp.1075-1081.

81) Tyler RG, 'A TENACIOUS BASE ISOLATION SYSTEM USING ROUND STEEL BARS', *BULL. NZ NAT. SOC. FOR EARTHQUAKE ENGINEERING,* 1978, Vol. 11, No. 4 , pp 273-81.

82) Tyler R. G., 'FURTHER NOTES ON A STEEL BRACED ENERGY ABSORBING ELEMENT FOR BRACED FRAMEWORKS', *BULL. NZ NAT. SOC. FOR EARTHQUAKE ENGINEERING*, 1985, Vol. 18, No. 3 , pp 270-79.

83) Villaverde R, Mosqueda G, 'ASEISMIC ROOF ISOLATION SYSTEM: ANALYTIC AND SHAKE TABLE STUDIES' *EARTHQUAKE ENGINEERING & STRUCTURAL DYNAMICS*, 1999, Vol.28, No.3, pp.217-234.

84) White MD, Jones N, 'EXPERIMENTAL QUASI-STATIC AXIAL CRUSHING OF TOP-HAT AND DOUBLE- HAT THIN-WALLED SECTIONS' *INTERNATIONAL JOURNAL OF MECHANICAL SCIENCES*, 1999, Vol.41, No.2, pp.179-208.

85) Wood RD. 'THE APPLICATION OF FINITE ELEMENT METHODS TO GEOMETRICALLY NONLINEAR STRUCTURAL ANALYSIS' *PhD THESIS*, University of Swansea, Wales, UK.

86) Xia C, Hanson RD, 'INFLUENCE OF ADAS ELEMENT PARAMETERS ON BUILDING SEISMIC RESPONSE' *JOURNAL OF STRUCTURAL ENGINEERING*, 1992, Vol. 118, No 7, pp 1903-1918.